Holistic and integrated energy system optimization in reducing diesel dependence of Canadian remote Arctic communities

by

Marvin Rhey D. Quitoras

A Dissertation Submitted in Partial Fullfillment of the
Requirements of the Degree of

DOCTOR OF PHILOSOPHY

in the Department of Mechanical Engineering

We acknowledge with respect the Lekwungen peoples on whose traditional territory the university stands and the Songhees, Esquimalt and WSÁNEĆ peoples whose historical relationships with the land continue to this day.

Holistic and integrated energy system optimization in reducing diesel dependence of Canadian remote Arctic communities

by

Marvin Rhey D. Quitoras

Supervisory Commitee

Dr. Curran Crawford, Supervisor
Department of Mechanical Engineering

Dr. Andrew Rowe, Departmental Member
Department of Mechanical Engineering

Dr. Madeleine McPherson, Outside Member
Department of Civil Engineering

Title: Holistic and integrated energy system optimization in reducing diesel dependence of Canadian remote Arctic communities
Author: Marvin Rhey D. Quitoras
Keywords: Canadian Arctic; Remote community; Indigenous peoples; Integrated energy system; Energy policy; Robust optimization; Uncertainty

ABSTRACT

This dissertation demonstrates novel holistic approaches on how to link policy, clean energy innovations, and robust energy modeling techniques to help build more resilient and cost-effective energy systems for the Canadian Arctic region and remote communities in general. In spite of the diversity among Arctic jurisdictions, various energy issues and challenges are shared pan-territorially in the North. For instance, 53 out of 80 remote communities in the Northern territories rely exclusively on diesel-based infrastructures to generate electricity, with heating oil as their primary source of heat. This critical dependence on fossil fuels exposes the Indigenous peoples and other Canadians living in the North to high energy costs and environmental vulnerabilities which is exacerbated by the local and global catastrophic effects of climate change in the Arctic. Aside from being strong point sources of greenhouse gases and other airborne pollutants, this reliance on carbon-intensive sources of energy elevates risk of oils spills during fuel transport and storage. Further, conventional transportation mode via ice roads is now increasingly unreliable because of the rising Arctic temperatures which is twice the global average rate. As a result, most fuels are being transported by small planes which contribute to high energy costs and fuel poverty rates, or via boats which also increases the risk of oil spills in the Arctic waters.

Methodologically, this thesis presents a multi-domain perspective on how to accelerate energy transitions among Northern remote communities. In particular, a multi-objective optimization energy model was developed in order to capture complex trade-offs in designing integrated electrical and thermal energy systems. In comparison with traditional single-objective optimization approach, this technique offers diversity of solutions to represent multiple energy solution philosophies from various stakeholders and practitioners in the North. A case study in the Northernmost community of the Northwest Territories demonstrates the applicability of this framework – from modeling a range of energy solutions (supply and demand side aspects) to exploring insights and recommendations while taking into account uncertainties. Overall, this dissertation makes a set of contributions, including:

- Development of a robust energy modeling framework that integrates complex trade-offs and multiple overlapping uncertainties in designing energy systems for the Arctic and remote communities in general;
- Extension of previous Arctic studies – where focused has solely been on the electricity sector – by integrating heating technology options in the proposed modeling framework in conjunction with methods on obtaining 'high performance' buildings in the North;
- Overall energy system performance evaluation when integrating heat and electricity sectors, as well as the role of battery storage systems and diesel gener-

ator on facilitating variable renewable energy generation among isolated communities;

- Formulation of a community-scale energy trilemma index model which helps design policies that are accelerating (or hindering) energy transitions among remote communities by assessing quantitatively challenges relating to energy security, affordability, and environmental sustainability;

- Synthesized holistic insights and recommendations on how to create opportunities for Indigenous peoples-led energy projects while discussing interwoven links between energy system operations, relationship building and stakeholders engagement, policy design, and research (energy modeling and analysis).

Collectively, the new methods and recommendations demonstrated herein offer evidence-based decision making and innovative solutions for policy makers, utility companies, Indigenous peoples, and other stakeholders in the Arctic and beyond.

Contents

List of Figures

List of Tables

Nomenclature

The number after each abbreviation and symbol is the page number where the nomenclature is **first** used.

Abbreviations

ASHP	Air-source Heat Pump, 57
BAU	Business as Usual, 46
BT	Battery, 22
CCOS	Cycle Charging Operation Strategy, 34
CONV	Converter, 22
DG	Diesel Generator, 22
DHW	Domestic Hot Water, 60
DT	Deterministic, 115
GA	Genetic Algorithm, 25
GHG	Greenhouse Gas Emissions, 94
GNWT	Government of Northwest Territories, 121
HOMER	Hybrid Optimization of Multiple Energy Resources, 6
HRES	Hybrid Renewable Energy System, 7
IEA	International Energy Agency, 7
iHOGA	improved Hybrid Optimization by Genetic Algorithms, 100
IPP	Independent Power Producer, 92
KiBaM	Kinetic Battery Model, 32
LA	Lead Acid, 106

LFOS	Load Following Operation Strategy, 34
LI	Lithium Ion, 106
MILP	Mixed Integer Linear Programming, 26
MINES	Multi-objective INtegrated Energy System, 24
MOP	Multi Objective Problem, 22
MVHR	Mechanical Ventilation with Heat Recovery, 81
NCPC	Northern Canada Power Corporation, 151
NOAA	National Oceanic and Atmospheric Administration, 1
NOCT	Nominal Operating Cell Temperature, 30
NSGA-II	Non-dominated Sorting Genetic Algorithm - II, 61
NTPC	Northwest Territories Power Corporation, 36
NWT	Northwest Territories, 1
NWT	Northwest Territories, 19
PPA	Power Purchase Agreement, 92
PV	Photovoltaic, 22
QEC	Qulliq Energy Corporation, 152
RB	Reliability-based Optimization, 94
RE	Renewable Energy, 94
RO	Robust Optimization, 97
SHGC	Solar Heat Gain Coefficient, 65
STC	Standard Test Conditions, 30
UNDRIP	United Nations Declaration on the Rights of Indigenous Peoples, 5
URRC	Utility Rates Review Council, 120
WEC	World Energy Council, 66
WT	Wind Turbine, 22

WT	Wind turbine, 9
WWF	World Wildlife Fund, 6
WWR	Windows-to-wall ratio, 65

Symbols

$\xi_j(\mu_o, \sigma_o)$	Discrete samples of stochastic variables, 101
α	Wind power law exponent, 31
α_{hr}	Heat recovery efficiency, 65
α_p	Temperature coefficient of power, 30
$\bar{U}$	Annual mean wind speed, 31
η_{gen}	Wind turbine generator efficiency, 31
η_i	Infiltration air changes per hour, 65
$\eta_{mp,STC}$	Maximum power point efficiency of PV under STC, 30
η_v	Ventilation air changes per hour, 65
Γ	Complete gamma function, 31
λ_{fi}	Failure rate of the ith component, 103
λ_{ri}	Repair rate of the ith component, 103
ρ_a	Air density, 31
ρ_w	Water density, 64
$\tau\alpha$	Effective transmittance-absorptance product of PV, 30
τ_i	Outage history of the ith component, 103
φ_μ	Mean value of the original time-series, 101
φ_σ	Standard deviation of the original time-series, 101
$\varphi_{new}(t)$	New time-series of the uncertain parameter, 101
A	Rotor area of the wind turbine, 31
A_b	Total surface area of the building, 65

c	Scale parameter, 31
C_p	Wind power coefficient, 31
c_{BT}	Fraction of capacity that may hold available charge of BT, 32
C_{inst}	Installation cost of the hybrid system, 9
$c_{p,a}$	Air specific heat, 65
$c_{p,b}$	Building heat specific capacity, 65
$c_{p,w}$	Water specific heat, 64
CC	Capital cost, 9
COP	Coefficient of Performance of ASHP, 76
DG_{LF}	Load factor of DG, 28
dT	Building hourly temperature variation, 65
dt	Simulation timestep, 65
EF	Emission factor, 10
$F(u)$	Percent of time hourly mean speed exceeds u, 31
F_0	Fuel curve intercept coefficient, 34
F_1	Fuel curve slope coefficient, 34
f_{pv}	PV derating factor, 30
$fuel_{cons}$	Fuel consumption, 10
GHI	Global Horizontal Irradiance, 30
h	Hub height, 31
h_a	Anemometer height, 31
HG	Heat gain, 65
HL	Heat losses, 65
HL_i	Heat losses due to infiltration, 65
HL_t	Heat losses due to transmission, 65
HL_v	Heat losses due to ventilation, 65

i	System component, 9
i_g	Inflation rate, 9
$I_{c,max}$	Maximum charge current, 32
$I_{d,max}$	Maximum discharge current, 32
k	Variability about the mean wind speed, 31
k_{BT}	Rate constant of BT, 32
LCC	Life Cycle Cost, 28
M	Mass of the building, 65
$MTBF_i$	Mean Time Between Failure, 103
$MTTR_i$	Mean Time To Repair, 103
N	Number of components of the hybrid system, 9
n	Life of the energy system in years, 9
N_{BT}	Number of BT in the storage bank, 34
$O\&M$	Operations and maintenance costs, 9
P_w	Power output of the WT, 31
P_{batt}	Power stored from the BT, 9
$P_{deficit}$	Insufficient supply of power from the power sources, 8
$P_{DG,r}$	Rated capacity of DG, 34
P_{DG}	Power produced by DG, 34
P_{excess}	Excess electricity, 28
P_{gen}	Overall power generated from the system, 10
P_{load}	Load demand, 100
P_{pv}	Solar PV generation, 30
P_{RE}	Power produced by RE, 9
P_{served}	P_{load} served, 9
$P_{w,r}$	Rated power output of the WT, 32

POA	Incident irradiance, 30
POA_{NOCT}	Solar radiation at which NOCT is defined, 30
POA_{STC}	Incident irradiance at STC, 30
Q_i	Quantity per unit of the system component, 9
q_0	Stored energy, 33
$q_{1,0}$	Available charge at the beginning of the timestep, 33
q_1	Available charge at the end of the timestep, 33
$q_{2,0}$	Bound charge at the beginning of the timestep, 33
q_2	Bound charge at the end of the timestep, 33
Q_{dhw}	Daily average demand for DHW, 64
Q_{LT}	Lifetime throughput of a single storage, 34
q_{max}	Maximum capacity of the BT, 32
Q_{sh}	Thermal energy demand for space heating, 65
Q_{thrpt}	Annual storage throughput, 34
r	Discount rate, 9
$R_{BT,f}$	Storage float life, 34
R_{BT}	Battery bank life, 33
RC	Replacement cost, 9
RE_{pen}	RE penetration, 9
$Risk_{coeff}$	Risk coefficient, 101
S	Salvage value, 10
SOC	State of charge of the battery, 28
SOC_{sp}	Set point state of charge, 35
T	Overall time period considered, 8
t	Time, 27
$T_{a,NOCT}$	Ambient temperature at which NOCTis defined, 30

T_a	Ambient temperature, 30
$T_{c,NOCT}$	Nominal operating cell temperature, 30
$T_{c,STC}$	PV cell temperature under STC, 30
T_c	PV cell temperature, 30
T_{in}	Set indoor temperature, 65
T_{out}	Outdoor temperature, 65
$T_{w,c}$	Cold water temperature, 64
$T_{w,h}$	Hot water temperature, 64
U	Overall heat transfer coefficient of the building, 65
u	Wind velocity, 31
U_i	Uniformly distributed number between [0,1], 103
u_r	Rated wind speed, 32
u_{ci}	Cut-in wind speed, 32
u_{co}	Cut-out wind speed, 32
V_i	Building infiltrated volume, 65
V_v	Building ventilated volume, 65
$V_{d,p}$	Daily consumption of hot water per person, 64
Y_{pv}	rated capacity of the PV array, 30
Z	Other costs associated in building the energy system, 10

Acknowledgements

I want to thank:

God. Thank you for Your faithfulness all throughout this PhD journey. Embarking on a PhD (and absolutely everything) is meaningless without Your presence.

My family. Mama, Papa and Adeng – thank you for supporting me on this journey. Pursuing a PhD is hard, doing it abroad is beyond words. Thank you for keeping me grounded and allowing me to continue reaching my often too ambitious dreams. Thank you for reminding me that relationship/family is more important than all the success this world could offer.

Oxford Centre for Christian Apologetics and Ravi Zacharias International Ministries. Thank you for influencing me to become a scientist and a Christian, and that it is definitely okay to be both. Thank you for defending the Christian faith with so much clarity and grace in open forums across prestigious universities worldwide.

Dr. Curran Crawford. Thank you Curran for believing in my capacity to do this work. Being mentored by you is such an honor. Without your guidance and supervision, all this would not have been possible.

Dr. Paul Rowley. Paul, thank you for opening the world of energy policy to me. Thank you for always highlighting the value of incorporating real-world energy issues and challenges in my energy modeling work.

Dr. Pietro Campana. Thank you for answering all of my questions when I was still building my energy model. Grateful for your willingness to support and guide me from start to end of my PhD.

Dr. Martha Lenio. Thank you for sharing your experience in dealing with Indigenous peoples to build actual energy projects in the North. Your mentorship has helped me framed the significance of my work from the perspective of the Indigenous peoples.

IESVic. Thank you Sue, Pauline and Jeremy for all the administrative support in my doctoral work. Thank you for dealing with my complicated travel claims!

Funders. I would like to acknowledge financial support for my PhD project from the following organizations: Marine Environmental Observation, Prediction and Response Network (MEOPAR), Polar Knowledge Canada, Mitacs, World Wildlife Fund - Canada and the University of Victoria.

Friends. Forever grateful to be able to meet and establish wonderful friends/family from all over the world along this PhD journey: Ninang Lois, Daniel, Sandi, Joe, Charity, Yina, Masa, Zehui, Risa, Keiko, Lucas, Harry, Bohan, Kuya Dennis, Manuel, Mylene, Charles and Ruth. Hoping to cross paths again in the future!

Maraming salamat!

Marvin Rhey Dumo Quitoras
Victoria, BC, Canada

Dedication

To all persons of color and to the Indigenous Peoples.

"It is in collectivities that we find reservoirs of hope and optimism."
— Angela Y. Davis

Chapter 1

Introduction

The Arctic is experiencing some of the worst local and global catastrophic effects of climate change today. According to the Arctic report card of the National Oceanic and Atmospheric Administration (NOAA) [1], it is in fact warming twice as fast as the rest of the globe. This has also been supported and very well documented in various reports [2]. Unfortunately, this situation resulted to gradual diminishing of ice cover in Northern latitude areas and introduced risks to every community situated in the Arctic region.

The Arctic serves as a massive temperature regulator not just for the Northern Hemisphere but for the whole planet [3]. The capacity of the Arctic to reflect heat is measured by how well a surface, such as snow or ice, bounces heat back into space. However, with the shrinking Arctic sea ice extent[1], caused by the rising air temperatures, more heat is infiltrated in the earth's surface and it caused dramatic increase of warming in the world.

According to Perera et al. [4], climate induced extreme weather events and variations are critical in energy systems planning as it affect both the demand of energy and the resilience of energy supply systems. In the Canadian Arctic, fossil fuels (predominantly diesel) have been the primary source of electricity and heat at the residential, commercial, institutional and community levels [5]. This reliance on fossil fuels exposes the Indigenous peoples living in the North[2] to high energy costs and environmental vulnerabilities which is exacerbated by rapid ongoing climate changes in the region.

Fig. 1.1 presents that nearly 40% of Canada's landmass is considered part of the Arctic, and is home to approximately 150,000 inhabitants, of which close to 80% is Indigenous [7]. Along with Fig. 1.1, Table 1.1 shows that majority of Northern remote communities rely exclusively from diesel for their energy needs, especially in the NWT and Nunavut. Unavailability of data makes it more difficult to quantify how much diesel is used for heating, but it is estimated to be three times more than the amount of fuel used for electricity [6]. In terms of energy use per sector, the NWT is the most energy intensive territory in Canada as compared to Yukon and Nunavut. Yukon, on Fig. 1.2, shows that the energy demand share between transportation, industrial, commercial and residential is in the 20 - 30% range [8].

[1] Sea ice extent is a measure of the surface area of the ocean covered by sea ice.

[2] The North in Canada politically refers to the territories of Yukon, Northwest Territories (NWT) and Nunavut. Also, the Indigenous peoples in Northern Canada consist of the First Nations, Métis and Inuits.

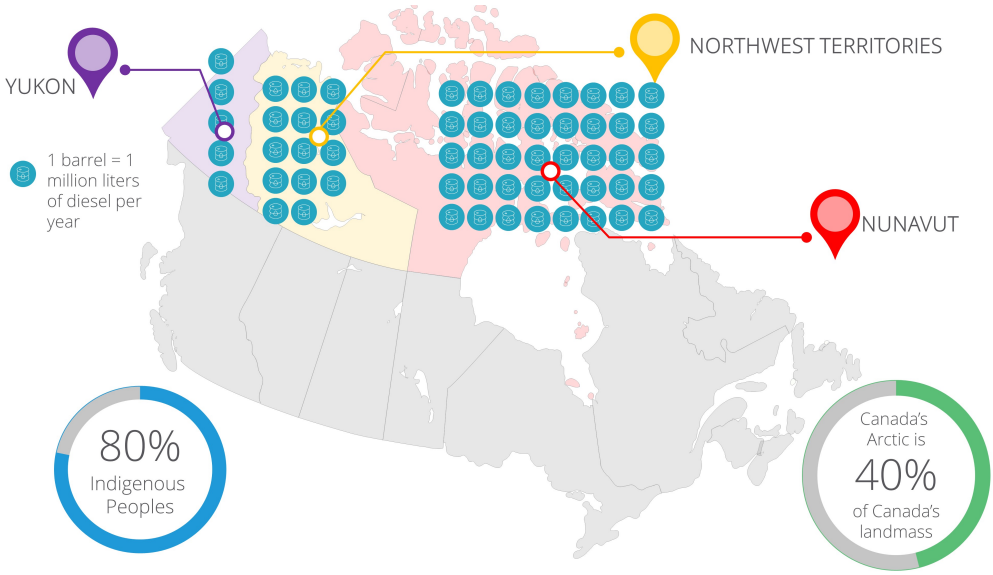

Figure 1.1: Diesel consumption in Northern territories of Canada [6].

Table 1.1: Number of remote communities in Northern territories with their corresponding primary sources of electricity generation [9].

Source	Yukon	NWT	Nunavut
Diesel	5	23	25
Hydro	16	9	0
Natural gas	0	2	0

The NWT and Nunavut, on the other hand, represent approximately 60% of energy demand from its industry sector. However, note that the data presented is driven by the existing industry activity by the year 2013. For instance, the mining operation in these regions could create important swings (up and down) in energy demand, and it might vary per year.

1.1 Motivation and relevance

The energy situation in the Canadian North is notably different from the rest of the country. For example, the energy use per capita in the North is more than twice the Canadian average [10]. Their electricity prices are also significantly higher as compared to other provinces in Canada as shown in Fig. 1.3. In particular, households in the NWT and Nunavut pay more than twice the Canadian average electricity rate of 12.9 cents per kWh. Yukon pays 13.6 cents per kWh, which is closer to, but still above the Canadian average [11]. Some of the fossil fuel generation costs in the North is also listed in Table 1.2.

Fig. 1.4 shows that the average household fuel poverty rate in Canadian provinces is 8% last 2015. A household is described as experiencing fuel poverty when it spends more than 10% of its income on utility bills. Study illustrates that households in the Atlantic provinces and Saskatchewan experience the most fuel poverty in the country [13]. However, the research excluded Northern territories because of the

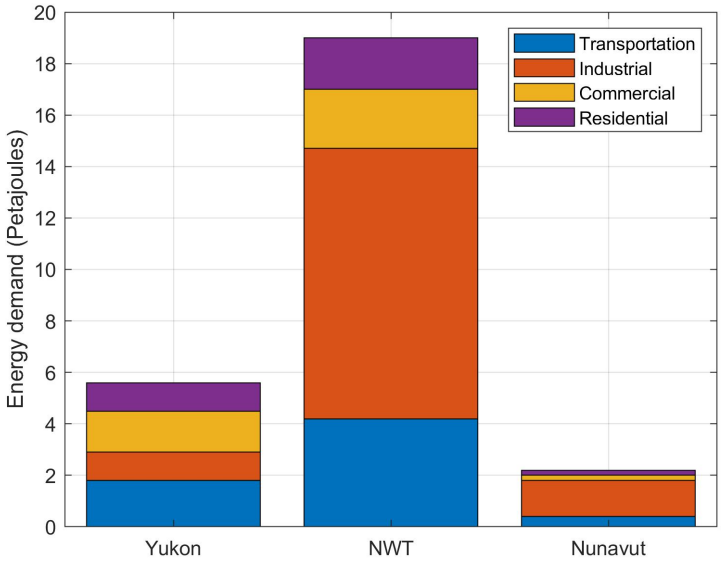

Figure 1.2: End-use energy demand per sector in the three territories of Canada [8].

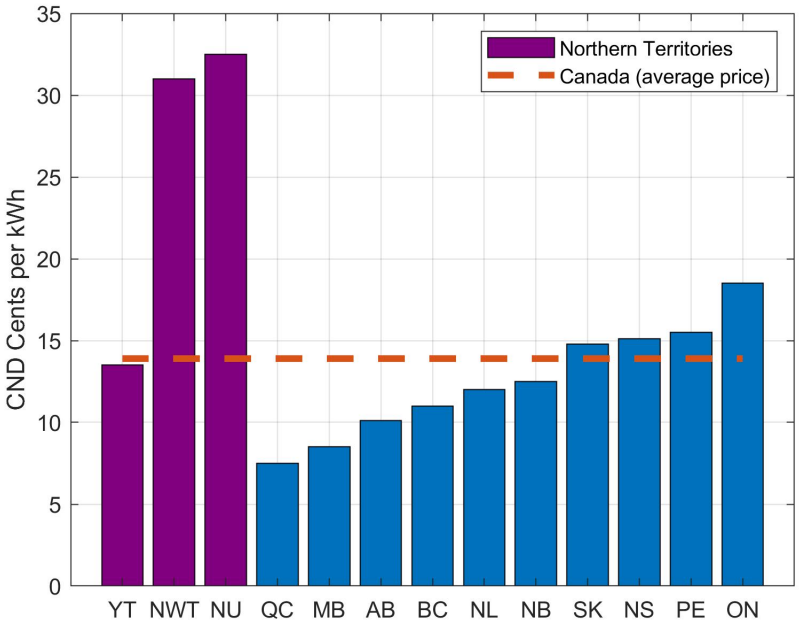

Figure 1.3: Representative territorial and provincial electricity prices in Canada [11].

unique energy challenges being faced by Indigenous remote communities in the Arctic. Specifically, energy costs in the region are highly subsidized through local and federal government programs. In context, the government of Nunavut spends an average of $60.5 million CND each year to subsidize the use of diesel fuel in their territory [14].

The mode of transporting fuels in the North also impacts the high energy costs in the region. Most fuels are shipped from Southern Canada through ice roads and scheduled in bulk. Unfortunately, due to climate change, this mode of transporta-

Table 1.2: Fossil fuel generation costs in Northern Communities [12].

Territory	Community	Fossil Fuel Generation (MWh)	Fuel ($/kWh)	Other Costs ($/kWh)	Total Costs ($/kWh)
NWT	Inuvic-Diesel	16,996	0.33	0.31	0.64
	Inuvic-Natural gas	11,330	0.27	0.31	0.58
	Tuktoyaktuk-Diesel	4,142	0.29	0.31	0.61
	Fort McPherson-Diesel	3,424	0.34	0.31	0.66
Nunavut	Iqaluit-Diesel	60,741	0.29	0.21	0.50
	Cambridge Bay-Diesel	10,267	0.29	0.21	0.50
	Rankin Inlet-Diesel	17,625	0.28	0.21	0.49
	Baker Lake-Diesel	9,518	0.27	0.21	0.48
Yukon	Old Crow-Diesel	2,264	0.54	0.22	0.76
	Destruction Bay-Diesel	1,789	0.19	0.22	0.41

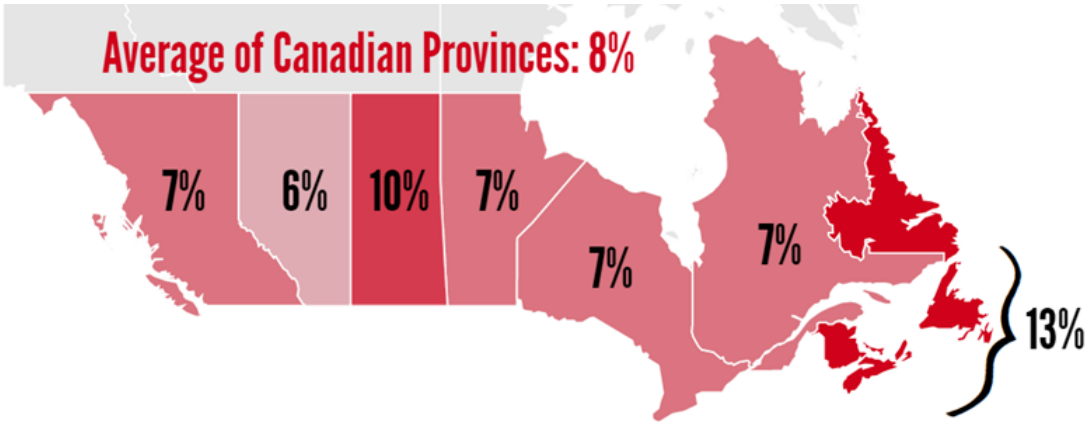

Figure 1.4: Household fuel poverty rates in Canadian provinces in 2015 [13].

tion has become unreliable as most of the ice roads are freezing later and melting earlier. Consequently, fuels have to be shipped via boats, which also increases risk of oil spills in the Arctic waters. This situation is a big challenge for communities especially when there is a delay of fuel deliveries. For example, during the summer of 2019 in Paulatuk, NWT, the annual diesel barge did not arrive because of extreme fall ice conditions that shut down marine traffic through the area. The territorial government had to fly-in 600,000 litres of diesel to the community of 265 people to keep the mostly obsolete diesel generators running. This operation cost $1.75 million CND over dozens of flights. Fig. 1.5 shows an air-shipping activity in transporting fuels in remote communities in Canada.

As mentioned, dependence on fossil fuels also exposes the community to high risk of oil spills during fuel transport and storage. For instance, more than 9.1 million litres of diesel has been spilled in the NWT and Nunavut since the 1970s. More than half of the leaks are from trucks and storage tanks [16]. Outside of Canada, a state of emergency was introduced in Norilsk, Russia after 20,000 tons of diesel leaks into the Arctic river system [17]. The fuel was intended to be stored in the community to ensure continuous supply of power.

Ultimately, understanding the role and the current situation of Indigenous peo-

Figure 1.5: Air-shipping activity in transporting fuels in remote communities [15].

ples in the North is just as important in framing the motivation and relevance of this work. In particular, this thesis aims to create open dialogues between Indigenous peoples and various stakeholders in the North on how to create more Indigenous-led energy projects. According to A SHARED Future Research Team [18], Canada is in the midst of two most challenging issues in the contemporary era: (1) addressing the global climate change crisis by exploring pathways towards a low carbon economy, and (2) "decolonizing" Canadian laws and energy policies by implementing the United Nations Declaration on the Rights of Indigenous Peoples (UNDRIP) [19] and the Truth and Reconciliation Commission of Canada's Calls to Action [20]. Hence, along with the transition to more sustainable forms of energy, this work aims to contribute on a much larger transition for Indigenous communities which is the transition towards self-determination, economic reconciliation and energy sovereignty (to be fully described in Chapter 4).

1.2 Diverging from fossil fuels

This section provides a brief overview on previous studies conducted for transitioning Northern communities of Canada from being fossil fuel dependent towards alternative and clean sources of energy. Note that a more detailed literature review has been conducted in the three main Chapters of this thesis (Chapter 2 - 4).

1.2.1 Unfreezing renewable energy potential

There is a great potential to deploy RE technologies in the remote communities of the Canadian Arctic. For instance, the Government of NWT has commissioned Hatch Ltd. to conduct a feasibility study of wind power generation in Sachs Harbour, NWT. The study [21] investigated potential sites and turbine options for the integration of wind power to the community. Hatch installed two meteorological ("met") stations in the area. The first one was 30m high and was located 6.5 km west of the airport while the other met station was located 300m south of the airport, and measured the wind at 4.2m height from the ground using heated sensors. The data captured by the instruments covered July 8, 2005 to September 18, 2009. However, the data were screened out to detect icing events as well as identify missing

and erroneous measurements. As such, only three full years of the data were considered for the analysis. The WindFarmer commercial software from DNV GL [22] was used in finding the suitable location for a possible wind project in the community. Four proposed sites were identified (between 54m-60m elevation), located from 1 to 6km west of the Sachs Harbour village. They estimated a wind energy production of around 280 MWh/yr for each identified sites. Additionally, last May 2017, Clean Energy-Wood Group (formerly SgurrEnergy Ltd.) [23] released its wind feasibility report for Inuvic High Point, NWT. Based on the preliminary modeling from SgurrEnergy, a considerable financial and greenhouse gas savings can be achieved, ranging from $1.6 million CND to nearly $3 million CND in fuel savings, and from nearly 4,000 tonnes to 7,000 tonnes of greenhouse emissions annually [24]. A similar and earlier study done by Aurora Research Institute [25] has also been carried out to predict the wind energy potential of Sachs Harbour.

Nunavut, unlike Yukon and NWT, relies 100% from diesel to generate power, see Fig. A.2. There are recent developments from the Government of Nunavut to start exploring the potential of RE for their communities. According to a report made by Karanasios and Parker [26], solar potential in Nunavut is estimated to be 567 - 691 kWh/kWp[3] in Iqaluit while the average wind speed in the other communities range from 5m/s in Coral Harbour to 7.7 m/s in Whale Cove. Further, they have also mentioned significant savings in diesel consumption by integrating wind and solar resources into the local diesel systems for the communities of Sanikiluaq, Iqaluit, Rankin Inlet, Arviat and Baker Lake. In addition, Pinard [27] studied the wind potential of Nunavut with more detail. Using RETScreen [28], he identified ten communities for potential wind development projects, which was reduced to five communities after further studies. Detailed modeling was then conducted through Hybrid Optimization of Multiple Energy Resources (HOMER) [29] identifying Iqaluit as the best location for a first project involving large turbines, and followed by Sanikiluaq for small wind turbines. Pinard recommended the Government of Nunavut to install meteorological mast to accurately measure wind resources in the community, and to initiate a prefeasibility study to further examine the area.

1.2.2 Hybrid energy systems

World Wildlife Fund (WWF) completed the most recent set of feasibility studies done for Northern communities of Canada [30]. Their investigations showed that the deployment of hybrid diesel-solar-wind-battery system would economically reduce diesel consumption in the Canadian Arctic. They used HOMER software for the pre-feasibility stage of their study and an in-house mathematical optimization model during the feasibility phase. HOMER determines the most feasible energy system configuration by applying a full factorial design of experiments and choosing the configuration with the minimum NPC. With its user-friendly interface, HOMER is probably the most widely used software in evaluating feasibility of hybrid energy systems among remote communities.

The solution proposed by WWF can be implemented through a microgrid system. A number of definitions can be found on literature [31] describing a microgrid system. Simply, it is a configuration of interconnected loads and distributed energy resources operating as a single integrated energy system. A typical microgrid includes major

[3]kWp is the peak power of a PV system or panel

components such as load, power source (either conventional or RE) and for most cases, a back-up source of power which could either be in the form of diesel generator or battery storage. Lastly, this system can either be grid connected or can operate on island mode.

1.3 Overview in energy systems modeling

Integrating renewables to the current energy system of the Arctic is a complex task. Components and subcomponents of a hybrid renewable energy system (HRES) have to be modeled into a one integrated energy system. According to Biberacher [32], a model is a simplified description of the reality with the purpose of highlighting certain relations that will make the best prediction of future developments possible. In the case of energy systems, Biberacher further described that a model is defined as a framework of relations, be they technical, economic, or social, which describe the actual processes under investigation. The International Energy Agency (IEA) also defined energy models as abstractions of reality that simplify the world into "bite sized" pieces in order to fit within certain sets of mathematical methodologies [33]. They vary in scale from local to global, in sector from electricity or transportation-only to economy wide. These models could also be capable of simulating, optimizing, forecasting or even backcasting and they can all be applied for academic purposes, guide policy-making, or for investment planning of the private and government sectors.

Energy system is complex in nature. Thus, this complexity requires simplification during actual modeling. However, the choice of this simplification influences the validity and accuracy of the model being developed. In practice, the usefulness and quality of every model can be verified by the level to which the objectives (identified beforehand) are attained. Further, IEA argued in their report [33], that all models rely in imperfect inputs, parameters, assumptions, and omission. Hence, while there exists a wealth of advance energy modeling tools, important questions remain about how to effectively implement these models to help stakeholders in their decision-making process.

1.3.1 Simulation versus optimization

There are two basic classes of energy models as described by Lund et al. [34]: optimization and simulation models. A simulation model can be defined as a representation of a system used to simulate and envisage the behaviour of the system under a given set of conditions. The term optimization, on the other hand, is typically used synonymously with a modelling approach where a number of decision-variables are computed that minimize or maximize an objective function subject to various modeling constraints. These decision variables are typically energy system design characteristics. Note that these approaches sometimes overlap and thus a hybrid model, in this context, exists.

Further, optimization is typically associated with a detailed consideration of the current system as starting point to identify the optimal way moving forward. On the other hand, the current system is of less importance for simulation models but details many options in modeling technologies and possible energy systems configurations in the future. In simulation models, the primary focus is to analyse and compare

alternatives and/or scenarios with respect to key parameters in energy modeling such as costs, supply and demand, and emissions, among others. In other words, scenarios are compared based on several criteria rather than establishing an optimal strategy through quantitative analyses based on one criterion. Therefore, simulation models can be classified as a type of scenario model.

Ultimately, the key difference of the two modeling approaches is whether the model itself is capable of identifying one optimal solution or not. As discussed, optimization models are expected to produce optimization decisions based on restrictions or constraints set in the model as combined with its predefined objective function. On the contrary, simulation models will give the user prerogative in making crucial decisions based on a variety of considerations as reflected with various scenarios of the model. Lastly, both have different ways of dealing with risks and uncertainties associated with the energy model. Optimization tends to execute quantitative risk assessment and sensitivity analysis to address uncertainties while simulation typically employs qualitative assessment.

1.3.2 Optimal design criteria

The components and subcomponents of the entire HRES are interconnected and need to be optimized as one integrated energy system. This section presents some of the most common objective functions that can be formulated in the energy model. From a modeling perspective, these objective functions will direct the optimal performance of an energy system. These objectives are often conflicting when optimized simultaneously and is associated with various energy solution priorities from various decision makers among remote communities.

1.3.2.1 Energy system reliability

Reliability of the energy system is an important aspect of any modeling technique given the intermittency of the renewable sources of energy. The energy system should be designed to meet the load at any given point of time by dispatching power from the renewables, diesel generator or the back-up battery.

The reliability of a system can be expressed in terms of Loss of Power Supply Probability ($LPSP$). It is defined as the long-term average fraction in which no power is supplied by a power system over the total electrical load [35]. It will be further described in Sec 2.2.1.1 as part of the constraints formulation of the proposed modeling framework in this dissertation. The mathematical expression of $LPSP$ over a given time period T (8760 h) can be written as:

$$LPSP = \frac{\sum_{t=1}^{T} P_{deficit}(t)}{\sum_{t=1}^{T} P_{load}(t)} \tag{1.1}$$

where $P_{deficit}$ pertains to the insufficient supply of power from the renewables and diesel, as well as the available energy from the BT storage:

$$P_{deficit}(t) = P_{load}(t) - (P_{RE}(t) + P_{DG}(t) + P_{batt}(t-1)) \tag{1.2}$$

where P_{load} is the electricity demand (kW), P_{RE} is the power produced by the renewables (kW), and P_{batt} is the power stored from the BT (kW).

The concept of Loss of Load Probability ($LOLP$) was first introduced by Calabrese [36]. It is a measure of the probability that a system demand will exceed capacity during a given period; often expressed as the estimated number of days over a long period (frequently 10 years or the life of the system). It can be mathematically described as [37]:

$$LOLP = \frac{\sum_{t=1}^{T} Deficit\,load\,time}{Total\,period\,of\,time} \tag{1.3}$$

The $LOLP$ approach is commonly implemented in sizing stand-alone solar energy system [38] but it has also been used in optimizing HRES taking into consideration its subcomponents [39].

If the system is grid-connected, $P_{deficit}$ is assumed to be always zero since power can be bought anytime from the energy market. Thus, RE penetration (RE_{pen}) in the HRES will be considered instead, and is defined as:

$$RE_{pen} = \frac{\sum_{t=1}^{T} P_{RE}(t)}{\sum_{t=1}^{T} P_{served}(t)} \tag{1.4}$$

where P_{served} is the electrical load served.

1.3.2.2 Energy system cost

The economic impact of building an energy system is as important as making it efficient and technically feasible. As such, economic criteria in optimizing an HRES will be discussed here.

The net present value (NPV) of an energy system is the summation of the present value of all present and future cash flows involved in operating the HRES. All cash flows are converted to the initial moment of the system (year 1) taking into account inflation and discount rates. Mathematically, NPV can be illustrated in Eq. 1.5 as adapted from [40].

$$NPV = \sum_{i=1}^{N} Q_i \times \left[(CC_i + RC_i) + \sum_{t=1}^{n} O\&M_i \times \frac{(1+i_g)^t}{(1+r)^t} \right] + C_{inst} \tag{1.5}$$

where N is the number of components of the hybrid system (PV,WT, etc.), Q_i is the quantity per unit of the system component i, CC is the capital cost, RC is the sum of the replacement costs of component i during the system life minus the residual cost of component i at the end of the system life time n (all of them converted to the initial life of the system), $O\&M$ is the operations and maintenance costs of component i, i_g is the inflation rate, r is the discount rate, and C_{inst} is the installation cost of the hybrid system.

The cost effectiveness of an energy system is probably the most common criterion in optimizing HRES, usually in the form of $LCOE$. It is defined as the lifetime

cost of the system over its total energy production. Eq. 1.6 shows a simple and mathematical representation of this concept.

$$LCOE = \frac{\sum_{t=1}^{n} \frac{CC(t)+O\&M(t)+Z(t)}{(1+r)^t}}{\sum_{t=1}^{n} \frac{P_{gen}}{(1+r)^t}} \tag{1.6}$$

where Z is all other costs associated in building the energy system and P_{gen} is the power generated from the system.

Life cycle cost (LCC) is an economic parameter that associates all costs of each HRES component throughout its entire life cycle (from design to recycling) [40], [41]. In equation form, it can be stated as:

$$LCC = \sum_{t=1}^{T} CC_i + RC_{i,NPV} + O\&M_{i,NPV} - S_{i,NPV} \tag{1.7}$$

where S is the salvage value and all subscript of 'NPV' denotes the net present value of each component i.

1.3.2.3 Environmental emission

One of the goals of incorporating renewables to a hybrid system is to reduce environmental emissions of a stand-alone power generator fueled by fossil fuel such as diesel. Therefore, it is important to account for the emissions being contributed by diesel and the indirect emissions from other HRES components. Most studies use CO_2 as a representative of pollutant emissions in quantifying the environmental impact of an energy system [42]. In equation form, CO_2 emissions can be written as:

$$CO_{2emission} = \sum_{t=1}^{T} fuel_{cons}(t) \times EF \tag{1.8}$$

where $fuel_{cons}$ is the fuel consumption and EF is the emission factor, which depends on the type of fuel and diesel engine characteristics.

1.4 Research gaps

The introduction of HRES results to a more dynamic and complex system that requires innovative modeling approaches to effectively model energy sources that are conventionally separated. Further, in order to determine the full spectrum of feasible configurations resulting from hybrid systems and to capture the complexities of conflicting objectives in the decision making process of various stakeholders in the North, the single-objective function approach in optimization of previous studies has to be improved. Thus, the first research gap identified in this work is the lack of mathematical representations on conflicting design objectives when optimizing HRES. Solution diversity, as implemented through a multi-objective approach, is an important aspect of optimization that was lacking in previous studies conducted for Arctic communities.

Literature survey conducted in Chapter 3 indicates that most research applied to Northern Canada has been focused on electricity aspects. According to Gilmour et al. [43], heating is the most dominant form of energy use in the territories with diesel and heating oil[4] as the most frequent fuel used to generate heat. For instance, 2011 reports showed that Northeners consumed 219 million litres of diesel (and some propane) for heating alone. To put this figure into perspective, in the same year 76 million litres of diesel were consumed for power generation [9] making heat more than 70% of the combined heat and electricity demand of Canada's territories. Due to the unavailability of heat load data for most Northern communities, it is critical to perform domestic heating simulations to fully investigate all forms of energy solutions in the North.

Energy system component sizing methods in conjunction with demand side modeling, specifically of heat load reductions, are generally scarce in literature. Most work done for the Arctic was centered on supply-side alternatives without taking into account the significant impact of the demand aspect of the energy system. In particular, the value of high performance building enclosures must be investigated in order to meet deep decarbonization targets in the North. This energy solution is significantly cheaper to implement in comparison with building new energy systems with intermittent renewable resources. According to previous study, heating can also be expensive enough that some households are forced to live in cold homes, which can increase the risk of physical and mental health problems. The risk of respiratory illness doubles as well with kids living in cold homes, while risk of cardiovascular disease and arthritis are common among adults [16].

As heating is a dominant form of energy use in the North, heating technology options must then be part of the energy modeling work being conducted for Arctic communities. Specifically, it was not found in literature studies incorporating the operational impact of various heating technologies in the overall performance of an energy system. In considering the viability of these heating options, flexibility of integration for current and future energy systems must also be taken into account.

Battery storage systems are critical in addressing fluctuations caused by load profiles of remote communities along with the variability coming from the renewables. Previous work done for Northern communities of Canada employed a simplistic representation of modeling battery storage systems in tracking its performance because of the computational expense involved in modeling renewables with battery storage. Although this practice is accepted in the energy modeling community, some improvements must be incorporated to fully understand the flexibilities being provided by batteries. In the Arctic region, the relation of below freezing temperatures on the capacity of battery storage must be modeled together with a suitable dispatch strategy to better capture battery's impact on the overall performance of the energy system.

Integrating heat and electricity sectors can provide flexibility on energy system infrastructures if operated properly. In can also increase renewable energy penetration since the energy sources are integrated and they can address multiple loads (thermal and non-thermal) for the community. This approach on integrated energy

[4]Heating Oil is a generic industry term that covers a variety of potential products, formulations, and compositions. Standard Road Diesel #2, Diesel #1, Kerosene, K-1, Jet Fuel, JP-1, Agricultural Diesel, Diesel #2, Home Heating Oil / Fuel Oil #4, or Home Heating Oil / Fuel Oil #6 may be sold and used for heating [43].

systems modeling is available in literature, but application to remote communities is generally limited especially in the Arctic.

The future development of energy systems in Northern communities is rife with uncertainties, and energy modelers should be able to capture this on a non-deterministic fashion. In majority of previous studies involving energy systems modeling, uncertainties are typically treated by performing sensitivity analysis for a given range of input parameters. This technique provides understanding of the uncertainty space and up to a certain extent, the future risks involved in understanding the complexities of an integrated energy system. However, this way of performing sensitivity analysis should be complemented with further investigation on the impact of uncertainties in a non-deterministic and more robust approach.

Ultimately, design strategies for sustainable energy systems in the North demand holistic approaches, as policy, technological development and complex energy systems are inherently intertwined. Most studies conducted for Arctic communities were focused on quantitative energy modeling without describing its real-world applications on the energy policy space, and how to address the trilemma of challenges relating to energy security, affordability and environmental sustainability. This multi-domain perspective along with the use of emerging energy modeling approaches will help inform decisions in balancing trade-offs from various energy solution viewpoints of different stakeholders in the North and remote communities in general.

1.5 Study objectives and research questions

Poelzer et al. [44] described the critical role of the Arctic region in the global transition towards carbon neutral forms of energy by transferring knowledge to other remote communities – within and beyond the bounds of the Arctic – than can use and build more sustainable energy systems of their own. Hence, the primary objective of this dissertation is to:

> *Chart feasible pathways towards sustainable and decarbonized energy systems by developing robust energy system model that captures a multi-domain perspective on key drivers influencing the evolving energy landscape in the Canadian Arctic and remote communities in general.*

Specifically, this work aims to address the gaps of previous studies undertaken for Northern remote communities by developing energy modeling frameworks that represent unique considerations of various stakeholders and practitioners in the territories of Canada. The methodology employed was a combination of highly participatory research methods through active consultations with the local community (via local partners) and the application of state-of-the-art modeling techniques for energy systems integration.

Relative to the previous and recent studies done for the Canadian Arctic, several research gaps are identified and the primary research objective is established. In addition, the following research questions will guide the intended research outputs of this PhD work:

1. How to integrate multiple and conflicting solution philosophies in designing/modeling energy system among remote communities?

2. How can electricity generation alternatives be effectively integrated in the Northern communities of Canada?
3. How can electricity and heating generation systems be effectively linked into one integrated energy system?
4. What heating alternatives will be viable in the North while considering flexibility of integration for current and future energy systems?
5. What low-cost initiatives are available to accelerate clean energy transformations in remote communities?
6. What are the trade-offs between optimal solutions in transitioning towards alternatives to diesel energy?
7. What are the socio-economic impacts of implementing new sustainable energy solutions in isolated Arctic communities?
8. How to effectively integrate uncertainties in energy systems modeling in the Arctic given energy resource variability and future climate change impacts in the region?
9. How do extreme temperature events impact battery (BT) storage operation in the Arctic region?
10. How to advance diesel reduction initiatives in Northern latitude communities while considering risks from multiple uncertainties?
11. How can private, government and non-government entities support Indigenous-led energy projects?

1.6 Key contributions

The primary contribution of this thesis is the advancement of the frontier of knowledge in energy systems planning among Northern remote communities. By establishing the connection between research, development and the implementation of state-of-the-art modeling techniques, risk and opportunities in the energy transition of Arctic communities were explored. In particular, the novel contributions of this work are listed below:

In Chapter 2,

1. Development of a multi-objective optimization framework that integrates complex trade-offs for Northern latitude community energy systems and other remote communities in general;
2. Robust simulation and optimization algorithms that can size components of a hybrid microgrid system while evaluating the impact of various operational strategies;
3. The baseline simulation results of the energy system model have been validated against widely accepted software HOMER;

4. A case study for Sachs Harbour, the Northernmost community in the NWT with extreme winter conditions has been completed, demonstrating applicability of the model to other Arctic and remote communities;

5. The utility of insights from a multi-objective algorithm have been demonstrated.

In Chapter 3,

1. Development of a time-series heat load building model coupled with the concurrent electrical load of Northern latitude communities;

2. Assessment of heat source alternatives such as ASHP and electric baseboard heaters while evaluating overall impact on the integrated energy system;

3. Demand side modeling incorporating a building enclosure-focused approach and overview of possible energy efficiency measures which are key in holistically addressing energy solutions in remote communities;

4. Dynamic simulation and optimization algorithms that can capture complex trade-offs in the energy system design space using the Multi-objective INtegrated Energy System (MINES) modeling framework;

5. Formulation of a community-scale energy trilemma index model using outputs from the multi-objective algorithm which can holistically encapsulate various energy solutions and viewpoints relevant to policy makers and stakeholders in remote communities.

In Chapter 4,

1. Development of a robust Multi-objective INtegrated Energy System (MINES) model that captures decision-maker attitudes towards multiple overlapping uncertainties in designing integrated energy systems;

2. Assessment of lead acid and lithium-ion BT storage systems while taking into account impacts of BT capacity decrease from freezing temperatures in cold climate settings;

3. Adaptation of holistic energy solutions in transitioning towards robust and sustainable energy systems while addressing trade-offs and uncertainties in reducing diesel dependence;

4. Formulation of insights and recommendations on how to address barriers and opportunities in implementing strong energy policies and risk hedging strategies in remote communities.

1.7 Thesis outline

Following this introduction, the three main chapters of this thesis were introduced. Each chapter represents a journal publication which is either published or under review as shown in Table 1.3.

Table 1.3: Thesis outline and publication status summary.

Chapter	Title	Publication status
2	Exploring electricity generation alternatives for Canadian Arctic communities using a multi-objective genetic algorithm approach	Published in *Energy Conversion and Management*
3	Remote community integrated energy system optimization including building enclosure improvements and quantitative energy trilemma metrics	Published in *Applied Energy*
4	Towards robust investment decisions and policies in integrated energy systems planning: Evaluating trade-offs and risk hedging strategies for remote communities	Submitted and under review in *Applied Energy*

Chapter 2 builds from previous studies conducted by WWF for Canadian Arctic communities. The development of the MINES model was first proposed in this chapter. The functionality of the tool was demonstrated with a case study in Sachs Harbour, Northernmost community in the NWT. Various electricity generation alternatives were modeled in comparison with their current diesel-based system, while minimizing both levelised cost of energy and fuel consumption of the diesel generator. This chapter presents the first set of investigations where trade-off analyses have been proven to be relevant in capturing conflicting design objectives from various stakeholders in the North.

Chapter 3 extends the modeling framework developed in Chapter 2 by integrating both electric and heating sectors. Demand side modeling was also introduced in conjunction with the supply-side aspect of the integrated energy system. High-performance building enclosures were also assessed, together with some heating technologies (baseboard heater and air-source heat pump) that could be viable in the Arctic. Finally, community-scale energy trilemma index model was formulated to quantifiably assess holistic energy solutions determined through the multi-objective optimization approach of MINES. This trilemma model is an effective tool to communicate whether new policies are hindering or moving towards the desired position (in reference to the three axes), and what interwoven links between various stakeholders are needed to accelerate energy transitions for the community.

Chapter 4 expands further the modeling framework described in Chapter 2 and 3. In particular, multiple overlapping uncertainties were integrated in the energy model in order to inform energy policies and investment decisions for Indigenous communities in the North. Varying risk attitudes of decision makers towards uncertainties were also taken into account and demonstrated. Policies to enhance Indigenous-led energy projects, and how to promote synergies between various stakeholders in the North were highlighted in this chapter as well.

Finally, Chapter 5 summarizes the key findings of the previous chapters, and offers recommendations for future work.

Chapter 2

Exploring electricity generation alternatives for Canadian Arctic communities using a multi-objective genetic algorithm approach

This paper was published in **Energy Conversion and Management** journal:

M. R. Quitoras, P. E. Campana, and C. Crawford, *"Exploring electricity generation alternatives for Canadian Arctic communities using a multi-objective genetic algorithm approach,"* Energy Convers. Manag., vol. 210, no. April, pp. 1–19, Apr. 2020. Available online at: https://doi.org/10.1016/j.enconman.2020.112471

CRediT authorship contribution statement[1]

Marvin Rhey Quitoras: Conceptualization, Methodology, Software, Validation, Formal analysis, Investigation, Resources, Data Curation, Writing - Original Draft, Visualization, Funding acquisition

Pietro Elia Campana: Conceptualization, Resources, Writing - Review & Editing, Supervision

Curran Crawford: Conceptualization, Writing - Review & Editing, Supervision, Project administration, Funding acquisition

This chapter builds from previous studies conducted by WWF for Canadian Arctic communities. The development of the MINES model was first proposed in this chapter. The functionality of the tool was demonstrated with a case study in Sachs Harbour, Northernmost community in the NWT. Various electricity generation alternatives were modeled in comparison with their current diesel-based system, while minimizing both levelised cost of energy and fuel consumption of the diesel generator. This chapter presents the first set of investigations where trade-off analyses have been proven to be relevant in capturing conflicting design objectives from various stakeholders in the North.

[1]Refer to Appendix B for description

Abstract

Indigenous peoples in the Northern communities of Canada are experiencing some of the worst catastrophic effects of climate change, given the Arctic region is warming twice as fast as the rest of the world. Paradoxically, this increasing temperature can be attributed to fossil fuel-based power generation on which the North is almost totally reliant. At the moment, diesel is the primary source of electricity for majority of Arctic communities. In addition to greenhouse gas and other airborne pollutants, this situation exposes risk of oil spills during fuel transport and storage. Moreover, shipping fuel is expensive and ice roads are harder to maintain as temperatures rise. As a result, Northern governments are burdened by rising fuel prices and increased supply volatility.

In an effort to reduce diesel dependence, the multi-objective microgrid optimization model was built in this work to handle the complex trade-offs of designing energy system for an Arctic environment and other remote communities. The tool uses a genetic algorithm to simultaneously minimize levelised cost of energy and fuel consumption of the microgrid system through dynamic simulations. Component submodel simulation results were validated against an industry and academic accepted energy modeling tool. Compared to previous energy modeling platforms, proposed method is novel in considering Pareto front trade-offs between conflicting design objectives to better support practitioners and policy makers. The functionality of the method was demonstrated with a case study on Sachs Harbour, in the Northernmost region of the Northwest Territories. The algorithm selected a fully hybrid wind-solar-battery-diesel system as the most suited technically, economically and environmentally for the community. The robustness of the results was assessed by performing system failure analysis of the model results. Overall, the modeling framework can help decision makers in identifying trade-offs in energy policy to transition the Canadian Arctic and other remote communities towards more sustainable and clean sources of energy.

Keywords

Arctic environment; Energy model; Microgrid; Renewable energy; Optimization; Genetic algorithm

2.1 Introduction

More than 50 Indigenous remote communities in the Northern territories[2] rely exclusively on fossil fuels, predominantly diesel, as their primary source of electricity [9] as presented in Fig. 2.1 and Table 2.1. The communities are exposed to high energy costs and environmental vulnerabilities which are made worse by the changing Arctic environment. According to the Pembina Institute [45], remote communities in Canada collectively consume more than 90 million liters of diesel fuel every year for electricity generation. Out of the total amount, 59 million liters of diesel (Fig. 2.1) are transported to the North to serve the electricity demand of almost 100,000 Canadians of which 80% are Indigenous.

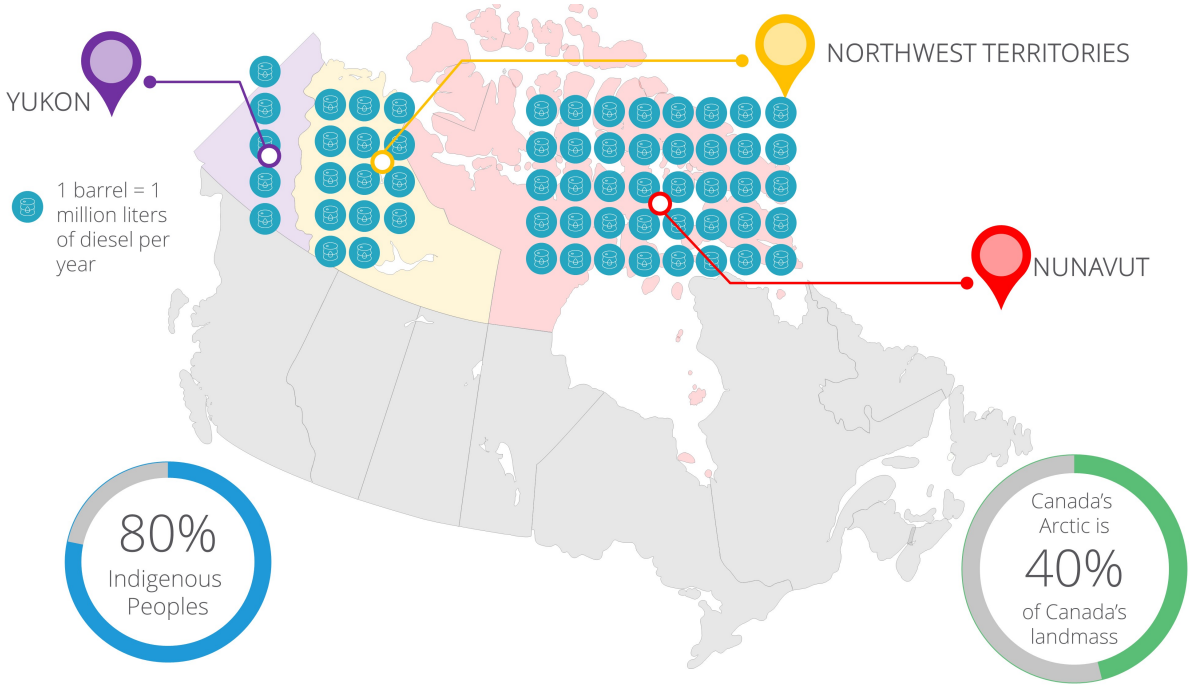

Figure 2.1: Diesel consumption in Northern territories of Canada. Data Source:Natural Resources Canada [6]

Canada's Arctic covers over 40% of the country's landmass and an area of growing importance internationally [7]. Both the federal and local governments are working together to reduce dependence on diesel as primary source of energy, in large part to their desire to lower emissions and contribute to Canada's commitment to the Paris agreement [46]. Further, decreasing the carbon footprint of the Canadian Arctic will introduce significant impact not just from a country perspective but on a global scale considering the continuous increase of air temperature in Northern latitude communities. The Arctic serves as a massive temperature regulator [3]; its white ice bounces heat back into the space. However, with shrinking Arctic sea ice extent caused by rising air temperatures[3], more heat can infiltrate in the earth's surface

[2]The North in Canada politically refers to the territories of Yukon, Northwest Territories (NWT) and Nunavut; its geographical location as compared to the rest of Canada can be seen in Fig. 2.1.

[3]The warming of Arctic air temperatures has been caused not only by the increase in greenhouse gas concentrations (from burning fossil fuels and other sources), but also the deposition of soot ice on Arctic ice [47].

Table 2.1: Number of remote communities in Northern territories with their corresponding primary sources of electricity generation [9].

Source	Yukon	NWT	Nunavut
Diesel	5	23	25
Hydro	16	9	0
Natural gas	0	2	0

and cause dramatic increases in warming in the world.

Protecting Canada's Arctic from oil spills is also one of the concerns of the government to lessen the environmental impact of shipping diesel. A significant amount of fuel never makes it to Northern communities but is lost to fuel spills during fuel transport and storage. According to Environment and Natural Resources Canada [48], roughly 9.1 million liters of diesel has been spilled in Nunavut and NWT since the 1970s, and more than 50% of the leaks are from trucks and storage tanks [16]. Further, the United Nation's International Maritime Organization [49] has stated that a single spill could have devastating and lasting effects on the fragile Arctic marine and coastal environments. The World Wildlife Fund (WWF) has been specifically studying the impact of oil spills in the Arctic [50].

To address energy issues, the Northern territories conduct regular Energy Charrettes to bring together representatives and energy experts to tackle challenges and identify energy solutions in the North [8]. Overall, affordability is the most important concern for Indigenous communities. This can be attributed to the high cost of electricity prices in the NWT and Nunavut as shown in Fig. 2.2(a). Households in these communities pay more than twice the Canadian average electricity price of 12.9 CND cents/kWh. Yukon, on the other hand, pays 13.6 CND cents/kWh which is closer to Canada's average price [11]. Hydropower is the primary source of electricity in Yukon while NWT and Nunavut is primarily diesel (Table 2.1) making those two regions the focus of the government in shifting to clean sources of energy. In Fig.2.2(a), the comparative residential electricity prices[4] for the three territories are subsidized by the government. Full costs, based on the first 1000 kWh consumed in winter during 2015, can be seen in Fig. 2.2(b) [9]. These subsidies have policy implication for every system transition.

Another significant issue in the North is the method of transporting fuel to the remote communities. Most fuels are shipped from Southern Canada [8] through ice roads and scheduled in bulk. However, this mode of transportation is increasingly unreliable due to climate change resulting in Canada's ice roads freezing later and melting earlier in the year [51]. As a result, most fuels are shipped by small plane, making electricity prices even more expensive, or via boats, which increases the risk of oils spills in the Arctic waters. All of these factors – rising electricity prices, fuel supply volatility, catastrophic warming of the Arctic at twice the global average rate [52], environmental emissions and the likelihood of oil spills – are driving the

[4]Territorial electricity prices in the graph are based on residential rates in the capital city of each territory: Yellowknife, NWT; Whitehorse, YT and Iqaluit, NU. Provincial prices reflect rates in major cities in each province: Vancouver, BC; Edmonton, AB; Regina, SK; Winnipeg, MB; Toronto, ON; Montréal, QC; Moncton, NB; Halifax, NS; Charlottetown, PE; and, St. John's, NL [11].

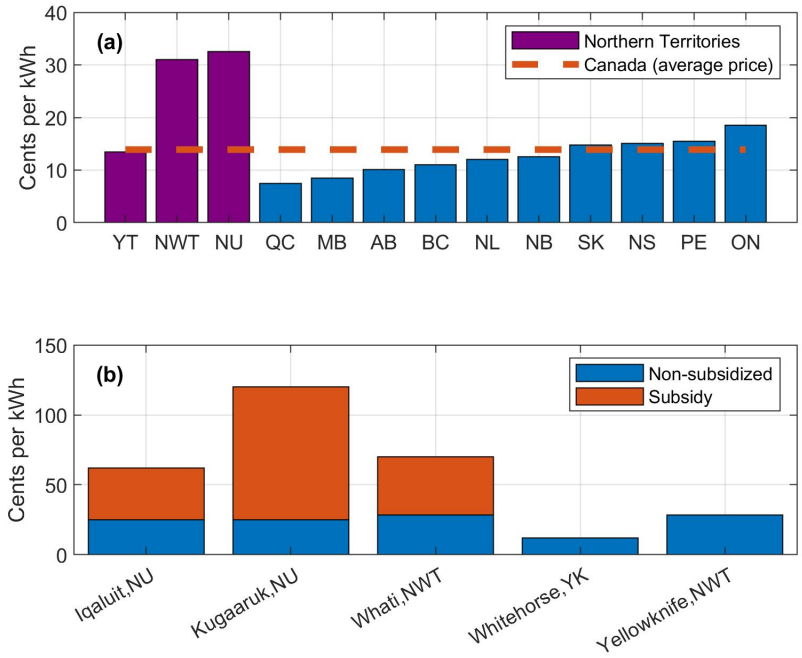

Figure 2.2: Electricity prices: (a) Representative territorial and provincial residential electricity prices in Canada[11] ; (b) Full costs of residential electricity rates in selected communities in the North [9]

Canadian government to unfreeze the renewable energy (RE) potential of its Arctic communities.

With this framing in mind, the motivating research question for this study is: ***How can electricity generation alternatives be effectively integrated in the Northern communities of Canada?***

2.1.1 Energy systems modeling

Energy systems modeling provides a tool to help answer this research question. Biberacher [32] defined a model as a simplified description of reality with the goal of highlighting certain relations and to make the best prediction of future developments possible. In the case of energy systems, Biberacher further described a model as a framework of relations encompassing the technical, economic and social aspects of a system under evaluation. The International Energy Agency also defined energy models as abstractions of reality that simplify the world into "bite sized" pieces in order to fit within certain sets of mathematical methods [33]. They vary in scale from local to global, in sector from electricity or transportation-only, to economy wide. These models are variously capable of simulating, optimizing, forecasting or even backcasting. They can be applied for academic purposes, to guide policy-making, or for investment planning of the private and government sectors.

WWF Canada completed the most recent feasibility study of RE technologies in the North [53]. Over a 25-year planning horizon, their investigations showed that the deployment of hybrid diesel-solar-wind-battery system would economically reduce diesel consumption in Northern remote communities. They used Hybrid Optimization of Multiple Energy Resources (HOMER) software [29] for the pre-

feasibility stage of their study and an in-house mathematical optimization model of RE integration based on a long term generation expansion planning approach during the feasibility phase. For both cases, they minimized Net Present Cost (NPC) in order to determine the most feasible configuration of the energy system. HOMER finds the most feasible configuration by applying a full factorial design of experiments and choosing the configuration with the minimum NPC. With its user-friendly interface, HOMER is probably the most widely used software in evaluating feasibility of microgrid systems.

Kim et al. [54] used HOMER in studying the feasibility of displacing a diesel generator (DG) as the only source of power for a tourist spot in the South China Sea, Malaysia. Results of their case study showed that a 20% reduction in NPC is available from solely using a DG versus having a Hybrid Renewable Energy System (HRES) composed of wind turbine (WT), solar photovoltaic (PV), converter (CONV) and back-up sources of power from DG and batteries (BT). Sen et al. [55] employed HOMER to meet the load demand coming from a residential, institutional, commercial, agricultural and small scale industry in India. The authors also presented post-HOMER analysis to discuss issues that might influence the realization of the optimal solution of their model.

HOMER has also been implemented to find the optimum sizing of a solar powered system to maintain water quality which impacts the fishery production system in Indonesia [56]. Additionally, Hafez and Bhattacharya [57] conducted four different studies using synthetic load generated from HOMER and resource data for Waterloo, Ontario, Canada. The study included diesel-only, a fully renewable-based, a diesel-renewable mixed, and an external grid-connected microgrid configuration. Montuouri et al. [58] dealt with the economic evaluation of a biomass gasification plant using HOMER while studying the integration of RE in microgrid coordinated with demand response resources. High profitability was demonstrated when using demand response to handle renewable variability. Lastly, Amutha and Rajini [59] examined growing energy demand among domestic, industrial, agricultural areas in a remote village in India through HOMER. The optimal options for RE based electrification were compared with the extended grid electricity distribution network for which the costs of extending lines to rural facilities were proven to be expensive.

A wide range of other modeling tools aside from HOMER, can be used in energy system design. There is already a large body of literature reviewing the features of various software-tools that can be used in simulating and optimizing an energy system. For example, interested readers are referred to the work of Tozzi and Jo [60], Ringkjøb et al. [61] and Connolly et al. [62] for broad and comprehensive analyses of various tools available to the energy modeling community.

Unlike the single objective function implemented in HOMER, Ming et al. [63] argued that the optimization of HRES should follow a multi-objective problem (MOP) approach for most cases. According to a study made by Konak et al. [64], MOP objectives are generally conflicting but they have to be considered simultaneously in describing complex engineering optimization problems. Thus, it is important to investigate a set of solutions versus a single solution (as is the case for conventional optimization techniques) while satisfying more than one objective function. Such solution diversity, as implemented through a multi-objective approach, is a research gap among recent energy studies done for the Arctic environment. This multi-objective approach of optimizing energy systems unlocks the full spectrum of

Table 2.2: Common objective functions in optimizing HRES according to literature.

Classification	Objective function	References
System reliability	Loss of Power Supply Probability ($LPSP$)	[65], [66]
	Loss of Load Probability ($LOLP$)	[38], [67]
System cost	Net Present Value (NPV)	[68], [69]
	Levelised Cost of Energy ($LCOE$)	[70], [71]
	Life Cycle Cost (LCC)	[70], [72]
Environmental	Fuel emissions	[63], [72]

solutions in the energy system design space.

Several examples of objective functions in solving MOP can be seen in Table 2.2. More detailed information of each objective can be found in the cited references; the specific objective functions used in this research work are further described in Sec. 2.2.1.1.

2.1.2 Research gap and study objectives

A research gap was identified in terms of addressing the complexity of designing energy systems for a unique environment like the Arctic. Decision makers study the Arctic from different viewpoints, thus, there exist multiple solution philosophies in exploring design alternatives that could work in Northern remote communities (to be discussed further in Sec. 2.2.1.1). Hence, the primary objective of this study is to extend the previous work of WWF by introducing a new modeling paradigm that can represent the complex trade-offs between priorities when designing an energy system for an Arctic community and remote communities in general. Since HOMER only considers NPC, it does not fully capture relevant aspects of the energy situation for Northern communities. This is also the case for WWF's in-house energy modeling tool, which is similarly based on NPC with an even simpler modeling treatment for its BT storage and a conventional dispatch strategy. Thus, the proposed method of this study aims to provide additional capabilities as compared to existing energy modeling platforms, and use the results to provide insights to policy makers in solving the *"trilemma"* of challenges relating to energy security, environmental emissions and energy economics.

Compared to previous and recent studies, the novelty of the present work is in developing a multi-objective optimization framework that captures complex trade-off in designing energy system for remote communities, while ensuring high power supply reliability with minimum impact to the environment and cost of living to the Indigenous peoples in the North. The tool is applicable beyond the bounds of the Canadian Arctic but its functionalities will be described through a case study while observing its relevance on an international perspective as well.

Relative to current energy trends and the research gap exposed in recent studies to capture trade-offs caused by the complexity of designing energy system within and beyond Arctic communities, the key contributions of this work can be summarized as:

1. Development of a multi-objective optimization framework that integrates com-

plex trade-offs for Northern latitude community energy systems and other remote communities in general;

2. Robust simulation and optimization algorithms that can size components of a hybrid microgrid system while evaluating the impact of various operational strategies;

3. The baseline simulation results of the energy system model have been validated against widely accepted software HOMER;

4. A case study for Sachs Harbour, the Northernmost community in the NWT with extreme winter conditions has been completed, demonstrating applicability of the model to other Arctic and remote communities;

5. The utility of insights from a multi-objective algorithm have been demonstrated.

The rest of the article is organized as follows. Section 2.2 describes the models developed for the study and Section 2.2.4 presents information regarding the specific Arctic community that was studied. Section 2.3 summarizes the results, with conclusions and future work given in Section 2.4.

2.2 Methods

The schematic diagram of a prototypical hybrid energy system studied in this work is presented in Fig.2.3. It consists of WT, solar PV, BT storage and back-up power from a DG. A bi-directional converter was also modeled so power can flow in both directions (DC bus to AC bus and vice versa). Each distributed energy resource (wind, solar and various sources of power generation and energy storage) can be modeled individually. However, with the proposed Multi-objective INtegrated Energy System (MINES) model in this study, a system-of-systems approach was employed wherein the constituent systems were brought together in one integrated microgrid system as presented in Fig. 2.3 and Fig. 2.4.

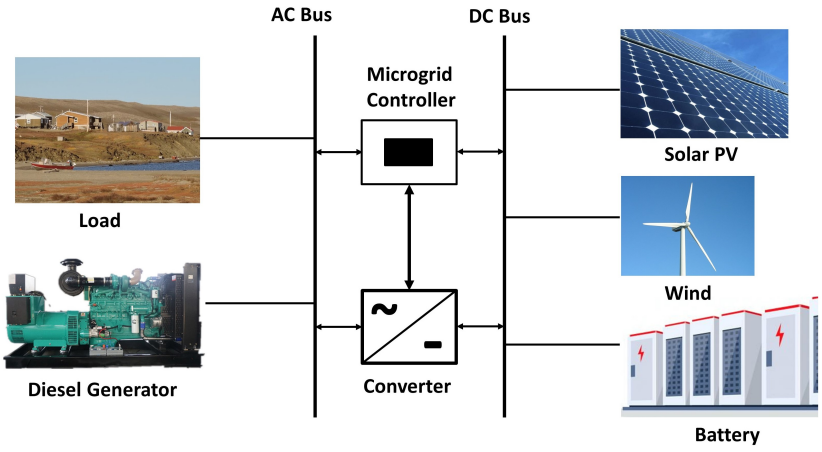

Figure 2.3: Schematic layout of a hybrid solar-wind-battery-diesel energy system.

2.2.1 Optimization module

A general constrained minimization problem may be written as follows:

$$\begin{aligned} \min_{x} \quad & f_s(x) && \mathrm{s} = 1, 2, ..., S \\ \text{s.t.} \quad & h_p(x) = 0 && \mathrm{p} = 1, 2, ..., P \\ & g_e(x) \leq 0 && \mathrm{e} = 1, 2, ..., E \end{aligned} \tag{2.1}$$

where x is the decision vector (set of variables to be optimized); $f_{\mathrm{s}}(x)$ is the objective function while $h_{\mathrm{p}}(x)$ and $g_{\mathrm{e}}(x)$ are the sets of equality and inequality constraints, respectively. The indices refer to the number of objective functions as well as the constraints of the model.

A genetic algorithm (GA) model has been developed to solve the optimization problem described in this study. It was first proposed by John Holland [73] and then widely utilized for optimization problems as popularized by Goldberg [74]. It is an optimization approach to determine the best outcome for a mathematical model following a certain set of constraints. Fig. 2.4 shows a flowchart of the GA as applied to modeling energy systems. It starts by inputting relevant information for the model such as load profile, meteorological data, equipment specifications and projected costs, among others; constraints were also added in the algorithm. The model generates initial set of individuals of a population randomly selected in each step of the algorithm which serve as basis for the next iteration [75]. The GA analyses random sizes of each component in the HRES while satisfying the load demand at each timestep. Each of the solutions in the population comprises a range of numbers called an individual, vector or chromosome [40]. After the first random configuration, the initial population set is evaluated based on the objective/fitness function defined in the model. This corresponds to minimizing costs, maximizing system reliability, and others. The three operators (selection, crossover, mutation) then come into play. The selection operator selects the predefined percentage of the initial population base on their fitness values [76]. The crossover operator generates new individuals by combining the information contained within a pair of parents with the goal of attaining higher fitness values. The process of looking for greater fitness values continues at each iteration and a mutation operator is needed to prevent the model getting stuck in a local minimum. Mahbub et al. [77] describes this concept as *"survival of the fittest"* ensuring that only the best individuals (solutions) have the chance to reproduce to the next generation. These new generations are produced in a loop until the termination criteria is met and the optimized solution is found.

Campana et al. [78] used GA as an optimization technique to find the best mix among power sources, storage systems and back-up sources of power while minimizing Life Cycle Cost (LCC) and maximizing power system reliability. Meanwhile, Konak et al. [64] provided an overview and tutorial of implementing a GA in an energy system model while describing its applicability in solving problems with multiple objectives. As well, Yang et al. [79] utilized a GA to optimally size a stand-alone hybrid solar-wind system with Loss of Power Supply Probability ($LPSP$) as their objective function. The decision variables included in their research were the number of solar PV modules, WT, slope angle of the PV array and the installation height of the WT. At the end of their case study, they found that a hybrid system with 3-5 days' battery nominal storage is suitable for the desired $LPSP$ of 1% and 2%.

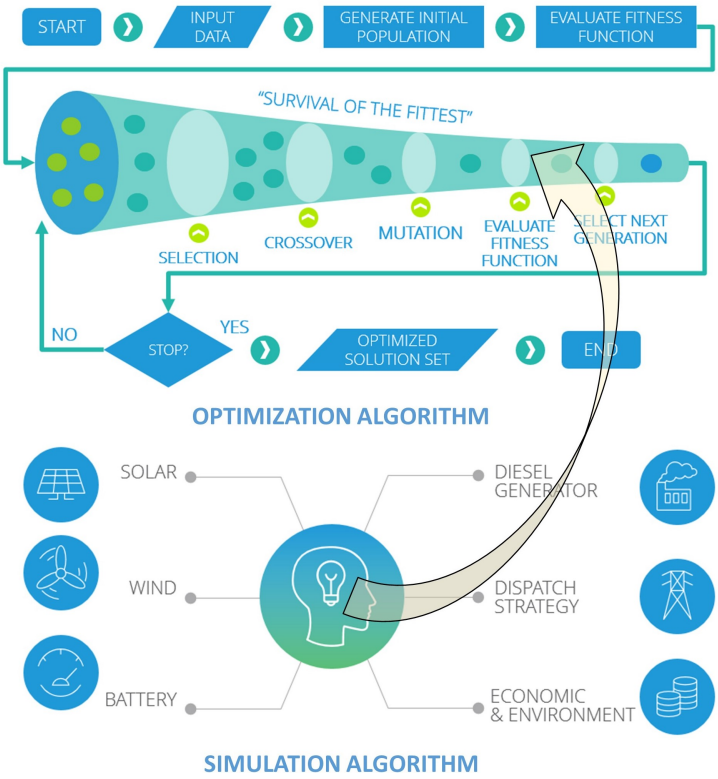

Figure 2.4: Flowchart of the optimization and simulation process.

For this study, the GA approach was implemented in a MATLAB® platform and the settings of the optimization parameters are listed in Table 2.3.

There are other optimization approaches that can be used in designing an energy system such as the classical optimization methods of linear programming or Mixed Integer Linear Programming (MILP). However, they are rarely used for multi-objective optimization functions and can only be applied to restricted types of problems due to non-linearities and other factors in real-world applications. Simplification of non-linear problems results in a lack of accuracy in the optimization process. In contrast, good performance for a wide range of different optimization problems is a significant advantage of GA [40]. It is commonly applied to solve different combinatorial optimization problems with a high number of feasible solutions that makes the application of MILP and other classical optimization methods

Table 2.3: GA configuration parameters.

Parameter	Description
Algorithm	Variant of NSGA II [80]
Generations	200
Population	100
Crossover function	Heuristic
Crossover rate(%)	90
Mutation function	Non-uniform
Tournament size	2

challenging [81]. Further, non-linearities of different variables, multiple objective functions and constraints can be handled effectively by GA. Most importantly, GA requires information only from the objective/fitness function since the algorithm does not require derivatives which is the conventional way of finding minimum or maximum of a certain optimization problem; hence, it is able to deal with various non-linearities which are present in designing complex energy systems. Furthermore, the computational time is relatively low as compared to other optimization methods [82]. Interested readers are referred to the work of Tezer et al. [40] for evaluation of various multi-objective optimization approaches for sizing components of stand-alone HRES.

2.2.1.1 Objective functions, constraints and other output parameters

Based on the previous Energy Charrettes among the territories, affordability is a major concern for Indigenous peoples in the North [83]. Thus, the first objective in the optimization process is to minimize the Levelised Cost of Energy ($LCOE$). As compared to previous studies with NPC as the only objective function, $LCOE$ was necessary for this work to better understand the cost impact in terms of the actual electricity price being paid by the community versus the subsidy support from the government. The typical $LCOE$ equation [84] was modified in order to consider the full spectrum of costs from the design to recycling (salvage value) stage as shown in Eq. 2.2.

$$LCOE = \frac{\sum_{t=1}^{n} \frac{CC_i(t)+O\&M_i(t)+Z_i(t)-S_i}{(1+r)^t}}{\sum_{t=1}^{n} \frac{P_{gen}}{(1+r)^t}} \tag{2.2}$$

where t is time (year); r is the discount rate (%); n is the total life of the energy system (year); CC is the capital cost ($) per unit of the system's component i; $O\&M$ is the operations and maintenance costs ($/year); Z is all other costs associated with the project ($/year); S is the salvage value ($); and P_{gen} is the power generated from the microgrid system (kWh/year).

The second objective is in line with Canada's goal to offset diesel [85] as the primary source of energy to remote communities. It was applied in the model by minimizing fuel consumption ($fuel_{cons}$) of the diesel generator. The mathematical equation involved is illustrated in Section 2.2.2.4 as part of the DG model.

The two objective functions arise from different stakeholders (community and policy makers) with varying solution philosophies to solve energy issues in the North. Power coming from the DG might be a cheaper option for the communities, but it degrades the Arctic environment. It might give energy security for remote areas but the risk of oil spills during fuel transport and storage will continue to be a concern for everyone living in the region. All of these competing factors can be effectively evaluated if they can be simultaneously considered and optimized in the model.

Various constraints were also implemented as part of the optimization algorithm. To consider energy security for example, $LPSP$ is set to 0%. An $LPSP$ of 100% means that the demand is never satisfied and an $LPSP$ of 0% means that the load is always satisfied. For instance, Nelson et al. [65] in their report, targeted an $LPSP$ of 0.0003 which corresponds to having a loss of power supply of approximately 1

day in 10 years. Other research work that implemented this technique can be found here [66], [86]. The mathematical expression of $LPSP$ over a given time period T (8760 h) can be written as:

$$LPSP = \frac{\sum_{t=1}^{T} P_{deficit}(t)}{\sum_{t=1}^{T} P_{load}(t)} \tag{2.3}$$

where $P_{deficit}$ pertains to the insufficient supply of power from the renewables and diesel, as well as the available energy from the BT storage:

$$P_{deficit}(t) = P_{load}(t) - (P_{RE}(t) + P_{DG}(t) + P_{batt}(t-1)) \tag{2.4}$$

where P_{load} is the electricity demand (kW);P_{RE} is the power produced by the renewables (kW); and P_{batt} is the power stored from the BT (kW).

The full set of constraints considered to run the optimization module of MINES are:

$$constraints \begin{cases} LPSP \leq 0\% \\ SOC_{min} \leq SOC(t) \leq SOC_{max} \\ RE_{pen} \geq 30\% \\ P_{excess} \leq 30\% \\ LCOE \leq 0.70 \frac{\$}{kWh} \\ DG_{LF} \geq 30\% \end{cases} \tag{2.5}$$

where SOC is the state of charge of the BT (%); RE_{pen} is the RE penetration (%); P_{excess} is the excess electricity (%); and DG_{LF} is the load factor of the DG (%). The 30% RE_{pen} target was based on the conservative assumption of including a portion of RE in the energy mix of the location being studied which is currently 100% diesel. The 30% P_{excess} was to avoid oversizing each component of the HRES. To establish a competitive price for the community as compared to their current price of electricity, an $LCOE$ limit of 0.70 CND $/kWh was imposed in the model, similar to the current price of Whati, NWT (Fig. 2.2(b)). The 30% DG_{LF} constraint was to avoid running the DG at partial load which is damaging for the generator and will be further discussed in Sec 2.3.1. The user can also change and add additional constraints in MINES or pick one objective function and formulate it as a constraint.

An example of an output parameter that can also be extracted from the model relates to the life cycle emissions of the system. Emission factors from Roberts et al. [42] were adapted for this study and it is shown in Table 2.4. As compared to considering the emissions from fuel only, a life cycle approach covers both direct and indirect emissions generated during the manufacturing, transportation and decommissioning stages from all components of the microgrid system.

In addition to $LCOE$, another economic performance metric was introduced in Table 2.11. The metric was parameterized as Life Cycle Cost (LCC) of the energy system. It served as one of the simulation outputs of the model to complement $LCOE$ and to capture the full cost of the system throughout its entire life cycle [40]. It is also the numerator of the modified $LCOE$ equation in Eq. 2.2.

Table 2.4: Emission factors in evaluating HRES [42].

Component	Indirect EF[a]		Direct EF[b]	
PV	0.059	$kgCO_2eq/kWh$	-	-
WT	0.02	$kgCO_2eq/kWh$	-	-
CONV	42.835	$kgCO_2eq/kW$	-	-
BT	59.42	$kgCO_2eq/kWh$	-	-
DG	454.293	$kgCO_2eq/kW$	2.64	$kgCO_2eq/L$
Diesel fuel	0.530	$kgCO_2eq/L$	-	-

[a] Emissions generated during the manufacturing, transportation and disposal stages.
[b] Emissions generated during the operation stage.

Table 2.5: Dimension of the discrete variables in the optimization algorithm.

Parameter	Value
WT quantity	0 - 500
WT capacity (kW)	95,95,100,100
PV quantity	0 - 500
PV capacity (kW)	15,25,20,25.025
BT quantity	0 - 500
BT capacity (kWh)	55,13.9,7.37,9.24
DG quantity	0 - 100
DG capacity (kW)	300,320,225,150
CONV quantity	0 - 10
CONV capacity (kW)	200,250,270,300
Operation strategy	LFOS and CCOS

2.2.1.2 Design optimization variables

The decision variables used for this research are divided into three groups. The first group of variables pertains to the individual capacity of all components of the HRES in Fig. 2.3 (solar PV, WT, BT, DG and CONV). The second group relates to the quantity of each component as listed in Table 2.5. The third group refers to the operation dispatch strategies of the integrated microgrid system. In total, there were 11 discrete decision variables carried out in the model.

2.2.2 Simulation module

The simulation module is part of the overall energy system model. Simulation results were evaluated per generation in MINES, in the form of fitness function on a one hour timescale over a year (Fig. 2.4). Community-scale models usually employ 1-hour temporal resolution on a one-year timeframe to size and investigate components of the energy system. Regional-scale models, on the other hand, use low temporal resolution (every 5 years or per decade) to capture a broader space in their study. One-hour temporal scale on a yearly basis is a common academic practice [42], [87] in sizing components of the microgrid system of a specific community. Increasing

the temporal resolution of the model will be too computationally expensive for the model to converge to a solution in a design relevant timeframe. For this reason, sensitivity analysis is implemented in this work in order to address uncertainties and to test the robustness of the results of the model.

The mathematical models of each subcomponent of the microgrid system will be discussed in the following subsections.

2.2.2.1 Solar Photovoltaic model

The amount of solar PV output is based on the resource potential of a given location which is parameterized by the Global Horizontal Irradiance (GHI). It pertains to the intensity of solar radiation striking the horizontal surface of the earth. This parameter has been translated to its corresponding radiation incident on the surface of the PV array (POA) by quantifying POA's three radiation components, namely beam radiation, reflected radiation, and diffuse radiation. Methods proposed by Duffie and Beckman [88] as well as Erbs et al. [89] were used at this point of the PV model. After identifying POA, the mathematical expression to quantify PV generation is then expressed as follows [90]:

$$P_{pv} = Y_{pv}\left(\frac{POA}{POA_{STC}}\right)[1 + \alpha_p(T_c - T_{c,STC})]f_{PV} \tag{2.6}$$

where P_{pv} is the power delivered by the PV array (kW); Y_{pv} is the rated capacity of the PV array (kW); POA_{STC} is the incident radiation at standard test conditions (STC) (1 kW/m^2); α_p is the temperature coefficient of power (%/°C); T_c is the PV cell temperature in the current timestep (°C); $T_{c,STC}$ is the PV cell temperature under STC (25 °C); and f_{pv} is the derating factor (%) which accounts for reduced PV output in real-world operating conditions.

The PV cell temperature (T_c) per timestep as described in Eq. 2.6 was accounted using the approach given in Eq. 2.7 [90].

$$T_c = \frac{T_a + (T_{c,NOCT} - T_{a,NOCT})\left(\frac{POA}{POA_{NOCT}}\right)\left[1 - \frac{\eta_{mp,STC}(1 - \alpha_p T_{c,STC})}{\tau\alpha}\right]}{1 + (T_{c,NOCT} - T_{a,NOCT})\left(\frac{POA}{POA_{NOCT}}\right)\left(\frac{\alpha_p \eta_{mp,STC}}{\tau\alpha}\right)} \tag{2.7}$$

where T_a is the ambient temperature (°C); $T_{c,NOCT}$ is the nominal operating cell temperature (NOCT) (°C); $T_{a,NOCT}$ is the ambient temperature at which NOCTis defined (20 °C); POA_{NOCT} is the solar radiation at which NOCT is defined (0.8 kW/m^2); $\eta_{mp,STC}$ is the maximum power point efficiency of PV under STC (%); and $\tau\alpha$ is the effective transmittance-absorptance product of the PV module valued at 0.9 according to Duffie and Beckman [88]. The PV parameters used in the simulation are shown in Table 2.6.

2.2.2.2 Wind turbine model

Jain [91] and Burton et al. [92] defined basic to complex concepts of modeling wind as applied to an energy system. The most fundamental approach to correlate wind

Table 2.6: Solar PV parameters used in the simulation.

Parameter	Unit	Values per technology type			
		1	2	3	4
Manufacturer	-	Generic	Schneider Electric	Schneider Electric	Huawei
f_{pv}	%	80	85	85	96
α_p	%/°C	-0.44	-0.41	-0.41	-0.41
$\eta_{mp,STC}$	%	14.70	17.30	17.30	17.30
Lifetime	years	10	25	25	25

speed and wind power is:

$$P_w(t) = \frac{1}{2}\rho_a A C_p u(t)^3 \eta_{gen} \tag{2.8}$$

where P_w is the output power of the WT (kW); ρ_a is the air density (kg/m^3), A is the rotor area (m^2); C_p is the power coefficient (%); u is the wind speed (m/s) at time t; and η_{gen} is the efficiency of the generator (%).

The extractable power output of the wind resource is influenced by the hub height of the turbine. In general, as hub height increases, wind speed increases as well (known as wind shear). The magnitude of wind shear differs per site and is dependent on factors like wind direction, wind speed and atmospheric stability. By determining wind shear, the modeler can extrapolate the wind speed or wind-power-density to other heights by using the following equations:

$$\begin{aligned} P_w(h) &= P_w(h_a)\left(\frac{h}{h_a}\right)^{3\alpha} \\ u(h) &= u(h_a)\left(\frac{h}{h_a}\right)^{\alpha} \end{aligned} \tag{2.9}$$

where $P_w(h)$ and $P_w(h_a)$ are power generated (kW) at hub height h (m) and anemometer height h_a (m), respectively, and α is the power law exponent (•); same analogy applies in terms of wind speed u (m/s).

Wind speed is a stochastic quantity. Thus, to model wind speeds, a statistical distribution, typically a Weibull distribution for hourly wind speed is needed. The distribution follows the function [92] given in Eq. 2.10.

$$F(u) = exp\left(\left(-\frac{u}{c}\right)^k\right) \tag{2.10}$$

where $F(u)$ describes the percent of time hourly mean speed exceeds u (%); c is a scale parameter (•); and k pertains to the variability about the mean (•). The relation of annual mean wind speed $\bar{U}$ and c is in Eq. 2.11.

$$\bar{U} = c\Gamma\left(1 + \frac{1}{k}\right) \tag{2.11}$$

where Γ is the complete gamma function (•).

Table 2.7: Wind turbine parameters used in the simulation.

Parameter	Unit	Values per technology type			
		1	2	3	4
Manufacturer	-	XANT	Northern Power	XANT	Northern Power
Rated power	kW	95	95	100	100
Hub height	m	38	37	31.8	30
Lifetime	years	20	20	20	20

Further to the theoretical extractable wind power in Eq. 2.8, the WT model for this study incorporated actual power curves from the turbine manufacturers and wind power was approximated using the piecewise interpolation function in Eq 2.12 [93].

$$P_w(u) = \begin{cases} P_{w,r}\frac{u^2-u_{ci}^2}{u_r^2-u_{ci}^2} & \text{if } u_{ci} < u < u_r, \\ P_{w,r} & \text{if } u_r < u < u_{co}, \\ 0 & \text{if } otherwise. \end{cases} \tag{2.12}$$

where $P_{w,r}$ is the rated power output of the WT (kW); u_{ci} is the cut-in wind speed or the speed where the turbine starts producing energy (m/s); u_{co} is the cut-out wind speed or the speed where the turbine stops operating (m/s); and u_r is the rated wind speed on which the rated power of the turbine is produced.

The wind turbine specifications used in the simulation are shown in Table 2.7 and their corresponding power curves are presented Fig. 2.5. The manufacturers of the chosen wind turbine types have extensive track records in Northern Canada and Alaska. The turbines have been proven to operate even in cold climate conditions. Finally, the actual power generated by the WT was calibrated by considering the variation of air density with a method adapted from [42].

2.2.2.3 Kinetic battery storage model

The energy storage model used for the study follows the Kinetic Battery Model (KiBaM) of Manwell and McGowan [94]. It is a two-tank model based on the approach of chemical kinetics. It assumes that the charge can be stored in two ways – either as immediately available or as chemically bound.

KiBaM requires determination of three parameters in order to describe the behavior of the lead acid BT: q_{max} is the maximum capacity of the BT (Ah); c_{BT} is the fraction of capacity that may hold available charge of the BT (•); and k_{BT} is the rate constant of the BT (•). Considering the nominal system voltage, the mentioned parameters were used in quantifying the respective maximum BT charge power (given $I_{c,max}$ in Eq. 2.13) and maximum BT discharge power (given $I_{d,max}$ in Eq. 2.14) per timestep.

$$I_{d,max} = \frac{-k_{BT}c_{BT}q_{max} + k_{BT}q_{1,0}e^{-k_{BT}\Delta t} + q_0 k_{BT}c_{BT}(1-e^{-k_{BT}\Delta t})}{1 - e^{-k_{BT}\Delta t} + c(k_{BT}\Delta t - 1 + e^{-k_{BT}\Delta t})} \tag{2.13}$$

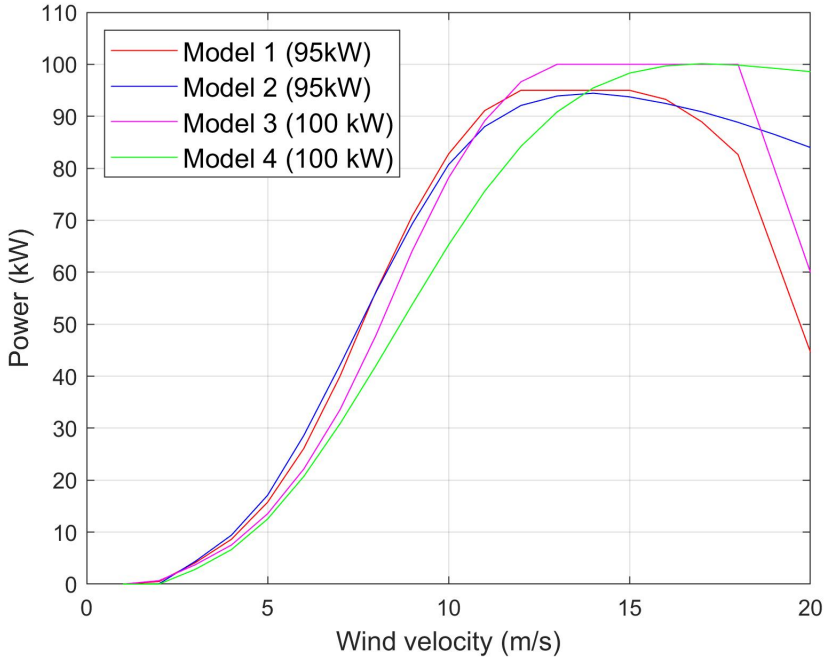

Figure 2.5: Power curves of the wind turbines used in the simulation.

$$I_{c,max} = \frac{k_{BT}q_{1,0}e^{-k_{BT}\Delta t} + q_0 k_{BT}c_{BT}(1 - e^{-k_{BT}\Delta t})}{1 - e^{-k_{BT}\Delta t} + c(k_{BT}\Delta t - 1 + e^{-k_{BT}\Delta t})} \tag{2.14}$$

where $q_{1,0}$ is the available charge at the beginning of the timestep (Ah) and q_0 is the stored energy. Meanwhile, the resulting available (q_1) and bound (q_2) charges at the end of every timestep were approximated by the succeeding equations.

$$q_1 = q_{1,0}e^{-k_{BT}\Delta t} + \frac{(q_0 k_{BT}c_{BT} - I)(1 - e^{-k_{BT}\Delta t})(Ic_{BT}(k_{BT}\Delta t - 1 + e^{-k_{BT}\Delta t})}{k_{BT}} \tag{2.15}$$

$$q_2 = q_{2,0}e^{-k_{BT}\Delta t} + \frac{q_0(1 - c_{BT})(1 - e^{-k_{BT}\Delta t}) - I(1 - cBT)(k_{BT}\Delta t - 1 + e^{-k_{BT}\Delta t})}{k_{BT}} \tag{2.16}$$

$$q_0 = q_{1,0} + q_{2,0} \tag{2.17}$$

where $q_{2,0}$ is the bound charge at the beginning of the timestep (Ah).

The model assumes the convention that the power surplus from the renewables will cause negative current indicating that the BT is charging and the power deficit will translate to a positive current leading to discharge of power from the BT. The simulation adapts the BT degradation (R_{BT}) model of HOMER. Mathematically, storage degradation is determined using the following equation with both use and

Table 2.8: Battery storage parameters used in the simulation.

Parameter	Unit	Values per technology type			
		1	2	3	4
Manufacturer	-	Generic	Rolls/Surrette	BAE Batterien GmbH	BAE Batterien GmbH
Nominal capacity	kWh	55	13.9	7.37	9.24
Nominal voltage	V	720	2	2	2
q_{max}	Ah	76.4	6950	3.68	4620
c_{BT}	-	0.927	0.267	0.369	0.355
k_{BT}	1/h	0.989	0.385	0.832	0.869
Roundtrip %	%	97	80	90	90
SOC_{min}	%	30	30	30	30
Q_{thrpt}	kWh/yr	240,000	19,434.10	7,728	9,744
$R_{BT,f}$	years	20	20	20	20

aging components:

$$R_{BT} = \begin{cases} \frac{N_{BT} Q_{LT}}{Q_{thrpt}} & \text{if } limited\,by\,throughput, \\ R_{BT,f} & \text{if } limited\,by\,time, \\ min\left(\frac{N_{BT} Q_{LT}}{Q_{thrpt}}, R_{BT,f}\right) & \text{if } limited\,by\,both. \end{cases} \tag{2.18}$$

where N_{BT} is the number of BT in the storage bank (•); Q_{LT} is the lifetime throughput of a single storage (kWh); Q_{thrpt} is the annual storage throughput (kWh/yr); and $R_{BT,f}$ is the storage float life (years).

The storage specifications used in the simulation model are listed in Table 2.8.

2.2.2.4 Diesel generator model

In various models [95], [96], a linear relationship is assumed between fuel consumption ($fuel_{cons}$) and the corresponding DG output. Mathematically, it is defined as:

$$fuel_{cons} = F_0 P_{DG,r} + F_1 P_{DG} \tag{2.19}$$

where F_0 is the fuel curve intercept coefficient (L/h/kW$_{\text{rated}}$); F_1 is the fuel curve slope coefficient (L/h/kW); $P_{DG,r}$ is the rated capacity of DG; and P_{DG} is the instantaneous power coming from the DG (kW).

The simulation parameters for the generator are presented in Table 2.9.

2.2.3 Operation strategies

Two operation strategies were implemented in the model: Load following (LFOS) and Cycle charging (CCOS). For both strategies, the generator only operates when the renewables cannot meet the load and the BT cannot discharge power. However, when the dispatch is in LFOS mode (Fig. 2.6), the generator produces just enough power to meet the instantaneous load per timestep unless it reaches the minimum

Table 2.9: Diesel generator parameters used in the simulation.

Parameter	Unit	Values per technology type			
		1	2	3	4
Manufacturer	-	Generic	Generic	Generic	Generic
Rated capacity	kWh	300	320	225	150
F_0	L/h/kW$_{\text{rated}}$	0.08145	0.08145	0.08145	0.08145
F_1	L/h/kW	0.246	0.246	0.246	0.246
c_{BT}	-	0.927	0.267	0.369	0.355
DG_{LF}	%	30	30	30	30
Lifetime	hours	15,000	15,000	15,000	15,000

power of the DG based on DG_{LF}. In CCOS, on the other hand, the DG runs at full rated capacity (Fig. 2.7) and will continue to operate and charge the BT up to a pre-set SOC (SOC_{sp}). Regardless of the operational strategy, any excess electricity production was assumed to be dispatched to a dummy load.

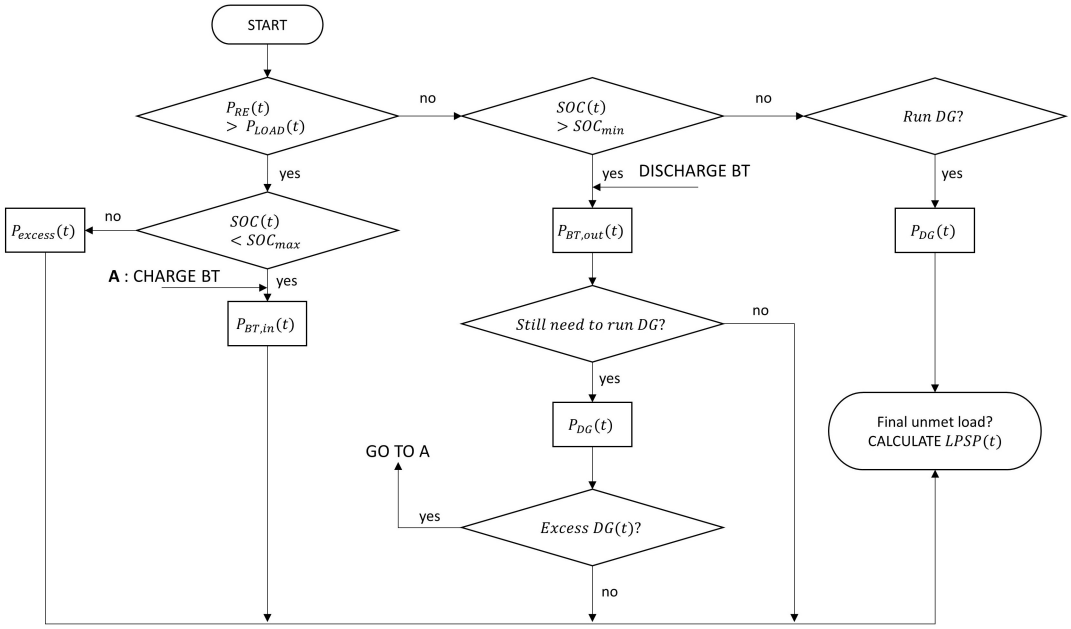

Figure 2.6: Flowchart of load following operation strategy.

Finally, to manage power flows from the DC bus to AC bus and vice versa, the simulation parameters for the converter listed in Table 2.10 were used.

2.2.4 Case study input data

The proposed method was applied to the Northernmost community in NWT: Sachs Harbour (Lat: 71.9884 N; Long: 125.23935 W). The community is located on Banks Island in the High Arctic as presented in Fig. 2.8. It has a population of about 130 and it is the ancestral territory of the Inuvialuit [97]. The community's main source of electrical power is diesel with a total generating capacity of 795 kW. The diesel generation facility is owned and operated by the Northwest Territories Power

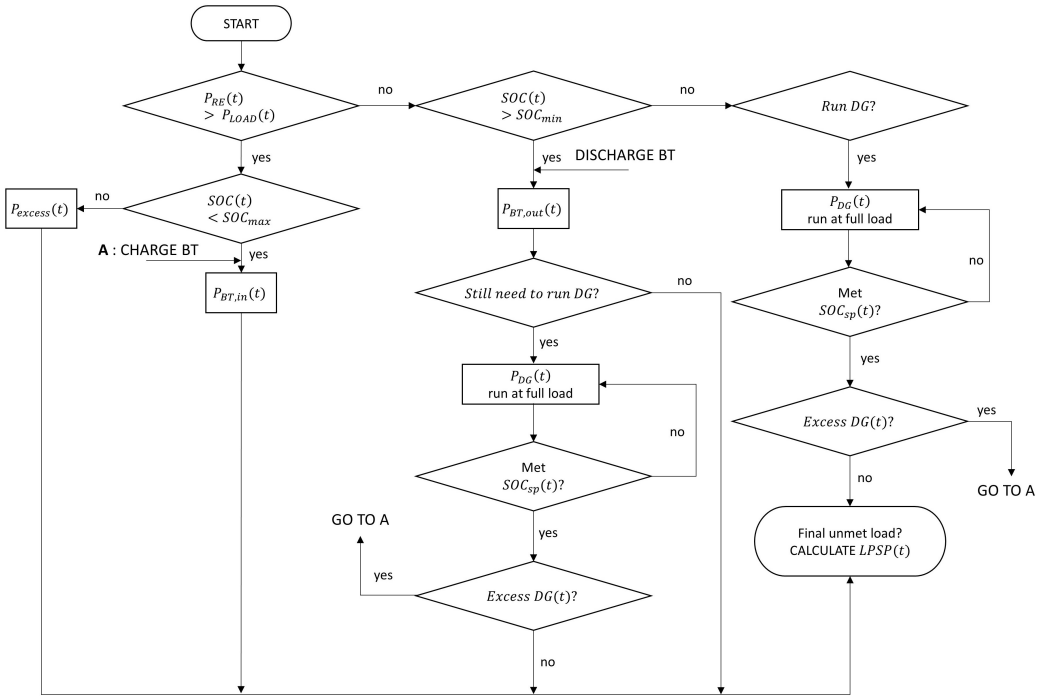

Figure 2.7: Flowchart of cycle charging operation strategy.

Corporation (NTPC). The fuel is shipped by Marine Transportation Services by barge once a year through NTPC's fuel service division. Since year-round road access to the community is not available, fuel is shipped via plane if the barge is unable to deliver the community's fuel.

Fig. 2.9(a) shows the hourly load profile of Sachs Harbour. The actual load data came from NTPC with a 15-minute temporal resolution for one year. The maximum and minimum loads are 220 kW and 70 kW, respectively. The average daily consumption profile for the different seasons is also shown in Fig. 2.9(b).

Actual wind tower measurements with a 10-minute temporal resolution were extracted from July 8, 2005 to September 29, 2009; data was requested for this study from the GNWT office. The data was initially used for the wind energy feasibility project done by GNWT. The wind meteorological instruments were located 6.5 km

Table 2.10: Converter parameters used in the simulation.

Parameter	Unit	Values per technology type			
		1	2	3	4
Manufacturer	-	Generic	Generic	Generic	Generic
Rated capacity	kW	200	250	270	300
Inverter %	%	95	95	95	95
Relative capacity [a]	%	100	100	100	100
Rectifier %	%	90	90	90	90
Lifetime	years	20	20	20	20

[a] Relative capacity of the rectifier in relation to the inverter .

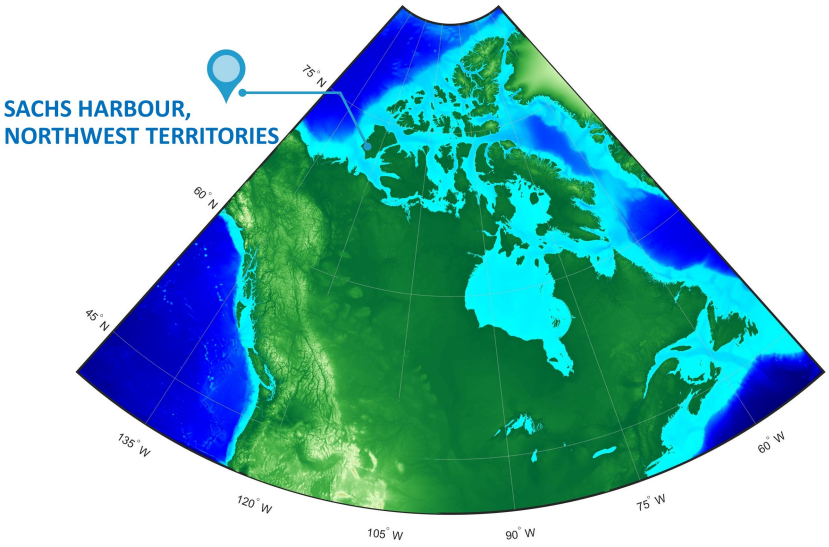

Figure 2.8: Geographical location of Sachs Harbour in reference to rest of Canada.

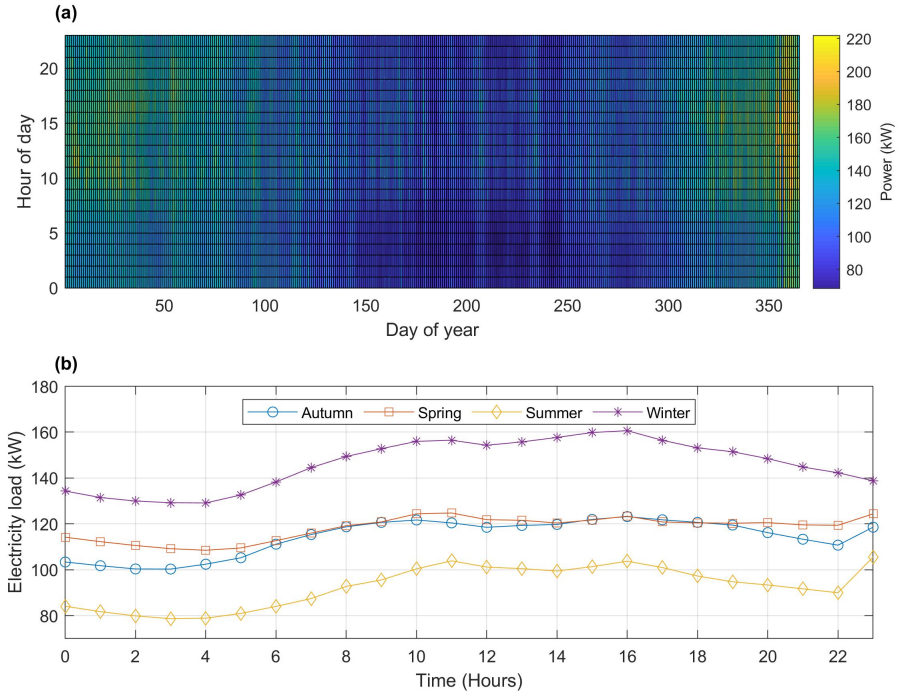

Figure 2.9: Electricity load consumption of Sachs Harbour: (a) Average hourly load profile for one year; (b) Average hourly load profile for the different seasons.

west of the Sachs Harbour airport along the main road. It was equipped with three anemometers and one wind vane at three measurement heights as presented in Fig. 2.10(a). The variations of the wind velocity every 10 minute at 30m height is also shown in Fig. 2.10(b). All anemometers used were NRG 40 model and the wind vane was a NRG 200P model. Fig. 2.11 shows that the dominant wind direction of the community is blowing from the southeast.

Actual wind shear was calculated from the three respective wind measurement heights and wind velocity was extrapolated at a 40m height according to the method

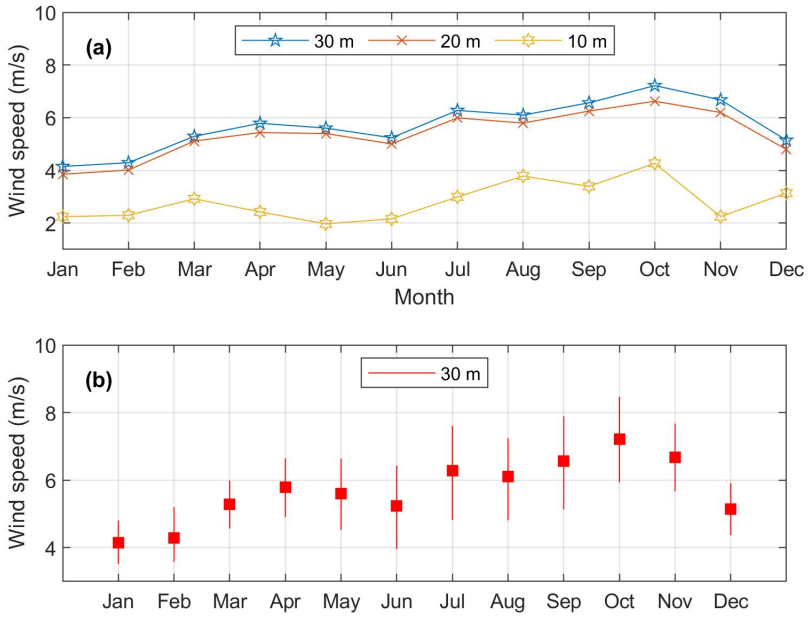

Figure 2.10: Wind speed profile of Sachs Harbour from July 8, 2005 to Sept 29, 2009: (a) Average monthly wind speed at three measurement heights; (b) Average monthly wind variations of wind speed recorded for every 10 minutes.

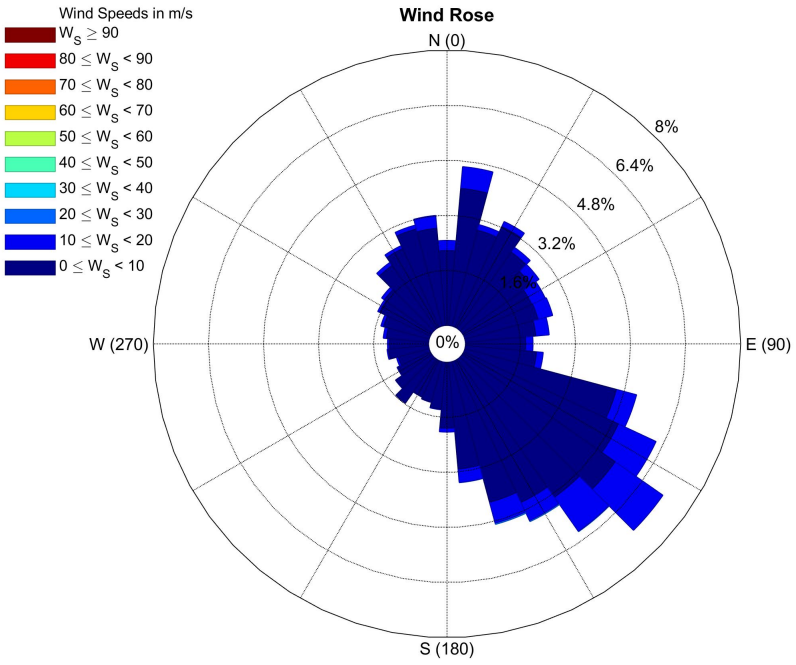

Figure 2.11: Wind rose profile of Sachs Harbour.

discussed in Sec 2.2.2.2. The resulting wind profile after the extrapolation is presented in Fig. 2.12, with its corresponding histogram and Weibull fit distribution shown in Fig. 2.13. High wind speed registries can be observed during autumn and the mean wind velocity for the year is around 8m/s at a 40m height.

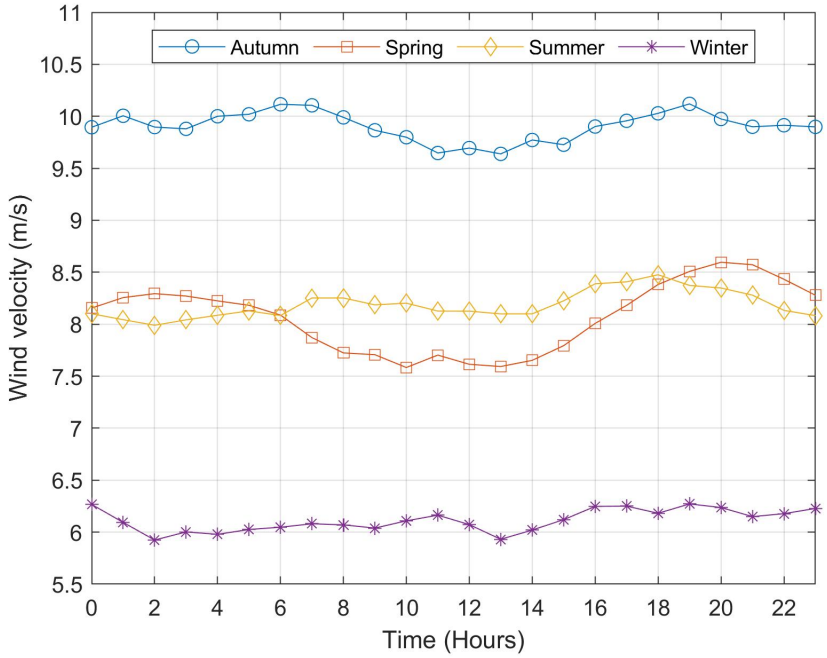

Figure 2.12: Average extrapolated wind speed of Sachs Harbour at 40m elevation for different seasons.

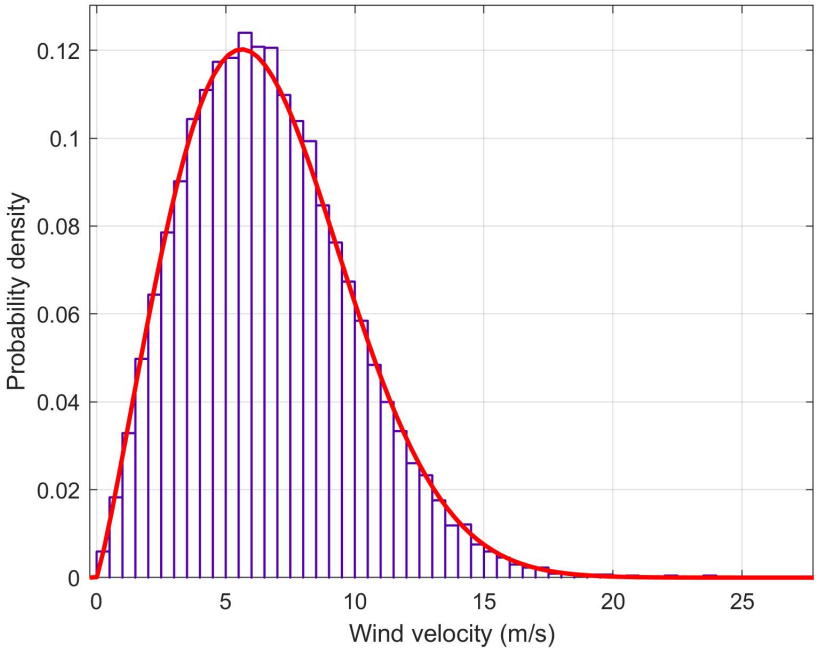

Figure 2.13: Histogram (violet bar) and Weibull fit distribution (red curve) of the extrapolated wind speed data at 40m elevation.

Other meteorological variables such as *GHI* and the community's temperature profile are shown in Fig. 2.14(a) and Fig. 2.14(b), respectively. The solar resource is low during autumn and winter due to extreme freezing temperature conditions. The data for *GHI* was extracted from GNWT's HOMER simulation file while the

temperature timeseries data was retrieved from Meteonorm [98].

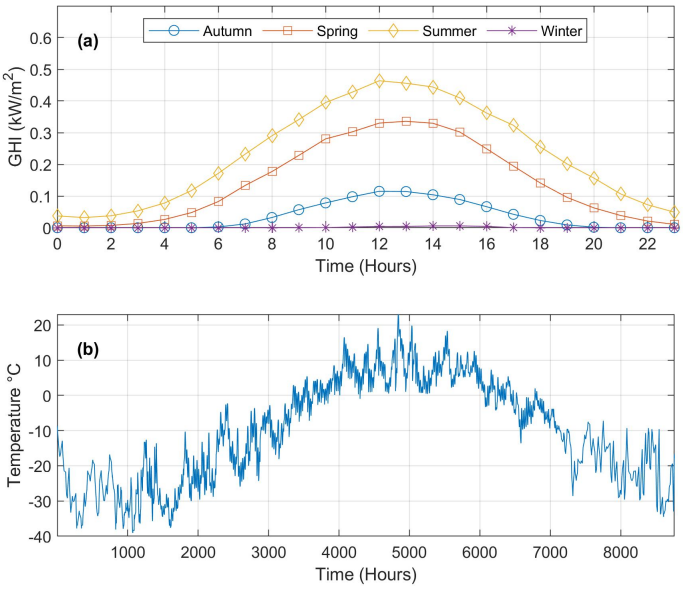

Figure 2.14: Other meteorological variables in Sachs Harbour: (a) Average hourly Global Horizontal Irradiance; (b) Hourly temperature profile for one year.

2.3 Results and discussion

This section presents the simulation and optimization results using the input data discussed in Sec. 2.2.4. The impact of the two operation strategies on the overall microgrid system was explored and sensitivity analysis was performed to investigate multiple system configurations that can be viable for Sachs Harbour. The robustness of the results was tested by modeling system component failure of each component of the hybrid system. Policy insights were framed considering various quantitative outputs extracted from MINES. At the end of this section, the results from the model were verified using an industry and academic accepted energy modeling tool, HOMER.

2.3.1 Optimization and simulation results

The optimized configurations of the energy system are shown in the form of a Pareto front in Fig. 2.15. The number of generations and population used to run the GA model is 200 and 100, respectively. Population size specifies the number of individuals in each generation. With a large population size, the GA analyses the solution space more thoroughly, thereby, reducing the chance that the algorithm is stuck in a local minimum versus the desired global minimum. However, a large population size also causes GA to run more slowly. As presented in Fig. 2.16, a wide range of values for the objective functions can be seen at the beginning of the optimization process but start to converge to a solution roughly at the 90th generation moving forward. This shows that MINES can no longer improve the $LCOE$ and $fuel_{cons}$;

thus, the solution has been attained. The total number of possible combinations given the constraints in Eq. 3.5 and the dimensions of optimization variables listed in Table 2.5 is 2.8613 x 10^{14}. The algorithm converged to a solution in roughly 3h using a Windows 10 computer equipped with a 64-bit operating system, an Intel Core i7-7700HQ 2.800GHz and 16 GB of RAM.

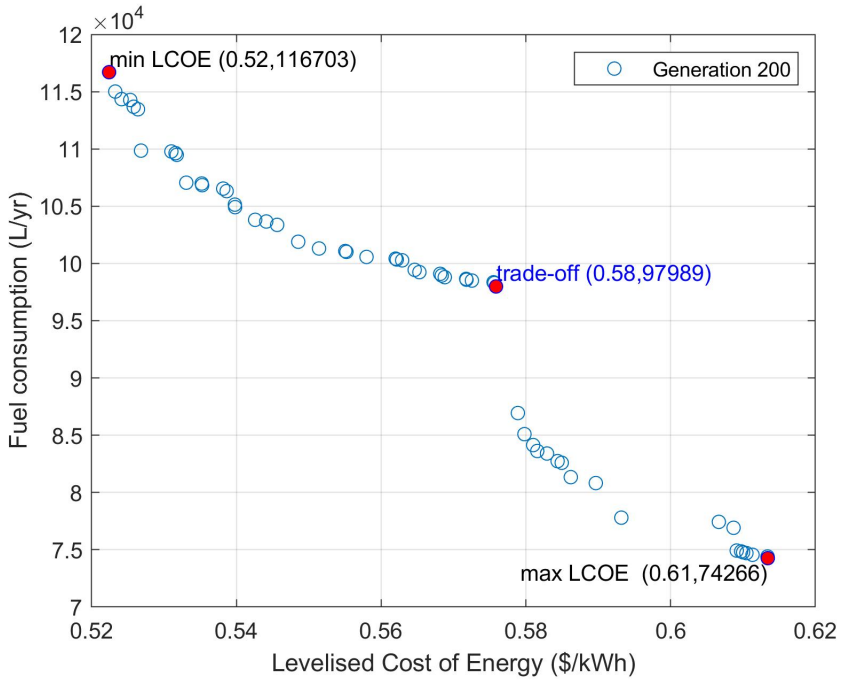

Figure 2.15: Pareto front of the last generation and the identified solutions of interest.

Solutions of interest from the Pareto front are highlighted in Fig. 2.15 and listed in Table 2.11. It can be observed that lowering $fuel_{cons}$ resulted in an increase in $LCOE$ which was attributable to limiting the operation of the DG and replacing it with RE technologies. The uppermost left red marker in Fig. 2.15 represents the solution with lowest $LCOE$ and highest $fuel_{cons}$. On the other hand, the lowest right red marker corresponds to a solution with the highest $LCOE$ and lowest $fuel_{cons}$. The red marker at the middle of the curve is considered a trade-off solution for both $LCOE$ and $fuel_{cons}$. The discontinuities in the Pareto front were caused by the discrete characteristics of the optimization variables (as discussed in Sec 2.2.1.2) and the restrictions imposed in the constraints of the optimization algorithm which were mainly to limit the vast search space of solutions.

The power generated by the WT is the highest among all other sources of energy in the system for the three solutions. This reflects strong wind resource in the region and a viable option specifically for Sachs Harbour. Due to extended winter conditions in the Arctic, the share of solar PV is minimal and unmet load has to be met by either DG or discharging the power coming from the BT. The variations of SOC for the three solutions is presented in Fig. 2.17. The SOC profile of each BT was influenced by the operational dispatch strategy of the system as discussed in Sec. 2.2.3. The flows of electricity from the DC and AC bus were also constrained by the selected 250 kW CONV of the system which is the same for all three cases.

As listed in Table 2.11, the algorithm selected CCOS as the most appropriate

Table 2.11: Configuration characteristics of the three solutions of interest determined from the Pareto front.

Parameter	Unit	Optimization results		
		Min. $LCOE$ and Max. $fuel_{cons}$	Trade-off Point	Max. $LCOE$ and Min. $fuel_{cons}$
PV	kW	100 (25kW x 4)	500 (25kW x 20)	175 (25kW x 7)
WT	kW	190 (95kW x 2)	190 (95kW x 2)	285 (95kW x 3)
BT	kWh	4,481 (9.24kWh x 485)	4,592 (9.24kWh x 497)	4,462 (9.24kWh x 483)
DG	kW	225 (225kW x 1)	225 (225kW x 1)	225 (225kW x 1)
CONV	kW	250 (250kW x 1)	250 (250kW x 1)	250 (250kW x 1)
Strategy	-	CCOS	CCOS	CCOS
P_{pv}	kWh	81,457	407,285	142,550
P_{w}	kWh	818,800	823,921	1,235,882
$P_{BT,out}$	kWh	396,062	322,482	274,602
$P_{BT,in}$	kWh	393,032	319,610	272,550
P_{DG}	kWh	356,400	299,250	226,800
$LPSP$	%	0	0	0
RE_{pen}	%	71.64	80.45	85.87
P_{excess}	%	9.14	26.08	29.94
$fuel_{cons}$	L/yr	116,703	97,989	74,266
CO_2[a]	$tCO_{2\text{-eq}}$/yr	770	736	646
CC	CND $	5,023,520	6,535,030	7,603,810
$LCOE$	CND $/kWh	0.522406	0.575872	0.61342
LCC	CND $	9,580,800	10,561,300	11,250,000

[a] Lifecycle CO_2 emissions of the energy system

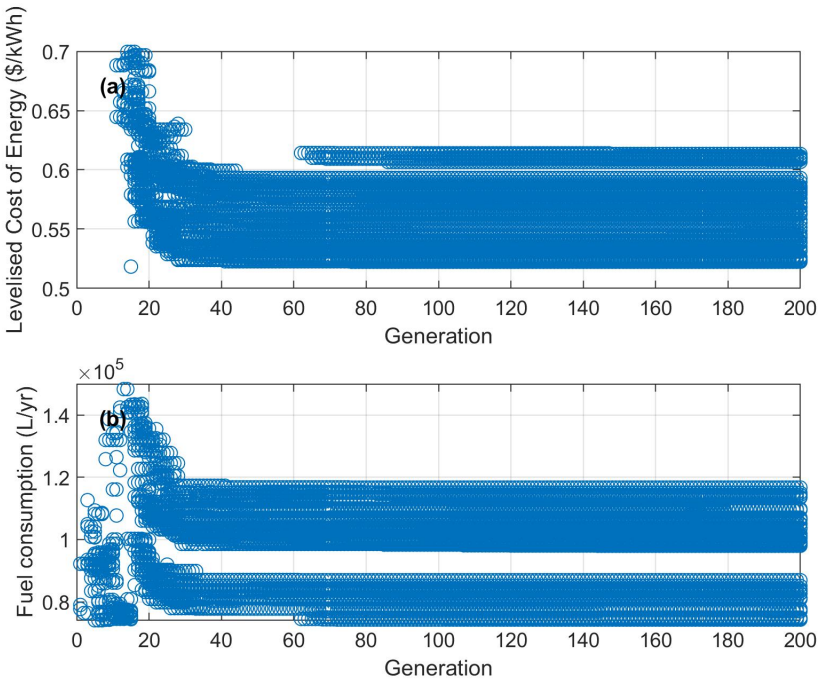

Figure 2.16: Variations of the objective functions during the multi-objective optimization process: (a) Levelised Cost of Energy objective function; (b) Fuel consumption objective function.

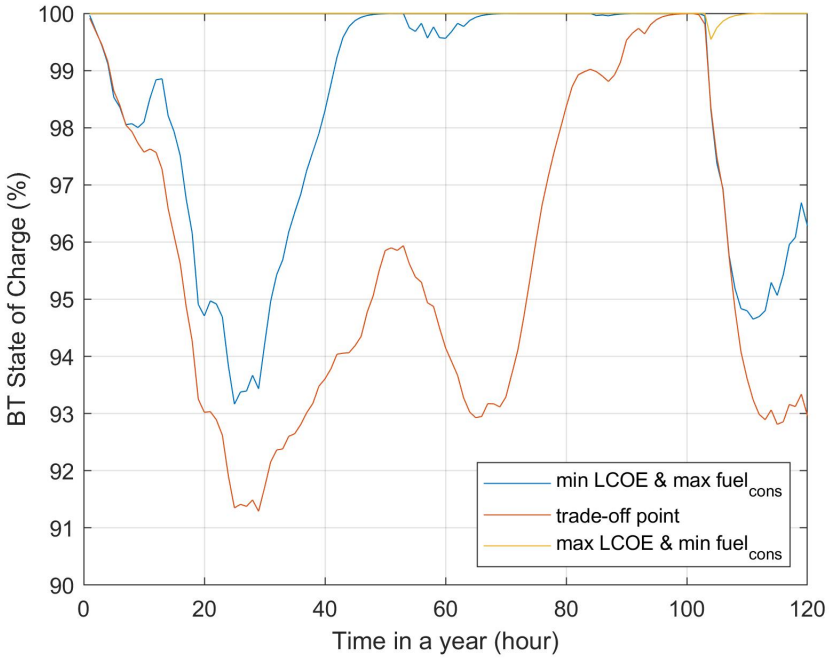

Figure 2.17: Performance variations of the state of charge of the BT for the three solutions of interest.

operation strategy for the three solutions. This shows that operating the DG uninterrupted in low power load mode can lead to higher fuel consumption resulting in higher oil residue in the engine as well. The residue has a negative impact on the

functional behaviour of the engine and it decreases the expected lifespan of the generator. As a result, operations and maintenance costs of the DG increase whenever it is being partially utilized.

The effect of modifying the operation strategies was evaluated by changing the power dispatch and running the model once again. In Fig. 2.18, it can be noticed how the Pareto front moved right after constraining the operation strategy to LFOS. From this behaviour, it can be inferred that the CCOS is a better option economically for the microgrid system. In other words, running the DG at full rated capacity is more favorable than running it based on the unmet load per timestep. In addition, the engine cools down when running the generator in low load mode. As a result, the fuel is partially burned which produces relatively higher hydrocarbon emissions as compared to running it at full load.

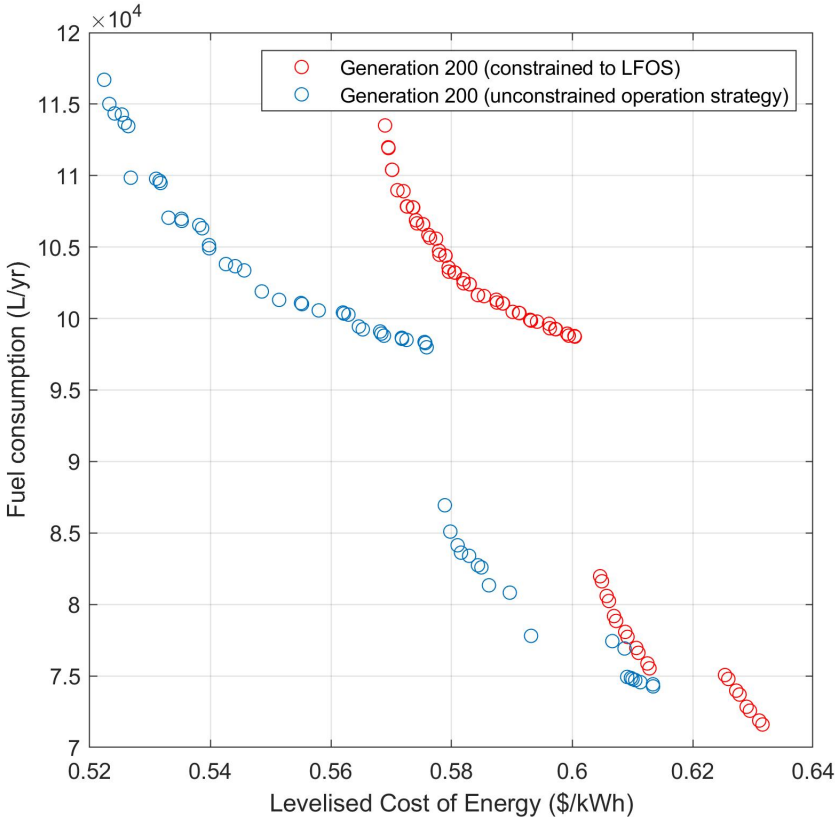

Figure 2.18: Plot showing how the Pareto front moved away from the unconstrained operation strategy to being limited to load following dispatch of power.

The energy mix of the system both hourly and monthly is presented in Fig. 2.19. For example, in a given year, it is possible that some of the load will be met only by WT or DG. Hence, for presentation purposes, a portion of the simulation results were selected where all available power sources were represented to show the actual variation of dispatch of power hour by hour. As expected, power output coming from the DG was higher during CCOS than LFOS (Fig. 2.19(a) and Fig. 2.19(b)) since the former was running at full load capacity until the pre-set SOC_{sp} of 80% was attained. The latter, on the other hand, dispatches exact power from DG based on the load not served by the renewables and BT. However, it can be observed that

regardless of the operation strategy (Fig. 2.19(c) and Fig. 2.19(d)), wind has a significant share in meeting the load demand of Sachs Harbour.

The pre-set SOC_{sp} of 80% is an input parameter in the model which is only applicable when the system runs at CCOS. The value was set to 80% in order to prevent the BT from spending at a low SOC level which helps the storage bank from being damaged. Further, this will reduce the number of times the DG starts (since it is always running at full load) and it will also limit the number of charge-discharge cycles of the BT .

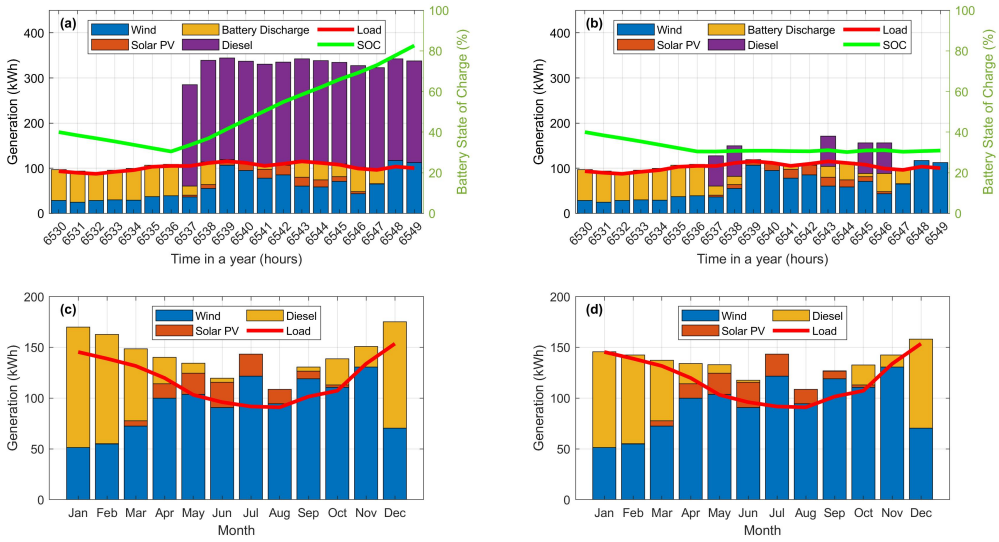

Figure 2.19: The solution with minimum LCOE and maximum fuel consumption was modified in terms of operation strategy to see the effect on the simulation results: (a) Hourly simulation results under Cycle Charging strategy; (b) Hourly simulation results under Load Following strategy; (c) Average monthly simulation results under Cycle Charging strategy; (d) Average monthly simulation results under Load Following strategy.

2.3.2 Design space sensitivity analysis

A sensitivity analysis was conducted by investigating other feasible energy system configurations for Sachs Harbour given the same optimization variables and restrictions implemented earlier in the study. Fig. 2.20 shows the location of each scenario in the Pareto space. Due to the currently available DG facility in the community and to seek realistic results, all configurations included DG and it was treated as a back-up source of power for the community along with the BT . Scenarios such as PV-DG, WT-DG and PV-WT-DG resulted in only one solution point on the Pareto front. As expected, a BT is required for RE integration. Multiple points, on the other hand, were determined to be feasible after running the optimization algorithm for PV-BT-DG and WT-BT-DG. The Pareto front of the original system configuration (PV-WT-BT-DG) was retained in order to compare other feasible cases. Configurations with multiple solution points in the Pareto space reflect more flexibility for the community in their decision making process relative to sizing and

designing each component of the energy system. The GA failed to find a feasible solution using DG as the only available source of power because of the restrictions given in the constraints and the goal of minimizing $fuel_{cons}$.

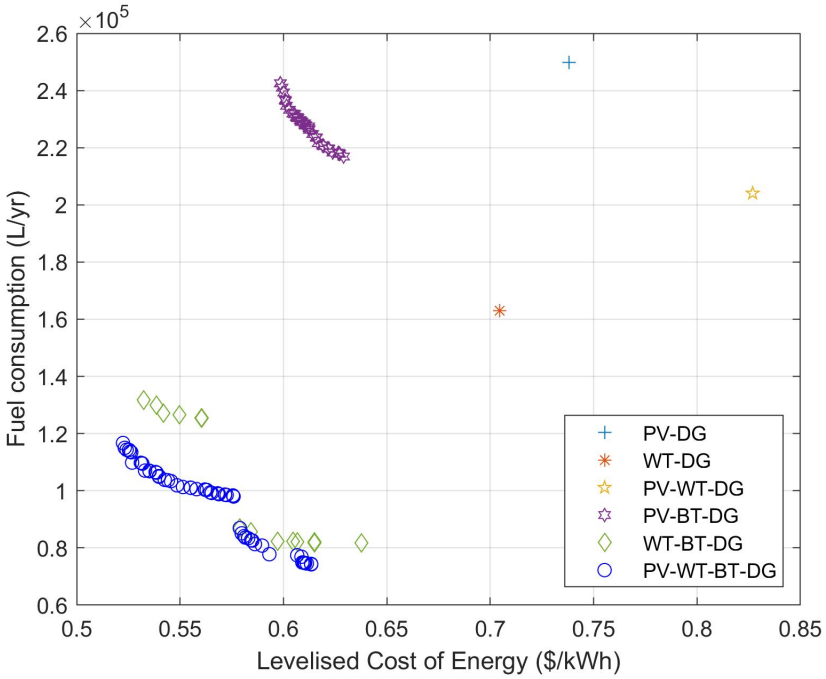

Figure 2.20: Pareto front of different scenario configurations.

Fig. 2.21 shows the annual generation of each scenario configuration and its corresponding emission reduction. Other performance metrics for each case are presented in Table 2.12 based on the lowest $LCOE$ of all possible combinations of various components of the hybrid microgrid system. For all scenarios, an $LPSP$ of 0% was imposed on the model to ensure load was met by either renewables, BT or DG; their optimal capacities are influenced by the range of the optimization variables in Table 2.5. Increasing the range of those variables translates to a wider search space and can add more time before the algorithm converges to a solution. For comparison with other scenarios, it was also assumed that a business-as-usual (BAU) case of DG with a capacity of 300 kW[5] was simulated in the model. Table 2.12 shows that the PV-WT-BT-DG hybrid system is the most suited energy system in the community of Sachs Harbour considering lowest values of its $LCOE$ and LCC. The proposed system has a significant amount of diesel fuel saved amounting to 353,407 L/yr in reference to the BAU scenario.

2.3.3 Optimal system complexity

As the optimal system is complex with all types of components present, analysis of system component failure based on the PV-WT-BT-DG hybrid system configuration was also simulated in MINES. This section also highlights the robustness of the optimal results against uncertainties caused by the renewables in the hybrid system.

[5]Sachs Harbour has a total generating capacity of 795 kW composed of three DG units with a capacity of 175 kW, 300 kW and 320 kW respectively. However, the generators are old (43-year-old plant) and they mostly run below 200 kW.

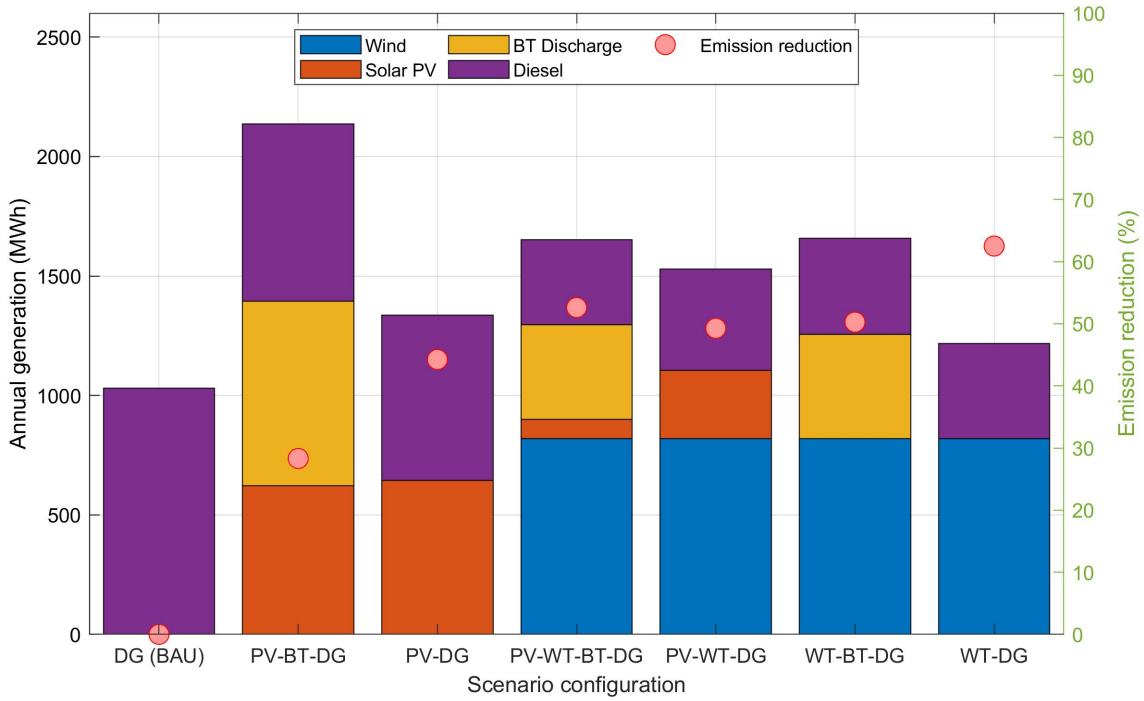

Figure 2.21: Annual power generation and projected emission reduction based on the lowest LCOE of each Pareto front of various system configuration.

Fig. 2.22 shows the resulting system's $LCOE$ and $fuel_{cons}$ if one component fails and the system has to continue operation to meet the demand. This reflects challenges with seasonal repair in the North. It was observed that the DG was critical to the overall performance of the microgrid, resulting in 27% $LPSP$ assuming it failed. Failure of all other system components (PV or WT or BT or CONV), on the other hand, would not affect the security of power supply ($LPSP = 0\%$) but resulted in an increase in P_{DG} and $fuel_{cons}$ to compensate for the unavailability of a system component as shown in Table 2.13. Due to the significant share of power produced by the two WT and assuming it both failed during system operation, the $fuel_{cons}$ would increase by 228% (382,895 L/yr) as compared to a no-failure-scenario of the hybrid system. Similarly, a failure of the microgrid's CONV would force all the renewables and the BT storage to shut down, requiring the DG to operate as the community's only source of power; this case has an estimated 255% increase (414,280 L/yr) of $fuel_{cons}$. Failure of the BT in the system resulted in 71% increase in $fuel_{cons}$ due to the unavailability of a storage device to store surplus power (to be discharged if there is power deficit in the system) forcing the DG to run more often. Due to the PV's minimal share in meeting the demand, the estimated increase in $fuel_{cons}$ if it fails is only 13% (132,028 L/yr).

Assuming all the components of the hybrid system are the same and one WT is in operation, the model estimated a 41% decrease in $fuel_{cons}$ from the 382,895 L/yr mentioned earlier. Meanwhile, $fuel_{cons}$ is almost the same after doubling or increasing the capacity of the BT storage along with one WT operating, due to the microgrid's designed power dispatch (CCOS). Under this scheme, the DG operates until the SOC_{sp} of 80% is attained. In effect, the majority of the power deficit from

Table 2.12: Projected annual diesel displaced and emission reductions with the lowest LCOE configuration in the Pareto front of each possible combination of the hybrid microgrid system.

System	Diesel displaced (MWh)	Diesel fuel saved (L)	Emission reductions ($tCO_{2\text{-eq}}$)	*LCOE* (CND $/kWh)	*LCC* (CND $)
DG (BAU)	-	-	-	1.11	20,357,700
PV-BT-DG	291	227,568	460	0.60	10,975,500
PV-DG	339	220,279	719	0.74	13,377,800
PV-WTBT-DG	675	353,407	854	0.52	9,580,800
PV-WT-DG	606	266,055	800	0.83	15,165,300
WT-BT-DG	629	338,303	816	0.53	9,765,020
WT-DG	632	307,138	1,015	0.70	12,900,300

the renewables was met by the DG instead of discharging the BT. The 220 kW peak load of Sachs Harbour and the 225 kW optimized capacity of the DG also affected this result.

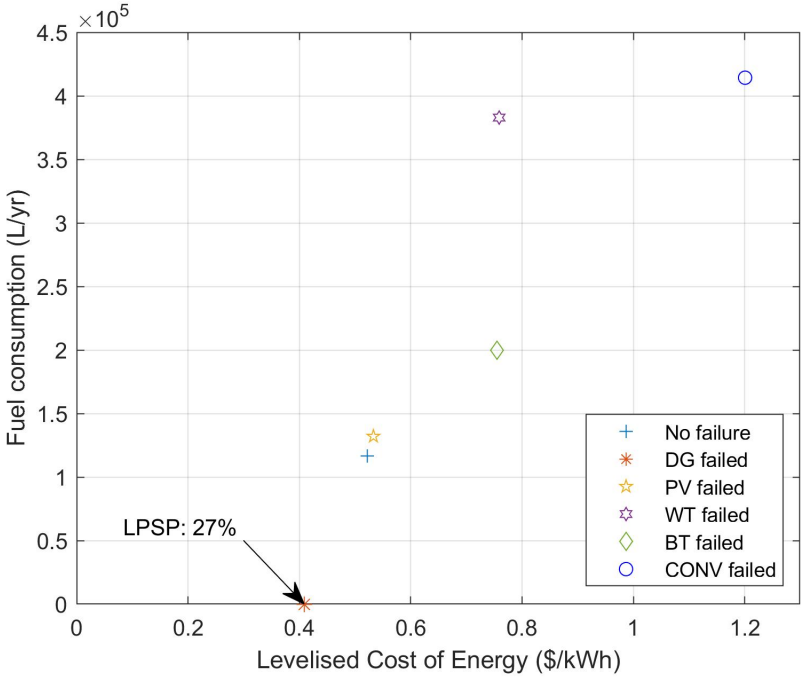

Figure 2.22: System component failure simulation of the fully hybrid (PV-WT-BT-DG) microgrid system.

2.3.4 Policy implications

Huntington et al. [99] argued that the purpose of energy modeling is to produce insights and not just numbers. Hence, this section provides policy insights that can be extracted from the analytical outputs of MINES. The proposed model can

Table 2.13: Impact of system component failure in the overall performance of the fully hybrid (PV-WT-BT-DG) microgrid system.

Cause of system failure	$LPSP$ (%)	$LCOE$ (CND $/kWh)	$fuel_{cons}$ (L/yr)	P_{DG} (kWh/yr)
No failure	-	0.52	116,703	356,400
DG	27.12	0.41	-	-
PV	-	0.53	132,028	403,200
WT	-	0.76	382,895	1,169,325
BT	-	0.75	199,753	444,362
CONV	-	1.2	414,280	1,031,471

guide decision makers in transitioning Northern communities of Canada to more sustainable sources of energy. Similarly, given specific inputs, the quantitative model outputs from the tool can be applicable as well even beyond the bounds of the Canadian Arctic.

As discussed earlier, MINES generates sets of feasible solutions, in the form of a Pareto front, by analyzing possible combinations of various energy resources including the BT storage. For example, as of writing, Sachs Harbour has been awarded 10M CND from the federal and territorial governments to replace its 43-year-old diesel facility by 2020 [100]. With MINES, the policy makers can be informed of the investment pathways in upgrading diesel facilities from other Northern communities or spending its money to advance RE projects in the Canadian Arctic region. With the multi-objective nature of the model, policy makers can weigh different priorities and targets (energy security, affordability, environmental impact) which vary per community in the North. Specifically, the Pareto front can give insights to the decision making process of policy makers in giving preference to certain solution over the other by analyzing trade-off points and its corresponding pros and cons.

Fig. 2.23 shows the projected savings in subsidizing fuel cost as compared to DG (BAU) and the proposed hybrid system (PV-WT-BT-DG). The full cost of energy using the DG to meet the demand is 111 CND cents/kWh which is comparable to the price of Kugaaruk, Nunavut in Fig 2.2(b). The full cost of energy for the hybrid system, on the other hand, is 52 CND cents/kWh as listed in Table 2.12. The green bar in Fig. 2.23 pertains to the actual electricity price charged to the consumers of Sachs Harbour which is at 28 CND cents/kWh. The orange bar represents the subsidy price covered by the government to pay the full cost of producing electricity. Assuming full implementation of the proposed hybrid system, the government can save 70% from its budget in subsidizing the electricity cost of the community. The savings can then be allocated in increasing RE investments in Sachs Harbour or other areas in the NWT. The savings were calculated in reference to the actual subsidy paid by the government instead of savings per household in order to avoid uncertainty caused by disaggregating the community load data.

Another policy application of the model is in terms of the carbon pricing scheme in the Canadian territories [101]. As a signatory to the Pan-Canadian Framework for Clean Growth and Climate Change, GNWT committed to meeting a federal benchmark for carbon price by 2019. With this context, MINES can also be a tool

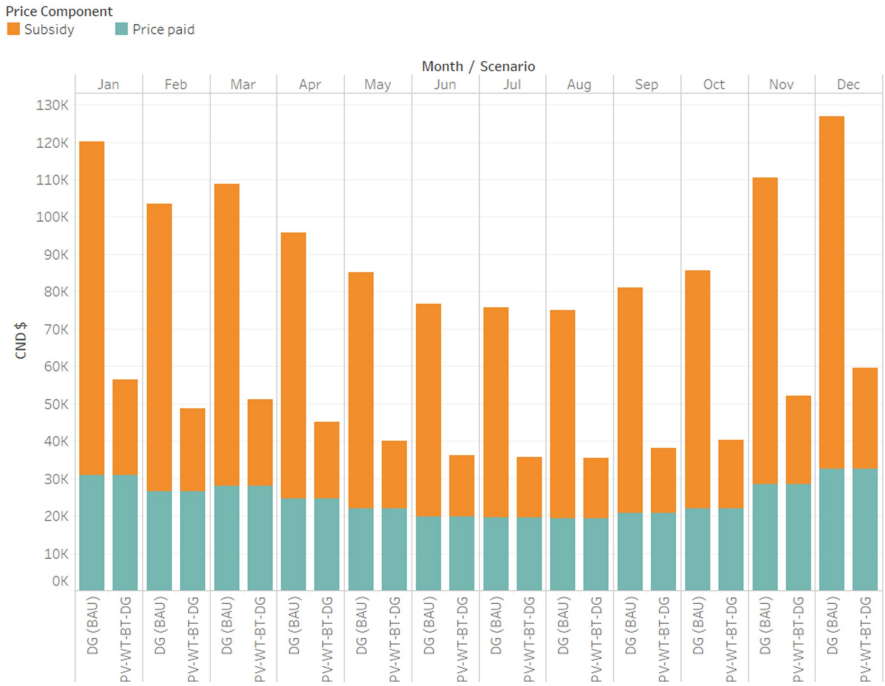

Figure 2.23: Comparative estimate of cost of energy for Sachs Harbour using diesel generator as its only source of power and the proposed hybrid microgrid system consists of wind, solar PV, battery storage and diesel generator.

in updating NWT's carbon price in the future to increase the penetration of RE while ensuring minimum impact on the cost of living in the Northern communities. This can be achieved by analyzing trade-offs between environmental emissions, cost of energy, energy security and other parameters that can be quantitatively analyzed by MINES.

2.3.5 Validation

The results of the model were validated using an industry and academic accepted energy modeling tool, HOMER. Since the presented multi-objective model and the full factorial optimization approach of HOMER are incomparable, the simulation results were analyzed instead.

The percentage error equation implemented in validating the results of the model is in Eq. 2.20.

$$\%Error = \frac{|HOMER - MINES|}{|MINES|} \tag{2.20}$$

For comparison, one point in the Pareto front in Fig. 2.18 was chosen. For example, the components of the solution with the lowest $LCOE$ under LFOS was extracted and simulated in HOMER. Results in Table 2.14 show that the difference is negligible between the two energy modeling tools. As well, it implicitly validates the optimization algorithm since the simulation process is linked to the GA as shown in Fig. 2.4. This validation proves that the model can be used in sizing individual components of the hybrid system on a more robust fashion. In addition, the multi-objective approach implemented in the study is more applicable in examining the

Table 2.14: Validation of simulation results with HOMER.

Parameter	Unit	Simulation results		
		HOMER	MINES	% Error
P_{pv}	kWh	138,053	138,136	0.06%
P_w	kWh	825,181	818,800	0.78%
P_{DG}	kWh	266,633	271,093	1.65%
P_{excess}	%	12.84	12.51	2.57%
$fuel_{cons}$	L/yr	111,426	113,439	1.77%
SOC[a]	%	568,955	570,632	0.25%
CC	CND $	5,179,598	5,179,600	0%
$LCOE$	CND $/kWh	0.57610	0.56998	1.06%
LCC	CND $	10,565,080	10,453,200	1.06%

[a] For the sake of comparison, SOC per timestep was summed up for one whole year and compared to HOMER.

complex trade-offs of priorities in designing energy system for an Arctic community or remote areas elsewhere.

2.4 Conclusions

In this work, a study was completed looking at alternatives in displacing diesel for power generation among Arctic communities in Canada. Solution diversity – as implemented in a multi-objective optimization approach – was established to be a research gap among recent energy studies done in an Arctic environment. Hence, MINES was proposed in order to investigate the complex trade-offs in designing a microgrid power system. A metaheuristic algorithm, specifically GA, was employed in the model as it can solve different combinatorial optimization problems and it can handle non-linearities as compared to classical optimization methods such as MILP which is rarely used for handling MOP.

Through GA, various components of the microgrid system were optimally sized. It was demonstrated with a case study on Sachs Harbour, the Northernmost region of the NWT. From the optimization process, a fully hybrid PV-WT-BT-DG-CONV has been proposed. The Pareto front confirmed the expected trend of the energy system: as $fuel_{cons}$ decreases, the system's $LCOE$ increases due to the integration of renewables and the BT storage, displacing diesel power in the energy mix. Three points on the Pareto front were analyzed focusing on solutions with minimum $LCOE$, maximum $LCOE$ and a point at the middle of the curve which was established to be a trade-off point. The three solutions of interest follow an $LPSP$ of 0% to ensure that the demand was met every timestep. A RE_{pen} above 70% was observed with wind having the largest share of power in the system. This reflects the excellent wind resource in the region and its technical viability.

The system with the lowest $LCOE$ in the Pareto front has a projected $LCOE$ of 52 CND cents/kWh versus an $LCOE$ of 111 CND cents/kWh for a diesel-only scenario (business-as-usual). The proposed hybrid system was also estimated to

displace 675 MWh/yr of energy from diesel and it save 353,407 L/yr of fuel. Power dispatch laws were also found to greatly affect the overall optimized system configuration, particularly the performance of the generator as a back-up source of power.

The robustness of the results of the model were investigated by performing system failure simulation of each component of the hybrid system. It was highlighted that the DG is the most critical component in the operation of the microgrid. Failure of all other system components, on the other hand, is not crucial in maintaining supply reliability ($LPSP = 0\%$) but will increase fuel consumption to compensate unavailability of other component in the microgrid to produce power. The results show that multiple system configurations are viable and the model giving more flexibility in the decision making process of the communities.

The application of energy modeling in giving insights to policy makers has been highlighted. With the proposed modeling tool, decision makers can weigh pros and cons in upgrading current diesel facilities in the North versus increasing their investments for RE projects in the future. For example, it was shown that the optimal HRES resulted in a 70% cost reduction in the government subsidy budget for the community of Sachs Harbour. Such savings can then be allocated to increasing the uptake of RE in the community for the future. Another potential policy application of MINES is in defining the appropriate carbon price in the NWT. The tool is also flexible beyond the specific energy situation for different Arctic communities. The objective functions, constraints and other variables in the model can be altered, and policy insights can be framed from the quantitative model outputs.

To justify reliability of the simulation results, the proposed model was validated against HOMER and negligible percentage error was found between the two tools. The validation also implicitly validated the employed GA approach since the simulation and optimization algorithms were interlinked in the discussed methodology of this research.

Overall, the proposed model constitutes a useful energy modeling platform in solving challenges relating to energy affordability, environmental emissions and energy security in the North and other remote communities within and beyond Canada. Ultimately, through research and community engagement that stem from critical empathy, respect and reciprocity, the energy model framework is capable of quantifying project risk and performance will be used to help Indigenous communities return to more harmonious coexistence with nature to ensure their continued economic viability and quality of life.

Chapter 3

Remote community integrated energy system optimization including building enclosure improvements and quantitative energy trilemma metrics

This paper was published in **Applied Energy** journal:

M. R. Quitoras, P. Elia, P. Rowley, and C. Crawford, *"Remote community integrated energy system optimization including building enclosure improvements and quantitative energy trilemma metrics,"* Appl. Energy, vol. 267, no. March, p. 115017, 2020. Available online at: https://doi.org/10.1016/j.apenergy.2020.115017

CRediT authorship contribution statement[1]

Marvin Rhey Quitoras: Conceptualization, Methodology, Software, Validation, Formal analysis, Investigation, Resources, Data curation, Writing - original draft, Visualization, Funding acquisition

Pietro Elia Campana: Software (Heat load model), Writing - review & editing, Supervision

Paul Rowley: Conceptualization, Resources, Writing - review & editing, Project administration, Supervision

Curran Crawford: Conceptualization, Writing - review & editing, Supervision, Project administration, Funding acquisition

This chapter extends the modeling framework developed in Chapter 2 by integrating both electric and heating sectors. Demand side modeling was also introduced in conjunction with renewable energy options. High-performance building enclosures were also assessed, together with some heating technologies (baseboard heater and air-source heat pump) that could be viable in the Arctic. Finally, community-scale energy trilemma index model was formulated to quantifiably assess holistic energy solutions determined through the multi-objective optimization approach of MINES.

[1]Refer to Appendix B for description

Abstract

Design strategies for sustainable energy systems in remote communities require holistic approaches, as policy, technological development and complex energy systems operation are inherently intertwined. The present work takes a multi-domain perspective in which various energy solution philosophies co-exist. In particular, a multi-objective energy system model has been developed to determine the optimal configuration of integrated electrical and thermal energy systems for Sachs Harbour, the Northernmost community in the Northwest Territories of Canada. From the four scenarios implemented in the model, the Pareto front curves show that the fuel consumption can vary from 0 – 700,000 L/yr while the cost of energy is in the range of 0.5 – 2.7 CND $/kWh. Further, a comparative dynamic simulation has been carried out to analyze the impacts of using electric baseboard heaters versus air-source heat pumps. The results indicate that load fluctuations caused by the variations of the heat pumps' coefficients of performance negatively impact the operation of the energy system. These demand fluctuations result in a larger battery storage requirement, along with an increase in overall energy system costs. Building enclosure improvements alone were found to reduce space heating loads by up to 40%. Finally, nine solutions of interest from the Pareto front were quantified and tested in the energy trilemma index model. From the multiple viable configurations, the proposed solution was estimated to have a weighted average trilemma score of 73.3. Overall, the use of such innovative modeling approaches in real-world applications can support policy makers to make informed decisions in balancing trade-offs from various energy solution viewpoints.

Keywords

Energy system optimization; Air-source heat pump; Integrated energy system; Energy trilemma; Fuel poverty; Building enclosure

3.1 Introduction

The diversity of Arctic jurisdictions, spanning unique geographical locations from central municipalities to very isolated communities, and the predominant reliance upon obsolete diesel infrastructure play pivotal roles in the energy situation of Canada's North[2] today [5]. Arctic communities have a critical dependence on energy services – heating, transportation, and electricity – for their safety, sustainability, and economic growth [43]. For decades, fossil fuels (mostly diesel) have been the primary source of energy in the territories of Canada as they are not connected to the North American electricity or natural gas grids. This situation exposes the Indigenous peoples and other Canadians living in the North to high energy costs and environmental vulnerabilities which is exacerbated by rapid ongoing climate changes in the region. Also, traditional transportation modes including winter roads are now increasingly unreliable because of the rising Arctic temperatures which impact access to reliable fuel sources. As a result, energy prices for households in Nunavut and the Northwest Territories (NWT) pay more than 30 CND cents/kWh (even after subsidy) for their electricity bills which is three times higher the national average electricity price [11] as presented in Fig. 3.1.

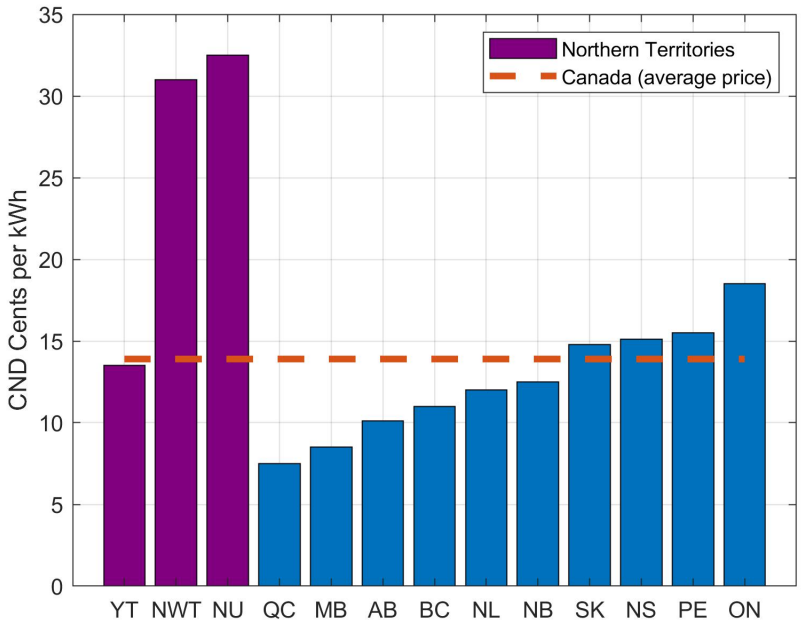

Figure 3.1: Household electricity prices in major cities for each province and territory (after subsidy) in 2016; data from National Energy board of the Government of Canada [11].

Poelzer et al. [44] described the Arctic as a region that can play a critical part in the global transition to carbon neutral forms of energy by transferring knowledge to other remote communities that can use and build more sustainable integrated

[2]The North in Canada politically refers to the territories of Yukon, Northwest Territories (NWT) and Nunavut; the use of the term Canada's Arctic for this work is inclusive of the three territories mentioned.

energy systems of their own. Hence, this research adopts a community in Northern Canada as a case study of the developed energy modeling framework and highlights the potential of the Arctic from a global perspective. As a country with more than 40% of its landmass belonging to the Arctic region [7], Natural Resources Canada [102] launched its Indigenous Off-diesel Initiative program to support Indigenous communities in developing and implementing ambitious plans to reduce diesel use for heat and power.

3.1.1 Overview of the energy situation in the North and various energy system modeling approaches

The Northern territories are facing energy challenges unique in Canada: high rates of fuel poverty[3], volatile fuel prices (both for heating and electricity), increased risk of fuel oil spills during fuel transport and storage, catastrophic rise of Arctic temperatures at twice the global average rate [103], and the financial burden of significant government subsidies for energy costs. These challenges leave the communities exposed to various risks. For example, during the summer of 2019 in Paulatuk, NWT, the annual diesel barge did not arrive because of extreme fall ice conditions that shut down marine traffic through the area. The territorial government had to fly-in 600,000 litres of diesel to the community of 265 people to keep the mostly obsolete diesel generators running. This operation cost $1.75 million CND over dozens of flights [16].

Recent studies have explored accelerating implementation of diesel alternatives and other energy solutions in the Arctic. Along with other organizations, the World Wildlife Fund (WWF) is at the forefront of assessing techno-economic feasibility of various low carbon technologies for the region. For instance, a two-step procedure was applied in the pre-feasibility stage of the WWF study [30]. First, 25 communities in Nunavut were analyzed based on high-level renewable resource profiles (solar and wind) and energy consumption of each municipality; 13 areas were then selected to advance for further analysis using Hybrid Optimization of Multiple Energy Resources (HOMER) software [29] developed by the National Renewable Energy Laboratory in the United States. HOMER determines the most feasible configuration by applying a full factorial design of experiments and choosing the configuration with minimum Net Present Cost (NPC) [104].

For the feasibility phase [53], WWF developed a Mixed Integer Linear Programming model to improve the results of their pre-feasibility assessment. They used community-specific data and timelines to provide a community-level simulation for each year over a 20-year period. The study considered more detailed parameters that were only broadly approximated in the pre-feasibility study, including diesel generator efficiency curves, wind-turbine power curves and unit capacity of renewable energy (RE) equipment as well as battery storage. For both stages of the study, WWF concluded that a microgrid or a Hybrid Renewable Energy System (HRES) composed of wind turbine (WT), solar photovoltaic (PV), power converter (CONV) and back-up sources of power from a diesel generator (DG) and batteries (BT) would be economic for such Northern communities.

[3] A household may be described as experiencing fuel poverty when it spends more than 10% of its income on utilities [13].

To investigate various energy modeling approaches without necessarily focusing on the Arctic, this section looks at various modeling techniques as applied to integrated energy systems. For instance, Sugihara et al. [105] developed a multi-objective optimization model for designing urban energy system alternatives in Osaka, Japan. The model simultaneously minimized cost, primary energy consumption and carbon dioxide emissions of the energy service system delivering electric and thermal energy in an integrated manner. Similarly, Lo Cascio et al. [106] studied an integrated energy system model consisted of small scale urban electrical, thermal and gas grids. The economic and environmental metrics evaluated in the study were quantified and verified with the commercial proprietary software, Honeywell UniSim Design Suite. Orehounig et al. [107] carried out an energy hub method in integrating decentralized energy systems at a neighborhood scale. The energy hub concept managed the relation between input and output energy flows in order to evaluate energy-autonomy and ecological performance of integrated energy systems. Cabrol and Rowley [108] conducted a simulation analysis of building-integrated air-source heat pump (ASHP) systems for various locations in the United Kingdom. The study also investigated the impacts of varying building enclosure characteristics. The results showed that the total operational costs and carbon dioxide emissions were lower for ASHP than for a comparative gas boiler heating system. Renaldi et al. [109] investigated a similar study by looking at heating system electrification through heat pumps installation in combination with renewable power generation. Through linear programming as formulated in Pyomo 4.0 and solved with CPLEX 12.6.2, the main optimization problem of the study was to find the optimal size and operational profile of the energy system in order to minimize total cost. Their study concluded that the renewable energy incentive programs/tariffs made the heat pump systems cost competitive against conventional heating systems.

3.1.2 Research gaps and research questions

The literature survey indicates that various component sizing methods for integrated energy system are available, but are not yet applied to remote communities especially in the Arctic. Also apparent from previous work – component sizing methods in conjunction with demand side modeling, specifically of heat load reductions, are generally scarce. Most studies focused on the supply side aspect of optimization and neglected the impact of demand-side modeling, specifically the effect of high-performance building enclosures. The latter is significantly cheaper to implement in achieving decarbonization targets, as opposed to building new energy systems with intermittent renewable resources. In some cases, heating can also be expensive enough that some households are forced to live in cold homes, which can increase the risk of physical and mental health problems [16]. Hence, this study proposes a holistic and integrated energy systems approach in modeling and evaluating various energy solutions in Northern remote communities.

Specifically, previous Arctic energy system investigations will be improved by considering the complex trade-offs of designing integrated energy system in remote communities through multi-objective optimization. Policy makers study the North from different viewpoints, thus, there exist multiple solution philosophies in investigating a wide array of energy solutions in reducing diesel dependence in the territories of Canada. For this purpose, a Multi-objective INtegrated Energy System

(MINES) [110] model, based on a Genetic Algorithm (GA), has been formulated to determine the drivers of energy vulnerabilities to better understand the *trilemma* of challenges relating to energy security, affordability and environmental sustainability. In line with this, a quantitative approach to describe and address the energy trilemma has also been found lacking in previous studies.

Another gap from the literature is related to domestic heating analysis, as most research applied to Northern Canada has been focused on electricity aspects. According to Gilmour et al. [43], heating is the most dominant form of energy use in the territories with diesel and heating oil[4] as the most frequent fuel used to generate heat. In 2011, reports showed that Northeners consumed 219 million litres of diesel (and some propane) for heating alone. To put this figure into perspective, in the same year 76 million litres of diesel were consumed for power generation [9] making heat more than 70% of the combined heat and electricity demand of Canada's territories.

This paper will give significant focus and discussion on heat loads to complement the vast research that has been undertaken already for the electricity sector among Northern remote communities. For instance, Fig. 3.2(a) shows the amount of domestic heat generated in the Arctic territories of Canada wherein heating oil is the largest heating source across the three territories because of its reliability, especially during winter. Further, Fig. 3.2(b) illustrates that the annual home heating costs in the NWT are significantly higher than in southern regions of Canada like Edmonton. Wood is also widely used for home heating in combination with other heat sources such as heating oil and propane [111]. However, unlike Yukon and the NWT, Nunavut and communities farther North in the Arctic circle have limited access to wood and other types of biomass, thus limiting its use as a viable heat source among Nunavummiut [9].

Considering the expensive fuel prices in Northern remote communities, the unique energy profile in the Arctic which is predominantly heating, and the drive to respond to a rapidly changing Arctic environment while improving quality of life in the region, the motivating research questions for this work are the following:

1. How can electricity and heating generation systems be effectively linked into one integrated energy system?

2. What heating alternatives will be viable in the North while considering flexibility of integration for current and future energy systems?

3. What low-cost initiatives are available to accelerate clean energy transformations in remote communities?

4. What are the trade-offs between optimal solutions in transitioning towards alternatives to diesel energy?

5. What are the socio-economic impacts of implementing new sustainable energy solutions in the Arctic region?

[4]Heating Oil is a generic industry term that covers a variety of potential products, formulations, and compositions. Standard Road Diesel #2, Diesel #1, Kerosene, K-1, Jet Fuel, JP-1, Agricultural Diesel, Diesel #2, Home Heating Oil / Fuel Oil #4, or Home Heating Oil / Fuel Oil #6 may be sold and used for heating [43]

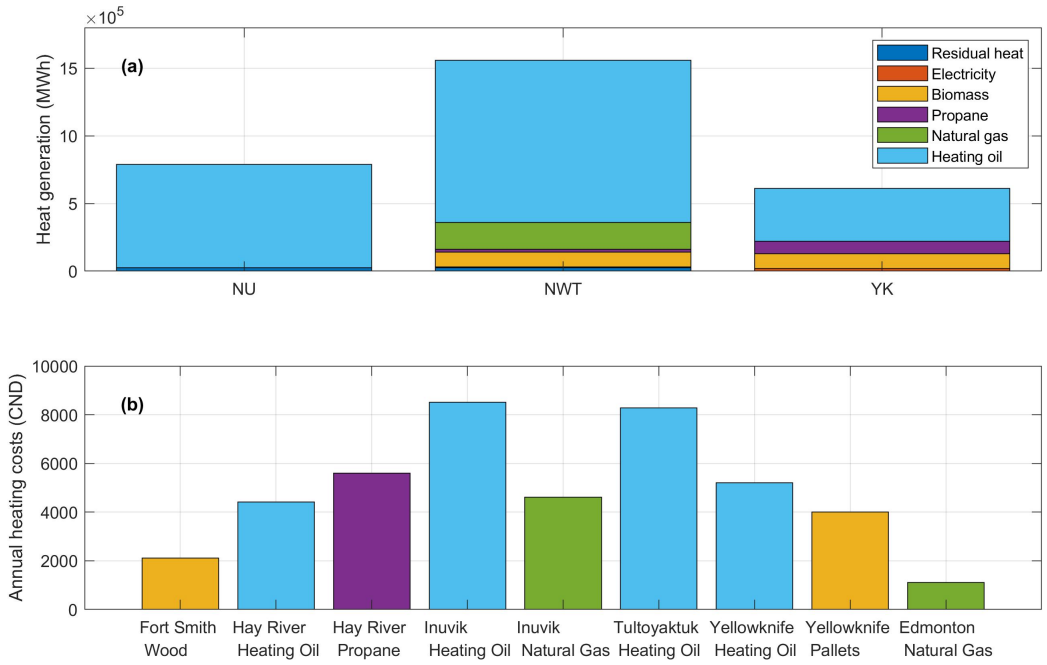

Figure 3.2: Heat load: (a) Heat generation by source across all territories [9]; (b) Annual community home heating costs in NWT [111].

3.1.3 Study objectives and key contributions

Just recently, WWF released its latest energy report [112] for the North by including heat in their HOMER analyses. However, it was a simplistic representation of an energy system by diverting and assuming that all excess electricity from the HRES will be used to meet the heat demand of a community. Thus, the main objective of this work is to contribute and bridge the gaps of previous Northern energy feasibility studies and answer the previously mentioned research questions by having a holistic and combined investigation of the electrical and thermal energy systems.

The primary contribution of this work is in establishing the connection between research, development and the implementation of emerging modeling approaches in real-world decision-making process concerning energy planning in remote communities. Additionally, the five key research questions of this study are addressed by the specific key contributions of this work:

1. Development of a time-series heat load building model coupled with the concurrent electrical load of Northern latitude communities;

2. Assessment of heat source alternatives such as ASHP and electric baseboard heaters while evaluating overall impact on the integrated energy system;

3. Demand side modeling incorporating a building enclosure-focused approach and overview of possible energy efficiency measures which are key in holistically addressing energy solutions in remote communities;

4. Dynamic simulation and optimization algorithms that can capture complex trade-offs in the energy system design space using the Multi-objective INtegrated Energy System (MINES) modeling framework;

5. Formulation of a community-scale energy trilemma index model using outputs from the multi-objective algorithm which can holistically encapsulate various energy solutions and viewpoints relevant to policy makers and stakeholders in remote communities.

The rest of the article is organized as follows: Section 3.2 describes the models developed for the study. To demonstrate functionality of the models developed in Section 3.2, Section 3.2.5 presents relevant information for the community of Sachs Harbour (a community in the NWT) ; the information presented will serve as input data for the models. Section 3.3 summarizes the results of the test case for the method, with conclusions presented in Section 3.4.

3.2 Methods

Multiple combinations of technologies can be considered in designing an integrated energy system. In the specific instance of the current case study, the microgrid system consists of WT, solar PV, BT, DG and a bi-directional converter to handle power flows from the DC bus to AC bus and vice versa (Fig. 3.3). In terms of load, the modeled microgrid system must meet both heat demand (space heating and domestic hot water (DHW) and electricity (lighting and consumption from home appliances) for each 1 hour timestep over a given year. As shown in Fig. 3.4, a system-of-systems approach was implemented across the simulation and optimization algorithms wherein the constituent sub-systems are brought together in one integrated electrical and thermal energy system.

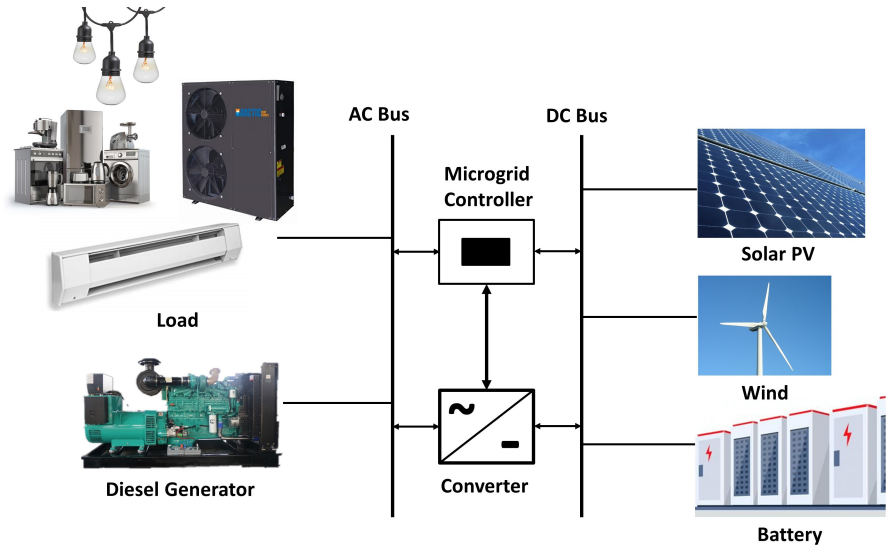

Figure 3.3: Schematic diagram of an integrated electrical and thermal energy system.

3.2.1 Genetic algorithm optimization

To capture the complex trade-offs in designing integrated energy systems, a multi-objective approach is implemented which utilizes a meta-heuristic optimization process based upon on a Genetic Algorithm (GA). This is a population-based search and

optimization method which mimics the process of natural evolution [113]. Specifically, the Non-dominated Sorting Genetic Algorithm - II (NSGA-II) of Deb et al [114] has been adapted for this work as it has the generic ability to handle multi-objective trade-offs and Pareto pursuit. This has been demonstrated in various research works such as that of Evins et al. [115], Forde et al. [116], Roberts et al. [42] and Zhang et al. [117], among others.

A GA approach was chosen to be the most appropriate algorithm for this study as it can solve multi-objective and non-linear optimization problems without requiring information from derivatives of the objective functions. Also, the required computational time is still relatively low as compared to other optimization techniques since the integrated energy system in question does not possess a large number of design variables and constraints [15]. Its reliability, accuracy and convergence in finding global optimal solutions have been proven in studies conducted by Campana et al. [87] and Zhang et al. [117], among others. As presented in Fig. 3.4, a GA initiates the optimization process by collecting input parameters and randomly generating an initial population sets of individuals (solutions), and evaluating their corresponding fitness function. Each iteration encompasses a competitive selection process among the individuals where the vector of solutions with the highest fitness function values are recombined through GA techniques (mutation, elitism and crossover) with a purpose of attaining higher fitness values. The recombination process stops once the convergence criterion is satisfied and the optimal solution is found. The output of a multi-objective GA is a Pareto frontier curve wherein the non-dominant solutions are further analyzed to better understand trade-offs in minimizing one objective function over the other (to be further described in Section 3.3).

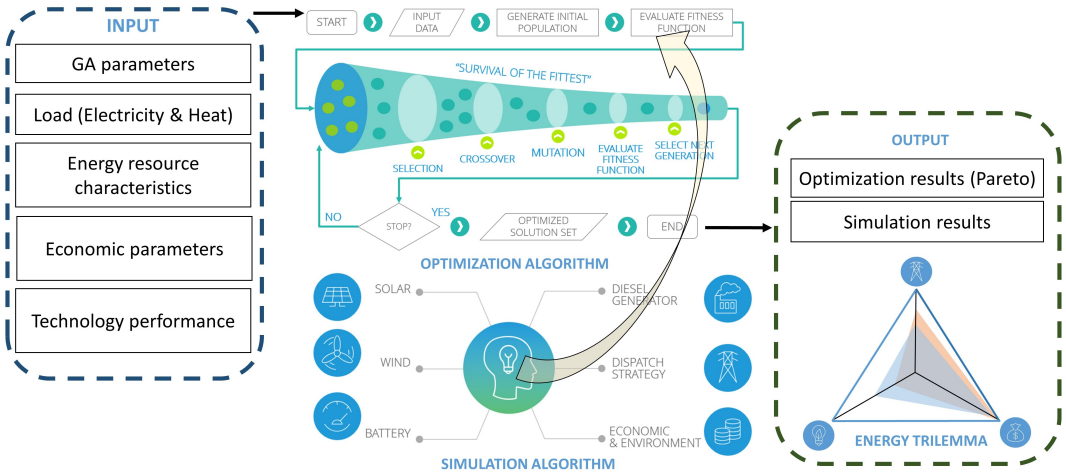

Figure 3.4: Multi-objective INtegrated Energy System (MINES) modeling framework.

The set of GA input parameters for this work is shown in Table 3.1 and the approach was implemented in a MATLAB® platform.

3.2.1.1 Objective functions

Energy affordability is a primary concern based on the previous Energy Charettes exercise done in the Northern territories [83]. Hence, the first objective function that was formulated for this study is minimizing the Levelised Cost of Energy ($LCOE$).

Table 3.1: GA configuration parameters.

Parameter	Description
Algorithm	Variant of NSGA-II [114]
Generations	200
Population	100
Crossover function	Heuristic
Crossover rate(%)	90
Mutation function	Non-uniform
Tournament size	2

This economic parameter encapsulates the impact of the cost of energy to the community, together with the cost of subsidy support from the government. A modified $LCOE$ equation [84] that considers the full spectrum of costs from design to recycling (salvage value) as shown in Eq. 3.1 was used:

$$LCOE = \frac{\sum_{t=1}^{n} \frac{CC_i(t)+O\&M_i(t)+Z_i(t)-S_i}{(1+r)^t}}{\sum_{t=1}^{n} \frac{P_{gen}}{(1+r)^t}} \tag{3.1}$$

where t is time (year); r is the discount rate (%); n is the total life of the energy system (year); CC is the capital cost ($) per unit of the system's component i; $O\&M$ is the operations and maintenance costs ($/year); Z is all other costs associated with the project ($/year); S is the salvage value ($); and P_{gen} is the power generated from the microgrid system (kWh/year).

In modeling and planning energy systems, there are usually trade-offs between economic and environmental goals. For this work, minimizing fuel consumption ($fuel_{cons}$) was adopted as the second objective function to examine the interplay and trade-offs in reducing environmental emissions while ensuring low cost of energy for the community. The fuel curve describes the amount of fuel consumed by the generator in producing electricity. In this study, a linear relationship is assumed between $fuel_{cons}$ and the DG power output. This approach has been executed in previous studies done by Sharafi et al. [118], Morse [96], and Hoevenaars and Crawford [95], among others:

$$fuel_{cons} = F_0 P_{DG,r} + F_1 P_{DG} \tag{3.2}$$

where F_0 is the fuel curve intercept coefficient (L/h/kW$_{\text{rated}}$); F_1 is the fuel curve slope coefficient (L/h/kW); $P_{DG,r}$ is the rated capacity of DG; and P_{DG} is the instantaneous power coming from the DG (kW).

The linear relationship between $fuel_{cons}$ and the DG power output may not represent certain types of generators such as fuel cells or variable-speed diesels [119]. However, for the more common types of generators, constant-speed internal combustion generators and microturbines, the straight-line fuel curve is also an appropriate fit [119]. This has been proven with the fuel curves of the existing and new DG in a case study conducted by WWF [53]. The intercept and slope of the fuel curve are necessary so the model could extrapolate the data based on the discrete variable capacities of the DG as formulated in the GA. MINES then creates the generator

efficiency curve based on the power output of the DG and the chemical energy of the diesel fuel; this approach is adapted from HOMER [119].

3.2.1.2 Constraints and other output parameters

To depict real-world conditions in designing energy systems, certain constraints were formulated as part of the model. For example, Loss of Power Supply Probability ($LPSP$) as described in Eq. 3.3 [66] was set to 0%. This is to ensure energy reliability and that the load will be met by the energy system on an hourly timestep.

$$LPSP = \frac{\sum_{t=1}^{T} P_{deficit}(t)}{\sum_{t=1}^{T} P_{load}(t)} \tag{3.3}$$

where $P_{deficit}$ pertains to the insufficient supply of power from the renewables and diesel, as well as the available energy from the BT storage:

$$P_{deficit}(t) = P_{load}(t) - (P_{RE}(t) + P_{DG}(t) + P_{batt}(t-1)) \tag{3.4}$$

where P_{load} is the electricity demand (kW);P_{RE} is the power produced by the renewables (kW); and P_{batt} is the energy stored in the BT (kW).

The full set of constraints considered to run the optimization module in MINES are:

$$constraints \begin{cases} LPSP \leq 0\% \\ SOC_{min} \geq 30\% \\ RE_{pen} \geq 30\% \\ P_{excess} \leq 30\% \\ DG_{LF} \geq 30\% \end{cases} \tag{3.5}$$

where SOC is the state of charge of the BT (%); RE_{pen} is the RE penetration (%) [110]; P_{excess} is the excess electricity (%) [110]; and DG_{LF} is the load factor of the DG (%). To include a conservative assumption of introducing RE in the energy mix of the remote community, a 30% RE_{pen} was included in the constraints formulation. The 30% P_{excess}, meanwhile, was set to avoid excess energy caused by oversizing each component of the energy system. To prevent damaging the DG by running at very low partial loads, 30% DG_{LF} was imposed in the model. Similarly, the 30% minimum SOC was set to avoid damaging the storage bank by excessive discharge.

Furthermore, other output parameters that can be extracted in MINES correspond to life cycle emissions of the system. For this work, direct and indirect emission factors were adapted from Roberts et al. [42]. Unlike emissions coming from fuel combustion only, life cycle emissions approaches capture direct and indirect emissions from manufacturing, transportation and decommissioning stages of the energy system. Similarly, in terms of economics, the Life Cycle Cost (LCC) [40] also served as one of the model outputs to represent the sum of the cradle-to-grave economic costs of the integrated energy system for a project lifespan of 25 years.

Table 3.2: Dimension of the discrete variables in the optimization algorithm.

Parameter	Value
WT quantity	0 - 500
WT capacity (kW)	95,95,100,100
PV quantity	0 - 500
PV capacity (kW)	15,25,20,25.025
BT quantity	0 - 500
BT capacity (kWh)	55,13.9,7.37,9.24
DG quantity	0 - 100
DG capacity (kW)	300,320,225,150
CONV quantity	0 - 10
CONV capacity (kW)	200,250,270,300
Operation strategy	LFOS and CCOS

3.2.1.3 Multiple design optimization variables

As listed in Table 3.2, the 11 discrete decision variables were classified into three groups in the model. The first group reflects the individual capacity of all components of the integrated energy system as presented in Fig. 3.3 (solar PV, WT, BT, DG and CONV). The second classification corresponds to the quantity of each component. The last group refers to the dispatch of power implemented in the model.

3.2.2 Simulation

This section describes the simulation modules that were included in this work to evaluate the objective functions of the optimization algorithm in Fig. 3.4.

3.2.2.1 Heat load model

For the case study of Sachs Harbour (to be further described in 3.2.5), a building model was developed in order to simulate the combined DHW and space heating requirements of the community.

The daily average thermal energy demand per capita for DHW Q_{dhw} (Wh) is given by the following equation:

$$Q_{dhw} = \rho_w c_{p,w} V_{d,p} (T_{w,h} - T_{w,c}) \tag{3.6}$$

where ρ_w is the water density (kg/m^3); $c_{p,w}$ is the water specific heat (Wh/kg-°C); $V_{d,p}$ is the daily consumption of hot water per person (m^3); $T_{w,h}$ and $T_{w,c}$ are the hot and cold water temperatures (°C), respectively. The hourly average DHW consumption profile has been derived using the profile presented in Hendron and Burch [120]. The total energy consumption for DHW has been calculated by multiplying the thermal energy demand per capita by the number of inhabitants of the community.

The total space heating requirement has been estimated as the difference between the total thermal energy demand (data from Arctic Energy Alliance [121]) and the calculated total energy demand for DHW. To calculate the hourly load profile for

Table 3.3: Building simulation parameters to estimate heat load requirement of the community.

Parameter	Value
U (W/m^2-K)	0.5
T_{in} (°C)	18
α_{hr} (%)	0
η_v (1/h)	0.4
η_i (1/h)	0.4
SHGC (%)	50
WWR (%)	50

space heating, it was assumed that the building stock is composed of buildings with similar geometry and thermal characteristics. The hourly space heating requirement Q_{sh} has been calculated using the method described in Campana et al. [87].

$$Q_{sh} = HL - HG + Mc_{p,b}\frac{dT}{dt} \tag{3.7}$$

where HL is the heat losses (W); HG is the heat gain (W); M is the mass of the building (kg); $c_{p,b}$ is the building heat specific capacity (Wh/kg-°C); dT is the building hourly temperature variation (°C); and dt is the simulation timestep (h).

The heat losses takes into account loses due to transmission (HL_t) (W), ventilation (HL_v) (W) and infiltration (HL_i) (W). The heat gains caused by people, lighting system, and appliances have been neglected due to unpredictability, and this approach was adapted from Campana et al. [87]. It was also assumed that the internal building temperature is kept constant making dT/dt equal to zero. The heat gains due to solar radiation have been considered assuming a solar heat gain coefficient (SHGC) of 0.50 and a windows-to-wall ratio (WWR) of 0.50. An ideal temperature controller has been assumed to keep the indoor set-point temperature always constant. The rest of the building simulation parameters are listed in Table 3.3. HL_t, HL_v and HL_i are given by the following set of equations [87]:

$$HL_t = UA_b(T_{in} - T_{out}) \tag{3.8}$$

$$HL_v = (1 - \alpha_{hr})\eta_v V_v \rho_a c_{p,a}(T_{in} - T_{out}) \tag{3.9}$$

$$HL_i = \eta_i V_i \rho_a c_{p,a}(T_{in} - T_{out}) \tag{3.10}$$

where U is the overall heat transfer coefficient of the building (W/m^2-K); A_b is the total surface area of the building (m^2); T_{in} is the set indoor temperature (°C); T_{out} is the outdoor temperature (°C); α_{hr} is the heat recovery efficiency (%); η_v is the ventilation air changes per hour (1/h); η_i is the infiltration air changes per hour (1/h); V_v is the building ventilated volume (m^3); V_i is the building infiltrated volume (m^3); and $c_{p,a}$ is the air specific heat (Wh/kg-°C).

In the absence of an actual thermal load data, it should be noted that the heat demand simulation approach estimates the thermal energy consumption of the community as a whole rather than a detailed analysis of each individual building in

Sachs Harbour. Thus, the adapted heat load simulation process from Campana et al. [87] provides the worst case scenario in estimating the thermal demand of the community. This uncertainty in heat load variations will be addressed in Section 3.3.1.1.

3.2.2.2 Component models

The algorithm for the component sub-models (PV, WT, BT, DG) as laid out in Fig. 3.4 are detailed and have been previously described by the authors [110]. Also, a summary of the simulated characteristics of each component is listed in Tables 2.6 - 2.9.

3.2.3 Operation strategies

Two operation strategies were implemented in this work: Load following (LFOS) and Cycle charging (CCOS). The choice of dispatch strategy was also formulated as a design optimization variable in the MINES model. For both strategies, the DG only operates when the RE and BT cannot meet the load. With CCOS, the DG runs at 100% rated power until it reaches the pre-set SOC (SOC_{sp}) of the BT and the excess energy is either stored in the BT or used to serve a dummy load if the BT is at a 100% SOC on a given timestep. With LFOS, the DG outputs just enough power to meet the instantaneous load per timestep unless it reaches the minimum power of the DG based on DG_{LF}. Finally, to handle power flows from the DC bus to AC bus and vice versa, the simulation parameters for the converter listed in Table 2.10 were used.

3.2.4 Energy trilemma index model

The energy trilemma index model quantifies the three challenges (energy security, energy equity or affordability, and environmental sustainability) that have to be addressed in energy systems planning. These challenges can be described by three independent axes with their corresponding scoring or weighting, which have to be balanced as they imply trade-offs when looking at the impact of one axis over another. According to the World Energy Council (WEC), achieving high performance on all dimensions of the trilemma entails complex interwoven links between various sectors in the society [122]. WEC comparatively ranks 125 countries based on the specific indicators of the energy trilemma [122]. Fig. 3.5 shows Canada's energy trilemma score. The country performs strongly on energy security and affordability but needs improvement in environmental sustainability. It has to be noted that the score was benchmarked in comparison with the other countries present on WEC's database, as per the WEC trilemma score definition as a comparative metric.

ARUP Consulting argued that the three dimensions of the energy trilemma cannot be treated independently and that all three axes are equally important, so the optimum performance implies achieving high scores on all three [123]. The firm also graphically illustrated the importance of using the tool in achieving an informed decision in energy planning as shown in Fig. 3.6.

The original energy trilemma index model was developed in the context of benchmarking one country against another using a specific index structure and weighting. For this work, the generated model outputs from the MINES optimization model

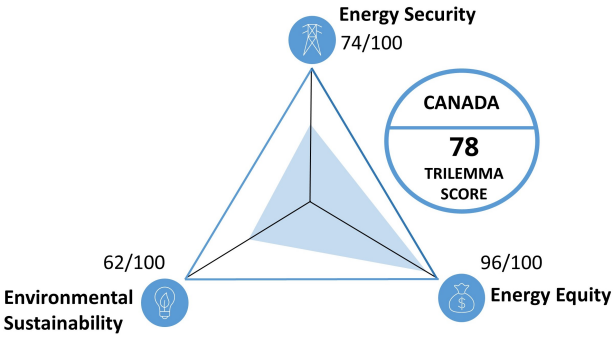

Figure 3.5: 2019 energy trilemma score of Canada according to the World Energy Council.

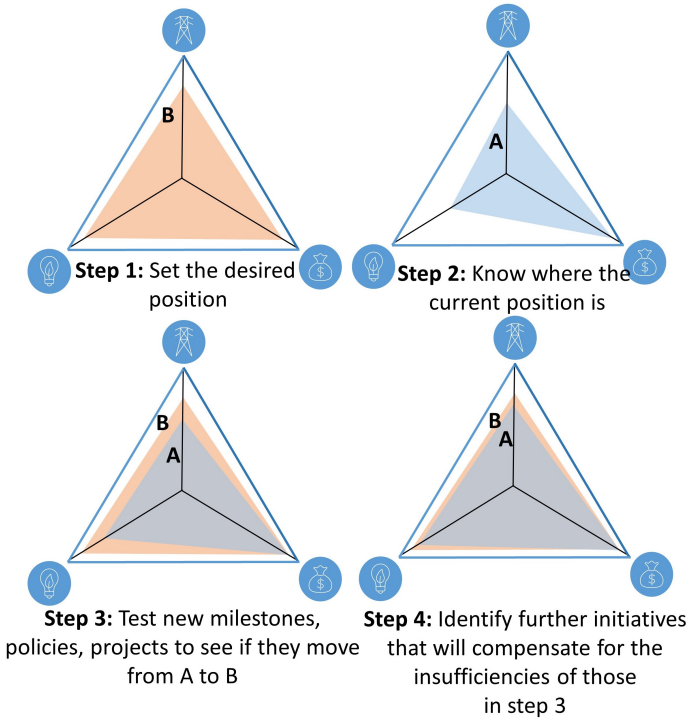

Figure 3.6: Graphical representation of energy trilemma index tool in understanding existing influences and drivers in balancing three components of the energy trilemma; adapted from ARUP Consulting Company [123].

will be extracted to specifically rank points of interest along the Pareto front, and to quantitatively assess the trade-offs inherent for each solution. In particular, the points of interest on the Pareto front will be benchmarked against other feasible solutions using the index structure presented in Tables 3.4 and 3.5.

3.2.5 Case study input data

The methods described in this section will be applied to a case study in Sachs Harbour (Lat: 71.9884 N; Long: 125.23935 W), the Northernmost community in the NWT. This Hamlet has a population of around 130 people with their main source of electricity and heat being diesel and heating oil, respectively. The fuel is shipped via barge once a year since year-round road access is not available.

Table 3.4: Community-scale energy trilemma index structure; the equal weightings represent the three axes of the energy trilemma as equally important and cannot be treated independently.

Indicator category	Parameter	Weight
Energy Security	$LPSP$	16.67%
	P_{excess}	16.67%
Energy Equity	LCC	16.67%
	$LCOE$	16.67%
Environmental Sustainability	$CO_{2\,emissions,life\,cycle}$	16.67%
	RE_{pen}	16.67%

Table 3.5: Rank and scoring table for the energy trilemma considering nine solutions of interest.

Rank	Score
1	100
2	90
3	80
4	70
5	60
6	50
7	40
8	30
9	20

Fig. 3.7 shows the simulated thermal load profile of Sachs Harbour using the methods detailed in Section 3.2.2.1. Fig. 3.8, meanwhile, clearly shows that the load profile of the community is predominantly from the heating load. The electrical load data has been directly provided by the Northwest Territories Power Corporation (NTPC). The maximum and minimum electrical loads are 220 kW and 70 kW, respectively. On the other hand, the peak load from the simulated heating demand is around 885 kW.

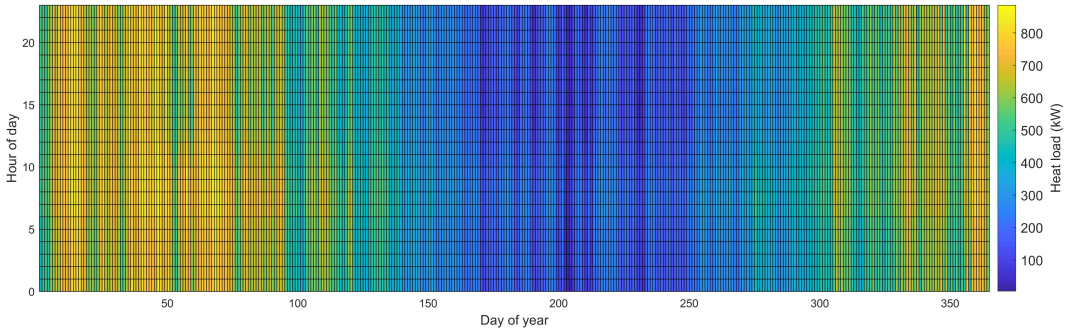

Figure 3.7: Heat map of thermal demand in Sachs Harbour over a year.

Although no on-site investigation has been done in terms of the actual conditions of building infrastructure in the community, a 2019 community survey from the NWT's Bureau of Statistics [124] indicated that the 30% of dwellings in Sachs Harbour have housing issues. The report focuses on housing indicators such as affordability, suitability and adequacy. A dwelling is described as affordable if the household is spending less than 30% of their income on housing costs. A house is considered adequate if it does not require major repairs. Suitability is defined as having the appropriate number of bedrooms against the number of occupants. No detailed discussion was given in the survey but it was assumed that the high heating demand is related to major housing repairs needed in specific houses and buildings in the community.

Further, wind tower data measurements at 30m height with 10-minute temporal resolution from July 8, 2005 to September 29, 2009 were supplied by the local government of the NWT for this work. The wind velocity data were extrapolated to a 40m height using the method described in Quitoras et al. [110]. As shown in Fig. 3.9(b), high wind speed registries can be observed during autumn and the mean wind velocity for the year is around 8m/s after extrapolating the data to a 40m height. Another climatic parameter that affects the operation of the energy system is the solar resource. Fig. 3.9(a) shows low GHI during autumn and winter due primarily to the high latitude of Sachs Harbour. The temperature profile of the community is in Fig. 3.15 and will be discussed further in the results section.

3.3 Results and discussion

This section presents the results from executing the methods discussed earlier. The outputs were further analyzed by performing scenario analyses of various energy system configurations while looking at practical implementation approaches to realize

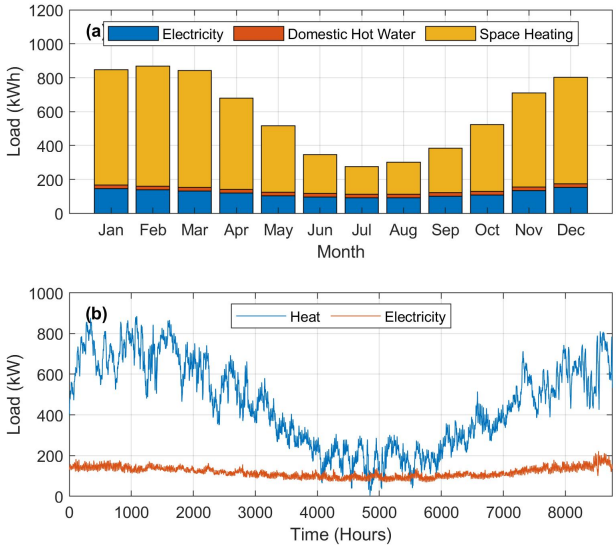

Figure 3.8: Integrated load of Sachs Harbour: (a) Average monthly load; (b) Hourly electricity and heat load.

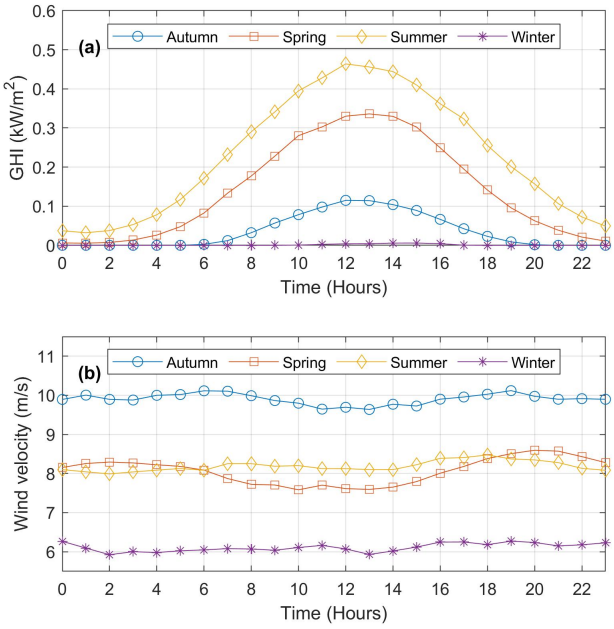

Figure 3.9: Meteorological data for Sachs Harbour for different seasons: (a) Average extrapolated wind speed at 40m elevation; (b) Average hourly Global Horizontal Irradiance (GHI).

the goals of this work. This section ends with a validation exercise for the proposed model.

3.3.1 Design optimization and simulation results

The full design space exploration by the GA of the energy system is shown in Fig. 3.10. The simulated heat load is assumed to be supplied by using electric appliances for DHW (specifically via instant water heating devices) and via electric baseboard heaters for space heating demands respectively. Fig. 3.11 presents the variations of the objective functions during the optimization process. It can be seen that a wide range of values are visible at the beginning of the optimization process, with convergence to uniform values evident from around the 130th generation forward. This means that the optimizer can no longer improve the calculated objective function values and a solution has been attained. Increasing the population size and the number of generations in the GA optimizer covers the solution space more thoroughly, but will cause the algorithm to run slowly. This investigation has been performed, but the Pareto front did not change and the solutions converged to uniform objective function values at the 130th (approximately) generation as well. This confirms that the chosen GA population size and the number of generations in Table 3.1 are sufficient to carry out the modeling work in this study.

In a multi-objective optimization, the superiority of a solution is determined by the concept of solution dominance [40]. In Fig. 3.10, the blue dots represent the dominated solution points while the points in orange (Pareto front) are the non-dominated solutions. Unlike in single-objective optimization problems where the output is presented as a candidate solution, output for a multi-objective optimization technique is presented as a set of candidate solutions. This approach yields diversity of solutions to be able to analyze trade-offs between two conflicting design objectives.

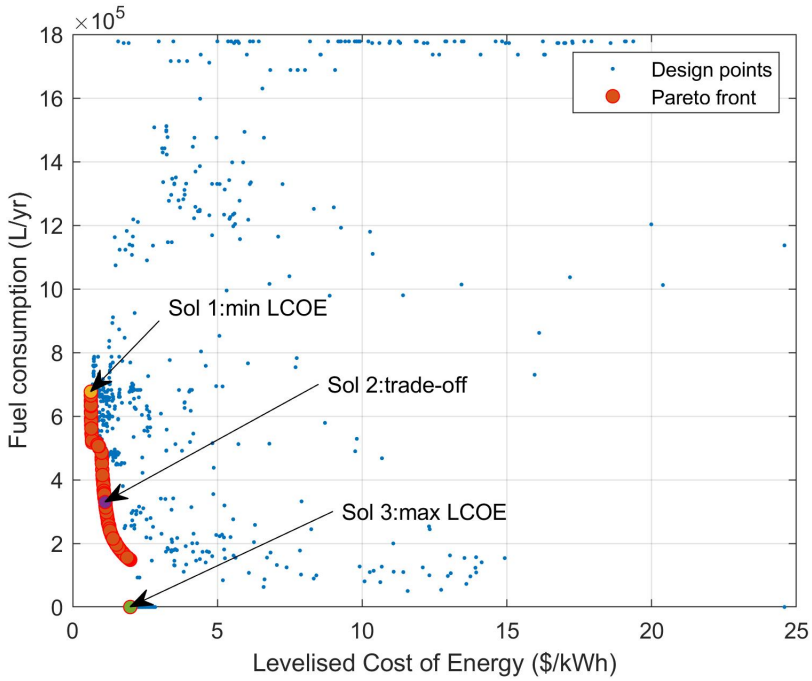

Figure 3.10: Full design space with the optimal Pareto front and the identified solutions of interest.

From the Pareto front in Fig. 3.10, it is clear that as $fuel_{cons}$ decreases, the $LCOE$ of the energy system increases. As described in the objective function for-

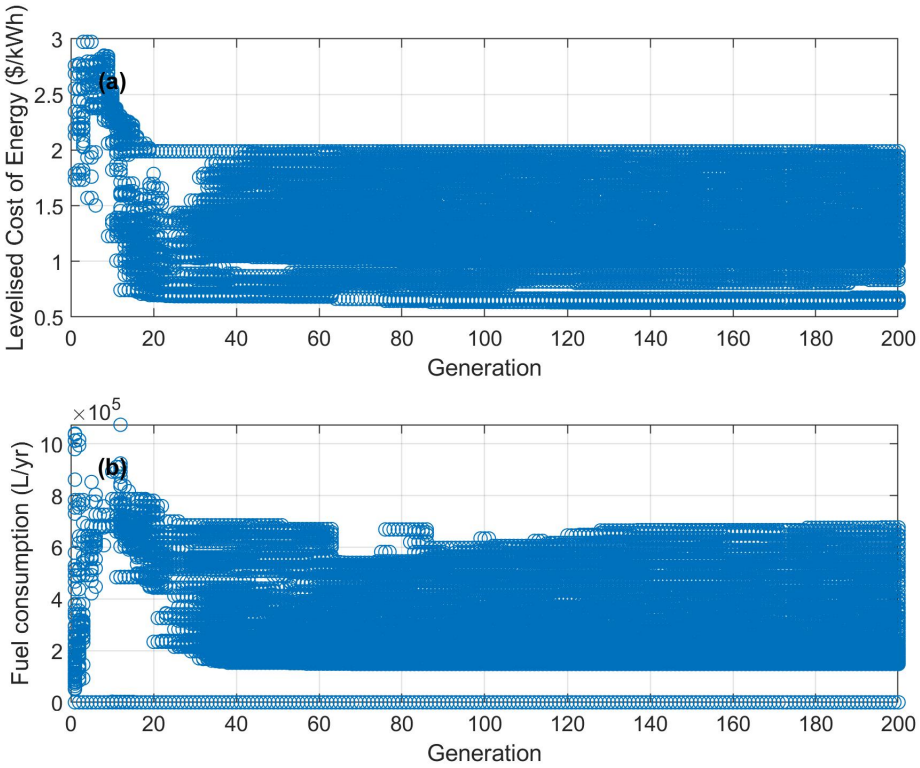

Figure 3.11: Variations of the objective functions with GA generations.

mulations, minimizing $fuel_{cons}$ impacts this aspect of the feasible solutions. In particular, this limits the operation of the DG and the power is compensated by including RE technology and BT storage. However, this reflects a trade-off wherein the resulting system's $LCOE$ increases. The discontinuity in the Pareto front is influenced by the lower and upper bounds of the discrete characteristics of the decision variables as shown in Table 3.2, and the restrictions implemented in the constraints formulation of the model. The reason for the final step-change at the tail end of the Pareto front will be explained in Section 3.3.1.1.

The three solutions of interest as specified in Fig. 3.10 are further examined and their system configurations are provided in Table 3.6. With the three solutions of interest, the WT has the largest share in meeting the energy demand. This reflects the strong wind resource in Sachs Harbour making it a viable option in displacing a significant proportion of the diesel power of the community. The BT storage helps stabilize the mismatch between the demand and the intermittency of RE. However, this causes an increase in the system's cost. In particular, solution 3 has a 100% RE_{pen} but the increased capacity in WT (5,225 kW) has to be matched with an appropriate level of BT storage (14,630 kWh) which is almost three times the capacity of solution 1 (4,620 kWh). A trade-off point (solution 2) located approximately at the middle of the Pareto front has a system configuration and characteristics that balance the results calculated from solutions 1 and 3. Solution 2 has all the system components presented in Fig. 3.3. The system's $LCOE$ (1.1212 CND $/kWh), however, has doubled from the solution 1 since it has higher RE capacity with a larger BT storage capacity. Nonetheless, the $fuel_{cons}$ of the DG is about 50% less than that of solution 1. This trade-off analysis is fundamental in analyzing all feasible

Table 3.6: Configuration characteristics of the three solutions of interest determined from the Pareto front of Scenario 1.

Parameter	Unit	Optimization results		
		Min. $LCOE$ and Max. $fuel_{cons}$	Trade-off Point	Max. $LCOE$ and Min. $fuel_{cons}$
PV	kW	650 (25kW x 26)	2,575 (25kW x 103)	-
WT	kW	855 (95kW x 9)	1,235 (95kW x 13)	5,225 (95kW x 55)
BT	kWh	4,620 (9.24kWh x 500)	14,410 (55kWh x 262)	14,630 (55kWh x 266)
DG	kW	1,125 (225kW x 5)	1,125 (225kW x 5)	-
CONV	kW	1,000 (200kW x 5)	1,200 (200kW x 6)	1,200 (200kW x 6)
Strategy	-	LFOS	LFOS	LFOS
P_{pv}	kWh	506,499	2,097,521	-
P_{w}	kWh	2,456,400	5,322,200	22,517,001
$P_{BT,out}$	kWh	150,143	656,701	825,357
P_{DG}	kWh	1,252,981	971,224	-
$LPSP$	%	0	0	0
RE_{pen}	%	68.11	88.43	100
P_{excess}	%	16.58	4.92	1.14
$fuel_{cons}$	L/yr	676,792	329,856	-
CO_2[a]	$tCO_{2\text{-eq}}$/yr	3,076	2,692	1,371
CC	CND $	22,873,000	51,822,100	120,575,000
$LCOE$	CND $/kWh	0.627133	1.12129	1.989
LCC	CND $	55,576,000	99,368,000	176,263,000

[a] Lifecycle CO_2 emissions of the energy system

options from the decision maker's point of view.

The optimal dispatch control strategy of the integrated energy system is LFOS. This result was influenced by the load profile of the system. Using the same decision variables in Table 3.2 and excluding the heat demand in Fig. 3.8(b), the MINES model was run again. Table 3.7 shows the comparison of the optimal configuration results for the system both with and without the heat load (cases 1 and 2 respectively). The tool selected CCOS as the optimal dispatch strategy when the load is only related to non-heating electrical demand. As mentioned previously in Sec 3.2.3, the two dispatch controls are similar except LFOS only produces enough power to meet the instantaneous load while CCOS operates at its rated power and excess energy is stored in the BT during operation. Hence, it can be deduced that the optimal dispatch approach could also greatly affect the optimal DG capacity of the system. From Table 3.7, it can be observed that the optimal DG capacity is influenced by the total energy demand along with the peak load. For example, in case 2, the peak electrical load for the system is 221 kW with an optimal DG capacity of 225 kW. Case 1, on the other hand, has a peak load of 1,036 kW with an optimal DG capacity of 1,125 kW. These optimal DG capacities ensure that the peak loads will be met throughout the year. However, how to dispatch these capacities from

Table 3.7: Comparison of optimal configuration of the system with and without the heat load.

Parameter	Unit	Optimization results	
		Case 1: Min. $LCOE$ (Elec and Heat)	Case 2: Min. $LCOE$ (Elec Only)
PV	kW	650 (25kW x 26)	100 (25kW x 4)
WT	kW	855 (95kW x 9)	190 (95kW x 2)
BT	kWh	4,620 (9.24kWh x 500)	4,481.4 (9.24kWh x 485)
DG	kW	1,125 (225kW x 5)	225 (225kW x 1)
CONV	kW	1,000 (200kW x 5)	250 (250kW x 1)
Strategy	-	LFOS	CCOS
P_{pv}	kWh	506,499	81,457
P_{w}	kWh	2,456,400	818,800
$P_{BT,out}$	kWh	150,143	396,062
P_{DG}	kWh	1,252,981	356,400
$LPSP$	%	0	0
RE_{pen}	%	68.11	71.64
P_{excess}	%	16.58	9.14
$fuel_{cons}$	L/yr	676,792	116,703
CO_2[a]	tCO$_{2\text{-eq}}$/yr	3,076	770
CC	CND $	22,873,000	5,023,520
$LCOE$	CND $/kWh	0.627133	0.522406
LCC	CND $	55,576,000	9,580,800

[a] Lifecycle CO_2 emissions of the energy system

the DG affects which dispatch control is optimal for the energy system taking into consideration the two conflicting design objectives mentioned previously.

The listed optimal subcomponent capacities in Table 3.7 are not sufficient to explain the selected optimal dispatch control given the complexity of the energy system. Hence, Fig.3.12 shows the impact of the load profile on the optimal hourly simulation dispatch. For both cases, it can be observed that running the DG is more flexible in meeting the fluctuations of the demand than discharging the BT as the latter's charge-discharge cycles are affected by the amount of excess and deficit power from RE. Changing the dispatch control to LFOS in case 2 would make the solution still feasible, but sub-optimal and dominated (Fig. 3.13(b)). On the other hand, running the DG just enough to meet the load deficit (LFOS) is more optimal in reducing the overall $fuel_{cons}$ of the system in case 1. In contrast, running the DG under CCOS would make the overall system sub-optimal and dominated as shown in Fig. 3.13(a). Although running the DG at full rated capacity is preferable and more efficient in general, doing so in this case is not necessary, as the WT and the PV are optimally scaled up (together with the instantaneous power coming from the DG) to meet the high demand and load fluctuations as compared to the previous case. Furthermore, the system tends to dispatch power coming from the DG during high demand season (winter) as there is not enough power to be discharged from

the BT.

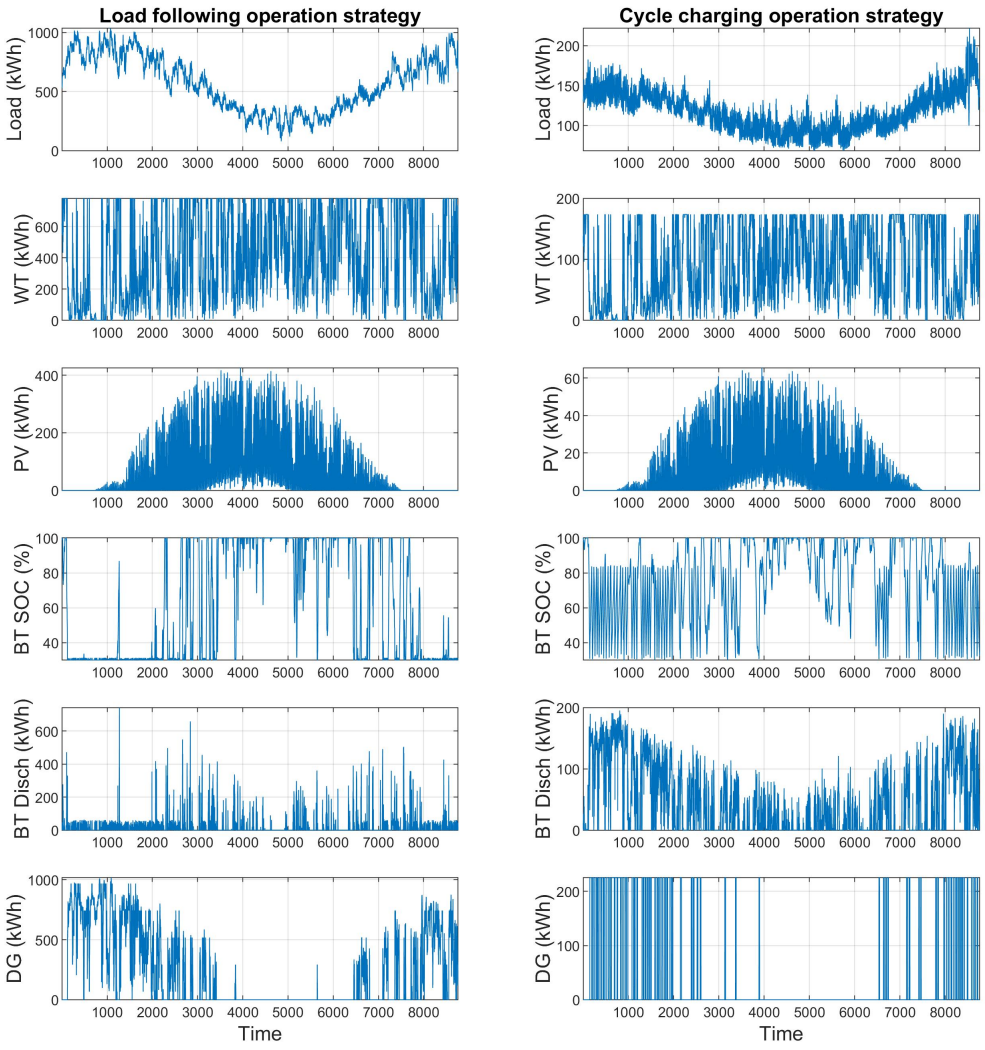

Figure 3.12: Impact of the load profile on the optimal simulation dispatch: (1) Case 1 (left column) is the simulation results (under load following) with the combined electricity and thermal load profiles; (2) Case 2 (right column) is the simulation results (under cycle charging) with electricity load profile only.

Note that increasing the value of the $LPSP$ from 0% is impractical as it would entail power outage. This would be even more costly for a Northern community such as Sachs Harbour as flown in fuel would be required to meet peaks in demand or the unmet load due to the increased $LPSP$. To illustrate this in a real-world context, this activity of flown in diesel fuel cost around $1.75 million CND over dozens of flights for the community of Paulatuk, NWT in 2019 [16].

3.3.1.1 Scenario evaluation and heating system flexibility

A scenario analysis was carried out in order to evaluate candidate heating technologies in Northern remote communities. In such contexts, district heating has always

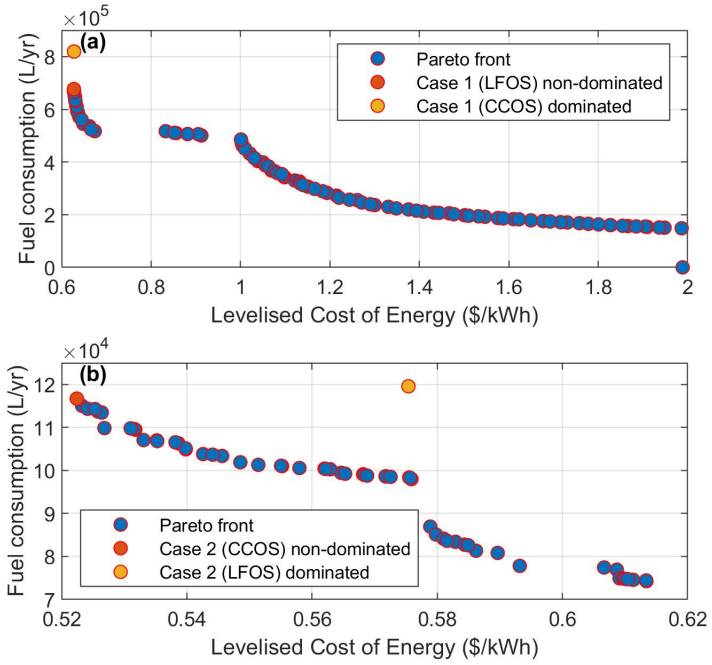

Figure 3.13: Changing the dispatch control would make the solution sub-optimal (dominated): (a) Case 1 Pareto front (under load following) with the combined electricity and thermal load profiles; (b) Case 2 Pareto front (under cycle charging) with electricity load profile only.

been challenging due to issues of installing pipe networks on permafrost to distribute heat in the community. A report from the local government of the NWT argued that even as construction techniques improve, challenges in building on permafrost have become more evident throughout the territory [125] especially for the Northernmost communities such as Sachs Harbour. Similarly, utilizing waste heat from the centralized diesel facility for the majority of communities in the North is not practical as it would also involve construction of piping networks that will distribute heat to houses and buildings. Also, since one of the objective functions in this study is to minimize $fuel_{cons}$, the resulting capacity factor of the DG is only around 10% - 20% which makes it even more impractical from an economic point of view.

Given these considerations, this section looks at the use of single dwelling air-source heat pumps (ASHP) as a potentially viable option along with the use of electric baseboard heaters which were included in the study's first optimization results (scenario 1). In particular, the evaluated scenarios together with their corresponding heat sources are presented in Table 3.8. This section focuses on the impact of the two heating technologies while Section 3.3.2 analyzes the impact of an 'enclosure first' approach to the building design. Meanwhile, to calculate the ASHP's electricity consumption, the empirical relationship between T_{out} and the heat pump's COP (efficiency) was used [87]:

$$COP = 2.79 + 0.036(T_{out}) + 0.0006036(T_{out}^2) \tag{3.11}$$

Baseboard heaters are thermodynamically close to 100% efficient; in this study it is assumed that 100% of the electrical energy consumed is converted to heat. Heat pumps, on the other hand, typically range from 200% to 300% efficient, supplying

Table 3.8: Scenarios implemented in the MINES model.

Scenarios	Electricity	Space Heating
Scenario 1	Home appliances including lighting and electric load for DHW	Baseboard Heater at $U = 0.5$ W/m^2-K
Scenario 2	Home appliances including lighting and electric load for DHW	Baseboard Heater at $U = 0.13$ W/m^2-K
Scenario 3	Home appliances including lighting and electric load for DHW	Baseboard Heater and ASHP[a] at $U = 0.13$ W/m^2-K
Scenario 4	Home appliances including lighting and electric load for DHW	Baseboard Heater and ASHP[b] at $U = 0.13$ W/m^2-K

[a] Baseboard heater kicks in if ASHP shuts off when outside temperature drops below -20 °C.

[b] ASHP only operates during summer and the baseboard heater runs for the rest of the seasons.

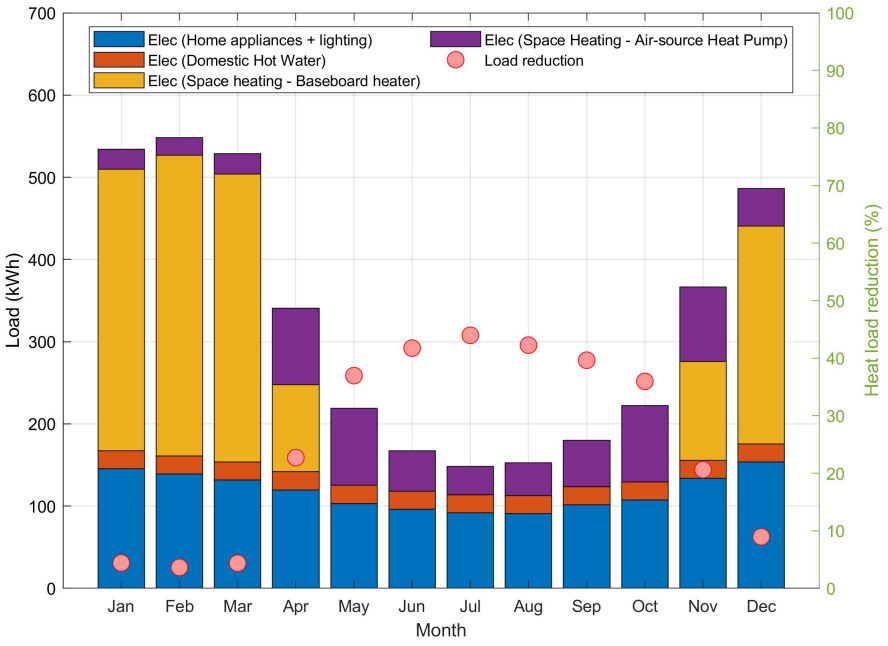

Figure 3.14: Scenario 3 heat load reduction caused by using ASHP and baseboard heater.

the same amount of heat from much less electrical energy. As shown in Fig. 3.14, a heat load reduction of about 40% (by using ASHP) is evident especially during the summer months in Sachs Harbour. However, using ASHP in the Arctic is quite challenging because of its low T_{out} profile (Fig. 3.15). In line with this, a company [126] manufacturing ASHP designed for the Arctic has been researched. The firm claim that their heat pumps can operate even in -20 °C with a COP of 2. For this work, when the T_{out} is below -20 °C, the ASHP shuts off and the baseboard heater kicks in (scenario 3 in Table 3.8).

In spite of the heat load reductions observed in Fig. 3.14, the hourly load fluc-

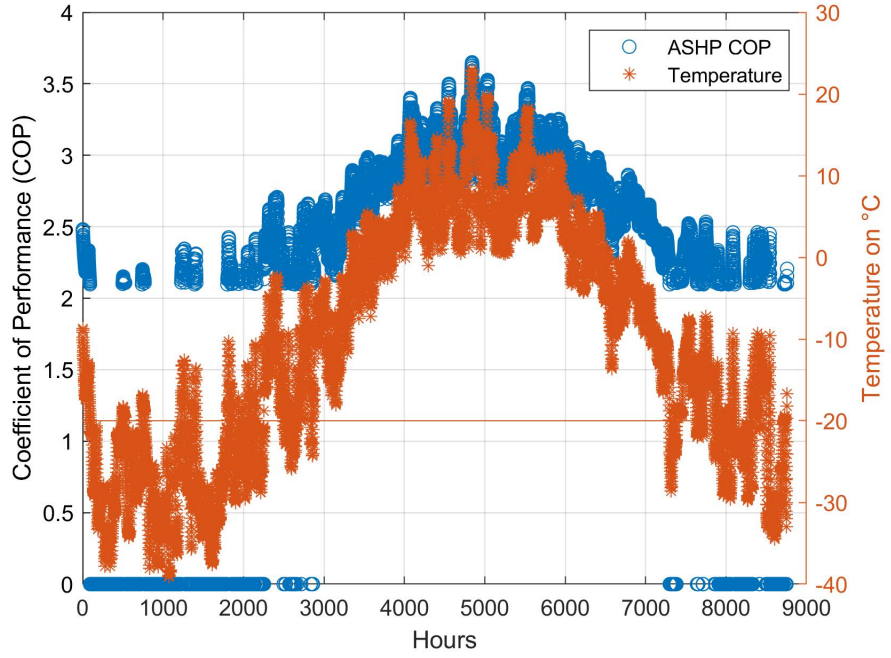

Figure 3.15: COP of ASHP in scenario 3; ASHP shuts off when outside temperature drops below -20 °C.

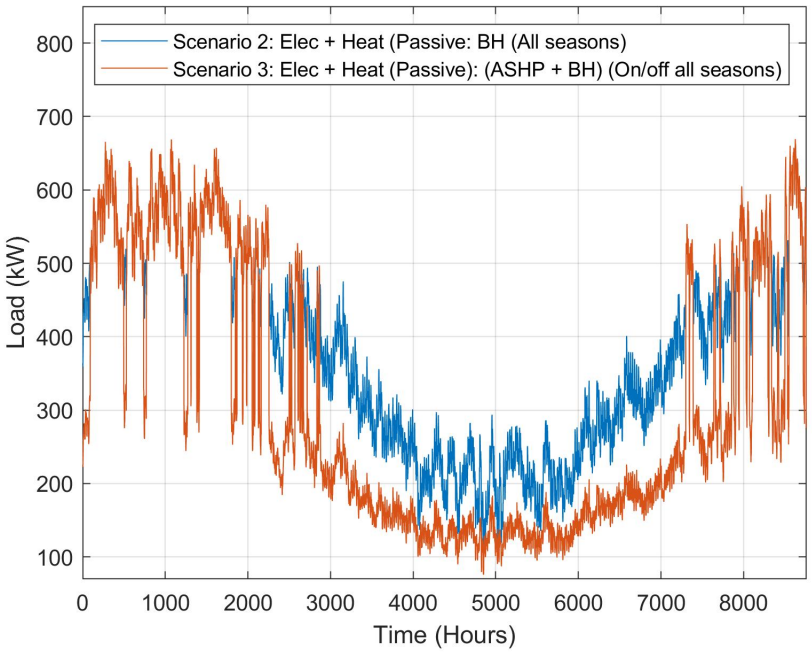

Figure 3.16: Hourly load fluctuations as the ASHP shuts off and the baseboard heater kicks in.

tuations (Fig. 3.16) caused by the on and off operation of the ASHP has a negative impact on the energy system. In particular, this resulted in an increased BT capacity (and a significant step-change at the tail end of the Pareto front) in order to handle the mismatch and fluctuations in the energy demand. From Fig. 3.17,

it can be seen that the optimal subcomponent capacities (DG and RE) of the 100 population/individuals (also known as the GA solutions) in the Pareto front of scenarios 2 and 3 are similar. This is also the case for the BT storage except for the last solutions/points at the tail end of the Pareto front. For example in scenario 2, the second to last solution in the Pareto front has a DG and BT storage included in its optimal system configuration. However, for lower than the optimal DG and BT capacities, the model can no longer find a non-dominated optimal solution where both DG and BT are acting as back-up sources of power. This is influenced respectively by the lower and upper bounds of the discrete optimization variables in Table 3.2; the constraints formulation, the two objective functions in the model, and the peak loads of the energy demand (to be explained subsequently on this section). As a result, the MINES model selected a zero DG capacity (lower bound in Table 3.2) for the last point in the Pareto front but it increased the BT storage capacity to compensate for the unavailability of the DG. This behaviour is consistent with the observed $fuel_{cons}$ variations in Fig. 3.11.

The amount of increase in BT capacity depends on the two peak loads present on the energy demand. In Fig. 3.18(a), non-parametric bimodal distributions of the integrated electrical and thermal loads are evident. In statistical terms, this bi-modal distribution, specifically the difference of the two maxima in scenario 2 is less than that of scenario 3. Hence, the optimal BT capacities at the tail end of scenario 3 is almost doubled as the difference of the two peak loads is also doubled (the same reason applies for scenario 2 as shown in Fig. 3.18).

The on and off operation of the ASHP may not be practical in real-world applications. Thus, scenario 4 (Table 3.8) has also been investigated. Under this case, the ASHP only operates during summer as ambient temperatures are more likely not below -20 °C. For the rest of the year, the baseboard heater runs. In Fig. 3.19(a)-(b), the resulting Pareto front and the objective function variations (whisker plots) of scenario 4 are almost the same as that for scenario 2 since the simulated energy demand is the same except during summer (as affected by the ASHP operation). However, it is observed in Fig. 3.19(c) that the Pareto front for scenario 2 is still more optimal than that for scenario 4. As described in the previous discussion, the fluctuation of loads caused by the variation of the ASHP's COPs resulted in a slight cost difference for the energy system, particularly due to the increase in BT storage capacity. This hourly variation of the COP in relation to the T_{out} has also been observed to affect district heating systems operation in a study made by Pavicevic et al. [127]. Their study, however, did not look at the impact upon the BT storage or upon the integrated energy system as a whole.

3.3.2 Building enclosure-focused approach

As described in Section 1, a household is considered to be fuel poor when it spends more than 10% of its net income on utilities. The Canada Energy Regulator's recent study [13] found that households in the Atlantic provinces and Saskatchewan experience the highest incidence of fuel poverty in Canada with rates of 13% and 10%, respectively. Notably, the Northern territories were excluded from this provincial-scale fuel poverty research because of the unique energy challenges faced by the people in the Arctic region. Paradoxically, the estimated fuel poverty rate in the North is about 8% using the average household utility expenditures data from CanmetEN-

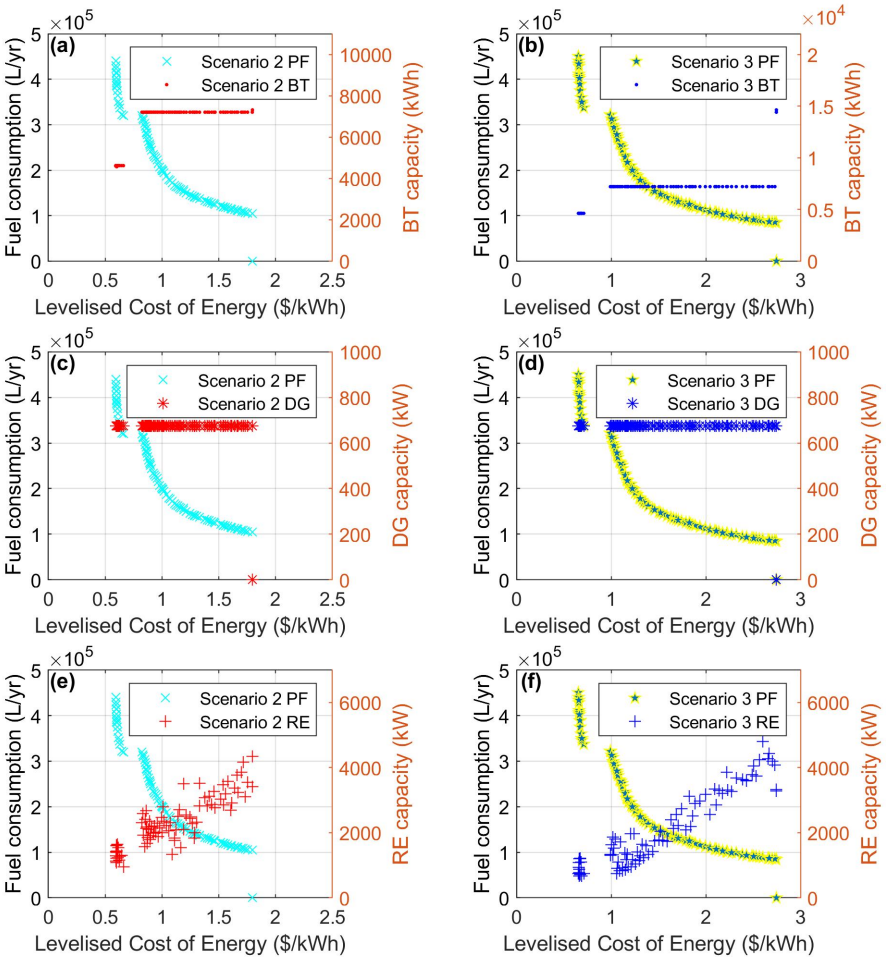

Figure 3.17: Comparison of subcomponents optimal capacity with Pareto front (PF) for scenarios 2 and 3: (a) BT storage - Scenario 2; (b) BT storage - Scenario 3; (c) DG - Scenario 2; (d) DG - Scenario 3; (e) RE - Scenario 2; (f) RE - Scenario 3.

ERGY [8]. However, it has to be noted that this includes a significant government subsidy for household utility bills.

To address fuel poverty impacts, provincial and federal governments have introduced energy efficiency programs especially for low income households [13]. In line with this, Efficiency Canada also launched its first Provincial Energy Efficiency Policy Scoreboard on 2019 [128] in order to assess policies and the overall energy efficiency performance of the country. However, the Northern territories have been excluded from the research conducted for the country's fuel poverty situation.

With this framing in mind, this section aims to give an overview of the impact of using less energy (through building enclosure improvements) to achieve the same or better energy services at lower cost and carbon emissions.

In the scenarios presented in Section 3.3.1.1, two types of building enclosures as a function of their whole-building U-values were evaluated in the MINES model. These two U-values (0.5 and 0.13) correspond approximately to the performance of a normal and passive building respectively in Sachs Harbour. The characteristics of a passive building varies depending on certain building standards. The Interna-

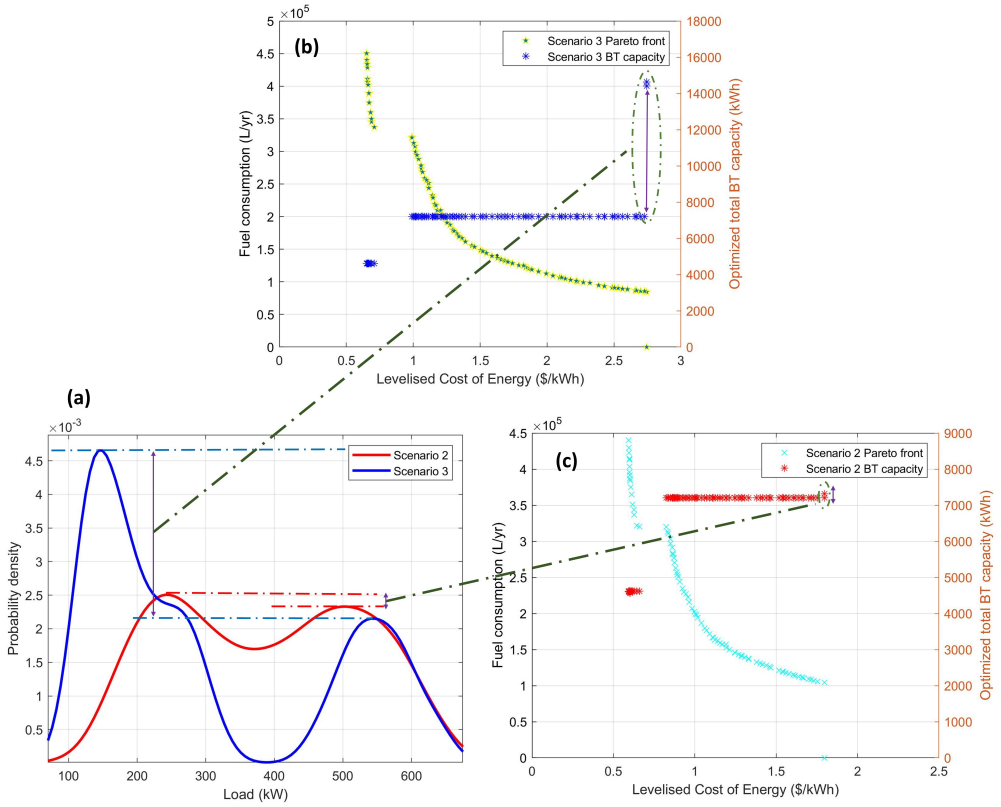

Figure 3.18: Comparison between scenario 2 and 3 optimization results: (a) Non-parametric bimodal distributions of integrated electrical and thermal loads; (b) Scenario 2 Pareto front with corresponding optimized BT capacity per population in GA; (c) Scenario 3 Pareto front with corresponding optimized BT capacity per population in GA.

tional Passive House Institute and the Passive House Institute US are two of the main organizations working on constructing high-performance building enclosures specifically in North America [129]. They administer similar Passive House criteria that might differ depending on climate zone and other factors.

Fig. 3.20 shows the projected energy saved by using high-performance building enclosures in Sachs Harbour. Reduced load estimates through other common methods of improving building performance such as installation of Mechanical Ventilation with Heat Recovery (MVHR) and maximizing air-tightness has also been conducted and the results are listed in Table 3.9. However, outputs show that improving the elements of building's enclosure (defined by its U-value) has the highest calculated load reduction (40%) as compared with the other two methods. Hence, it has been selected to be the focus of this section and it was reflected in the performed scenario evaluations in the model.

High-performance enclosures also impart significant benefits apart from reduced energy demand. In particular, the results of this approach offer thermal comfort and increased resiliency to extreme temperature events and power outages which are common among remote communities in the Arctic.

Table 3.10 lists the investment costs of improving building enclosures for new buildings, maintenance of existing buildings (plaster repairs, facade coating), and energy efficiency refurbishment of existing buildings (12 cm external insulation)

Table 3.9: Most common methods to improve energy performance among buildings.

Method	Metric	Normal Building	Passive Building	Heat Load Reduction
Use high insulation materials	U-value (W/m^2-K)	0.5	0.13 [130]	40%
Install MVHR	α_{hr} (%)	0	75 [131]	16%
Maximize airtightness	η_v (1/h)	0.4	0.3 [87]	6%

Table 3.10: Investment costs involved in building enclosure improvements [132].

Insulation thickness (Type)[a]	U-value[b]	Investment costs[d](CND \$/m^2)	
		Mean[c]	Best practice
30 cm (N)	0.15	407.31	334.74
20 cm (N)	0.20	327.72	311.34
16 cm (N)	0.23	297.29	278.56
12 cm (ER)	0.28	273.88	262.18
0 cm (M)	0.85 - 1.1	81.93	81.93

[a] N (New buildings); M (Maintenance of existing buildings – plaster repairs, facade coating); ER (Energy efficiency refurbishment)
[b] W/m^2-K
[c] Mean value from surveyed companies
[d] The present value (year 2020) of the investment costs were calculated using an inflation rate of 3.5% from 2004 (study from Jakob [132]).

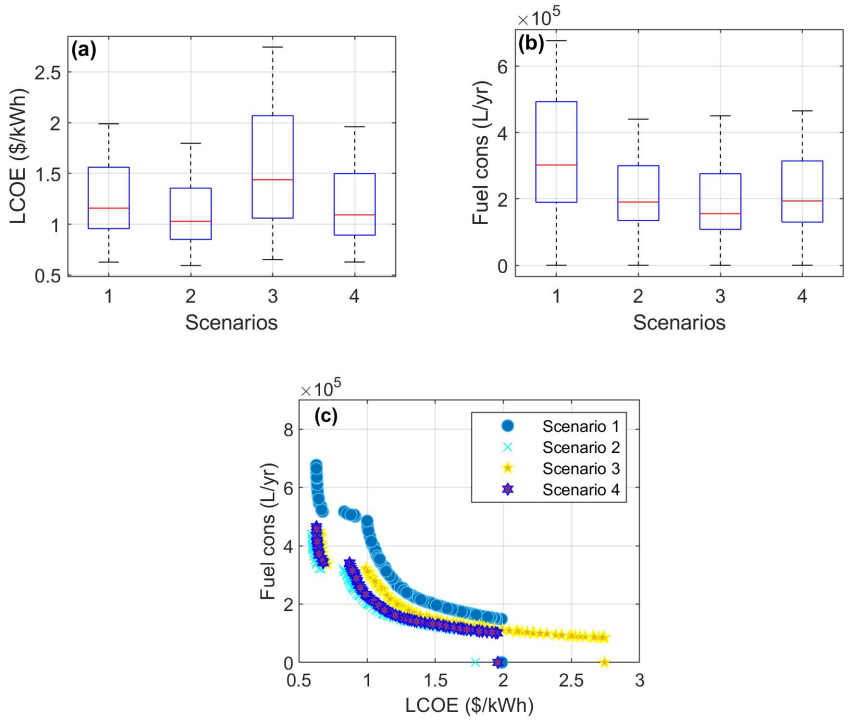

Figure 3.19: Design optimization results for the four scenarios: (a) Whisker plot showing the objection function variation of LCOE; (b) Whisker plot showing the objection function variation of fuel consumption; (c) Pareto fronts.

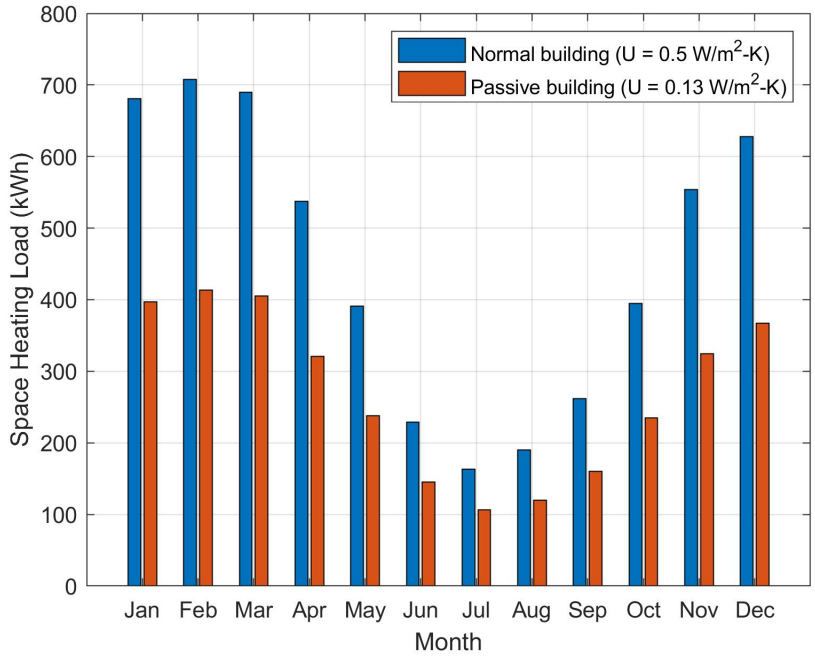

Figure 3.20: Average space heating load per month for the community of Sachs Harbour for using high-performance building enclosures.

[132]. With this data, the system configuration having the lowest $LCOE$ in scenario

2 was evaluated in the MINES model while looking at varying building enclosure improvements and its impact on cost and the overall performance of the energy system. Fig. 3.21(a) shows that the investment costs for building enclosures is relatively cheaper than investing in RE technologies. Further, Fig. 3.21(b) presents the robustness of the optimal configuration result against RE fluctuations and the variations of energy demand as impacted by the U-values of the specific types of building enclosures. It can be observed that the new building standards (U-values of 0.15, 0.2 and 0.23) and the energy efficiency refurbishment of existing buildings (U-value of 0.28) can withstand these variations while ensuring adequate supply of power and having approximately 0% $LPSP$ (0% - 0.24%) across the four U-values implemented in the model. This increase in $LPSP$ was affected by the increased space heating load as the U-value of the building increases. As a result, the capacity factor of the DG increased, but not enough to supply all the demand, especially to U-values ranging from 0.85 - 1.1 (maintenance of existing buildings). This increase in power output from the DG resulted to an increase on the LCC of the system. Note that this result is heavily influenced by the availability of investment costs data for building enclosures.

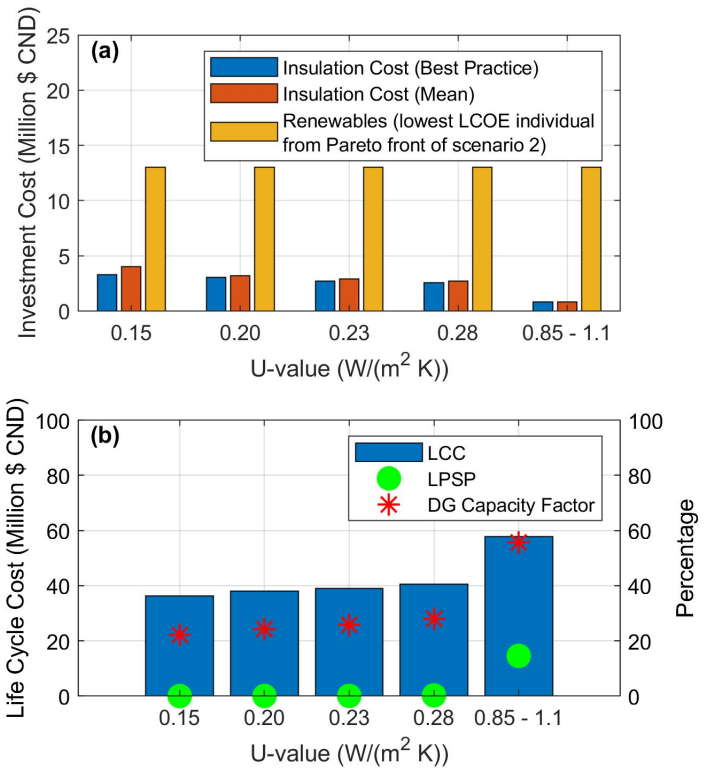

Figure 3.21: Projected impact of varying insulation thickness as a function of the building's U-value: (a) Investment cost; (b) Energy system performance (LPSP, DG capacity factor and LCC).

3.3.2.1 High-performance building enclosures versus renewables

It should be noted that in theory, the LCC savings from implementing a building enclosure-focused approach can be allocated towards investing in RE technology op-

tions for Sachs Harbour. Also, the reduced loads can reduce both the fuel poverty incidence in the Arctic region of Canada, as well as the level of public energy subsidies within such communities. However, prioritization as to which (or both) energy solution should be adopted must be considered in the context of the decision making processes of the various relevant stakeholders in the North. In this context, Fig. 3.22 presents an inverted pyramid concept for the implementation of the three main energy solutions relevant to both Northern Canada as well as for remote communities in general. Reducing loads and using energy efficiently are given preference as these are low-cost energy solutions compared to building energy systems with intermittent RE resources. These energy solutions are also not so dependent on complex energy management systems and can conform with existing and future upgrades in the energy system of specific communities. Hence, they must all be given consideration when implementing energy transition strategies, especially in challenging contexts such as the Arctic regions.

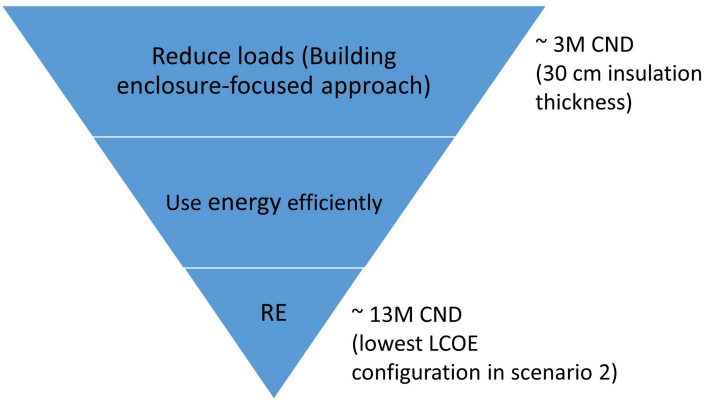

Figure 3.22: The inverted pyramid concept: How energy solutions should be prioritized (figure is adapted from RDH Consulting report [130].)

3.3.3 Balancing the energy trilemma

All of the energy solutions discussed so far in this work are key in holistically addressing energy challenges among Northern remote communities in order to maintain a reliable source of energy, ensure energy affordability, and to achieve deep decarbonization targets. The interplay between these goals can be quantified through the energy trilemma index model to assist decision makers. Huntington et al. [99] argued that the purpose of energy modeling is to produce insights and not just numbers. Hence, the formulated community-scale energy trilemma index model has value in its ability to powerfully communicate whether new policies are hindering or moving towards the desired position (in reference to the three axes) and what interwoven links between various stakeholders are needed to accelerate energy transitions for the community.

The method described in Section 3.2.4 was applied to scenario 2 as it yielded the best optimal results from the optimization process. In particular, the nine solutions of interest were assessed and the results are listed in Table 3.11 with the graphical representation shown in Fig. 3.23. The ranking process, the weightings applied, and the number of solutions evaluated in the Pareto front may vary depending on the insights and perspectives required from the energy model itself.

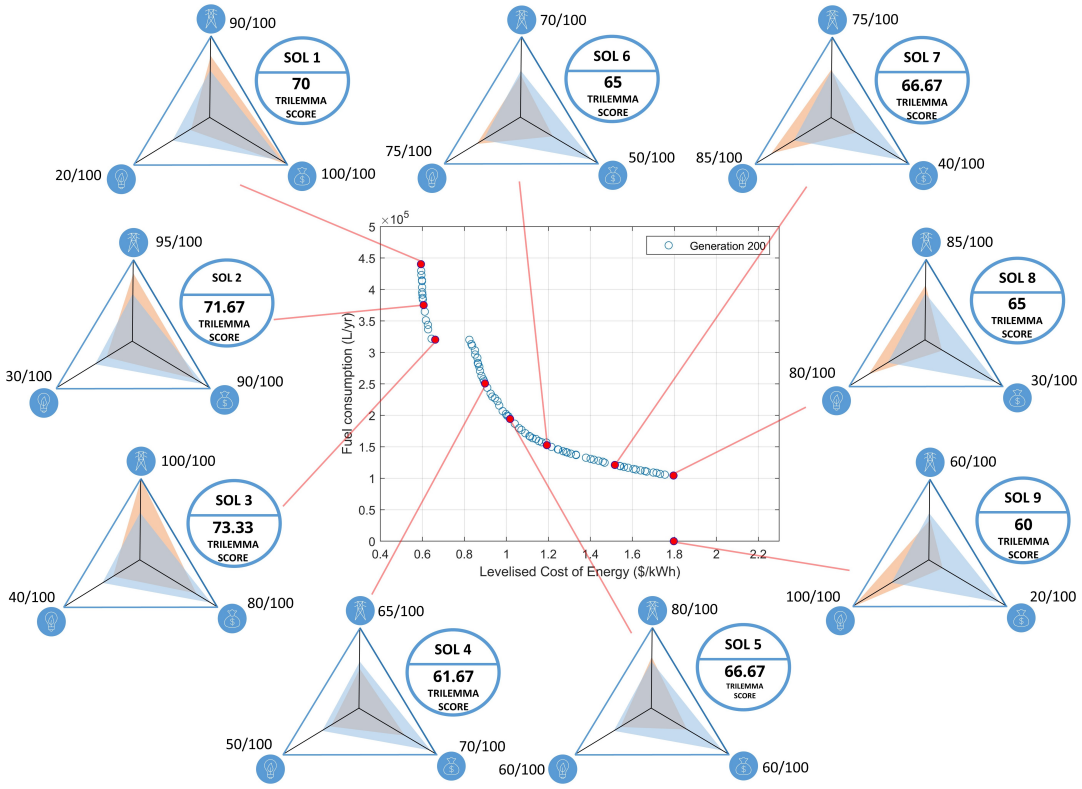

Figure 3.23: Energy trilemma index score (orange region) of scenario 2 overlaid on Canada's energy trilemma score (blue region).

As depicted in Fig. 3.23, solutions 1 - 3 have excellent scores in terms of the energy security and energy affordability indicators. However, it performed poorly on the third dimension, energy sustainability. In contrast, solutions 6 - 9 yielded best results in terms of the sustainability axis but the increased RE capacities and the high costs involved for these solution sets, negatively impacted its overall trilemma score. In particular, the energy affordability indicators are preferable from the first three solutions mentioned previously. The solutions at the middle of the curve (solutions 4 - 6) seem to perform satisfactorily in all three dimensions but their average trilemma score is significantly lower than that of the first three solutions. Overall, solution 3 garnered the highest weighted average trilemma score of 73.33 in comparison with the other eight solutions of interest. However, its overall trilemma score can still be improved by testing new milestones or policies in reference to the energy sustainability indicators. For example, applying an appropriate price to carbon emissions [101] might be a suitable trajectory to address this issue.

Similar to the multi-objective optimization results discussed in Section 3.3.1, balancing the three dimensions of the energy trilemma involves trade-offs. Thus, one goal for the modeler is to analyze these trade-offs and translate these into policy insights.

3.3.4 Results validation

As this work involves modeling of complex engineering systems, it is important to compare the results of the MINES model to other validated energy modeling tools with similar characteristics. This validation approach has been lacking in other

Table 3.11: Rank and scoring table of the community-scale energy trilemma index model relative to the 9 solutions of interest (can be adjusted by the modeler) in the Pareto front.

Solution	Security	Affordability	Sustainability	Overall Score	Rank
1	90	100	20	70	3
2	95	90	30	71.67	2
3	**100**	**80**	**40**	**73.33**	**1**
4	65	70	50	61.67	8
5	80	60	60	66.67	4
6	70	50	75	65	6
7	75	40	85	66.67	4
8	85	30	80	65	6
9	60	20	100	60	9

Table 3.12: Validation of simulation results with HOMER.

Parameter	Unit	Simulation results		
		HOMER	MINES	% Error
P_{pv}	kWh	506,195	506,498	0.06%
P_{w}	kWh	2,475,542	2,456,400	0.78%
P_{DG}	kWh	1,244,238	1,252,891	0.70%
SOC[a]	%	554,923	551,087	0.70%
CC	CND $	15,417,200	15,417,200	0%
$LCOE$	CND $/kWh	0.6139	0.5932	3.36%
LCC	CND $	36,965,330	35,721,900	3.36%

[a] For the sake of comparison, SOC per timestep was summed up for one whole year and compared to HOMER.

studies that involved energy system modeling.

In this work, the HOMER tool has been chosen to validate the results of MINES as it has been widely used and accepted in academia and industry (Section 3.1.1). Note that the respective model outputs cannot be compared directly, as HOMER employs single-objective optimization versus the multi-objective technique of this study. Instead, the simulation results were analyzed and compared. From Fig. 3.23, solution 1 has been selected and its configuration parameters were run in HOMER. The tool delivered results (with percentage errors for each) as shown in Table 3.12. This comparison shows consistent agreement across all parameters, and indicates successful validation of the optimization algorithm of the MINES model given the simulation and optimization algorithms are interlinked based on the modeling framework presented in Fig. 3.4.

3.4 Conclusions

The results presented in this work have been shown to have significant value in holistically addressing multi-domain energy challenges and candidate solutions in Northern remote communities of Canada and beyond. This work examined the interplay between three energy modeling approaches, namely: (1) supply side design optimization of integrated energy systems with intermittent RE resources and BT storage; (2) demand side impacts of building enclosure-focused approach; (3) energy trilemma enabling a quantitative trade-off between results from the two approaches and understanding its impact with the energy trilemma index model.

A multi-objective modeling framework was applied in this study to evaluate the complex trade-offs in designing integrated energy system. This technique offers comparison of a diversity of solutions between two conflicting design objectives to better support practitioners and policy makers. Based on the optimization results, a fully hybrid PV-WT-BT-DG-CONV solution has been proposed. Multiple systems of this configuration were found to be viable according to the resulting Pareto front, but each solution is unique and has to be analyzed considering real-world applications.

Viable heating alternatives were also investigated. As compared with electric baseboard heaters, ASHP can reduce space heating load by up to 40%. However, load fluctuations from the hourly variation of the heat pump's COP as influenced by the outside temperature were observed to negatively impact the overall performance of the energy system. In particular, this resulted in larger BT storage capacity components. The increase in BT storage was also found to be greatly affected by the peak load of the community. The constraints formulation, objective functions, and the discrete decision variables also influenced this result.

In conjunction with the previously mentioned optimization results, methods for improving building performance such as installation of MVHR, maximizing air-tightness, and optimizing building enclosures were also evaluated in the MINES model. Varying building enclosure characteristics (from normal to passive) were found to produce the highest building performance by reducing the space heating load by about 40% annually as compared with the other two methods pointed out earlier. Hence, it has been applied in the scenarios run in the model. The building enclosure-focused approach also offers non-energy benefits such as thermal comfort and increased resiliency in extreme temperature events and power outages.

Lastly, incorporating the results from the design space optimization and the impact of utilizing high-performance building enclosures provides a vast range of energy solutions for communities in Northern Canada. However, determination of which energy solutions to prioritize should also be considered in the decision making process of the community. Central to this aspect is the formulation of the community-scale energy trilemma index model. This tool processes the results from the MINES model, and quantifies various stakeholders' viewpoints by balancing the dimensions of the energy trilemma. For example, solution 3 from scenario 2 achieved the highest trilemma score of 73.33 in comparison with the other eight solutions of interest. It was highlighted that this weighted average trilemma score can still be improved by testing new milestones and policies affecting the energy situation of the community.

Chapter 4

Towards robust investment decisions and policies in integrated energy systems planning: Evaluating trade-offs and risk hedging strategies for remote communities

This paper was submitted and under review in **Applied Energy** journal:

M. R. Quitoras, P. Cabrera, P. Elia, P. Rowley, and C. Crawford, *"Towards robust investment decisions and policies in integrated energy systems planning: Evaluating trade-offs and risk hedging strategies for remote communities,"* Applied Energy *(under review).*

CRediT authorship contribution statement[1]

Marvin Rhey Quitoras: Conceptualization, Methodology, Software, Validation, Formal analysis, Investigation, Resources, Data curation, Writing - original draft, Visualization, Funding acquisition

Pedro Cabrera: Formal analysis

Pietro Elia Campana: Writing - review & editing

Paul Rowley: Conceptualization, Writing - review & editing

Curran Crawford: Conceptualization, Writing - review & editing, Supervision, Project administration, Funding acquisition

This chapter expands further the modeling framework described in Chapter 2 and 3. In particular, multiple overlapping uncertainties were integrated in the energy model in order to inform energy policies and investment decisions for Indigenous communities in the North. Varying risk attitudes of decision makers towards uncertainties were also taken into account and demonstrated. Policies to enhance Indigenous-led energy projects, and how to promote synergies between various stakeholders in the North were highlighted in this chapter as well.

[1]Refer to Appendix B for description

Abstract

Policy and investment decisions in transitioning remote communities towards clean sources of energy require innovative modeling approaches to capture uncertainties that impact overall performance of their integrated energy systems. This work introduces a novel robust modeling framework to enhance decision making process in energy systems planning, while taking into account decision-maker attitudes towards multiple overlapping uncertainties and various energy solution philosophies. In particular, multiple energy system configurations were evaluated by simultaneously minimizing the levelised cost of energy and fuel consumption for a specific community in the Northwest Territories of Canada. Combining the concepts of robustness and the stochastic nature of uncertain parameters in this multi-objective optimization framework elucidates the full spectrum of energy solutions available in the Arctic. Introducing known uncertainties in renewable energy characteristics was found to reduce the overall energy yields from the renewable energy technologies. For example, the deterministic renewable energy penetration of 69% from a specific energy system configuration reduced to a mean of around 51% after the inclusion of uncertainties via probabilistic simulation. Conversely, fuel consumption increased to 750,000 L/yr (mean) from its initial deterministic value of 447,470 L/yr. Holistic energy solutions which include not only supply aspects but also demand side considerations are also discussed. Specifically, a reduced community heating load of 40% was achieved via retrofit of high performance building fabric enclosures, and is described in conjunction with renewable energy supply options. Ultimately, insights and real-world applications have been synthesized to provide coherent recommendations on strategies to address energy security, energy affordability and environmental sustainability, along with meaningful propositions towards Indigenous peoples-led energy projects.

Keywords

Energy policy; Robust optimization; Uncertainty; Risk hedging strategies; Indigenous peoples; Energy sovereignty

4.1 Introduction

Understanding the dynamic complexities of energy systems, the long term consequences of investment decisions, and the critical role of implementing robust policy frameworks requires innovative approaches in dealing with energy systems planning uncertainties. Krey and Riahi [133] expounded that ignorance with respect to the multitude of uncertainties can be very costly, and highlighted the significance of improved capturing of the trade-offs and risks resulting from multiple systemic uncertainties. However, despite these risks, the challenges of understanding, assessing and communicating impacts of uncertainties for energy system policy makers remain significant and are poorly evaluated in previous research [134].

For example, Canada and 194 other countries of the United Nations Framework Convention on Climate Change reached a landmark agreement ("Paris Agreement") during the Conference of Parties 21 to accelerate and intensify the actions and investments needed for a sustainable low carbon future [135]. The goal of the agreement was to strengthen the global response to avoid the catastrophic effects of climate change by keeping a global temperature rise to well below 2°C and pursue preventive efforts to limit the increase to 1.5°C. According to Perera et al. [4], failure to address climate change mitigation and adaptation could specifically impact built and natural systems, leading to serious short and long-term issues, including partial or total energy supply disruptions. If not properly addressed, these consequences could be even worse in remote Arctic communities due to extreme climate events in the region. Hence, effective energy policies should consider multiple overlapping uncertainties encompassing impacts of climate change on extreme weather events, variability of power supply sources, and changing energy demand profiles, among others.

Focusing upon a a community in the remote Arctic region of Canada, this study demonstrates the importance of assessing uncertainties in developing a holistic energy modeling framework, and illustrates impact on energy policy and investment strategies from a broader perspective. Holistic energy considerations and trade-offs in transitioning Arctic communities from fossil-fuel dependency is also taken into consideration, while balancing the trilemma of challenges [136] relating to energy security, energy affordability and environmental sustainability.

4.1.1 Literature review

The literature survey conducted for this work presents an overview of existing energy policies and initiatives in reducing diesel dependence in Northern Canada. Further, this section describes techniques in modeling uncertainties in energy systems optimization as it is critical in designing strong policies and will inform decision making across various levels in achieving energy transitions.

4.1.1.1 Overview of energy policies in the Canadian North

To identify existing energy policies that accelerate and support energy transitions, a cross-Canada scan of diesel reduction initiatives and clean energy policies has been conducted by the Pembina Institute [137]. The study particularly focused on policies, programs and regulations that impact energy systems in remote Indigenous

communities at the federal, provincial, regulatory and utility levels. The three territories in the North[2] have various strategies to increase energy security and ensure affordable cost of energy, while transitioning to a lower-carbon economy. For example, the existing initiatives and policies designed for reducing diesel dependence in the NWT include [138]:

- Alternative Energy Technologies Program - provides funding for communities and commercial businesses in developing RE projects such as solar, wind, wood pellet heating, and biofuel/synthetic gas, among others;
- Community Government Building Energy Retrofit Program - supports upgrades to community government-owned buildings in order to reduce electrical and heat loads;
- Commercial Energy Conservation and Efficiency Program - encourages commercial businesses to conserve energy and improve their energy efficiency in the form of rebates;
- Energy Efficiency Incentive Program - designed to provide rebates for residents and non-profit organizations after purchasing energy efficient appliances, heating appliances, LED light bulbs, and drain water heat recovery systems;
- Net Metering - allows customers of the Northwest Territories Power Corporation (NTPC) to generate their own power and then send any surplus in the electricity grid of their community.

It should be highlighted that there is no documented Independent Power Producer (IPP) policy in the NWT, and IPP project proposals are subject to government and utility negotiations (to be further discussed in Section 4.3.4). A community-oriented IPP policy that offers competitive Power Purchase Agreements (PPAs) would potentially facilitate Indigenous community-led energy projects. For this reason, the Pembina Institute argued that the NWT is a critical jurisdiction in Canada given the number of Indigenous remote communities (Table 4.1) in the Territory [137].

4.1.1.2 Modeling uncertainty

Policy frameworks to meet decarbonization targets and energy security goals must contend with multiple and overlapping uncertainties [134]. Usher and Strachan [140] emphasized that previous studies on energy systems modeling have failed to address the significant uncertainties surrounding many aspects of the transition to a low-carbon future in an integrated and systematic manner. They argued that this is the result of: (i) challenges involved in applying solely a deterministic approach to a complex and multi-faceted problem that is inherently uncertain, and (ii) the issues associated with so much effort being input by the energy modeling community on pathways and technologies rather than uncertainties. Pfenninger et al. [141] provided a comprehensive study of current challenges on energy systems modeling

[2]The North in Canada politically refers to the territories of Yukon, Northwest Territories (NWT) and Nunavut; the use of the term Canada's Arctic for this work is inclusive of the three territories mentioned.

Table 4.1: Number of PPAs among Indigenous remote communities in Canada [139].

Jurisdictions	Number of communities[a]	Number of PPAs (inc. net metering)	Project types
British Columbia	25	4 current 3 developing	Micro-hydro Solar Biomass
Alberta	7	0 current	N/A
Saskatchewan	1	0 current	N/A
Manitoba	4	0 current	N/A
Ontario	25	7+ current 2 developing	Solar
Quebec	19	0 current	N/A
Newfoundland	16	0 current	N/A
Yukon	21	0 current 1 developing	Wind
NWT	26	1 current	Solar
Nunavut	25	0 current	N/A

[a] Indigenous remote communities - comprised of First Nations, Metis or Inuit peoples of Canada.

and efforts being taken to address them. One of the concerns they highlighted was in addressing the growing complexity of energy systems in terms of optimization approaches across various scales (spatial resolution), as shown in Fig. 4.1. From a modeling perspective, scale pertains to the boundary of a modeled system, so large-scale energy models cover an entire continental region with coarse temporal resolution, while small-scale energy models look at a residential or community level with a high temporal resolution. The inherent trade-offs in resolutions and simplifying assumptions influence the level of uncertainties in model outputs due to the associated computational demands in solving energy system optimization problems.

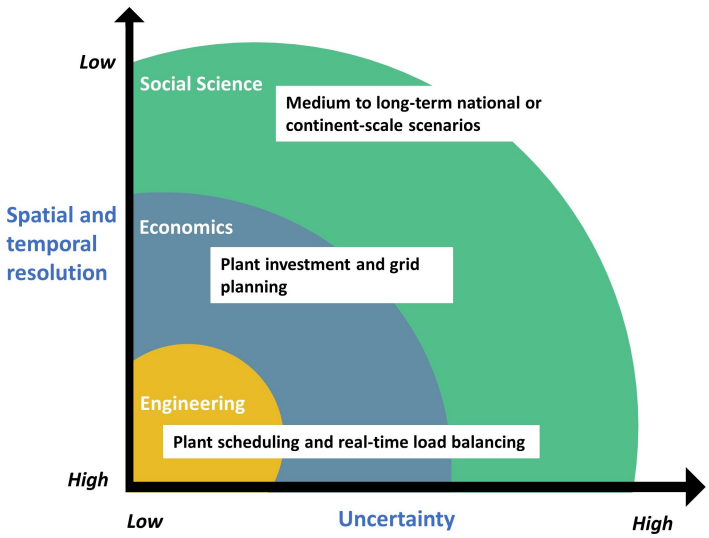

Figure 4.1: Optimization complexity across various spatial and temporal scales; adapted from [141].

In the majority of previous studies involving energy systems modeling, uncertainties are typically treated by performing sensitivity analyses for a given range of input parameters. This approach provides understanding of the uncertainty space and to a certain extent, the future risks involved in understanding the complexities of an integrated energy system. However, this approach should be complemented with further analysis exploring the impact of uncertainties in a non-deterministic fashion. For example, Mavromatidis et al. [142] conducted research on designing a distributed energy system for a Swiss neighborhood by performing two-stage stochastic programming that included multiple objective functions to capture decision-maker preferences on risks resulting from uncertainties. Hamarat et al. [143] focused on multi-objective robust optimization in specifying appropriate conditions for adapting energy policies by exploring transition pathways that lead to satisfactory results across a large ensemble of scenarios in the European Union. Similarly, Majewski et al. [144] carried out a minmax robust multi-objective optimization, through a mixed-integer linear programming formulation, to identify the trade-off between economic and ecological criteria in designing sustainable energy systems.

Reliability-based optimization (RB), meanwhile, is another optimization technique suitable for use in the presence of uncertainty. This method aims at finding the best solution that satisfies the constraints with a specified probability distribution [145]. Clark and DuPont [146] applied this approach in decreasing operations and maintenance costs in designing offshore renewable energy systems. Chu et al. [147] expanded the RB optimization process by creating surrogate models with metaheuristic methods such as genetic algorithm and simulated annealing. Despite the evident advantages of RB optimization, its real-world application is quite challenging due to high numerical costs involved in its solution of the reliability constraints [148].

In previous Arctic energy system studies, Ringkjob et al. [149] presented a stochastic long-term (2015 - 2050) energy model for a remote Arctic settlement in Longyearbyen, Svalbard. The TIMES modeling framework was employed. This model followed a linear programming approach to minimise the total system cost. The inherent trade-off of this long-term energy system analysis is its inability to track in detail the performance of each energy system component over the whole modeling horizon because of the computational expense of the energy model. Similarly, a high-level energy optimization study was presented in a work made by Chen et al. [150] for the Yukon territory in Canada. An inexact chance-constrained mixed integer model for mitigating Greenhouse Gas Emissions (GHG) was developed to investigate uncertainties for capacity expansion alternatives within the territory.

4.1.2 Research gaps and research questions

The literature survey indicates that various techniques for assessing uncertainties in energy systems modeling are available. However, executing such approaches and implementing them in the evaluation of a range of holistic energy solutions, especially in the Arctic region, are generally scarce. In general, previous work has taken a high-level focus on renewable energy (RE) pathways rather than looking at: (i) a wide array of energy solution initiatives (both supply and demand aspects), (ii) the technical details on the variability of the RE resources, and (iii) the types of energy storage available for both electricity and heating. The world's Northern re-

gions are unique and failure to incorporate these factors would have an impact on their energy system transitions because of the long time spans that these transitions require. Further, previous analyses on uncertainty modeling were found to be limited in terms of generating insights and recommendations from the energy model outputs, and designing adaptive and robust energy policies to accelerate energy transitions. Hence, this work builds upon the previous work of the authors in [151] wherein holistic energy solutions were introduced for the Canadian Arctic, balancing decision makers' diverse and multiple solution philosophies in addressing the energy trilemma.

With this framing in mind, the overarching research questions for this work are based on the current energy situation in the North as reflected in previous Energy Charettes[3], and the research gaps pointed out earlier. These research questions can be summarized as:

1. How to effectively integrate uncertainties in energy systems modeling in the Arctic given energy resource variability and future climate change impacts in the region?

2. How do extreme temperature events impact battery (BT) storage operation in the Arctic region?

3. How to advance diesel reduction initiatives in Northern latitude communities while considering risks from multiple uncertainties?

4. How can private, government and non-government entities support Indigenous-led energy projects?

4.1.3 Study objectives and key contributions

The main aim of this work is to bridge the gaps in previous research by establishing methods to address uncertainties in energy systems modeling, while taking into account coordinated climate and energy policies from the private sectors, Indigenous communities, governments, utilities, regulators, and other stakeholders. In particular, the four key research questions as mentioned previously are addressed by the novel contributions of this work:

1. Development of a robust Multi-objective INtegrated Energy System (MINES) model that captures decision-maker attitudes towards multiple overlapping uncertainties in designing integrated energy systems;

2. Assessment of lead acid and lithium-ion BT storage while taking into account impacts of BT capacity decrease from freezing temperatures in cold climate settings;

3. Adaptation of holistic energy solutions in transitioning towards robust and sustainable energy systems while addressing trade-offs and uncertainties in reducing diesel dependence;

[3]Energy Charette is a collaborative planning process where Northern communities, government and non-government organizations, industry, elders, Indigenous peoples, and energy experts come together to develop an energy strategy and plan for the future.

4. Formulation of insights and recommendations on how to address barriers and opportunities in implementing strong energy policies and risk hedging strategies in remote communities.

The rest of the article is organized as follows: Section 4.2 describes the model developed for the study. To demonstrate functionality of the energy model developed in this work, Section 4.2.6 presents relevant information for the case-study community, namely Sachs Harbour in the NWT; the information presented will serve as input data for the model. Section 4.3 summarizes the results of the test case for the method. Section 4.3.4 presents insights and recommendations for policy makers and various practitioners according to the quantitative outputs generated from the model. Finally, Section 4.4 presents the conclusions drawn from this study.

4.2 Methods

The schematic diagram of a prototypical integrated energy system studied in this work is shown in Fig. 4.2. It consists of wind turbine, solar PV, battery storage, diesel generator and a bi-directional converter to facilitate power flows from the DC bus to AC bus and vice versa. Thermal (space heating and domestic hot water) and electrical loads were modeled for each 1 h timestep over a given year.

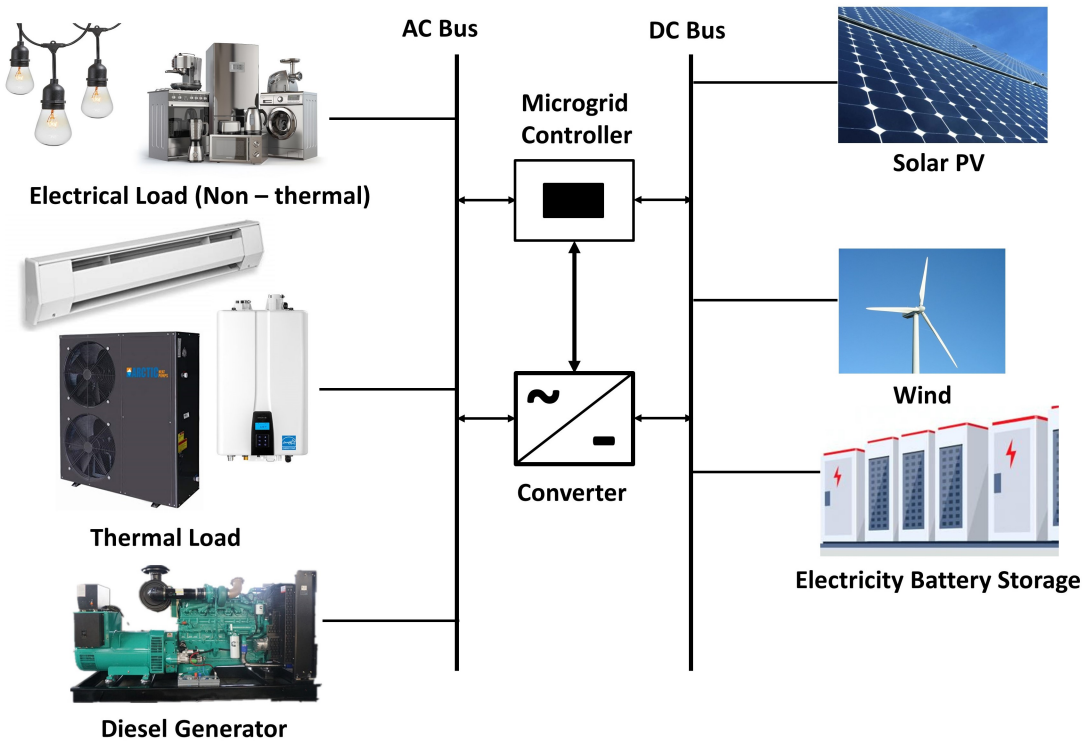

Figure 4.2: Schematic diagram of a prototypical integrated electrical and thermal energy system.

4.2.1 Robust optimization

The MINES model implements a multi-objective optimization approach to capture complex trade-offs in designing integrated energy systems. This technique opens a

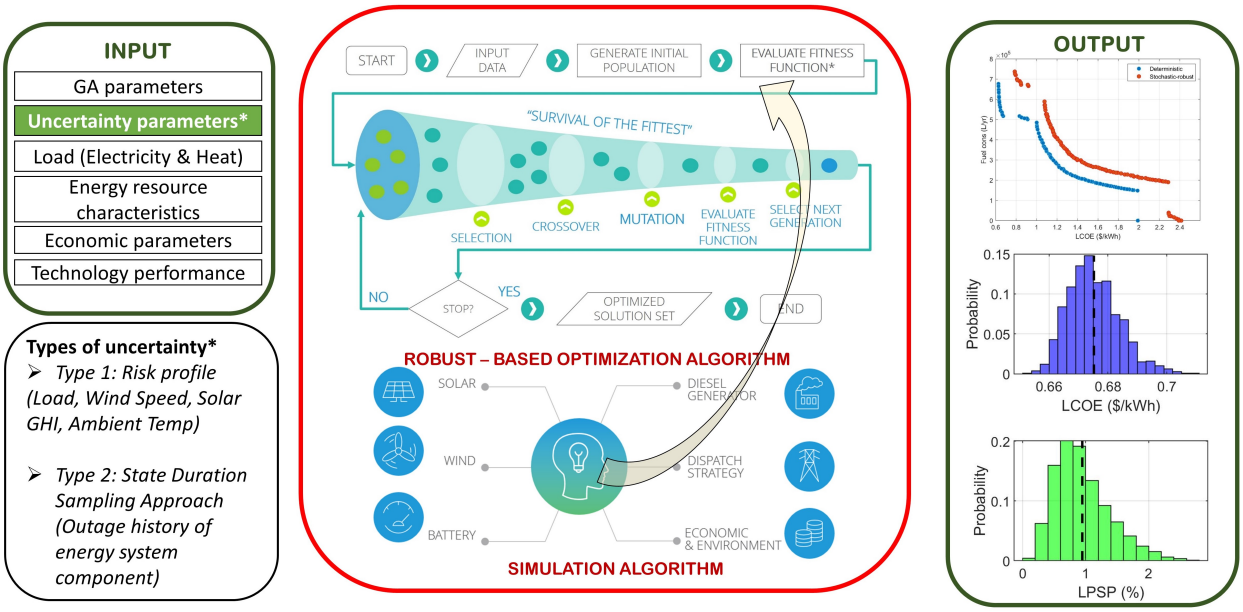

Figure 4.3: Overall energy modeling framework of MINES.

Table 4.2: GA configuration parameters.

Parameter	Description
Algorithm	Variant of NSGA-II [114]
Generations	200
Population	100
Crossover function	Heuristic
Crossover rate(%)	90
Mutation function	Non-uniform
Tournament size	2

diversity of solutions which are critical in capturing various solution philosophies in transitioning remote communities in the Arctic towards sustainable sources of energy. In particular, the Non-dominated Sorting Genetic Algorithm - II (NSGA-II) of Deb et al. [114] was adapted for this study. NSGA-II was selected as it has the generic ability to handle multi-objective trade-offs and Pareto front pursuit as proven in previous studies conducted by Evins et al. [115] and Forde et al. [116]. The set of Genetic Algorithm (GA) input parameters for this work is listed in Table 4.2 and the approach was implemented in a MATLAB® platform.

As discussed in Section 4.1.1.2, reliability and robust-based optimization techniques are two approaches that can be utilized when optimizing energy systems under deep uncertainty. For this work, the robust-based aspect was integrated into the optimization algorithm of the MINES model. There are many notions of robustness, including a good expected performance, a good worst-case performance, a low variability in performance, or a large range of disturbances still leading to acceptable performance [145]. Beyer and Sendhoff [152] conducted a comprehensive survey on robust optimization (RO), and described four types of uncertainties as related to real-world system designs; interested readers are referred to their work.

According to Gazijahani and Salehi [153], the undefined nature and poor avail-

ability of data about uncertain modeling parameters determine the most suitable approach in addressing uncertainties in a decision making framework. They argued that RO is the most suitable optimization technique in controlling the worst possible scenarios in designing microgrids due to the nature and the lack of full information of the uncertainties involved in the energy system. In this paper, a minmax principle was adapted to seek the optimal value of each decision variable under the worst-case realization of uncertainties. The mathematical representation of this concept is presented in Eq. 4.1 [154]:

$$min\Big[\sup_{\Xi} f_1(z,\xi), \sup_{\Xi} f_2(z,\xi), ..., \sup_{\Xi} f_M(z,\xi)\Big] \tag{4.1}$$

where $f_M(z,\xi)$ are the objective functions, $z \in Z$ represents a vector of decision variables, $\xi \in \Xi$ pertains to a vector of random variables, and sup(:) indicates the worst-case scenario of the specific objective function. The worst-case realizations of uncertainties (robust-based optimization) was adopted as it captures the unique considerations of decision makers in Arctic communities. Specifically, important aspects of energy planning in the North relates to catastrophic warming of the Arctic which is at twice the global average rate [30], as also observed in the variability of RE resources and extreme temperature events especially with extended winter conditions in the region. There is also a high possibility of power outages because of delayed fuel deliveries in Arctic communities. For instance, the territorial government had to fly-in 600,000 litres of diesel to the community of Paulatuk, NWT to keep the mostly obsolete diesel generators running during the summer of 2019. This operation cost $1.75 million CND over dozens of flights [16]. Another worst-case condition that RO-based optimization captures is related to the high risk of oil spills during fuel transport and storage. Recently, Norilsk, Russia was under a state of emergency after 20,000 tons of diesel leaks into the Arctic river system [17]. The fuel was intended to be stored for continuous supply of power in an Arctic community in Russia. Further, worst-case realization of uncertainties are critical for grid stability analysis since mathematical representation of actual power systems is based on extreme scenarios [155] in order to avoid grid failure, which is even more significant due to integration of intermittent renewables in isolated Arctic communities.

Aside from energy systems applications, RO has the generic ability to handle a wide variety of optimization problems and has been used extensively on other fields such as internet routing [156], business aircraft [157], machine scheduling [158], and intensity-modulated proton therapy [159], among others. RO has also been implemented in combination with various types of evolutionary algorithms as executed in previous studies done by Goh and Tan [160], Kuroiwa and Lee [161], and Wang et al. [162]. The algorithm behind the MINES modeling framework, NSGA-II, has also been applied in conjunction with RO as introduced by Deb and Gupta [163].

The justifications given for the RO approach and combining it with the multi-objective approach of the MINES model provides decision makers with the ability to balance and analyze trade-offs between investment decisions and environmental impacts of the energy system, while considering multiple overlapping uncertainties.

Table 4.3: Dimension of the discrete variables in the optimization algorithm.

Parameter	Capacity	Quantity	
		Lower Bound	Upper Bound
WT	95, 95, 100, 100 [kW]	0	500
PV	15, 25, 20, 25.025 [kW]	0	500
BT	55, 13.9, 7.37, 9.24 [kWh]	0	500
DG	300, 320, 225, 150 [kW]	0	100
CONV	200, 250, 270, 300 [kW]	0	10
Strategy	LFOS and CCOS	-	-

4.2.2 Quantifying complex trade-offs in the energy system design space

The multi-objective technique of MINES unlocks the full spectrum of energy solutions available in the Arctic. With this approach, a trade-off analysis can be done by analyzing two objective functions simultaneously. In this study, Levelised Cost of Energy ($LCOE$) (Eq. 4.2) [84] was formulated as the first objective function to represent energy affordability as a major concern based on the previous Energy Charettes in the NWT [83]:

$$LCOE = \frac{\sum_{t=1}^{n} \frac{CC_i(t)+O\&M_i(t)+Z_i(t)-S_i}{(1+r)^t}}{\sum_{t=1}^{n} \frac{P_{gen}}{(1+r)^t}} \tag{4.2}$$

where t is time (year), r is the discount rate (%), n is the total life of the energy system (year), CC is the capital cost ($) per unit of the system component i, $O\&M$ is the operations and maintenance costs ($/year), Z is all other costs associated with the project ($/year), S is the salvage value ($), and P_{gen} is the power generated from the energy system (kWh/year).

The DG's fuel consumption ($fuel_{cons}$), as shown in Eq. 4.3, was formulated as the second objective function in the model. This approach leads to a quantitative investigation of trade-offs between alternative sources of energy in the Arctic while observing low cost of energy (first objective function) for the community.

$$fuel_{cons} = F_0 P_{DG,r} + F_1 P_{DG} \tag{4.3}$$

where F_0 is the fuel curve intercept coefficient (L/h/kW$_{\text{rated}}$), F_1 is the fuel curve slope coefficient (L/h/kW), $P_{DG,r}$ is the rated capacity of DG, and P_{DG} is the instantaneous power coming from the DG (kW).

Table 4.3 shows the 11 discrete decision variables implemented in the model. The algorithm for the two operation strategies (Load Following Operation Strategy (LFOS) and Cycle Charging Operation Strategy (CCOS)) was explained by the authors in [110]. Also, the full set of constraints considered to run the optimization

module in MINES are:

$$constraints \begin{cases} LPSP \leq 0\% \\ SOC_{min} \geq 30\% \\ RE_{pen} \geq 30\% \\ P_{excess} \leq 30\% \\ DG_{LF} \geq 30\% \end{cases} \tag{4.4}$$

where $LPSP$ is the Loss of Power Supply Probability (%), SOC is the state of charge of the BT (%), RE_{pen} is the RE penetration (%), P_{excess} is the excess electricity (%), and DG_{LF} is the load factor of the DG (%). The mathematical formulation of each constraint and their respective justifications to include in the model were described previously by the authors in [110]. The component sub-models including the specific technology input parameters (solar PV, WT, BT, DG, CONV) as laid out in Fig. 4.2 were described in detail by the authors in [110].

4.2.3 Uncertainty propagation

Two types of uncertainties were introduced in MINES. The first type refers to the meteorological variables relevant for the community as well its load profile. The second type of uncertainty pertains to the operational reliability of each component in the integrated energy system. The two types of uncertainty ensure robustness of the energy system being proposed for remote communities in the Arctic.

4.2.3.1 Integrating risk hedging strategies in robust optimization

The first type specifically relates to uncertainties from the load profile of the community (P_{load}) as well as various meteorological parameters including Global Horizontal Irradiance (GHI), wind speed (u) and the ambient temperature (T_{out}). The approach is a modified version of the probability analysis being implemented through the improved Hybrid Optimization by Genetic Algorithms (iHOGA) software [164]. The iHOGA commercial software is a well-established tool in optimizing energy systems, both deterministically and probabilistically. Using iHOGA, Zubi et al. [165] conducted a techno-economic assessment of an off-grid PV system for developing regions to provide electricity for basic domestic needs. Dufo-Lopez et al. [166] conducted a similar study by optimizing a stand-alone hybrid solar-diesel-battery energy system for an off-grid health care facility while considering uncertainties from solar irradiance and the load demand. Other applications of the iHOGA software can be found in Fulzele and Daigavane [167], Fracastoro et al. [168], Bernal-Agustin et al. [169] and Cristobal-Monreal et al. [170], among others.

The probability analysis in iHOGA can be performed by taking into account the Gaussian probability distribution of the mean annual values of the system load, solar irradiance, wind speed and water flow (if there is a water turbine in the system). The software performs its simulation by assigning each uncertain parameter with five possible increments/reductions from the original time-series:

- Average
- Average + Standard Deviation

- Average - Standard Deviation
- Average + 3*Standard Deviation
- Average - 3*Standard Deviation

For example, the user can assign Average + Standard Deviation for load, and for the solar irradiance, wind and water flow data, the Average - Standard Deviation. This combination implies that there is an increment from the original time-series of the load data while there is a reduction in the other uncertain variables in reference to the original time-series [164]. In conjunction with the second type of uncertain parameters (relating to system reliability), this paper improves the iHOGA probabilistic technique by explicitly introducing decision-maker risk preferences (captured by a risk coefficient) towards the first types of uncertain parameters mentioned previously, and as shown in Eq. 4.5.

$$\varphi_{new}(t) = \overbrace{\left(\frac{\varphi_{old}(t)}{\varphi_{\mu}}\right)}^{\text{data normalization}} \underbrace{(\varphi_{\mu} \pm Risk_{coeff} \cdot \varphi_{\sigma})}_{\text{discrete samples (increment/reduction)}} \tag{4.5}$$

where $\varphi_{new}(t)$ is the new time-series of the uncertain parameter, obtained from its original mean value (φ_{μ}) and standard deviation (φ_{σ}). The original time-series was divided by its mean to ensure that each time-series will be proportional to the original. It can be observed that when the $Risk_{coeff}$ in Eq. 4.5 is zero, the algorithm reverts to a deterministic optimization (i.e old time-series is active). On the other hand, the probabilistic feature of MINES is active when the $Risk_{coeff}$ is set to a non-zero value. Specifically, this work introduces various risk attitudes of the decision maker towards uncertainty in energy system planning as presented in Table 4.4. The $Risk_{coeff}$ in the risk-averse column in Table 4.4 implies best performance of the energy system (i.e optimal value of the objective functions) against worst-case realizations of the uncertain parameters. Alternatively, the $Risk_{coeff}$ in the risk-seeking column appeals to a relatively more optimistic/risk-seeking decision-maker. An intermediate risk attitudes in the middle column (neither risk seeking nor risk averse) corresponds to a a risk-neutral decision-maker for this study.

The increment/reduction in the second term of Eq. 4.5 also pertains to the discrete samples $\xi_j(\mu_o, \sigma_o)$ of the stochastic variables wherein j is the number of samples (number of realization of uncertainties) and o is the uncertain variable. Through Latin Hypercube Sampling, the algorithm draws a total of j random samples from the probability distribution $\xi_j(\mu_o, \sigma_o)$ represented by its mean φ_{μ} and standard deviation φ_{σ}. Table 4.5 lists the respective means and standard deviations of the uncertain parameters described in this section.

4.2.3.2 Uncertainty on system reliability

To ensure robust operation of the energy system in the Arctic and avoid the possibility of having to fly-in emergency fuel to these remote communities (as what occured in Paulatuk, NWT during the summer of 2019 [16]), the $LPSP$ has been set to 0% as part of the model constraints (Eq. 4.4). The 0% $LPSP$ implies consistent and efficient operation of the entire energy system components. However,

Table 4.4: Risk coefficients as introduced in the robust-based optimization of the MINES model.

Uncertain Parameter	Risk seeking	Risk neutral	Risk averse
Load	+1	+2	+3
u	-1	-2	-3
GHI	-1	-2	-3
T_{out}	+1	+2	+3

Table 4.5: Meteorological and load uncertainty parameters/assumptions for Sachs Harbour.

Parameter	Mean	Standard Deviation	Number of Years[a]
Average u for a year	8.075 m/s	0.290 m/s[b]	10
Average T_{out} for a year	-10.31 °C	2.4°C[c]	55
Average daily GHI for a year	2.471 kWh/m^2	0.618 kWh/m[d]	-
Average combined daily thermal and electricity load for a year	9,277 kWh	927 kWh[e]	-

[a] Set of several years in reference to the standard deviation.
[b] Adapted from Tuktoyaktuk, NWT [171].
[c] Adapted from average temperature (1957 - 2012) increase for four communities in the NWT [172].
[d] Considered 25% of interannual variation [173].
[e] Considered 10% of interannual variation for P_{load}.

this ideal situation has to be investigated given the operational complexity of an integrated energy system. Hence, a sequential Monte Carlo state duration sampling has been incorporated in MINES to address uncertainty in reliability of the energy system components. This approach was adapted from the power system reliability simulation technique introduced by Billinton and Li [174], and uses component state duration distribution functions. In a two-state component representation, these distribution functions refer to the operating (uptime) and repair (downtime) state of a system component i, and are usually assumed to be exponential. According to Billinton and Li [174], this can be summarized in the following steps:

- ***Step 1:*** Identify initial state of energy system component (i). Generally, all components are assumed to be operational at least in the first hour. Following the initial state, let τ_i denote the state of the ith component:

$$\tau_i(t) = \begin{cases} 0 & \text{if } downstate \\ 1 & \text{if } upstate \end{cases} \tag{4.6}$$

- ***Step 2:*** Sample the state duration of each component i depending on its present state. For instance, given an exponential distribution, the sampling value of the state duration can be expressed as:

$$Upstate_i = round\left(\overbrace{-\frac{1}{\lambda_{fi}}}^{\text{MTBF}} \times ln(U_i)\right) \tag{4.7}$$

$$Downstate_i = ceil\left(\underbrace{-\frac{1}{\lambda_{ri}}}_{\text{MTTR}} \times ln(U_i)\right) \tag{4.8}$$

  where U_i is a uniformly distributed number between [0,1] corresponding to the ith component. If the present state is the down state, λ_{ri} will be the repair state of the ith component (1/h) (the annotated term in Eq. 4.8 is called Mean Time To Repair ($MTTR_i$ [42])). The *round* function of MATLAB® was used to round $Upstate_i$ to its nearest decimal or integer. If the present state is the up state, λ_{fi} will then be the failure rate of the ith component (1/h) (the annotated term in Eq. 4.7 is called Mean Time Between Failure ($MTBF_i$ [42])). The *ceil* function of MATLAB® was used to round $Downstate_i$ to its nearest integer greater than or equal to its value. Table 4.6 shows the uncertainty parameters used to generate outage history for each component i of the energy system.

- ***Step 3:*** Repeat Step 2 for each hour (1 - 8760) in the model, and record sampling values of each state duration for all components. A graphical representation of example chronological component state transition can be seen in Fig. 4.4(a) and (b).

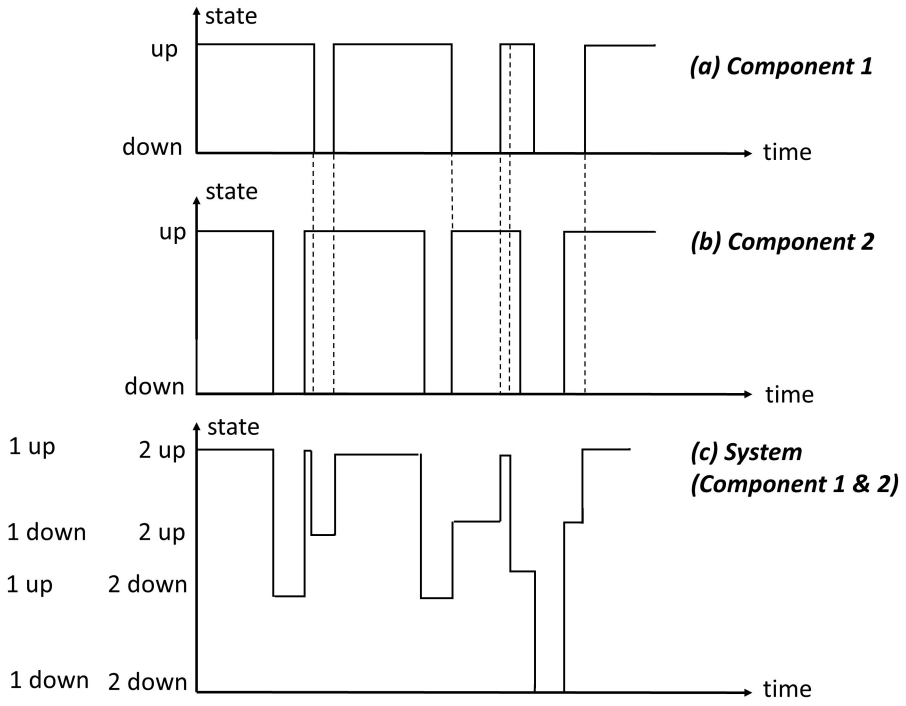

Figure 4.4: Chronological component state transition process of each component (a and b) and the overall system (c); adapted from [174].

- ***Step 4:*** As shown in Fig. 4.4(c), the chronological state transition of the overall system can then be obtained by combining the chronological component state transition processes for both components 1 and 2 (Eq. 4.9).

$$\tau_{system}(t) = \sum \tau_i(t) \tag{4.9}$$

Fig. 4.5 presents the overall uncertainty propagation process for the multiple overlapping uncertainties considered in this work. Specifically, the described uncertainty formulations result in a series of probability distribution functions relating to various outputs (system reliability, economics and environmental) in the MINES model. Similar to the iHOGA software [170], the mean of each performance metric

Table 4.6: Uncertainty parameters to generate outage history for each component of the energy system; approach was adapted from [174] and actual values were taken from [42].

Parameter	Value	Unit
$MTBF_{PV}$	2190	hours
$MTTR_{PV}$	80	hours
$MTBF_{WT}$	1,920	hours
$MTTR_{WT}$	80	hours
$MTBF_{DG}$	950	hours
$MTTR_{DG}$	50	hours
$MTBF_{CONV}$	87,600	hours
$MTTR_{CONV}$	80	hours

was taken into account in comparing all other feasible configurations of the energy system, and this will be reflected in the non-dominated individuals (optimal Pareto front) of MINES.

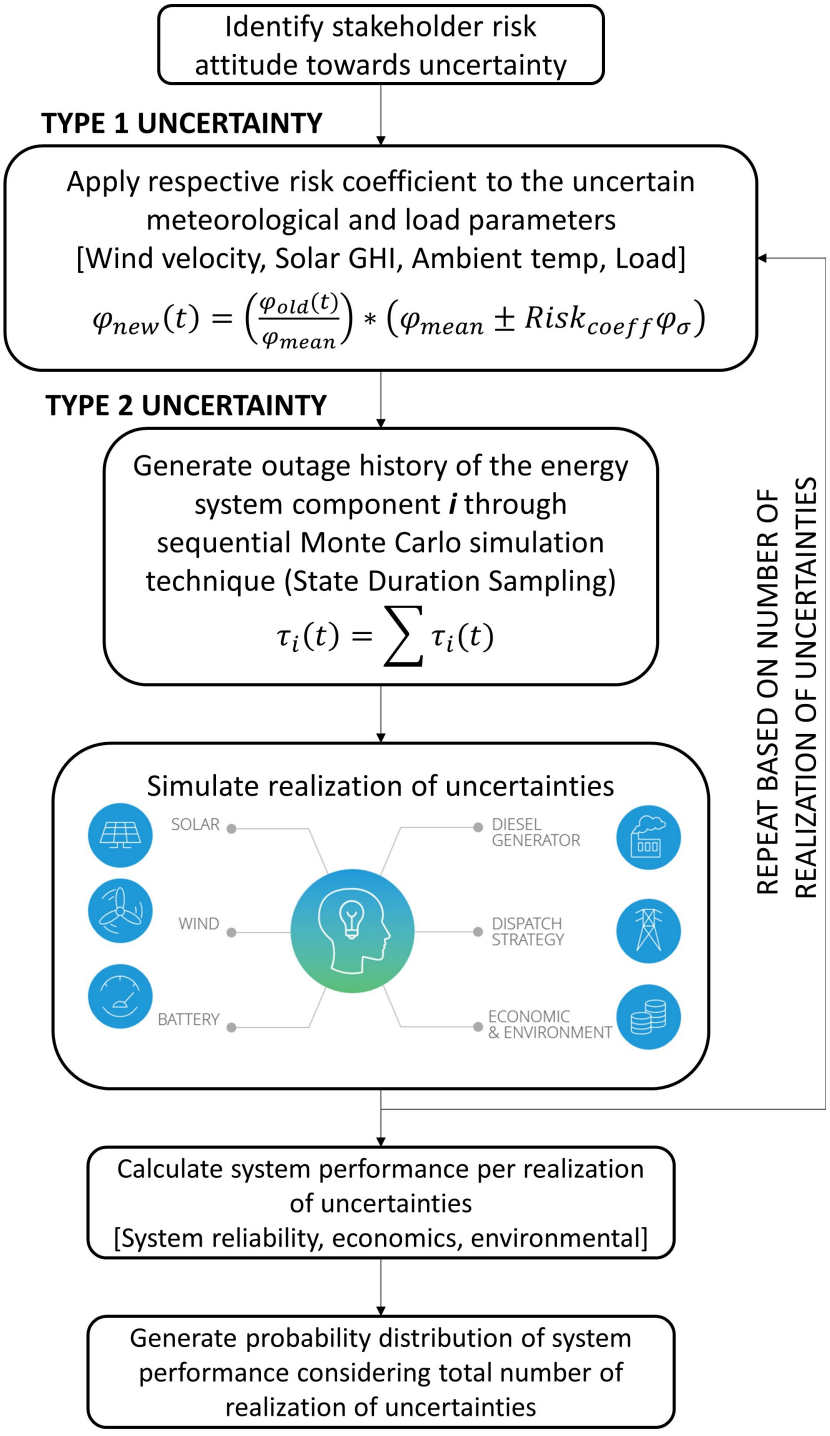

Figure 4.5: Uncertainty propagation of the proposed modeling framework.

4.2.4 Temperature effect on battery storage systems

The World Wildlife Fund conducted a set of feasibility studies [30] for the Canadian Arctic communities using the HOMER software [29]. HOMER is a tool originally

Table 4.7: Battery storage thermal parameters.

Parameter	Unit	Lead Acid	Lithium Ion
Model	-	T-105 with Bayonet Cap [175]	TR 25.6-25 Li-ion [176]
Manufacturer	-	Trojan Battery	Trojan Battery
Max operating temp.	°C	55	45
Min operating temp.	°C	-20	-20
Conductance to ambient	W/K	10	10
Specific heat capacity	J/kg-K	800	800
Fixed bulk temp.	°C	20	20

developed by the National Renewable Energy Laboratory in the United States. It determines the most feasible configuration of the energy system by applying a full factorial design of experiments, and choosing the configuration with minimum Net Present Cost (*NPC*) [104]. In this paper, the HOMER modeling framework was used to evaluate lead acid (LA) and lithium ion (LI) battery storage in cold climate regions using the modified Kinetic Battery Storage Model (KiBaM). In particular, the determined optimal capacity of the battery storage system from MINES will be further investigated by incorporating temperature effect on battery storage capacity.

The thermal parameters of the battery storage used for this work are listed in Table 4.7. The minimum and maximum operating temperature should be observed in simulating battery performance. Outside the given temperature range, the battery shuts off, and neither charging nor discharging is allowed. Fig. 4.6 shows the temperature versus capacity curve of the two types of battery considered in the simulation. In Table 4.7, conductance to ambient refers to the rate at which heat is exchanged between the battery components and the building where the battery is located. Specific heat capacity refers to the amount of heat energy the component absorbs, per kilogram of mass, before increasing in temperature by one degree Celsius. In order to demonstrate the impact of temperature on the overall energy system performance, the mentioned parameters will be considered in simulating the hourly dispatch of the battery after getting the deterministic optimal configuration of the energy system. In theory, this demonstrates the thermal variation of the battery at each time step in the model. However, only the fixed bulk temperature will be considered in the probabilistic optimization algorithm of MINES because: (i) in real-world applications, battery storage systems are typically installed in a building with thermal management, and (ii) this approach also reduces significantly the computational requirement of the optimization algorithm. In other words, this study assumed that the fixed bulk temperature of 20°C of the battery will be maintained through the temperature regulator installed in the building where the battery is located.

4.2.5 Computational expense and limitation of the MINES model

The integration of the uncertainty module in the overall modeling framework of MINES demands significant computational requirement in order to get the desired

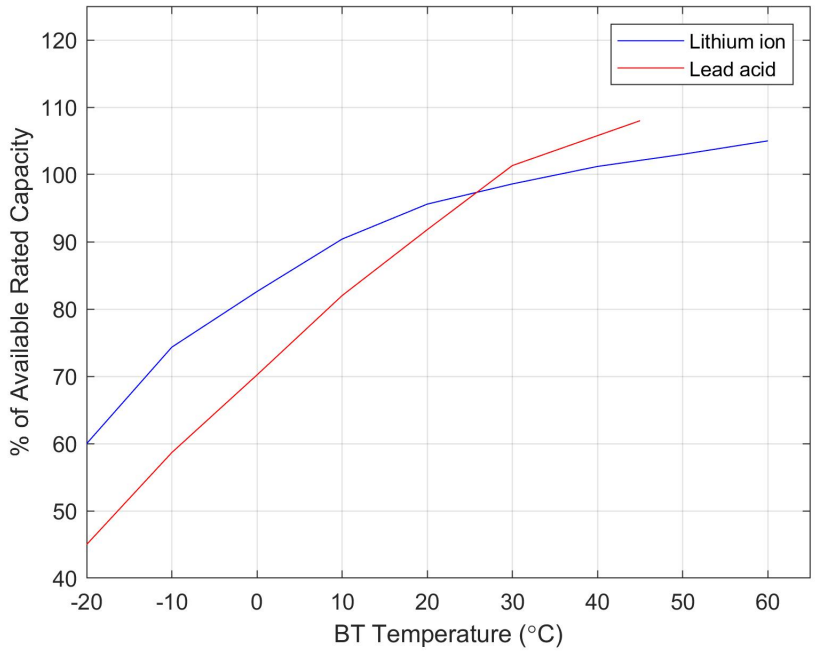

Figure 4.6: Temperature versus capacity curve of batteries; data extracted from Trojan Battery Company (T-105 with Bayonet Cap model for lead acid [175] and TR 25.6-25 Li-ion model for lithium ion [176]).

optimization output from the model. For instance, implementing parallel computing, the model implemented in MATLAB® converged to a solution roughly after 30 h by using 64-bit operating system, an Intel Core i7-7700HQ 2.800 GHz 4-core processor and 16 GB of RAM. For this reason, this work used state-of-the-art research parallel computing systems from Compute Canada [177] to decrease the computational requirement of the MINES model.

4.2.6 Case study input data

To test the methods described in this section, a case study was conducted for an Indigenous community in the Arctic. Sachs Harbour (Lat: 71.9884 N; Long: 125.23935 W), the Northernmost community in the NWT was selected for this purpose. This community has one of the most extreme winter conditions in Arctic Canada, and thus demonstrates the applicability of the modeling approach to other isolated communities in the region. All of the relevant meteorological information (GHI, u, T_{out}) and load demands (electrical and thermal) of the community have been presented in [151] and [110]. The heat load simulation conducted for this study was elaborated by the authors in [151].

4.3 Results and discussion

This section looks at the uncertainty modeling results generated from the MINES model. The investigation builds from the four scenarios presented in Table 4.8. The simulated thermal load of Sachs Harbour is assumed to be supplied by electric

Table 4.8: Scenarios implemented in the MINES model.

Scenarios	Electricity	Space Heating
Scenario 1	Home appliances including lighting and electric load for DHW	Baseboard Heater at U = 0.5 W/m^2-K
Scenario 2	Home appliances including lighting and electric load for DHW	Baseboard Heater at U= 0.13 W/m^2-K
Scenario 3	Home appliances including lighting and electric load for DHW	Baseboard Heater and ASHP[a] at U = 0.13 W/m^2-K
Scenario 4	Home appliances including lighting and electric load for DHW	Baseboard Heater and ASHP[b] at U = 0.13 W/m^2-K

[a] Baseboard heater kicks in if ASHP shuts off when outside temperature drops below -20 °C.

[b] ASHP only operates during summer and the baseboard heater runs for the rest of the seasons.

appliances for domestic hot water (DHW), such as instant water heating devices, and via electric baseboard heaters for space heating demand. Scenarios 3 and 4 use air-source heat pumps (ASHP) instead of the baseboard heater in the first two scenarios. Previous analysis by the authors [151] showed that the ASHP reduced spaced heating load by about 40% as compared to baseboard heaters. However, the simulation results indicated that load fluctuations caused by the variations of the heat pumps' coefficients of performance negatively impacted the operation of the energy system. In particular, these demand fluctuations resulted in a larger battery storage requirement, along with an increase in overall energy system costs. The authors also looked at the impact of building enclosure improvements as a function of the overall heat transfer coefficient of the building (U). The modeling results suggested that a passive house with an overall U-value of 0.13 W/m^2-K reduced space heating loads by about 40% as compared to a normal building. Collectively, scenario 2 was proven to have the best system performance as compared to the other three scenarios in Table 4.8.

4.3.1 Deterministic results

Fig. 4.7 shows the deterministic full design space and Pareto front of scenario 2 after minimizing simultaneously the $fuel_{cons}$ and $LCOE$ of the energy system in question for Sachs Harbour. The respective configurations of the three solutions of interest as specified in the Pareto front of Fig. 4.7 are listed in Table 4.9. Solution 1 corresponds to a solution with lowest $LCOE$ and highest $fuel_{cons}$. Solution 3, on the other hand, has no back-up DG which led the algorithm to increase the WT capacity of the system. It has a RE_{pen} of 100% but also resulted in a larger BT storage capacity to handle mismatch between demand and the RE resource. Consequently, this configuration has the most expensive $LCOE$ and Life Cycle Cost[4] (LCC) [40]. Solution 2, at the middle of the Pareto curve (trade-off point), balances the two solutions mentioned, and includes all the system components of the integrated energy

[4] LCC served as one of the model outputs to represent the sum of the cradle-to-grave economic costs of the integrated energy system for a project lifespan of 25 years.

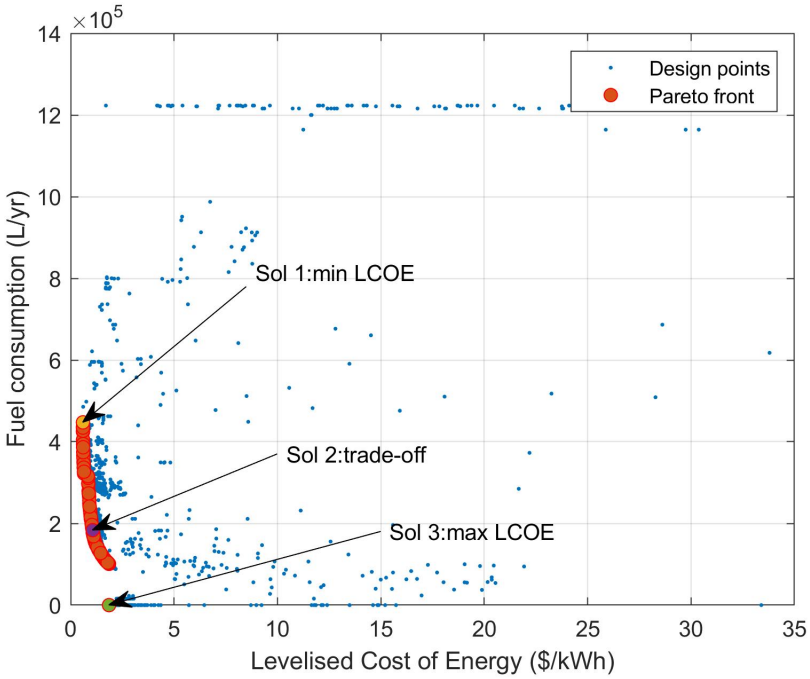

Figure 4.7: Scenario 2 deterministic results: full design space with the optimal Pareto front and the identified solutions of interest.

system. Note that the wind resource is able to meet the largest share of demand for the three solutions of interest. This reflects the viability of wind farm projects in the region. The inherent trade-off, however, is the resulting larger BT storage to handle wind's variability. This trade-off analysis is critical in the decision making process of energy system planners and stakeholders in the North.

4.3.1.1 Impact of temperature on battery storage performance

This work extends the deterministic results from [151] by looking at the impact of temperature on BT storage performance considering the thermal properties (Table 4.7) of both LA and LI batteries. Table 4.10 shows the simulation performance of two deterministically optimized energy systems with different types of BT storage systems. Note that the identified deterministic optimal capacity of each system component (PV, WT, BT, DG, CONV) for both configurations (case 1 and 2) were adopted from solution 1 in Table 4.9. Case 1, however, uses LA as its BT storage whereas case 2 uses LI. The technical and cost parameters of these two comparable storage systems were extracted from HOMER's database.

Fig. 4.8 presents hourly performance of LA and LI. At this stage of the study, the simulation assumed that the BT storage systems are located in a building without thermal management. Using a modified KiBaM model, HOMER tracks the variation of BT capacity in reference to temperature. For example, Fig. 4.8(b) and (d) shows a decrease in available energy content due to a decrease in operating temperature of the BT (also influenced by the ambient temperature profile of Sachs Harbour). For both storage types, it can be observed that the BT is neither charging nor discharging (Fig. 4.8(c) and (e)) whenever the operating BT temperature is outside the temperature ranges specified in Table 4.10.

Table 4.9: Deterministic configuration characteristics of the three solutions of interest determined from the Pareto front of Scenario 2.

Parameter	Unit	Optimization results		
		Sol 1: Min. $LCOE$	Trade-off Point	Sol 3: Max. $LCOE$
PV	kW	450.45 (25.025 kW x 18)	1,725 (25 kW x 69)	0
WT	kW	570 (95 kW x 6)	1,045 (95 kW x 11)	3,325 (95 kW x 35)
BT	kWh	4,620 (9.24 kWh x 500)	7,205 (55 kWh x 131)	7,315 (55 kWh x 133)
DG	kW	675 (225 kW x 3)	675 (225 kW x 3)	0
CONV	kW	600 (200 kW x 3)	800 (200 kW x 4)	800 (200 kW x 4)
Strategy	-	LFOS	LFOS	LFOS
P_{pv}	kWh	414,407	1,405,135	0
P_{w}	kWh	2,456,400	4,531,567	14,418,623
$P_{BT,out}$	kWh	151,831.41	365,881	513,951
P_{DG}	kWh	1,272,995	529,758	0
$LPSP$	%	0	0	0
RE_{pen}	%	69.27	91.81	100
P_{excess}	%	15.19	4.93	1.05
$fuel_{cons}$	L/yr	447,470	183,595	0
CO_2[a]	tCO$_{2\text{-eq}}$/yr	2,096	1,523	757
CC	CND $	15,117,673	37,839,517	79,936,645
$LCOE$	CND $/kWh	0.59387	1.06348	1.85487
LCC	CND $	35,756,756	64,031,794	111,681,201

[a] Lifecycle CO_2 emissions of the energy system

Table 4.10: Performance of lead acid and lithium ion batteries as applied to integrated energy system.

Parameter	Unit	Case 1: System with LA	Case 2: System with LI
BT max temp	°C	55	45
BT min temp	°C	-20	-20
CC_{BT}	CND $	1,345,500	1,840,916
$O\&M_{BT}$	CND $	797,439	644,352
P_{pv}	kWh	506,195	506,195
P_{w}	kWh	2,475,542	2,475,542
$P_{BT,out}$	kWh	73,897	118,806
$P_{BT,in}$	kWh	87,465	127,243
P_{DG}	kWh	1,331,850	1,280,713
$LPSP$	%	0	0
RE_{pen}	%	60.7	62.2
$fuel_{cons}$	L/yr	528,472	506,491
System CC	CND $	16,575,414	17,070,830
$LCOE$	CND $/kWh	0.6659	0.6784
LCC	CND $	40,092,700	40,846,160

In general, LI performs better than LA batteries. However, this superior performance of LI has a trade-off (in comparison with LA) in reference to the other parameters listed in Table 4.10. For instance, LA cost less up-front than LI but the former's $O\&M$ is more expensive than the latter. Further, the power generated from the back-up DG is relatively high in case 1 (system with LA) to compensate the limited amount of battery discharge from LA. This implies higher $fuel_{cons}$ and system cost as well. Consequently, this resulted to a cheaper overall system cost, both in terms of $LCOE$ and LCC. Note, however, that this result is heavily influenced by the BT storage data extracted from HOMER's database, and LA might also be a better option depending on its operating temperature range.

This section demonstrates the negative impact of installing BT storage systems in a building without thermal management. To depict real-world situations in this study and to improve the system performance of the overall integrated energy systems in Fig. 4.2, the robust optimization assumes that the BT storage is located in a temperature-controlled building in Sachs Harbour. A controlled temperature environment for batteries is also recommended by BT manufacturers such as Trojan [175].

4.3.2 Stochastic simulation results

In comparison with the sensitivity evaluation used in the author's previous study [151], this work carries out a probabilistic analysis using the two types of uncertainty introduced in the model (Section 4.2.3). This approach was first applied to the deterministic solution of scenario 2-solution 1 to test statistical convergence for an individual use case. Fig. 4.9 shows the coefficient of variation for the two

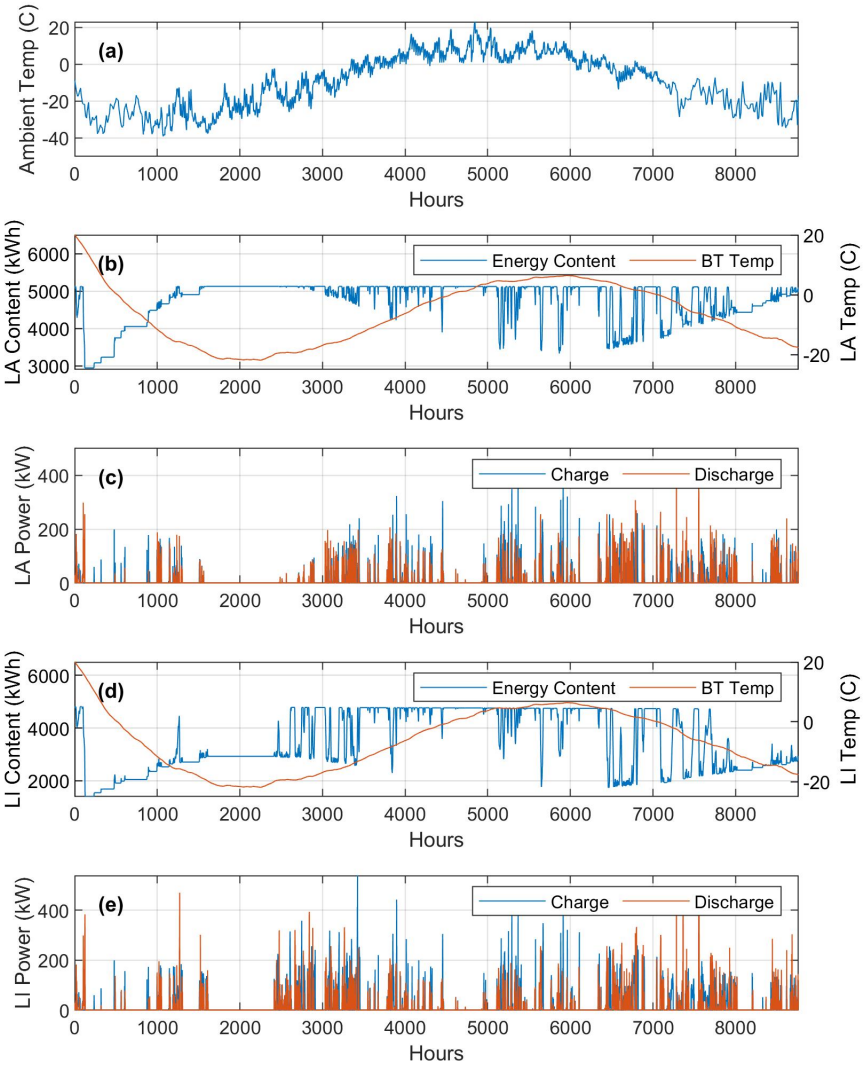

Figure 4.8: Example deterministic simulation results when there is no thermal management in a building where the battery storage systems are located: (a) ambient temperature of Sachs Harbour; (b) Energy content and operating temperature of lead acid BT; (c) Charge-discharge of lead acid BT; (d) Energy content and operating temperature of lithium ion BT; (c) Charge-discharge of lithium ion BT.

objective functions and it was demonstrated that 1000 samples were sufficient to carry out the probabilistic analysis for this work. The coefficient of variation shows the extent of variability of data in a sample in relation to the mean of the population. It represents, specifically, the ratio of the standard deviation to the mean, and is a useful statistic parameter in comparing the degree of randomness considering multiple overlapping uncertainties [178].

Fig. 4.10 presents a series of probability distribution functions that corresponds to various technical, economic and environmental outputs that can be extracted from the MINES model for a risk-seeking stakeholder or decision maker. For example,

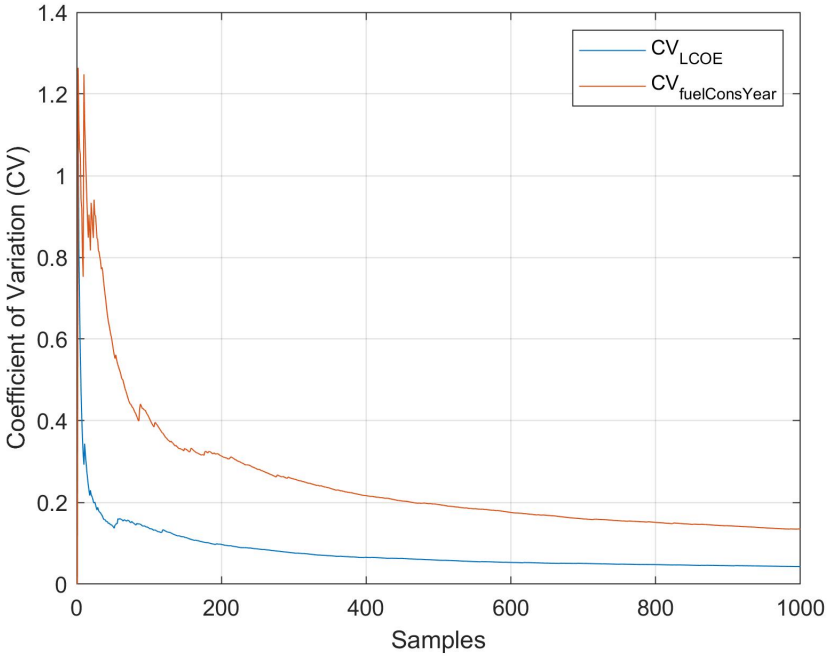

Figure 4.9: Risk seeking scenario 2-solution 1 coefficient of variation for the objective functions with 1000 samples.

solution 1 of scenario 2 has a mean RE_{pen} of approximately 51% after simulating 1000 times probabilistically as compared to its initial deterministic RE_{pen} of 69.27%. It can be observed that due to the uncertainties introduced in the model, the overall power generation from RE was reduced. This RE_{pen} is even lower when the risk preference shifts from risk seeking to risk averse. Consequently, the mean $fuel_{cons}$ of the DG increased to approximately 750,000 L/yr as compared to its initial deterministic value of 447,470 L/yr. This reflects that the DG was under-sized when multiple overlapping uncertainties were introduced in the model.

Fig. 4.11 shows the mean RE_{pen} decreases to approximately 20% when the preference of the decision maker towards uncertainty shifts from being risk seeking to risk averse. The mean $fuel_{cons}$, on the other hand, were further increased from approximately 750,000 L/yr (risk seeking) to 1,400,000 L/yr (risk averse). This implies increase in system costs ($LCOE$, $O\&M$, LCC) to ensure robust performance of the energy system under worst case realization of the uncertainties. Specifically, this is attributable the highest increment (in comparison with the other risk coefficients listed in Table 4.4) in energy demand and the reduction in the other uncertain variables (renewable resources and temperature).

A comparative analysis for the three solutions of interest in scenario 2 considering risk seeking preference of the decision maker and the probabilistic results of their respective $LCOE$ and $LPSP$ values are shown Fig. 4.12. In the presence of uncertainties, $LPSP$ of solution 3 is approximately 12% (mean) as this energy system configuration has no back-up DG. Hence, this solution is not resilient to extreme temperature events or any increase in energy demand in Sachs Harbour. The opposite can be observed for both solutions 1 and 2 wherein 675 kW capacity of DG are available (Table 4.9). This shows the critical role of DG to be able to maintain an $LPSP$ of approximately 1% - 2% (mean) for both solutions. Further,

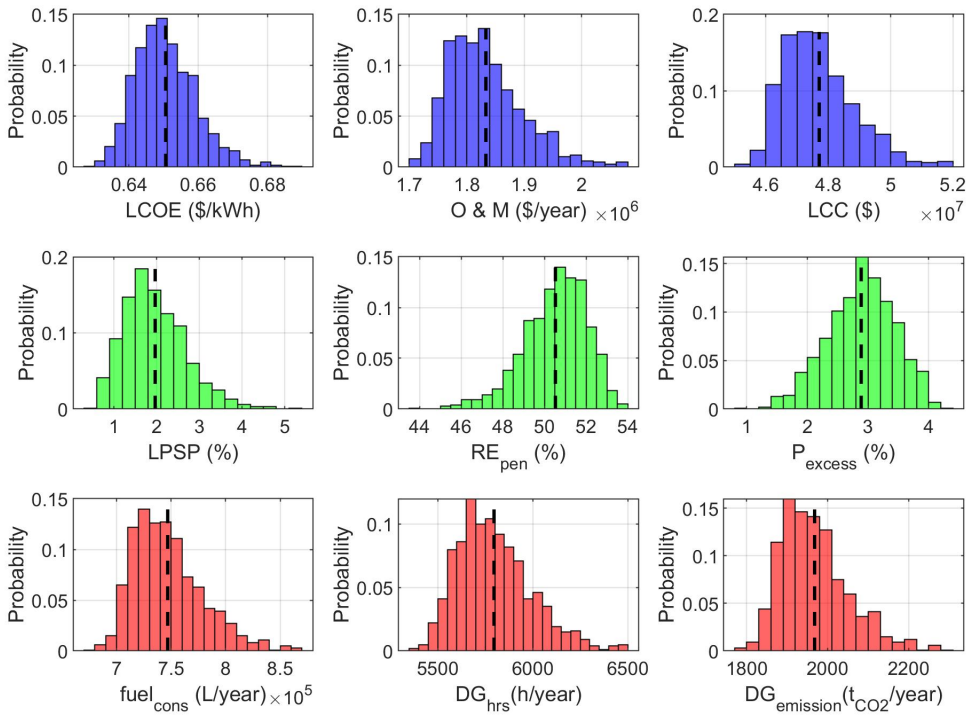

Figure 4.10: Risk seeking scenario 2-solution 1 series of probability distribution functions generated probabilistically using 1000 samples; dashed line refers to mean value.

this also implies that the constraint formulation of 0% $LPSP$ (Eq. 4.4) will be slightly violated (solutions 1 and 2) when multiple overlapping uncertainties are considered. Note that the probabilistic simulations done so far were taken from the deterministic optimization results, and hence, a separate robust optimization run will be performed in MINES wherein full compliance to the constraints formulation will be strictly observed. Fig. 4.12 also shows the range of $LCOE$ values with their respective probability once the $LPSP$ deviates from 0% (deterministic value across all solutions).

The hourly dispatch for solution 1 assuming risk seeking preference of the decision maker towards uncertainty is shown in Fig. 4.13. The hourly mean values of each source of energy is illustrated together with its variations due to uncertainties. For solutions where all system components are available, RE is treated as a priority dispatch before discharging available power from the BT storage and DG. Hence, a significant variation in power output from the DG (solution 1) can be observed as influenced by the multiple overlapping uncertainties introduced in the model. The lower bound of each hourly variation of the power output coming from the DG was affected by the 30% DG_{LF} constraint to avoid damaging the generator by running at very low partial loads.

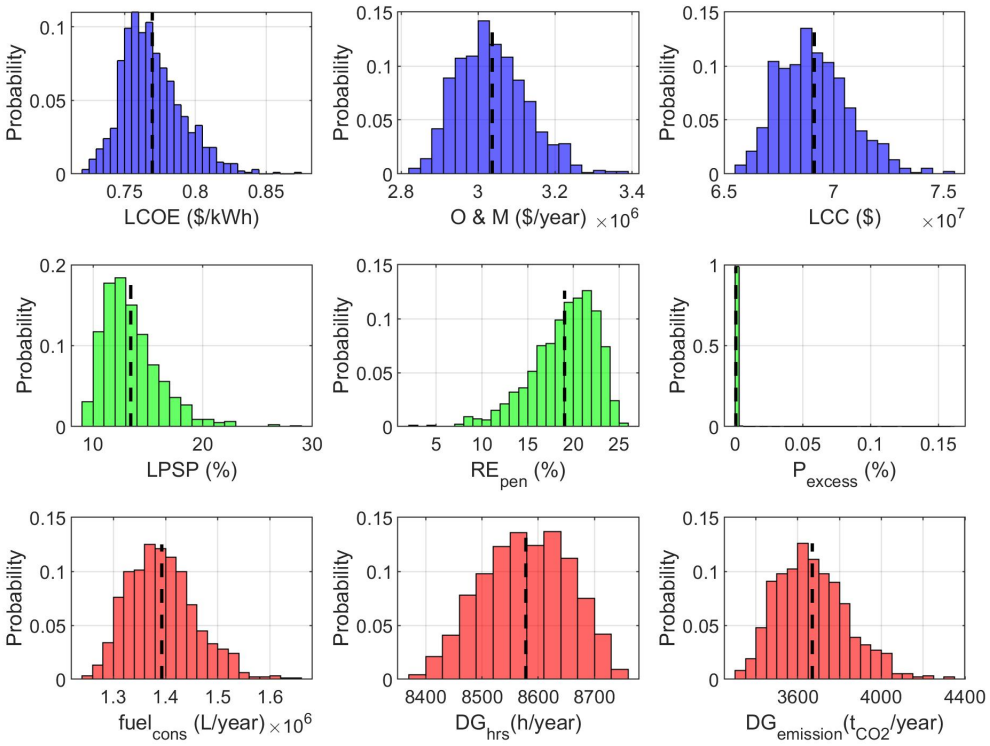

Figure 4.11: Risk averse scenario 2-solution 1 series of probability distribution functions generated probabilistically using 1000 samples; dashed line refers to mean value.

4.3.3 Robust optimization results

A comparison of the Pareto fronts generated deterministically (DT) and through the robust optimization process for scenario 2 considering risk attitudes of decision maker towards uncertainty are presented in Fig. 4.14. The non-deterministic solution was obtained using the same GA parameters listed in Table 4.2. Further, the last generation obtained from the deterministic algorithm of the MINES model was used as the first generation of the RO optimization. Doing this, along with parallel computing results in a relatively faster rate of convergence in obtaining the desired robust optimal capacities of the system components and the corresponding dispatch strategy for the integrated energy system.

It can be observed that the Pareto front tends to shift towards higher objective function values when the algorithm changed from DT to RO. This deviation implies higher *LCOE* for the system when uncertainties were incorporated in the model. In comparison with the DT optimal solutions, Table 4.11 shows an increase in the optimal capacity for majority of the system components (WT, PV, DG, CONV) except the BT storage. In the presence of uncertainties, this suggests that the RO algorithm assigns its preference to generate power from the DG over discharging the BT storage to meet load deficit. This is influenced by the charge-discharge cycles of the BT storage which is also affected by the renewables (wind and solar), treated as uncertain paremeters for this work. Hence, DG offers more flexibility whenever there is load deficit in the energy system. This result is critical for consideration

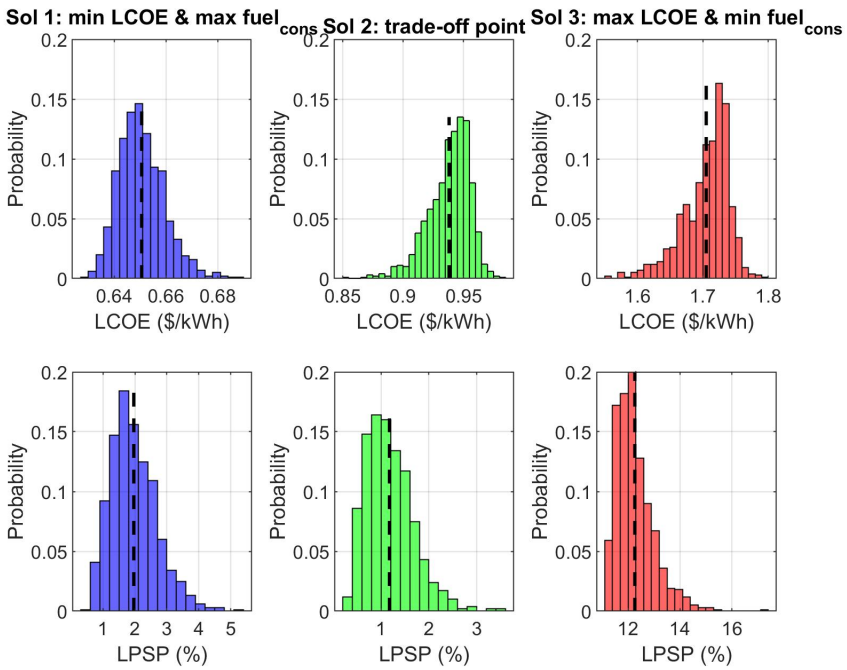

Figure 4.12: Risk seeking scenario 2 probabilistic simulations for the three solutions of interest generated from the deterministic optimization results; dashed line refers to mean value.

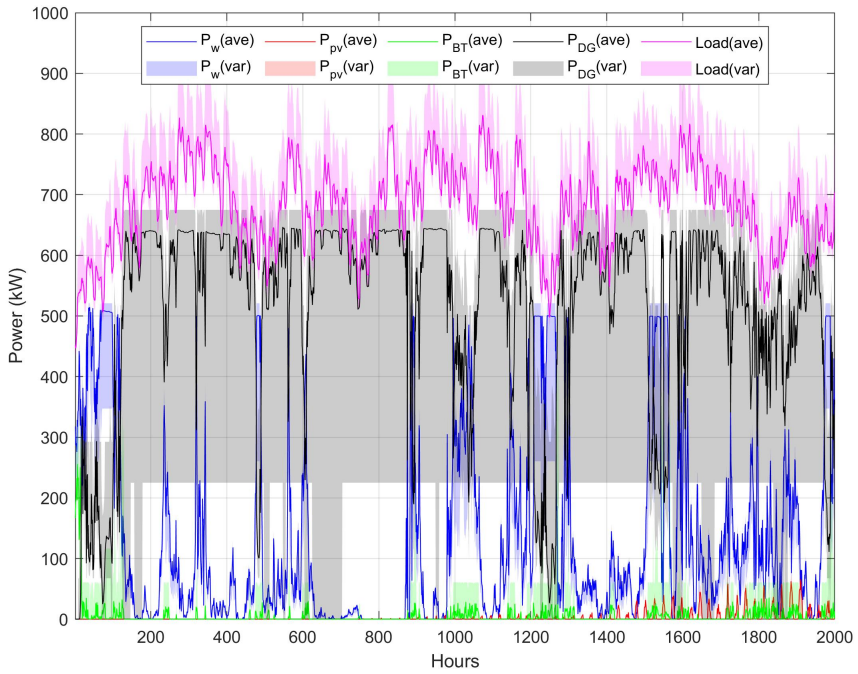

Figure 4.13: Hourly average (ave) and variation (var) of the deterministic optimal configuration in scenario 2 that was simulated probabilistically; assumed risk seeking preference of the decision maker.

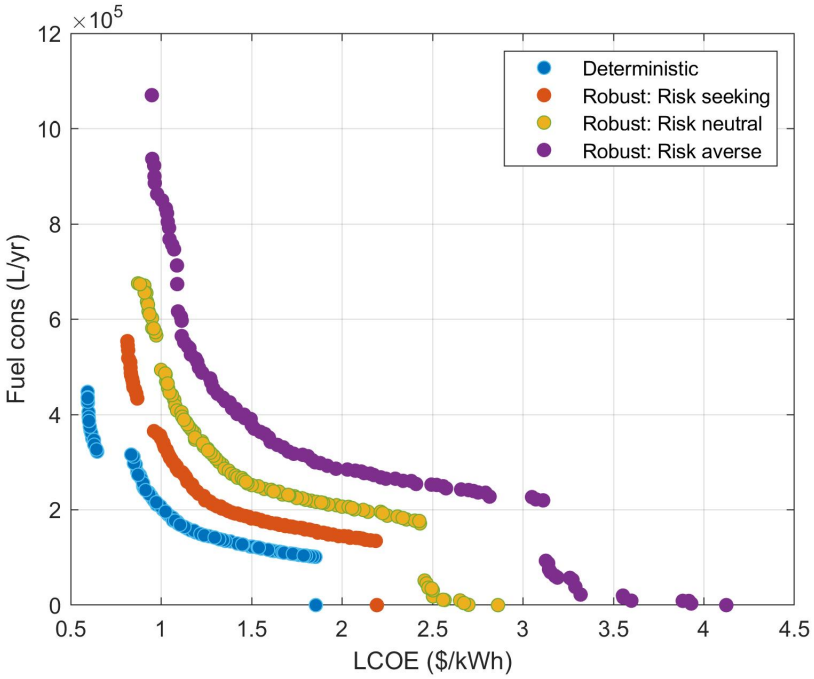

Figure 4.14: Scenario 2 Pareto front comparison for deterministic and robust optimization results with specific risk preferences.

among remote communities like Sachs Harbour wherein fuels are being delivered via barge once a year since year-round road access is not available.

The discontinuities in the Pareto fronts were influenced by the lower and upper bounds of the discrete characteristics of the decision variables shown in Table 4.3, and the restrictions implemented in the constraints formulation of the model. For instance, the final step-change at the tail end of the Pareto fronts were affected by the optimal capacities of the DG and BT storage. Specifically, the second to last solution in the deterministic Pareto front, for example, has a DG and BT storage included in its optimal system configuration. However, for lower than the optimal DG and BT capacities, the model can no longer find a non-dominated optimal solution where both DG and BT are acting as back-up sources of power. This concept of non-dominated solution applies to the robust optimization framework as well, and is integral to NSGA-II.

The risk attitudes of the decision maker towards uncertainty was observed to impact the optimal component capacities of the integrated energy system. As shown in Table 4.11, an increase in the component capacity implies higher system $LCOE$ and $fuel_{cons}$, from being risk seeking to risk averse across the three solutions of interest. This also reflects that the goal of having a robust energy system that can operate under extreme climate conditions has to be balanced with the possible implications of having an increased energy system $LCOE$ and $fuel_{cons}$. The increase in $fuel_{cons}$ is attributable to the uncertainties incorporated in the solar irradiance and wind speed of Sachs Harbour, ensuring that the load would still be met in spite of the randomness (uncertainty) of renewable resources.

Table 4.11: Configuration results comparison between deterministic (DT) and robust (RO) optimization with different risk preferences.

Parameter	Unit	Optimization results											
		Sol 1: Min *LCOE*				Sol 2: Trade-off				Sol 3: Max *LCOE*			
		DT	RO-RS	RO-RN	RO-RA	DT	RO-RS	RO-RN	RO-RA	DT	RO-RS	RO-RN	RO-RA
WT	kW	570	950	1,425	1,330	1,045	2,185	3,230	5,035	3,325	5,510	9,120	14,820
PV	kW	450	700	0	0	1,725	50	0	0	0	0	0	0
DG	kW	675	1,575	1,575	1,800	675	1,575	1,800	2,025	0	0	0	0
BT	kWh	4,620	4,620	4,324	4,620	7,205	7,205	7,205	7,205	7,315	7,315	7,315	7,315
CONV	kW	600	800	1,250	1000	800	1,000	1,350	1,250	800	2,000	1,750	1,500
Strategy	-	LFOS	LFOS	LFOS	LFOS	LFOS	LFOS	LFOS	LFOS	LFOS	LFOS	LFOS	LFOS
$fuel_{cons}$	L/yr	447,470	553,956	675,185	1,070,200	183,595	212,878	267,474	317,622	0	0	0	0
LCOE	CND $/kWh	0.59387	0.81333	0.87228	0.94848	1.0634	1.28017	1.42203	1.73301	1.85488	2.19247	2.86171	4.12364

[a] RS: Risk seeking; RN: Risk neutral; RA: Risk averse.

4.3.4 Implications for decision making

Huntington et al. [99] argued that the purpose of energy modeling is to produce insights and not just numbers. Hence, this section provides insights and recommendations based on the outputs presented in Section 4.3 and the overall modeling framework described in Section 4.2.

4.3.4.1 Multiple viable energy system configurations

Model insight: The results presented from the modeling work carried out for Sachs Harbour indicate that multiple energy system configurations were found to be viable in the North even in the presence of uncertainties. Specifically, Table 4.9 shows that wind can meet the largest share of the energy demand for the community, and this reflects that wind is a viable energy resource for remote communities in Northern Canada. Other system configurations were found to be feasible but with different levels of renewable energy penetration and capacities from back-up sources of energy such as BT storage and DG. Fig. 4.14 also shows that the risk preferences of decision makers towards uncertainties were also proven to impact the optimal configuration of the integrated energy system.
Context and recommendation: The first recommendation of this research is to develop a documented IPP policy in the NWT considering the feasibility of multiple renewables-based energy system in the Arctic. Note that power generation in Sachs Harbour is fully owned and operated by the Crown utility, Northwest Territories Power Corporation (NTPC). This is also the case for all Indigenous remote communities across the three territories in Northern Canada. Hence, building a renewable energy project, without a documented IPP policy in a region where there is a Crown utility, will be challenging since the majority of electric utilities worldwide, either publicly or privately owned, are regulated by utilities commission or public utilities board. For example, previous wind farm feasibility studies [21] have been conducted in Sachs Harbour but none of the projects were realized because of the lack of an explicit energy policy that supports renewable energy infrastructure development.

Demonstrating the viability of multiple energy system configurations in the North is essential not just in the energy transition towards more sustainable sources of energy but also fundamentally, for a much larger transition towards self-determination, economic reconciliation and energy sovereignty among Indigenous peoples. For this work, energy sovereignty is defined as the ability of Indigenous communities to own and operate their own energy systems, to use renewable sources of energy, to reduce dependence on burning fossil fuels, and to stop relying on corporation (Crown utility) for their energy needs [179]. The viability of these energy systems also provide opportunities to have Indigenous-owned renewable energy projects. The Yukon territory aims, for example, that at least 50% of IPP projects in the region must have Indigenous ownership component, government collaboration and significant flexibility on funding arrangements [180].

4.3.4.2 Community-specific (levelised) cost of energy

Model insight: Table 4.9 shows the *LCOE* for the three solutions of interest identified in Fig. 4.7. Table 4.11, on the other hand, presents *LCOE* for the the three solutions of interest in the presence of uncertainties while taking into account

varying risk preferences of the decision maker. The modeling results show that the cost of energy varies depending on the configuration of the integrated energy system, and is influenced by the amount of energy specific for the community of Sachs Harbour. *MINES* can handle different communities to calculate community-specific levelised cost of energy in the North and remote communities in general.

Context and recommendation: The second policy recommendation of this work is to re-assess the pricing structure in determining the applicable PPA rates as outlined in a certain IPP policy. Specifically, the community-specific *LCOE*, as shown in the modeling work of this research, should be recognized in awarding PPA contracts for renewable energy developers. As of writing, for example, the Qulliq Energy Corporation (QEC) is applying to the Utility Rates Review Council (URRC) of Nunavut to have a territory-wide flat PPA rate of $0.25 per kWh based on their proposed IPP policy [181]. The proposed rate is based on the average diesel fuel costs in the territory. This pricing structure proposed by QEC to the URRC will be a disadvantage to many renewable project proponents in areas where diesel fuel costs are higher. This is also not aligned with the motivation of having an IPP policy that supports the increase of renewable energy uptake in Nunavut which currently has the highest diesel dependency across all provinces and territories in Canada. Further, this low PPA rate will leave renewable energy project proponents to seek additional funding, and hence challenge the overall economic feasibility of their respective projects.

The techno-economic modeling work presented in this research calls for a holistic understanding of the full spectrum of costs in generating power from diesel facilities in the North as this understanding is critical in specifying and comparing eligible energy sources in an IPP policy. The Pembina Institute has released a report to ground financial conversations in understanding the true cost of diesel in remote communities [182]. It is composed of three cost clusters with specific cost inclusions per tier. The marginal cost of energy covers the direct costs (cost of fossil fuel and transportation, government taxes, and generation cost) for powering and heating homes and community buildings. Generating energy from diesel requires the use of an engine and generator, and therefore has additional associated costs for operations and maintenance as well as the amortized capital cost of the entire diesel facility. These can be bundled together with the marginal cost to describe the cost of service (the second cost cluster). Finally, the true cost of energy is the final tier that reflects the total burden on the community and wider society, which cannot be fully expressed in economic terms. The Pembina Institute described this cluster as health-related costs as a result of local air pollution; environmental costs due to diesel spills, contamination, and remediation; societal costs related to climate change; and local economic costs resulting from an expensive and limited energy supply. Additionally, there is the subsidy cost that the government has to pay to make energy affordable for remote communities.

Incorporating the full spectrum of costs associated in generating power from obsolete diesel infrastructures in specific remote community should be taken into account to provide consistency when assessing the competitiveness of alternative candidate RE projects. In particular, this holistic understanding of the true costs of diesel in remote communities could make the project economics (based on robust *LCOE* values such as those presented in Table 4.11) viable not just from a project proponent perspective, but also in terms of savings related to significant diesel sub-

sidies from the local government. To put this into perspective, the government of Nunavut spends an average of $60.5 million each year to subsidize the use of diesel fuel in the region [14]

4.3.4.3 Access to capital and transformational collaboration between stakeholders

Model insight: The modeling framework described in this work shows that trade-off analysis is critical in determining the vast range of potential energy solutions generated by the MINES model. In particular, it was shown in Fig. 4.14 that an increase in $LCOE$ is the inherent trade-off resulting from reducing diesel $fuel_{cons}$ of the integrated energy system due to the introduction of variable RE and BT storage. As shown in Table 4.11, this increase in $LCOE$ is significant when uncertainties and risk preferences of decision makers are introduced into the model. The other costs increases, in conjunction with the $LCOE$, is associated with the CC of the system.
Context and recommendation: Primarily, one of the main barriers for the transition of Indigenous communities towards clean and sustainable sources of energy is a lack of access to capital investments. At the moment, the First Nations Power Authority is the only North-American non-profit Indigenous owned and controlled organization developing power projects with Indigenous peoples [183]. Hence, this work recommends specific stipulations in the IPP policy on how to leverage capital investments for Indigenous peoples-led energy projects. Specifically, community partnerships with industry, utilities, and governments should be strengthened moving forward. These partnerships should include majority stake for Indigenous communities as this enables Indigenous stakeholders to influence distribution, reinvestment and future planning [184]. This tie-up leads to mutual benefits for all parties as the respective partners have the support from the Indigenous peoples who have the land base. Ultimately, such partnerships also represent a significant step towards economic reconciliation where Indigenous peoples are not just participants but key players and partners in the mainstream economy.

4.3.4.4 Renewable energy integration limits

Model insight: Integrating renewables in the current electricity grid of remote communities in the North requires a grid impact study from the Crown utility. Although there is an increase in renewable energy penetration for remote communities, stability of the grid to deliver reliable power to the community, especially to those which are most isolated, should be ensured. For instance, Sachs Harbour's solution 1 of scenario 2 has a mean RE_{pen} of approximately 51% after simulating probabilistically (considering risk seeking preference of the decision maker) while its initial deterministic RE_{pen} is 69.27%. This significant integration of intermittent renewables would be likely to cause stability and reliability issues if not properly addressed.
Context and recommendation: The 2030 Energy Strategy of the Government of Northwest Territories (GNWT) outlines the territory's long-term approach to addressing secure, affordable and sustainable energy supply for the region [185]. The strategy includes the introduction of GNWT's Renewable Electricity Participation Model as presented in Table 4.12. One of the intentions of this model is to increase Indigenous-led energy projects at various scales (from small scale (residential) to

Table 4.12: Renewable Electricity Participation Model in the NWT [185].

Category	Small-scale	Mid-scale	Large-scale
Participants	Residents/Business/ Community & Indigenous govts	Indigenous & Community govts	Indigenous & Community govts
Ownership	Direct-ownership	Community-ownership	Partnership with utility
Scale	Up to 15 kW	More than 15 kW	Not clearly identified
Financing	Self-financing + Potential govt grants	Self-financing + Potential govt grants	Partner financing
Revenue	Net metering: energy savings & credits	Payment for reduced cost of diesel	Low-risk interest

large-scale utility partnerships) in the NWT. This model also sets out guidelines to manage expectations on how much renewables can be installed by the communities in order to maintain grid reliability. For example, there is a 20% community solar capacity cap in the NWT because solar electricity causes the diesel generators (mostly obsolete) of the NTPC grid to work less efficiently [185].

With the modeling results generated from MINES, this research recommends for NTPC to consider suitable BT storage systems in order to increase renewable energy integration limits in the NWT. As shown in Table 4.10 and Fig. 4.8, it is also critical to consider the impact of temperature on BT capacity given the long and cold winters in the Arctic. It is recommended that these technology options be included in the Renewable Electricity Participation Model of the GNWT. The BT storage system can also be integrated in the net metering systems of the territory. This would enable residents/communities to store some of the power generated locally rather than selling everything back to the Crown utility. This set-up might potentially address grid reliability issues caused by the intermittency of renewables as well.

4.3.4.5 Demand-side energy solutions

Model insight: This work points out that a 40% space heating load reduction can be obtained when the overall U-value of the building enclosure is 0.13 W/m^2-K (equivalent to passive house performance).

Context and recommendation: According to the National Energy Board [10], energy costs are a major contributor to the high cost of living in the North, with per capita of energy use being twice the Canadian average. Hence, this work recommends that accelerating energy transitions in Arctic remote communities should be taken from a holistic perspective wherein energy solutions are not limited to the supply-side aspects but also to demand-side considerations. In particular, this work recommends evaluating building enclosure improvements especially in public housing among remote communities in the Northern territories. This does not only provide reductions in space heating loads but also offers non-energy benefits such as thermal comfort and increased resiliency in extreme temperature events. Supply-side energy solutions such as renewable energy integration is beneficial in meeting decar-

bonization goals, but they are generally expensive to implement. Thus, this research recommends policies that promote energy conservation and efficiency initiatives for the community. Aside from the ones in place right now in the NWT (Section 4.1.1.1), there should be a strict implementation of high-performance building standards in the region as prescribed by the International Passive House Institute [129].

4.4 Conclusions

The energy modeling framework presented in this work is useful in evaluating trade-offs and balancing risk hedging strategies in integrated energy systems planning. The risk preferences of decision makers towards uncertainty was found to influence the optimal capacity of the integrated energy system. Specifically, the Pareto front from the deterministic optimization tends towards higher optimal objective function values when the algorithm shifts to robust optimization which endogenises multiple overlapping uncertainties. This implies that the optimal capacities found deterministically were under-dimensioned considering possible increments and reductions from the load and other meteorological parameters relevant for Sachs Harbour. Uncertainties relating to system reliability were also proven to be critical in ensuring that the energy system will operate even in extreme climate conditions.

It was observed from one of the solutions of interest that due to uncertainties incorporated in the energy model, the deterministic RE_{pen} of 69.27% dropped to around 51% (mean) after simulating probabilistically. Conversely, the deterministic $fuel_{cons}$ of 447,470 L/yr increased to 750,000 L/yr (mean) to compensate for the reduced operation of the renewables. To ensure robust performance of the energy system under worst-case realization of uncertainties, increase in component capacity and the overall system costs ($LCOE$, LCC, CC) were demonstrated as the attitude of the decision maker shifts from being risk seeking to risk averse.

The probabilistic algorithm assigns its preference to the diesel generator over the battery storage whenever there is a load deficit in the system. This is due to the latter's charge-discharge cycling behavior being influenced by the amount of excess and deficit from the renewables, while the former's power can be dispatched promptly. An inherent trade-off, however, is the increase in environmental emissions from diesel generation to compensate for the unavailability or limited power being dispatched from the renewables and battery storage.

Real-world applications of the modeling approaches are also described, while taking into account holistic energy solutions not just for the Canadian Arctic region but remote communities in general. In particular, reaching decarbonization goals while ensuring affordable energy costs for remote communities is possible given the presence of robust policies that can accelerate and support the energy transition towards more sustainable sources of energy. Synergies between stakeholders (local governments, private sectors, utility corporations and Indigenous peoples) are also highlighted to be fundamental in achieving the desired energy transition for remote communities.

Chapter 5

Conclusions and recommendations

5.1 Summary

This thesis demonstrates novel holistic approaches to accelerate energy transitions among Northern remote communities. This was presented in the three main chapters of this work, Chapters 2, 3 and 4. Each chapter highlights methodological progression from the previous study for the purpose of addressing the research gaps mentioned previously in Section 1.4. Chapter 2 introduces the main energy modeling framework, MINES, developed for this dissertation. This tool embodies the multiple solution philosophies and conflicting design objectives from various stakeholders in the North, and thereby enables representation of complex trade-offs in designing an alternative energy system for remote communities. Chapter 3 improves the proposed modeling framework by integrating heat and electricity sectors, and by carrying out dynamic simulations of viable heating technologies in the Arctic region. This chapter also introduces a simplistic community-scale energy trilemma index model in order to quantitatively assess the set of optimal energy system configurations being extracted from MINES, in reference to the trilemma of challenges relating to energy security, affordability, and environmental sustainability. Chapter 4 builds from the holistic and integrated energy systems approach implemented in previous chapters, while improving way of handling uncertainties in energy systems modeling. In particular, the conventional sensitivity analysis approach was enhanced by adapting robust-based optimization technique in the overall modeling framework of MINES. In conjunction with the multi-objective feature of the proposed tool, this uncertainty modeling not just offers diversity of energy solutions but also ensures robust operation of the energy system in the presence of multiple overlapping uncertainties such as extreme climate events in the Arctic region. Varying risk preferences of the decision makers towards uncertainties are also presented.

Understanding that there is no one-size-fits-all solution for all of the communities in the North is fundamental for this work. Although the methods and approaches described in this dissertation are transferable to other remote communities, it should be noted that each community is unique especially in the territories. The energy situations in the Arctic communities are not necessarily homogeneous, and neither are their priorities and Indigenous community structures. Hence, the collective themes (graphical representation shown in Fig. 5.1) – formed as summary discussions of this work – should be complemented with further analysis if applied to other remote communities.

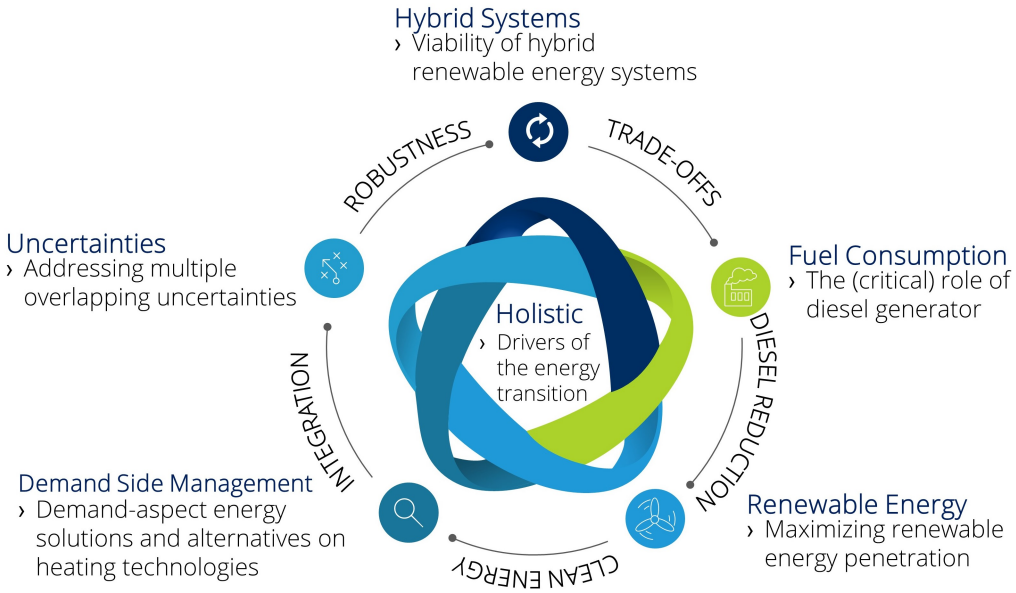

Figure 5.1: Graphical representation of the collective themes in this dissertation.

5.1.1 Viability of hybrid renewable energy systems

Various energy system configurations were found to be viable in this work in reference to the current fossil fuel-based energy system in the North. Across all three main chapters of this dissertation, the optimal combination of each energy system component was investigated by examining multiple points in the Pareto front. These points represent the non-dominated solutions/individuals generated from the optimization module of the MINES model. System $LCOE$ and $fuel_{cons}$ were formulated as the two conflicting design objectives for the case study conducted in Sachs Harbour. Specific solutions or points of interest were further analyzed by looking at the hourly dispatch of each configuration, and trade-off analyses were performed against a set of candidate solutions. This diversity of solutions implies more flexibility in the decision making process of various stakeholders and practitioners in the territories. The full spectrum of energy solutions demonstrated in this dissertation also support the significance of having a multi-objective approach in optimizing energy systems especially in Arctic remote communities wherein multiple energy solution philosophies exist.

5.1.2 The (critical) role of diesel generator

It was observed that minimizing $fuel_{cons}$ resulted to an increase in $LCOE$ which was attributable to limiting the operation of the DG and replacing it with renewables and the BT storage. The role of the back-up DG was also proven to be critical in ensuring energy system reliability for the community. In Chapter 2, the robustness of the proposed fully hybrid PV-WT-BT-DG-CONV was tested by performing system failure simulation on each component of the hybrid system. It was highlighted that the $LPSP$ increases to 27% assuming the DG failed. System failure associated on other components of the energy system, on the other hand, reflected no impact on the security of power supply ($LPSP = 0$) but resulted to an increase in P_{DG} and $fuel_{cons}$ to compensate for the unavailability of a particular system component.

Chapter 3 presents the robustness of the optimal configuration result against RE fluctuations and the variations of space heating demand as impacted by the U-values[1] of the specific type of building enclosures. The results demonstrated that the new building standards (U-values of 0.15, 0.2 and 0.23) and the energy efficiency refurbishment of existing buildings (U-value of 0.28) could withstood space heating load variations while ensuring adequate supply of power and having approximately 0% $LPSP$ (0% - 0.24%) across the four U-values (representing specific insulation thickness) shown in Table 3.10. However, the critical role of the DG was observed when $LPSP$ increased to approximately 20% with a U-value ranging from 0.85 - 1.1 (existing normal buildings). Specifically, the capacity factor of the DG increased to meet the increase in space heating demand, but not enough to supply all the heating load. This increase in power output from the DG also implied an increase on the LCC of the system.

The energy modeling work carried out in Chapters 2 and 3 were deterministic in nature, and a robust optimization approach was introduced in Chapter 4 to better capture multiple overlapping uncertainties in designing integrated energy systems. In comparison with the deterministic optimal solutions, an increase of optimal capacity for majority of the system components (WT, PV, DG, CONV) were observed for the three solutions of interest except the BT storage. In the presence uncertainties, this suggested that the probabilistic algorithm of MINES assigns its preference to generate power from the DG over discharging the BT storage to meet load deficit. Note that the charge-discharge cycles of the BT storage were driven by the renewables (wind and solar) which were treated as uncertain paremeters for this work. Thus, the DG offers more flexibility whenever there is a load deficit in the system. An inherent trade-off, however, is the increase in $fuel_{cons}$ which translates to an increase in $CO_{2\,emissions,life\,cycle}$ as well. This critical role of the DG should be well-considered in energy planning among remote communities like Sachs Harbour wherein fuels are being delivered via barge once a year since year-round road access is not available.

5.1.3 Maximizing renewable energy penetration

Of all the available sources of energy in the hybrid energy system, wind has been proven to meet the largest share of demand in Sachs Harbour. Along with solar, it was established how renewables could potentially displace diesel and heating oil among remote communities. However, the variability of renewables coupled with the fluctuations in energy demand are major design considerations in optimizing integrated energy systems, especially with the changing weather patterns in the Arctic region as impacted by climate change. With the set of investigations conducted in this work, the resulting Pareto front suggested increase in $LCOE$ as $fuel_{cons}$ decreases because of the introduction of renewables in the system. This also implied higher RE_{pen} for the community. Across the three main chapters of this work, the role of the BT storage was demonstrated to be necessary in facilitating variations from the renewables and fluctuations in the demand profile. Chapter 4 also described potential integration of BT storage systems in the existing net metering infrastructures in the territories. This would enable local residents in remote communities to store some of the power generated locally rather than selling everything back to the

[1] Units are in W/m^2-K

Crown utility. This set-up would potentially address grid reliability issues caused by the intermittency of the renewables and might increase the 20% community solar capacity cap in the NWT.

Integrating electricity and heating sectors was also presented to increase RE_{pen} in an energy system. For instance, this integration allows the WT, PV and DG to serve the thermal loads (space heating through ASHP or baseboard heaters) of the community. This energy system integration is important during extended winter conditions in the Arctic, wherein the solar resource is almost zero for the entire season. This also reduces reliance on heating fuel system which is a major source of environmental emission in the Arctic.

Increasing the utilization of renewables in remote communities requires strong policies that support development of renewable energy projects in the North. For example, full spectrum of costs (as described in Chapter 4) should be reflected in PPA rates among diesel-based systems to make the alternative RE-based projects competitive. Carbon price mechanism was also recommended to be executed in evaluating PPA rates for diesel project developers. In theory, the revenues from this carbon pricing scheme may then be allocated in creating more opportunities for Indigenous peoples-led renewable energy projects.

5.1.4 Demand-aspect energy solutions and alternatives on heating technologies

This work supports renewable energy pathways to decarbonize energy system among Northern remote communities. However, this work suggests a holistic perspective in achieving decarbonization targets in the Arctic region. For example, demand-aspect energy solutions should be incorporated in conjunction with renewable energy options for remote communities. Demand-side solutions are often cheaper to implement as compared to capital-intensive RE-based projects, and does not require major energy infrastructure upgrades. Some demand-aspect methods to improve building performance includes installation of mechanical ventilation heat recovery, maximizing air-tightness, and use of high-performance building enclosures. Having high-performance building does not only reduce space heating loads but also offers non-energy benefits such as thermal comfort, improved air quality, and increased resiliency to power outages and extreme climate events in the Arctic.

Alternatives on other viable heating technology options including ASHP and baseboard heaters were proven to be fundamental in recommending a full range of energy solutions in the North. The impact of these heating options on the overall performance of the energy system were also demonstrated in the modeling results shown in this work. For instance, due to the limited temperature operating range of ASHP in the Arctic, it was highlighted that the heat pumps' coefficients of performance negatively impacted the operation of the energy system and specifically caused space heating demand fluctuations. These demand fluctuations resulted to a larger BT storage requirement, along with an increase in overall energy system costs. The thermodynamically close to 100% efficiency of baseboard heater yielded better results because of the less fluctuations observed in the space heating demand of the community. The alternatives on heating options were further extended in Chapter 4 by including uncertainties in the analysis.

5.1.5 Addressing multiple overlapping uncertainties

Conventional energy systems modeling studies have failed to address uncertainties surrounding the energy transition towards more sustainable and clean sources of energy. Literature survey conducted for this dissertation implies that much effort has been given by the energy modeling community on pathways and technologies rather than uncertainties. Specifically, majority of previous studies rely on treating uncertainties by performing sensitivity analyses given a range of values for an input parameter. Although this provides understanding of the uncertainty space, this technique should be complemented with a non-deterministic approach to fully capture the multi-faceted problem of solving energy issues that are inherently uncertain. Chapter 4 provides a modeling framework to address multiple overlapping uncertainties in designing integrated energy systems while taking into account risk attitudes of the decision maker towards uncertainties. Robust optimization approach, in particular, was demonstrated to be the most suitable technique to ensure robust operation of the proposed energy system considering worst-case realization of uncertainties encompassing system reliability, load profile, and meteorological parameters relevant for Sachs Harbour. Results show that the Pareto optimal solutions found deterministically tends to shift towards higher optimal objective function values when uncertainties were introduced. This suggests that the energy system component capacities optimized deterministically were under-dimensioned considering uncertainties. It was also observed that the RE_{pen} of 69.27% from one of the energy system configurations presented dropped to around 51% (mean) after simulating probabilistically. Consequently, the $fuel_{cons}$ of the DG increased to approximately 750,000 L/yr (mean) as compared to its initial deterministic value of 447,470 L/yr to compensate for the reduced power generated from the renewables. Overall, the uncertainties introduced in the model and the risk preferences of stakeholders can improve decision making in energy system planning among remote communities.

5.1.6 Holistic understanding of the drivers of the energy transition

The energy transition among Indigenous communities in the North is part of a much larger transition towards self-determination, economic reconciliation and energy independence. This work recognized not just the unique physical environment of the Arctic in designing a robust energy system, but also the important role of Indigenous peoples themselves in driving energy transitions for their own communities. The energy landscape in the North is evolving, and this requires holistic approaches in understanding the interconnection between strong policy, emerging techniques in energy systems modeling, complexity of grid operations, and synergies needed among Indigenous peoples and various stakeholders in the Arctic. A multi-domain holistic perspective is integral to reach the overall goal of this project, and framing all the insights and recommendations in this dissertation are just as important as the numbers presented from the energy modeling framework developed for this study. The model is intended to be an additional decision support tool on how to balance all the complexities and trade-offs caused by various technical, economic, environmental, and socio-political aspects driving the energy transition in Northern remote communities and beyond.

Ultimately, understanding the value of holistic approaches in accelerating energy transitions elucidates the importance of technology push and demand pull policies [186], [187] in the adoption of multiple energy solution philosophies in the Arctic and remote communities in general. In particular, adoption of various energy solutions described in this dissertaion should be driven by multiple policy efforts across federal/provincial/territorial governments while taking into account trade-offs in priorities between meeting decarbonization targets and lowering fuel poverty rates within and beyond Northern latitutde communities of Canada.

5.2 Future work

Although this dissertation demonstrated novel contributions on having a multi-domain perspective in addressing energy challenges in the Canadian Arctic region and remote communities in general, there are still many aspects of energy systems modeling and analyses that can be done in order to synthesize more holistic insights to accelerate energy transitions. For instance, the implications of adjusting the 1 h timestep of MINES can be explored to investigate the impact of temporal resolution in designing integrated energy systems. Community-scale energy models usually employ 1 h timestep to maintain tractability of the overall energy system performance and its individual system components, and to ensure model run times manageable. From a modeling perspective, increasing the temporal resolution will increase the computational requirement of the energy model, especially when considering uncertainties, but it might provide additional technical insights to the intermittency of the renewables and its impact to size the energy system components.

Adding new technologies in the proposed energy system model is also valuable. For example, solar thermal and heat storage can be included in the modeling analysis done for remote Arctic communities. Since heating oil is the largest heating source across the three territories in the North, a viable alternative heating technology options can reduce their reliance on fossil fuel-based heating systems. This also implies reduction in environmental emission, lower risk of oil spills, and cheaper source of energy considering that heat is approximately 70% of the combined electricity and heat demand in the Canadian Arctic.

Improvement on the uncertainty module of MINES includes incorporation of cost uncertainties for the system components and price of diesel fuel. The volatility of diesel fuel prices, in particular, can be huge in the long term and this might be a strong argument to consider building renewables-based energy system projects in the North. It should be highlighted that most diesel infrastructures in Northern remote communities of Canada are obsolete which make it inefficient to produce power, and are also strong point sources of greenhouse gases and other airborne pollutants. Considering the trade-off analyses already presented in this work and the possible inclusion of uncertainty on diesel prices, the stakeholders can be provided with more informed decisions on their investment pathways in upgrading their obsolete diesel facilities versus advancing alternative energy solutions that can primarily increase renewable energy uptake in their region.

Climate change risks are significant in developing energy system design strategies for Arctic communities. The high energy costs and environmental vulnerabilities exacerbated by the rapid ongoing climate changes in the region are critical and should be captured in energy systems planning moving forward. Hence, incorpo-

rating climate change variations, especially for Northern latitude communities, is recommended as this may impact the optimal size of renewable energy technologies and battery storage in the system. Some uncertainties, associated with observational gaps and climate model biases, can be reduced when continued research from atmospheric scientists are taken into account as well.

Considering aggressive efforts from the local and federal governments of Canada to reduce diesel dependence among remote communities, the development of a functioning territorial carbon market(s) in the North can have a significant impact given full carbon pricing implementation within the region. From a modeling perspective, this policy implementation may push the Pareto fronts presented in this dissertation towards lower diesel fuel consumption. This will also provide additional insights for policy makers in terms of understanding the implication of carbon prices within their territories.

Finally, the modeling framework of MINES has the generic ability to handle other remote communities aside from the case study presented in this dissertation. For instance, this model has been applied in establishing the first Inuit energy cooperative in Gjoa Haven, Nunavut through a partnership with World Wildlife Fund - Canada. Moving forward, and through the Indigenous Off-Diesel Initiative program of Natural Resources Canada, the model will be applied to other remote communities to frame robust policies in accelerating energy transitions both in the Northern territories and other provinces in the country. Together with the previously mentioned recommendations for future work, a probabilistic and holistic energy planning approach facilitates simultaneous evaluation of demand, supply and cost considerations under uncertainty for other remote Indigenous communities in Canada.

Bibliography

[1] National Oceanic and Atmospheric Administration, *Arctic Report Card*, 2017. [Online]. Available: https://www.businessinsider.com/arctic-warming-twice-fast-planet-2016-12 (visited on 11/08/2018) (cit. on p. 1).

[2] C. Joyce, *Arctic Is Warming Twice As Fast As World Average*, 2014. [Online]. Available: https://www.npr.org/2014/12/18/371438087/arctic-is-warming-twice-as-fast-as-world-average (visited on 10/15/2019) (cit. on p. 1).

[3] R. Letzter, *2016 was the worst year ever in the Arctic*, 2016. [Online]. Available: https://www.businessinsider.com/arctic-warming-twice-fast-planet-2016-12 (visited on 11/07/2019) (cit. on pp. 1, 19).

[4] A. T. Perera, V. M. Nik, D. Chen, J. L. Scartezzini, and T. Hong, "Quantifying the impacts of climate change and extreme climate events on energy systems," *Nature Energy*, vol. 5, no. 2, pp. 150–159, 2020, ISSN: 20587546. DOI: 10.1038/s41560-020-0558-0. [Online]. Available: http://dx.doi.org/10.1038/s41560-020-0558-0 (cit. on pp. 1, 91).

[5] D. Cherniak, V. Dufresne, L. Keyte, A. Mallett, and S. Schott, "Report on the State of Alternative Energy in the Arctic," Tech. Rep. September, 2015 (cit. on pp. 1, 55).

[6] Pembina Institute, *Diesel, renewables, and the future of Canada's remote communities*, 2019. [Online]. Available: https://www.pembina.org/blog/remote-microgrids-intro (visited on 07/01/2019) (cit. on pp. 1, 2, 19).

[7] High Commission of Canada in the United Kingdom, *The Canadian Arctic*, 2018. [Online]. Available: https://www.canadainternational.gc.ca/united%7B%5C_%7Dkingdom-royaume%7B%5C_%7Duni/bilateral%7B%5C_%7Drelations%7B%5C_%7Dbilaterales/arctic-arctique.aspx?lang=eng (visited on 02/05/2020) (cit. on pp. 1, 19, 56).

[8] CanmetENERGY, "Energy Policy Context and Market Characterization for the Development of a Northern Communities Energy Technology Intervention Strategy," Tech. Rep. September, 2015 (cit. on pp. 1, 3, 20, 80).

[9] Standing Senate Committee on Energy Environment and Natural Resources, "Powering Canada's Territories," Tech. Rep., 2014 (cit. on pp. 2, 11, 19–21, 58, 59, 151, 152).

[10] National Energy Board, "Energy Facts - Energy Use in Canada's North," Tech. Rep., 2011 (cit. on pp. 2, 122).

[11] Government of Canada (National Energy Board), *Market Snapshot: Explaining the high cost of power in northern Canada*, 2017. [Online]. Available: https://www.neb-one.gc.ca/nrg/ntgrtd/mrkt/snpsht/2017/02-03hghcstpwr-eng.html?=undefined%7B%5C&%7Dwbdisable=true (visited on 10/14/2019) (cit. on pp. 2, 3, 20, 21, 55).

[12] D.-h. Kim, R. Lambert, and R. G. Lambert, "Diverging from Diesel - Technical Report," Tech. Rep. December, 2013, pp. 130–136 (cit. on p. 4).

[13] Canada Energy Regulator, *Market Snapshot: Fuel poverty across Canada – lower energy efficiency in lower income households*, 2017. [Online]. Available: https://www.cer-rec.gc.ca/nrg/ntgrtd/mrkt/snpsht/2017/08-05flpvrt-eng.html?=undefined%7B%5C&%7Dwbdisable=true (visited on 01/08/2020) (cit. on pp. 2, 4, 56, 79, 80).

[14] Y. Touchette, P. Gass, and D. Echeverría, "Costing energy and fossil fuel subsidies in Nunavut : A mapping exercise," International Institute for Sustainable Development and World Wildlife Fund Canada, Tech. Rep., 2017, p. 32 (cit. on pp. 3, 121).

[15] M. A. Marin, "Long-Term Renewable Energy Generation Planning for Off-grid Remote Communities," PhD thesis, University of Waterloo, 2015 (cit. on pp. 5, 61).

[16] The Narwhal, *How can Canada's North get off diesel?* 2019. [Online]. Available: https://thenarwhal.ca/how-canadas-north-get-off-diesel/ (visited on 07/01/2019) (cit. on pp. 4, 11, 20, 56, 57, 75, 98, 101).

[17] S. Skarbo, *State of emergency in Norilsk after 20,000 tons of diesel leaks into Arctic river system*, 2020. [Online]. Available: https://siberiantimes.com/other/others/news/state-of-emergency-in-norilsk-after-20000-tons-of-diesel-leaks-into-arctic-river-system/ (visited on 06/09/2020) (cit. on pp. 4, 98).

[18] A SHARED Future Research Team, *"DECOLONIZING" CLEAN ENERGY POLICY IN CANADA?* 2019. [Online]. Available: https://yellowheadinstitute.org/2019/09/26/decolonizing-clean-energy-policy-in-canada/ (visited on 06/16/2020) (cit. on p. 5).

[19] United Nations, "'We the peoples...': The United Nations declaration on the rights of indigenous peoples," Tech. Rep., 2008. DOI: 10.1111/j.1467-8322.2008.00569.x (cit. on p. 5).

[20] Truth and Reconciliation Commission of Canada, "Truth and Reconciliation Commission of Canada: Calls to Action," Tech. Rep., 2015 (cit. on p. 5).

[21] Hatch Ltd., "Sachs Harbour Wind Scoping Study," Tech. Rep. April, 2017 (cit. on pp. 5, 119).

[22] DNV GL, *WindFarmer*, 2018. [Online]. Available: https://www.dnvgl.com/services/windfarmer-3766 (visited on 11/20/2018) (cit. on p. 6).

[23] John Wood Group PLC, *Wood Group*, 2018. [Online]. Available: https://www.woodgroup.com/who-we-are (visited on 11/21/2018) (cit. on p. 6).

[24] SgurrEnergyl, "Inuvik High Point Wind Feasibility Study," no. May, 2017 (cit. on p. 6).

[25] J.-P. Pinard and J. Maissan, "Sachs Harbour Wind Energy Pre- Feasibility Study," Aurora Research Institute, Tech. Rep., 2009. [Online]. Available: https://nwtresearch.com/sites/default/files/sachs-harbour-wind-energy-pre-feasibility-study.pdf (cit. on p. 6).

[26] K. Karanasios and P. Parker, "Recent Developments in Renewable Energy in Remote Aboriginal Communities, British Columbia, Canada," *Papers in Canadian Economic Development*, vol. 16, no. 0, pp. 65–81, 2016, ISSN: 0833-1871. DOI: 10.15353/PCED.V16I0.70. [Online]. Available: http://pced.uwaterloo.ca/index.php/pced/article/view/70 (cit. on pp. 6, 152).

[27] J.-p. Pinard and J. P. P. Consulting, "Potential for Wind Energy in Nunavut Communities Qulliq Energy Corporation," (cit. on p. 6).

[28] Natural Resources Canada, *RETScreen*, 2018. [Online]. Available: https://www.nrcan.gc.ca/energy/software-tools/7465 (visited on 12/11/2018) (cit. on p. 6).

[29] HOMER Energy, *HOMER Pro*, 2019. [Online]. Available: https://www.homerenergy.com/products/pro/index.html (visited on 09/17/2019) (cit. on pp. 6, 21, 56, 105).

[30] I. Das and C. Canizares, "Renewable Energy Deployment in Canadian Arctic - Phase I (Pre-Feasibility studies and community engagement report for Nunavut)," World Wildlife Fund, Waterloo Institute for Sustainable Energy, Tech. Rep., 2016 (cit. on pp. 6, 56, 98, 105).

[31] M. Stadler, G. Cardoso, S. Mashayekh, T. Forget, N. DeForest, A. Agarwal, and A. Schönbein, "Value streams in microgrids: A literature review," *Applied Energy*, vol. 162, pp. 980–989, 2016, ISSN: 03062619. DOI: 10.1016/j.apenergy.2015.10.081. [Online]. Available: http://dx.doi.org/10.1016/j.apenergy.2015.10.081 (cit. on p. 6).

[32] M. Biberacher, "Modelling and optimisation of future energy system using spatial and temporal methods. Dissertation," PhD thesis, University of Augsburg, 2004, p. 144 (cit. on pp. 7, 21).

[33] International Energy Agency, "RE-ASSUME : A decision maker's guide to evaluating energy scenarios modeling and assumptions," Tech. Rep. June, 2013 (cit. on pp. 7, 21).

[34] H. Lund, F. Arler, P. A. Østergaard, F. Hvelplund, D. Connolly, B. V. Mathiesen, and P. Karnøe, "Simulation versus optimisation: Theoretical positions in energy system modelling," *Energies*, vol. 10, no. 7, pp. 1–17, 2017, ISSN: 19961073. DOI: 10.3390/en10070840. arXiv: arXiv:1011.1669v3 (cit. on p. 7).

[35] B. Bhandari, K. T. Lee, G. Y. Lee, Y. M. Cho, and S. H. Ahn, "Optimization of hybrid renewable energy power systems: A review," *International Journal of Precision Engineering and Manufacturing - Green Technology*, vol. 2, no. 1, pp. 99–112, 2015, ISSN: 21980810. DOI: 10.1007/s40684-015-0013-z (cit. on p. 8).

[36] G. Calabrese, "Generating reserve capacity determined by the probability method," *IEEE Transactions of the American Institute of Electrical Engineers*, vol. 66, pp. 1439–1450, 1947. DOI: 10.1109/T-AIEE.1947.5059596 (cit. on p. 9).

[37] O. C. Otumdi, C. Kalu, and I. Markson, "Determination of Loss of Load Probability for Stand-Alone Photovoltaic Power System," vol. 2, no. 1, pp. 7–12, 2017. DOI: 10.11648/j.ep.20170201.12 (cit. on p. 9).

[38] A. Hadj Arab, F. Chenlo, and M. Benghanem, "Loss-of-load probability of photovoltaic water pumping systems," *Solar Energy*, vol. 76, no. 6, pp. 713–723, 2004, ISSN: 0038092X. DOI: 10.1016/j.solener.2004.01.006 (cit. on pp. 9, 23).

[39] M. Abdelaziz, M. Ali, and M. Eltamaly, *Modeling and Simulation of Smart Grid Integrated with Hybrid Renewable Energy Systems*. Springer International Publishing AG 2018, 2018, ISBN: 9783319647944. DOI: 10.1007/978-3-319-64795-1. [Online]. Available: https://link-springer-com.ezproxy.rgu.ac.uk/content/pdf/10.1007%7B%5C%%7D2F978-3-319-64795-1.pdf (cit. on p. 9).

[40] T. Tezer, R. Yaman, and G. Yaman, "Evaluation of approaches used for optimization of stand-alone hybrid renewable energy systems," *Renewable and Sustainable Energy Reviews*, vol. 73, no. December 2016, pp. 840–853, 2017, ISSN: 18790690. DOI: 10.1016/j.rser.2017.01.118 (cit. on pp. 9, 10, 25–28, 63, 71, 108).

[41] A. Askarzadeh and L. dos Santos Coelho, "A novel framework for optimization of a grid independent hybrid renewable energy system: A case study of Iran," *Solar Energy*, vol. 112, pp. 383–396, 2015, ISSN: 0038092X. DOI: 10.1016/j.solener.2014.12.013. [Online]. Available: http://dx.doi.org/10.1016/j.solener.2014.12.013 (cit. on p. 10).

[42] J. J. Roberts, A. Marotta Cassula, J. L. Silveira, E. da Costa Bortoni, and A. Z. Mendiburu, "Robust multi-objective optimization of a renewable based hybrid power system," *Applied Energy*, vol. 223, no. January, pp. 52–68, 2018, ISSN: 03062619. DOI: 10.1016/j.apenergy.2018.04.032. [Online]. Available: https://doi.org/10.1016/j.apenergy.2018.04.032 (cit. on pp. 10, 28, 29, 32, 61, 63, 103, 104).

[43] B. Gilmour, E. Oldfield, H. Platis, and E. Wicks, "Toward a positive energy future in Northern and remote communities," Tech. Rep., 2018 (cit. on pp. 11, 55, 58).

[44] G. Poelzer, G. H. Gjorv, G. Holdmann, N. Johnson, B. M. Magnusson, L. Sokka, M. Tsyiachiniouk, and S. Yu, "Developing Renewable Energy in Arctic and Sub-Arctic Regions and Communities," pp. 1–68, 2016 (cit. on pp. 12, 55).

[45] Pembina Institute, *Leading Canada's transition to clean energy*, 2019. [Online]. Available: https://www.pembina.org/ (visited on 07/01/2019) (cit. on p. 19).

[46] Government of Canada, *The Paris Agreement*, 2018. [Online]. Available: https://www.canada.ca/en/environment-climate-change/services/climate-change/paris-agreement.html (visited on 07/01/2019) (cit. on p. 19).

[47] P. K. Quinn, T. S. Bates, E. Baum, N. Doubleday, A. M. Fiore, M. Flanner, A. Fridlind, T. J. Garrett, D. Koch, S. Menon, D. Shindell, A. Stohl, and S. G. Warren, "Short-lived pollutants in the Arctic: Their climate impact and possible mitigation strategies," *Atmospheric Chemistry and Physics*, vol. 8, no. 6, pp. 1723–1735, 2008, ISSN: 16807324. DOI: 10.5194/acp-8-1723-2008 (cit. on p. 19).

[48] Environment and Natural Resources, *Spills*, 2019. [Online]. Available: https://www.enr.gov.nt.ca/en/spills (visited on 07/01/2019) (cit. on p. 20).

[49] S. Shankman, *Shipping's Heavy Fuel Oil Puts the Arctic at Risk. Could It Be Banned?* 2018. [Online]. Available: https://insideclimatenews.org/ (visited on 07/01/2019) (cit. on p. 20).

[50] M. S. Gearon, D. F. McCay, E. Chaite, S. Zamorski, D. Reich, J. Rowe, and D. Schmidt-Etkin, "SIMAP Modelling of Hypothetical Oil Spills in the Beaufort Sea for World Wildlife Fund (WWF)," Tech. Rep., 2014 (cit. on p. 20).

[51] D. Levin, *Ice Roads Ease Isolation in Canada's North, but They're Melting Too Soon*, 2017. [Online]. Available: https://www.nytimes.com/2017/04/19/world/canada/ice-roads-ease-isolation-in-canadas-north-but-theyre-melting-too-soon.html (visited on 07/01/2019) (cit. on p. 20).

[52] L. D. Bello, *The Arctic is warming twice as fast as the rest of the globe*, 2017. [Online]. Available: https://futurism.com/the-arctic-is-warming-twice-as-fast-as-the-rest-of-the-globe (visited on 07/01/2019) (cit. on p. 20).

[53] I. Das and C. Canizares, "Fuelling change in the arctic - Phase II (Feasibility studies on selected communities of Nunavut and Northwest Territories)," World Wildlife Fund, Waterloo Institute for Sustainable Energy, Tech. Rep., 2016 (cit. on pp. 21, 56, 62).

[54] I. Kim, J. A. James, and J. Crittenden, "The case study of combined cooling heat and power and photovoltaic systems for building customers using HOMER software," *Electric Power Systems Research*, vol. 143, pp. 490–502, 2017, ISSN: 03787796. DOI: 10.1016/j.epsr.2016.10.061. [Online]. Available: http://dx.doi.org/10.1016/j.epsr.2016.10.061 (cit. on p. 22).

[55] R. Sen and S. C. Bhattacharyya, "Off-grid electricity generation with renewable energy technologies inIndia: An application of HOMER," *Renewable Energy*, vol. 62, pp. 388–398, 2014, ISSN: 09601481. DOI: 10.1016/j.renene.2013.07.028. [Online]. Available: http://dx.doi.org/10.1016/j.renene.2013.07.028 (cit. on p. 22).

[56] I. Prasetyaningsari, A. Setiawan, and A. A. Setiawan, "Design optimization of solar powered aeration system for fish pond in Sleman Regency, Yogyakarta by HOMER software," *Energy Procedia*, vol. 32, pp. 90–98, 2013, ISSN: 18766102. DOI: 10.1016/j.egypro.2013.05.012. [Online]. Available: http://dx.doi.org/10.1016/j.egypro.2013.05.012 (cit. on p. 22).

[57] O. Hafez and K. Bhattacharya, "Optimal planning and design of a renewable energy based supply system for microgrids," *Renewable Energy*, vol. 45, pp. 7–15, 2012, ISSN: 0960-1481. DOI: 10.1016/j.renene.2012.01.087. [Online]. Available: http://dx.doi.org/10.1016/j.renene.2012.01.087 (cit. on p. 22).

[58] L. Montuori, M. Alcázar-Ortega, C. Álvarez-Bel, and A. Domijan, "Integration of renewable energy in microgrids coordinated with demand response resources: Economic evaluation of a biomass gasification plant by Homer Simulator," *Applied Energy*, vol. 132, pp. 15–22, 2014, ISSN: 03062619. DOI: 10.1016/j.apenergy.2014.06.075. [Online]. Available: http://dx.doi.org/10.1016/j.apenergy.2014.06.075 (cit. on p. 22).

[59] W. M. Amutha and V. Rajini, "Cost benefit and technical analysis of rural electri fication alternatives in southern India using HOMER," *Renewable and Sustainable Energy Reviews*, vol. 62, pp. 236–246, 2016, ISSN: 1364-0321. DOI: 10.1016/j.rser.2016.04.042. [Online]. Available: http://dx.doi.org/10.1016/j.rser.2016.04.042 (cit. on p. 22).

[60] P. Tozzi and J. H. Jo, "A comparative analysis of renewable energy simulation tools: Performance simulation model vs. system optimization," *Renewable and Sustainable Energy Reviews*, vol. 80, no. May, pp. 390–398, 2017, ISSN: 18790690. DOI: 10.1016/j.rser.2017.05.153. [Online]. Available: http://dx.doi.org/10.1016/j.rser.2017.05.153 (cit. on p. 22).

[61] H. K. Ringkjøb, P. M. Haugan, and I. M. Solbrekke, "A review of modelling tools for energy and electricity systems with large shares of variable renewables," *Renewable and Sustainable Energy Reviews*, vol. 96, no. August, pp. 440–459, 2018, ISSN: 18790690. DOI: 10.1016/j.rser.2018.08.002. [Online]. Available: https://doi.org/10.1016/j.rser.2018.08.002 (cit. on p. 22).

[62] D. Connolly, H. Lund, B. V. Mathiesen, and M. Leahy, "A review of computer tools for analysing the integration of renewable energy into various energy systems," *Applied Energy*, vol. 87, no. 4, pp. 1059–1082, 2010, ISSN: 03062619. DOI: 10.1016/j.apenergy.2009.09.026. [Online]. Available: http://dx.doi.org/10.1016/j.apenergy.2009.09.026 (cit. on p. 22).

[63] M. Ming, R. Wang, Y. Zha, and T. Zhang, "Multi-Objective Optimization of Hybrid Renewable Energy System Using an Enhanced Multi-Objective Evolutionary Algorithm," *Energies*, vol. 10, no. 5, p. 674, 2017, ISSN: 1996-1073. DOI: 10.3390/en10050674. [Online]. Available: http://www.mdpi.com/1996-1073/10/5/674 (cit. on pp. 22, 23).

[64] A. Konak, D. W. Coit, and A. E. Smith, "Multi-objective optimization using genetic algorithms: A tutorial," *Reliability Engineering and System Safety*, vol. 91, no. 9, pp. 992–1007, 2006, ISSN: 09518320. DOI: 10.1016/j.ress.2005.11.018 (cit. on pp. 22, 25).

[65] D. B. Nelson, M. H. Nehrir, and C. Wang, "Unit sizing and cost analysis of stand-alone hybrid wind/PV/fuel cell power generation systems," *Renewable Energy*, vol. 31, no. 10, pp. 1641–1656, 2006, ISSN: 09601481. DOI: 10.1016/j.renene.2005.08.031 (cit. on pp. 23, 27).

[66] B. S. Borowy and Z. M. Salameh, "Methodology for optimally sizing the combination of a battery bank and PV array in a Wind/PV hybrid system," *IEEE Transactions on Energy Conversion*, vol. 11, no. 2, pp. 367–373, 1996, ISSN: 08858969. DOI: 10.1109/60.507648 (cit. on pp. 23, 28, 63).

[67] J. H. Lucio, R. Valdés, and L. R. Rodrí guez, "Loss-of-load probability model for stand-alone photovoltaic systems in Europe," *Solar Energy*, vol. 86, no. 9, pp. 2515–2535, 2012, ISSN: 0038092X. DOI: 10.1016/j.solener.2012.05.021 (cit. on p. 23).

[68] R. Dufo-López and J. L. Bernal-Agustín, "Multi-objective design of PV-wind-diesel-hydrogen-battery systems," *Renewable Energy*, vol. 33, no. 12, pp. 2559–2572, 2008, ISSN: 09601481. DOI: 10.1016/j.renene.2008.02.027 (cit. on p. 23).

[69] S. Abedi, A. Alimardani, G. B. Gharehpetian, G. H. Riahy, and S. H. Hosseinian, "A comprehensive method for optimal power management and design of hybrid RES-based autonomous energy systems," *Renewable and Sustainable Energy Reviews*, vol. 16, no. 3, pp. 1577–1587, 2012, ISSN: 13640321. DOI: 10.1016/j.rser.2011.11.030. [Online]. Available: http://dx.doi.org/10.1016/j.rser.2011.11.030 (cit. on p. 23).

[70] A. R. Prasad and E. Natarajan, "Optimization of integrated photovoltaic-wind power generation systems with battery storage," *Energy*, vol. 31, no. 12, pp. 1607–1618, 2006, ISSN: 03605442. DOI: 10.1016/j.energy.2005.10.032 (cit. on p. 23).

[71] S. Diaf, D. Diaf, M. Belhamel, M. Haddadi, and A. Louche, "A methodology for optimal sizing of autonomous hybrid PV/wind system," *Energy Policy*, vol. 35, no. 11, pp. 5708–5718, 2007, ISSN: 03014215. DOI: 10.1016/j.enpol.2007.06.020 (cit. on p. 23).

[72] Y. Himri, A. Boudghene Stambouli, B. Draoui, and S. Himri, "Techno-economical study of hybrid power system for a remote village in Algeria," *Energy*, vol. 33, no. 7, pp. 1128–1136, 2008, ISSN: 03605442. DOI: 10.1016/j.energy.2008.01.016 (cit. on p. 23).

[73] R. Baños, C. Gil, B. Paechter, and J. Ortega, "A hybrid meta-heuristic for multi-objective optimization: MOSATS," *Journal of Mathematical Modelling and Algorithms*, vol. 6, no. 2, pp. 213–230, 2007, ISSN: 15701166. DOI: 10.1007/s10852-006-9041-6 (cit. on p. 25).

[74] S. Upadhyay and M. P. Sharma, "Selection of a suitable energy management strategy for a hybrid energy system in a remote rural area of India," *Energy*, vol. 94, pp. 352–366, 2016, ISSN: 03605442. DOI: 10.1016/j.energy.2015.10.134. [Online]. Available: http://dx.doi.org/10.1016/j.energy.2015.10.134 (cit. on p. 25).

[75] B. Jyoti Saharia, H. Brahma, and N. Sarmah, "A review of algorithms for control and optimization for energy management of hybrid renewable energy systems," *Journal of Renewable and Sustainable Energy*, vol. 10, no. 5, p. 053 502, 2018, ISSN: 1941-7012. DOI: 10.1063/1.5032146. [Online]. Available: http://aip.scitation.org/doi/10.1063/1.5032146 (cit. on p. 25).

[76] O. Erdinc and M. Uzunoglu, "Optimum design of hybrid renewable energy systems: Overview of different approaches," *Renewable and Sustainable Energy Reviews*, vol. 16, no. 3, pp. 1412–1425, 2012, ISSN: 13640321. DOI: 10.1016/j.rser.2011.11.011. [Online]. Available: http://dx.doi.org/10.1016/j.rser.2011.11.011 (cit. on p. 25).

[77] M. S. Mahbub, M. Cozzini, P. A. Østergaard, and F. Alberti, "Combining multi-objective evolutionary algorithms and descriptive analytical modelling in energy scenario design," *Applied Energy*, vol. 164, pp. 140–151, 2016, ISSN: 03062619. DOI: 10.1016/j.apenergy.2015.11.042. [Online]. Available: http://dx.doi.org/10.1016/j.apenergy.2015.11.042 (cit. on p. 25).

[78] P. E. Campana, Z. Yang, L. Anders, L. Hailong, and Y. Jinyue, "An Open-source Platform for Simulation and Optimization of Clean Energy Technologies," *Energy Procedia*, vol. 105, pp. 946–952, 2017, ISSN: 18766102. DOI: 10.1016/j.egypro.2017.03.423. [Online]. Available: http://dx.doi.org/10.1016/j.egypro.2017.03.423 (cit. on p. 25).

[79] H. Yang, W. Zhou, L. Lu, and Z. Fang, "Optimal sizing method for stand-alone hybrid solar-wind system with LPSP technology by using genetic algorithm," *Solar Energy*, vol. 82, no. 4, pp. 354–367, 2008, ISSN: 0038092X. DOI: 10.1016/j.solener.2007.08.005 (cit. on p. 25).

[80] M. Schoenauer, K. Deb, G. Rudolph, X. Yao, E. Lutton, J. J. Merelo, and H.-P. Schwefel, *Parallel Problem Solving from Nature - PPSN VI*. 2000, ISBN: 3540410562 (cit. on p. 26).

[81] M. Nemati, M. Braun, and S. Tenbohlen, "Optimization of unit commitment and economic dispatch in microgrids based on genetic algorithm and mixed integer linear programming," *Applied Energy*, vol. 210, pp. 944–963, 2018, ISSN: 0306-2619. DOI: 10.1016/j.apenergy.2017.07.007. [Online]. Available: https://doi.org/10.1016/j.apenergy.2017.07.007 (cit. on p. 27).

[82] Z. I. Id, N. Javaid, S. Iqbal, S. Aslam, and Z. A. Khan, "A Domestic Microgrid with Optimized Home Energy Management System," *Energies*, pp. 1–39, 2018. DOI: 10.3390/en11041002 (cit. on p. 27).

[83] Government of Northwest Territories, "2012 Northwest Territories Energy Charrette," Tech. Rep. January, 2013 (cit. on pp. 27, 61, 99).

[84] M. R. D. Quitoras, M. L. S. Abundo, and L. A. M. Danao, "A techno-economic assessment of wave energy resources in the Philippines," *Renewable and Sustainable Energy Reviews*, vol. 88, no. March 2017, pp. 68–81, 2018, ISSN: 18790690. DOI: 10.1016/j.rser.2018.02.016. [Online]. Available: https://doi.org/10.1016/j.rser.2018.02.016 (cit. on pp. 27, 62, 99).

[85] Natural Resources Canada, *Reducing diesel energy in rural and remote communities*, 2019. [Online]. Available: https://www.nrcan.gc.ca/climate-change/green-infrastructure-programs/reducing-diesel-energy-rural-and-remote-communities/20542 (visited on 07/03/2019) (cit. on p. 27).

[86] R. Ramakumar, I. Abouzahr, and K. Ashenayi, "A knowledge-based approach to the design of integrated renewable energy systems," *IEEE Transactions on Energy Conversion*, vol. 7, no. 4, pp. 648–659, 1992, ISSN: 15580059. DOI: 10.1109/60.182647 (cit. on p. 28).

[87] P. E. Campana, S. J. Quan, F. I. Robbio, A. Lundblad, Y. Zhang, T. Ma, B. Karlsson, and J. Yan, "Optimization of a residential district with special consideration on energy and water reliability," *Applied Energy*, vol. 194, pp. 751–764, 2016, ISSN: 03062619. DOI: 10.1016/j.apenergy.2016.10.005. [Online]. Available: http://dx.doi.org/10.1016/j.apenergy.2016.10.005 (cit. on pp. 29, 61, 65, 66, 76, 82).

[88] J. Duffie and W. Beckman, *Solar Engineering of Thermal Processes*, Fourth Edi. John Wiley & Sons, Inc. All, 2013, ISBN: 9780470873663 (cit. on p. 30).

[89] D. G. Eras, S. A. Klein, and J. A. Duffle, "Estimation of the diffuse radiation fraction for hourly, daily and monthly-average global radiation," vol. 28, no. 4, 1982 (cit. on p. 30).

[90] J. J. Roberts, A. A. Mendiburu Zevallos, and A. M. Cassula, "Assessment of photovoltaic performance models for system simulation," *Renewable and Sustainable Energy Reviews*, vol. 72, no. October 2016, pp. 1104–1123, 2017, ISSN: 18790690. DOI: 10.1016/j.rser.2016.10.022. [Online]. Available: http://dx.doi.org/10.1016/j.rser.2016.10.022 (cit. on p. 30).

[91] P. Jain, *Wind Energy Engineering*. New York: McGraw-Hill Companies, Inc., 2011, ISBN: 9780071714785. [Online]. Available: www.google.com (cit. on p. 30).

[92] T. Burton, N. Jenkins, D. Sharpe, and E. Bossanyi, *Wind Energy Handbook*, Second Edi. John Wiley & Sons, Ltd, 2011, ISBN: 0471359297. DOI: 10.1007/s007690000247. arXiv: arXiv:1011.1669v3 (cit. on pp. 30, 31).

[93] E. S. Sreeraj, K. Chatterjee, and S. Bandyopadhyay, "Design of isolated renewable hybrid power systems," *Solar Energy*, vol. 84, no. 7, pp. 1124–1136, 2010, ISSN: 0038092X. DOI: 10.1016/j.solener.2010.03.017. [Online]. Available: http://dx.doi.org/10.1016/j.solener.2010.03.017 (cit. on p. 32).

[94] J. F. Manwell and G. Jon, "Lead acid battery storage model for hybrid energy systems," vol. 50, no. 5, pp. 399–405, 1993 (cit. on p. 32).

[95] E. J. Hoevenaars and C. A. Crawford, "Implications of temporal resolution for modeling renewables-based power systems," *Renewable Energy*, vol. 41, pp. 285–293, 2012, ISSN: 09601481. DOI: 10.1016/j.renene.2011.11.013. [Online]. Available: http://dx.doi.org/10.1016/j.renene.2011.11.013 (cit. on pp. 34, 62).

[96] M. Matthew, "Assessing the operational robustness of the HOMER model for Marine Corps use in expeditionary environments," PhD thesis, Naval Postgraduate School, 2014 (cit. on pp. 34, 62).

[97] Northwest Territories Tourism, *Sachs Harbour*, 2019. [Online]. Available: https://spectacularnwt.com/destinations/western-arctic/sachs-harbour (visited on 07/05/2019) (cit. on p. 35).

[98] Meteonorm, *Meteonorm*, 2019. [Online]. Available: https://meteonorm.com/ (visited on 07/05/2019) (cit. on p. 40).

[99] J. L. Sweeney, "Modeling for Insights , not Numbers : the Experiences of the Energy Modeling Forum 1," *OMEGA*, vol. 10, no. 5, pp. 449–462, 1982 (cit. on pp. 48, 85, 119).

[100] O. Williams, *Sachs Harbour to receive new $10M diesel power plant*, 2019. [Online]. Available: https://cabinradio.ca/13683/news/economy/sachs-harbour-to-receive-new-10m-diesel-power-plant/ (visited on 08/14/2019) (cit. on p. 49).

[101] Government of the Northwest Territories, "Implementing Pan-Canadian Carbon Pricing in the Northwest Territories," Tech. Rep. July, 2017 (cit. on pp. 49, 86).

[102] Natural Resources Canada, *Indigenous Off-diesel Initiative*, 2020. [Online]. Available: https://impact.canada.ca/en/challenges/off-diesel (visited on 07/23/2020) (cit. on p. 56).

[103] B. Kentish, *Arctic is warming at twice the rate of the rest of the planet, scientists warn*, 2017. [Online]. Available: https://www.independent.co.uk/environment/arctic-warming-twice-rate-rest-of-planet-global-warming-snow-water-ice-permafrost-arctic-monitoring-a7710701.html (visited on 10/15/2019) (cit. on p. 56).

[104] L. Tribioli, R. Cozzolino, L. Evangelisti, and G. Bella, "Energy management of an off-grid hybrid power plant with multiple energy storage systems," *Energies*, vol. 9, no. 8, 2016, ISSN: 19961073. DOI: 10.3390/en9080661 (cit. on pp. 56, 106).

[105] H. Sugihara, J. Komoto, and K. Tsuji, "A multi-objective optimization model for determining urban energy systems under integrated energy service in a specific area," *Electrical Engineering in Japan (English translation of Denki Gakkai Ronbunshi)*, vol. 147, no. 3, pp. 20–31, 2004, ISSN: 04247760. DOI: 10.1002/eej.10275 (cit. on p. 57).

[106] E. Lo Cascio, D. Borelli, F. Devia, and C. Schenone, "Future distributed generation: An operational multi-objective optimization model for integrated small scale urban electrical, thermal and gas grids," *Energy Conversion and Management*, vol. 143, pp. 348–359, 2017, ISSN: 01968904. DOI: 10.1016/j.enconman.2017.04.006. [Online]. Available: http://dx.doi.org/10.1016/j.enconman.2017.04.006 (cit. on p. 57).

[107] K. Orehounig, R. Evins, and V. Dorer, "Integration of decentralized energy systems in neighbourhoods using the energy hub approach," *Applied Energy*, vol. 154, pp. 277–289, 2015, ISSN: 03062619. DOI: 10.1016/j.apenergy.2015.04.114. [Online]. Available: http://dx.doi.org/10.1016/j.apenergy.2015.04.114 (cit. on p. 57).

[108] L. Cabrol and P. Rowley, "Towards low carbon homes – A simulation analysis of building-integrated air-source heat pump systems," *Energy & Buildings*, vol. 48, pp. 127–136, 2012, ISSN: 0378-7788. DOI: 10.1016/j.enbuild.2012.01.019. [Online]. Available: http://dx.doi.org/10.1016/j.enbuild.2012.01.019 (cit. on p. 57).

[109] R. Renaldi, A. Kiprakis, and D. Friedrich, "An optimisation framework for thermal energy storage integration in a residential heat pump heating system," *Applied Energy*, vol. 186, pp. 520–529, 2017, ISSN: 03062619. DOI: 10.1016/j.apenergy.2016.02.067. [Online]. Available: http://dx.doi.org/10.1016/j.apenergy.2016.02.067 (cit. on p. 57).

[110] M. R. Quitoras, P. E. Campana, and C. Crawford, "Exploring electricity generation alternatives for Canadian Arctic communities using a multi-objective genetic algorithm approach," en, *Energy Conversion and Management*, vol. 210, no. April, pp. 1–19, Apr. 2020, ISSN: 0196-8904. DOI: 10.1016/j.enconman.2020.112471. [Online]. Available: http://dx.doi.org/10.1016/j.enconman.2020.112471 (cit. on pp. 58, 63, 66, 69, 99, 100, 107).

[111] Government of Northwest Territories, "Northwest Territories Energy Report," Tech. Rep. May, 2011 (cit. on pp. 58, 59).

[112] World Wildlife Fund Canada, "Renewble energy in Nunavut (Scoping Analysis)," Tech. Rep., 2019 (cit. on p. 59).

[113] L. H. Anh, L. S. Dong, V. Kreinovich, and N. N. Thach, *Econometrics for Financial Applications*. Springer Nature, 2018, ISBN: 9783319731490 (cit. on p. 61).

[114] K. Deb, A. Member, A. Pratap, S. Agarwal, and T. Meyarivan, "A fast and elitist multi-objective genetic algorithm:NSGAII," vol. 6, no. 2, pp. 182–197, 2002 (cit. on pp. 61, 62, 97).

[115] R. Evins, P. Pointer, R. Vaidyanathan, and S. Burgess, "A case study exploring regulated energy use in domestic buildings using design-of-experiments and multi-objective optimisation," *Building and Environment*, vol. 54, pp. 126–136, 2012, ISSN: 03601323. DOI: 10.1016/j.buildenv.2012.02.012. [Online]. Available: http://dx.doi.org/10.1016/j.buildenv.2012.02.012 (cit. on pp. 61, 97).

[116] J. Forde, C. J. Hopfe, R. S. McLeod, and R. Evins, "Temporal optimization for affordable and resilient Passivhaus dwellings in the social housing sector," *Applied Energy*, vol. 261, no. August 2019, p. 114 383, 2020, ISSN: 03062619. DOI: 10.1016/j.apenergy.2019.114383. [Online]. Available: https://doi.org/10.1016/j.apenergy.2019.114383 (cit. on pp. 61, 97).

[117] Y. Zhang, A. Lundblad, P. Elia, F. Benavente, and J. Yan, "Battery sizing and rule-based operation of grid-connected photovoltaic-battery system : A case study in Sweden Level of Confidence State of Charge," *Energy Conversion and Management*, vol. 133, pp. 249–263, 2017, ISSN: 0196-8904. DOI: 10.1016/j.enconman.2016.11.060. [Online]. Available: http://dx.doi.org/10.1016/j.enconman.2016.11.060 (cit. on p. 61).

[118] M. Sharafi and T. Y. Elmekkawy, "Multi-objective optimal design of hybrid renewable energy systems using PSO-simulation based approach," vol. 68, 2014, ISSN: 09601481. DOI: 10.1016/j.renene.2014.01.011 (cit. on p. 62).

[119] HOMER Pro 3.13, *Fuel Consumption Data*, 2020. [Online]. Available: https://www.homerenergy.com/products/pro/docs/latest/fuel%7B%5C_%7Dcurve.html (visited on 01/14/2020) (cit. on pp. 62, 63).

[120] R. Hendron and J. Burch, "Development of standardized domestic hot water event schedules for residential buildings," *Proceedings of the Energy Sustainability Conference 2007*, no. August, pp. 531–540, 2007. DOI: 10.1115/ES2007-36104 (cit. on p. 64).

[121] Arctic Energy Alliance, "Sachas Harbour Energy Profile," Tech. Rep., 2008, p. 2016. DOI: 10.1351/goldbook.e02112 (cit. on p. 64).

[122] World Energy Council, "World Energy Trilemma Index — 2017," Tech. Rep., 2017, p. 145 (cit. on p. 66).

[123] ARUP, "Five-minute guide: Energy trilemma," 2019. [Online]. Available: https://www.arup.com/perspectives/publications/promotional-materials/section/five-minute-guide-to-the-energy-trilemma (cit. on pp. 66, 67).

[124] NWT Bureau of Statistics, "Housing Indicators," Tech. Rep., 2019, pp. 30–33 (cit. on p. 69).

[125] Government of Northwest Territories, "NWT Climate Change Impacts and Adaptation Report," Tech. Rep., 2008, pp. 1–31. [Online]. Available: www.enr.gov.nt.ca/%7B%5C_%7Dlive/documents/content/NWT%7B%5C_%7Dclimate%7B%5C_%7Dchange%7B%5C_%7Dimpacts%7B%5C_%7Dand%7B%5C_%7Dadaptation%7B%5C_%7Dreport.pdf (cit. on p. 76).

[126] Arctic Heat Pumps, *Arctic Cold Climate Heat Pumps*, 2019. [Online]. Available: https://www.arcticheatpumps.com/ (visited on 01/10/2020) (cit. on p. 77).

[127] M. Pavičević, T. Novosel, T. Pukšec, and N. Duić, "Hourly optimization and sizing of district heating systems considering building refurbishment – Case study for the city of Zagreb," *Energy*, vol. 137, pp. 1264–1276, 2017, ISSN: 03605442. DOI: 10.1016/j.energy.2017.06.105 (cit. on p. 79).

[128] Energy Efficiency, *Canadian Provincial Energy Efficiency Scoreboard*, 2019. [Online]. Available: http://www.efficiencycanada.org/ (visited on 01/11/2020) (cit. on p. 80).

[129] T.-P. Frappé-Sénéclauze, D. Heerema, —. Karen, and T. Wu, "Accelerating Market Transformation for High-Performance Building Enclosures," no. September, 2016. [Online]. Available: www.pembina.org. (cit. on pp. 81, 123).

[130] RDH Building Engineering Ltd., "Window Design for Canada ' s North," Tech. Rep., 2016 (cit. on pp. 82, 85).

[131] E. Burrell, *What is Mechanical Ventilation with Heat Recovery (MVHR)?* 2015. [Online]. Available: https://elrondburrell.com/blog/passivhaus-mechanical-ventilation-heat-recovery/ (visited on 01/11/2020) (cit. on p. 82).

[132] M. Jakob, "Marginal costs and co-benefits of energy efficiency investments. The case of the Swiss residential sector," *Energy Policy*, vol. 34, no. 2 SPEC. ISS. Pp. 172–187, 2006, ISSN: 03014215. DOI: 10.1016/j.enpol.2004.08.039 (cit. on pp. 82, 83).

[133] V. Krey and K. Riahi, "Risk Hedging Strategies under Energy System and Climate Policy Uncertainties," International Institute forApplied Systems Analysis, Laxenburg, Austria, Tech. Rep. August, 2009 (cit. on p. 91).

[134] S. Pye, N. Sabio, and N. Strachan, "An integrated systematic analysis of uncertainties in UK energy transition pathways," *Energy Policy*, vol. 87, pp. 673–684, 2015, ISSN: 03014215. DOI: 10.1016/j.enpol.2014.12.031. [Online]. Available: http://dx.doi.org/10.1016/j.enpol.2014.12.031 (cit. on pp. 91, 92).

[135] United Nations Framework Convention on Climate Change, *What is the Paris Agreement?* 2018. [Online]. Available: https://unfccc.int/process-and-meetings/the-paris-agreement/what-is-the-paris-agreement (visited on 12/16/2018) (cit. on p. 91).

[136] A. A. M. H. A. Asbahi, F. Z. Gang, W. Iqbal, Q. Abass, M. Mohsin, and R. Iram, "Novel approach of Principal Component Analysis method to assess the national energy performance via Energy Trilemma Index," *Energy Reports*, vol. 5, pp. 704–713, 2019, ISSN: 23524847. DOI: 10.1016/j.egyr.2019.06.009. [Online]. Available: https://doi.org/10.1016/j.egyr.2019.06.009 (cit. on p. 91).

[137] D. Heerema and D. Lovekin, "Power Shift in Remote Indigenous Communities A cross-Canada scan of diesel reduction and clean energy policies," Tech. Rep. July, 2019. [Online]. Available: www.pembina.org. (cit. on pp. 91, 92).

[138] Energy and Mines Ministers Conference, "Clean Technology Integration in Remote Communities: Policies, Programs, and Initiatives by Federal, Provincial, and Territorial Governments," Tech. Rep. August, 2018 (cit. on p. 92).

[139] D. Lovekin, B. Dronkers, and B. Thibault, "Power purchase policies for remote Indigenous communities in Canada: Research on government policies to support renewable energy projects," World Wildlife Fund, Pembina Institute, Tech. Rep., 2016, p. 101 (cit. on p. 93).

[140] W. Usher and N. Strachan, "Critical mid-term uncertainties in long-term decarbonisation pathways," *Energy Policy*, vol. 41, pp. 433–444, 2012, ISSN: 03014215. DOI: 10.1016/j.enpol.2011.11.004. [Online]. Available: http://dx.doi.org/10.1016/j.enpol.2011.11.004 (cit. on p. 92).

[141] S. Pfenninger, A. Hawkes, and J. Keirstead, "Energy systems modeling for twenty-first century energy challenges," *Renewable and Sustainable Energy Reviews*, vol. 33, pp. 74–86, 2014, ISSN: 13640321. DOI: 10.1016/j.rser.2014.02.003. [Online]. Available: http://dx.doi.org/10.1016/j.rser.2014.02.003 (cit. on pp. 92, 93).

[142] G. Mavromatidis, K. Orehounig, and J. Carmeliet, "Comparison of alternative decision-making criteria in a two-stage stochastic program for the design of distributed energy systems under uncertainty," *Energy*, vol. 156, pp. 709–724, 2018, ISSN: 03605442. DOI: 10.1016/j.energy.2018.05.081. [Online]. Available: https://doi.org/10.1016/j.energy.2018.05.081 (cit. on p. 94).

[143] C. Hamarat, J. H. Kwakkel, E. Pruyt, and E. T. Loonen, "An exploratory approach for adaptive policymaking by using multi-objective robust optimization," *Simulation Modelling Practice and Theory*, vol. 46, pp. 25–39, 2014, ISSN: 1569190X. DOI: 10.1016/j.simpat.2014.02.008. [Online]. Available: http://dx.doi.org/10.1016/j.simpat.2014.02.008 (cit. on p. 94).

[144] D. E. Majewski, M. Wirtz, M. Lampe, and A. Bardow, "Robust multi-objective optimization for sustainable design of distributed energy supply systems," *Computers and Chemical Engineering*, vol. 102, pp. 26–39, 2017, ISSN: 00981354. DOI: 10.1016/j.compchemeng.2016.11.038. [Online]. Available: http://dx.doi.org/10.1016/j.compchemeng.2016.11.038 (cit. on p. 94).

[145] K. Deb, S. Gupta, D. Daum, J. Branke, A. K. Mall, and D. Padmanabhan, "Reliability-based optimization using evolutionary algorithms," *IEEE Transactions on Evolutionary Computation*, vol. 13, no. 5, pp. 1054–1074, 2009, ISSN: 1089778X. DOI: 10.1109/TEVC.2009.2014361 (cit. on pp. 94, 97).

[146] C. E. Clark and B. DuPont, "Reliability-based design optimization in offshore renewable energy systems," *Renewable and Sustainable Energy Reviews*, vol. 97, no. September, pp. 390–400, 2018, ISSN: 18790690. DOI: 10.1016/j.rser.2018.08.030. [Online]. Available: https://doi.org/10.1016/j.rser.2018.08.030 (cit. on p. 94).

[147] L. Chu, "Reliability Based Optimization with Metaheuristic Algorithms and Latin Hypercube Sampling Based Surrogate Models," *Applied and Computational Mathematics*, vol. 4, no. 6, p. 462, 2015, ISSN: 2328-5605. DOI: 10.11648/j.acm.20150406.20 (cit. on p. 94).

[148] M. A. Valdebenito and G. I. Schuëller, "A survey on approaches for reliability-based optimization," *Structural and Multidisciplinary Optimization*, vol. 42, no. 5, pp. 645–663, 2010, ISSN: 1615147X. DOI: 10.1007/s00158-010-0518-6 (cit. on p. 94).

[149] H. K. Ringkjøb, P. M. Haugan, and A. Nybø, "Transitioning remote Arctic settlements to renewable energy systems – A modelling study of Longyearbyen, Svalbard," *Applied Energy*, vol. 258, no. November 2019, p. 114079, 2020, ISSN: 03062619. DOI: 10.1016/j.apenergy.2019.114079. [Online]. Available: https://doi.org/10.1016/j.apenergy.2019.114079 (cit. on p. 94).

[150] J. P. Chen, G. Huang, B. W. Baetz, Q. G. Lin, C. Dong, and Y. P. Cai, "Integrated inexact energy systems planning under climate change : A case study of Yukon Territory , Canada," *Applied Energy*, vol. 229, no. August, pp. 493–504, 2018, ISSN: 0306-2619. DOI: 10.1016/j.apenergy.2018.06.140. [Online]. Available: https://doi.org/10.1016/j.apenergy.2018.06.140 (cit. on p. 94).

[151] M. R. Quitoras, P. Elia, P. Rowley, and C. Crawford, "Remote community integrated energy system optimization including building enclosure improvements and quantitative energy trilemma metrics," *Applied Energy*, vol. 267, no. March, p. 115 017, 2020, ISSN: 0306-2619. DOI: 10.1016/j.apenergy.2020.115017. [Online]. Available: https://doi.org/10.1016/j.apenergy.2020.115017 (cit. on pp. 95, 107–109, 111).

[152] H. G. Beyer and B. Sendhoff, "Robust optimization - A comprehensive survey," *Computer Methods in Applied Mechanics and Engineering*, vol. 196, no. 33-34, pp. 3190–3218, 2007, ISSN: 00457825. DOI: 10.1016/j.cma.2007.03.003 (cit. on p. 97).

[153] F. S. Gazijahani and J. Salehi, "Robust Design of Microgrids with Reconfigurable Topology under Severe Uncertainty," *IEEE Transactions on Sustainable Energy*, vol. 9, no. 2, pp. 559–569, 2018, ISSN: 19493029. DOI: 10.1109/TSTE.2017.2748882 (cit. on p. 97).

[154] G. Petrone, J. Axerio-Cilies, D. Quagliarella, and G. Iaccarino, "A probabilistic non-dominated sorting ga for optimization under uncertainty," *Engineering Computations (Swansea, Wales)*, vol. 30, no. 8, pp. 1054–1085, 2013, ISSN: 02644401. DOI: 10.1108/EC-05-2012-0110 (cit. on p. 98).

[155] J. Zrum, S. Sumanik, and M. Ross, "Modelling of remote diesel-based power systems in the Canadian territories," Yukon Research Centre, Yukon College, Tech. Rep., 2019 (cit. on p. 98).

[156] E. K. Doolittle, H. L. Kerivin, and M. M. Wiecek, "Robust multiobjective optimization with application to Internet routing," *Annals of Operations Research*, vol. 271, no. 2, pp. 487–525, 2018, ISSN: 15729338. DOI: 10.1007/s10479-017-2751-5. [Online]. Available: https://doi.org/10.1007/s10479-017-2751-5 (cit. on p. 98).

[157] Z. Tang, J. Périaux, G. Bugeda, and E. Oñate, "Lift maximization with uncertainties for the optimization of high lift devices using multi-criterion evolutionary algorithms," *2009 IEEE Congress on Evolutionary Computation, CEC 2009*, pp. 2324–2331, 2009. DOI: 10.1109/CEC.2009.4983230 (cit. on p. 98).

[158] J. W. Herrmann, "A genetic algorithm for minimax optimization problems," *Proceedings of the 1999 Congress on Evolutionary Computation, CEC 1999*, vol. 2, pp. 1099–1103, 1999. DOI: 10.1109/CEC.1999.782545 (cit. on p. 98).

[159] W. Chen, J. Unkelbach, A. Trofimov, T. Madden, H. Kooy, T. Bortfeld, and D. Craft, "Including robustness in multi-criteria optimization for intensity-modulated proton therapy," *Physics in Medicine and Biology*, vol. 57, no. 3, pp. 591–608, 2012, ISSN: 00319155. DOI: 10.1088/0031-9155/57/3/591. arXiv: 1112.5362 (cit. on p. 98).

[160] C. K. Goh and K. C. Tan, "Evolving the tradeoffs between Pareto-optimality and robustness in multi-objective evolutionary algorithms," *Studies in Computational Intelligence*, vol. 51, pp. 457–478, 2007, ISSN: 1860949X. DOI: 10.1007/978-3-540-49774-5_20 (cit. on p. 98).

[161] D. Kuroiwa and G. M. Lee, "On robust multiobjective optimization," *Journal of Nonlinear and Convex Analysis*, vol. 15, no. 6, pp. 1125–1136, 2014, ISSN: 18805221 (cit. on p. 98).

[162] L. Wang, Q. Li, R. Ding, M. Sun, and G. Wang, "Integrated scheduling of energy supply and demand in microgrids under uncertainty: A robust multi-objective optimization approach," *Energy*, vol. 130, pp. 1–14, 2017, ISSN: 03605442. DOI: 10.1016/j.energy.2017.04.115. [Online]. Available: http://dx.doi.org/10.1016/j.energy.2017.04.115 (cit. on p. 98).

[163] K. Deb and H. Gupta, "Introducing robustness in multi-objective optimization," *Evolutionary Computation*, vol. 14, no. 4, pp. 463–494, 2006, ISSN: 10636560. DOI: 10.1162/evco.2006.14.4.463 (cit. on p. 98).

[164] R. Dufo-Lopez, "iHOGA User's manual," Tech. Rep. February, 2020 (cit. on pp. 100, 101).

[165] G. Zubi, R. Dufo-lópez, G. Pasaoglu, and N. Pardo, "Techno-economic assessment of an off-grid PV system for developing regions to provide electricity for basic domestic needs : A 2020 – 2040 scenario," *Applied Energy*, vol. 176, no. 2016, pp. 309–319, 2016, ISSN: 0306-2619. DOI: 10.1016/j.apenergy.2016.05.022. [Online]. Available: http://dx.doi.org/10.1016/j.apenergy.2016.05.022 (cit. on p. 100).

[166] R. Dufo-lópez, E. Pérez-cebollada, J. L. Bernal-agustín, and I. Martínez-ruiz, "Optimisation of energy supply at off-grid healthcare facilities using Monte Carlo simulation," *Energy Conversion and Management*, vol. 113, pp. 321–330, 2016. DOI: 10.1016/j.enconman.2016.01.057 (cit. on p. 100).

[167] J. B. Fulzele and M. Daigavance, "Sc cience Direct t Des ign and Optimiz zation of f Hybrid PV-Win nd Renew wable En nergy," *Materials Today: Proceedings*, 2018. DOI: 10.1016/j.matpr.2017.11.151 (cit. on p. 100).

[168] G. Zubi, G. Vincenzo, J. M. Lujano-rojas, K. El, and D. Andrews, "The unlocked potential of solar home systems ; an effective way to overcome domestic energy poverty in developing regions," *Renewable Energy*, vol. 132, pp. 1425–1435, 2019, ISSN: 0960-1481. DOI: 10.1016/j.renene.2018.08.093. [Online]. Available: https://doi.org/10.1016/j.renene.2018.08.093 (cit. on p. 100).

[169] R. Dufo-López, J. L. Bernal-Agustín, J. M. Yusta-Loyo, J. A. Domínguez-Navarro, I. J. Ramírez-Rosado, J. Lujano, and I. Aso, "Multi-objective optimization minimizing cost and life cycle emissions of stand-alone PV-wind-diesel systems with batteries storage," *Applied Energy*, vol. 88, no. 11, pp. 4033–4041, 2011, ISSN: 03062619. DOI: 10.1016/j.apenergy.2011.04.019 (cit. on p. 100).

[170] R. Dufo-López, I. R. Cristóbal-Monreal, and J. M. Yusta, "Stochastic-heuristic methodology for the optimisation of components and control variables of PV-wind-diesel-battery stand-alone systems," *Renewable Energy*, vol. 99, pp. 919–935, 2016, ISSN: 18790682. DOI: 10.1016/j.renene.2016.07.069 (cit. on pp. 100, 104).

[171] J.-p. Pinard, "Wind Monitoring Update for Tuktoyaktuk," Tech. Rep. 867, 2009 (cit. on p. 102).

[172] Government of Northwest Territories, "CLIMATE OBSERVATIONS IN THE NORTHWEST TERRITORIES (1957-2012)," Tech. Rep., 2012 (cit. on p. 102).

[173] F. R. Martins, S. A. Silva, E. B. Pereira, and S. L. Abreu, "The influence of cloud cover index on the accuracy of solar irradiance model estimates," *Meteorology and Atmospheric Physics*, vol. 99, no. 3-4, pp. 169–180, 2008, ISSN: 01777971. DOI: 10.1007/s00703-007-0272-5 (cit. on p. 102).

[174] R. Billinton and W. Li, *Reliability assessment of electric power systems using Monte Carlo methods*. Springer Science+Business Media New York, 1994, ISBN: 9781489913487 (cit. on pp. 103, 104).

[175] Trojan Battery Company, *T-105 Deep-Cycle Flooded*, 2020. [Online]. Available: https://www.trojanbattery.com/product/t-105/ (visited on 07/04/2020) (cit. on pp. 106, 107, 111).

[176] ——, *TR 25.6-25 Li-ion Deep-Cycle Lithium*, 2020. [Online]. Available: https://www.trojanbattery.com/product/tr-25-6-25-li-ion/ (visited on 07/04/2020) (cit. on pp. 106, 107).

[177] West Grid, *What is Compute Canada*, 2020. [Online]. Available: https://www.westgrid.ca/faq%7B%5C_%7Dprospective%7B%5C_%7Dusers/what%7B%5C_%7Dcompute%7B%5C_%7Dcanada (visited on 06/29/2020) (cit. on p. 107).

[178] A. Hayes, *Coefficient of Variation (CV)*, 2020. [Online]. Available: https://www.investopedia.com/terms/c/coefficientofvariation.asp (visited on 07/13/2020) (cit. on p. 112).

[179] V. Brown, *This is what Indigenous energy sovereignty looks like*, 2019. [Online]. Available: https://briarpatchmagazine.com/articles/view/indigenous-climate-action (visited on 06/16/2020) (cit. on p. 119).

[180] Government of Yukon, "Yukon's Independent Power Production Policy," Tech. Rep. October, 2018, p. 15. [Online]. Available: https://yukon.ca/sites/yukon.ca/files/emr/emr-yukon-independent-power-production-policy.pdf (cit. on p. 119).

[181] Qulliq Energy Corporation, *Qulliq Energy Corporation Application for Commercial and Institutional Power Producers Pricing Structure*, 2020. [Online]. Available: https://www.qec.nu.ca/customer-care/generating-power/commercial-and-institutional-power-producer-program (visited on 07/16/2020) (cit. on p. 120).

[182] D. Lovekin and D. Heerema, "The True Cost of Energy in Remote Communities," Pembina Institute, Tech. Rep. March, 2019. [Online]. Available: https://www.pembina.org/pub/diesel-true-cost (cit. on p. 120).

[183] First Nations Power Authority, *First Nations Power Authority: Bringing Experience and Expertise to First Nations*, 2020. [Online]. Available: https://fnpa.ca/home-3/ (visited on 06/16/2020) (cit. on p. 121).

[184] B. Morin, *Can First Nations Power Authority transform the energy industry?* 2019. [Online]. Available: https://www.nationalobserver.com/2019/11/24/news/can-first-nations-power-authority-transform-energy-industry (visited on 06/16/2020) (cit. on p. 121).

[185] Government of Northwest Territories, "2030 Energy Strategy of Northwest Territories," Tech. Rep., 2018 (cit. on pp. 121, 122).

[186] M. Peters, M. Schneider, T. Griesshaber, and V. H. Hoffmann, "The impact of technology-push and demand-pull policies on technical change - Does the locus of policies matter?" *Research Policy*, vol. 41, no. 8, pp. 1296–1308, 2012, ISSN: 00487333. DOI: 10.1016/j.respol.2012.02.004. [Online]. Available: http://dx.doi.org/10.1016/j.respol.2012.02.004 (cit. on p. 130).

[187] S. Samant, P. Thakur-Wernz, and D. E. Hatfield, "Does the focus of renewable energy policy impact the nature of innovation? Evidence from emerging economies," *Energy Policy*, vol. 137, no. May 2019, p. 111 119, 2020, ISSN: 03014215. DOI: 10.1016/j.enpol.2019.111119. [Online]. Available: https://doi.org/10.1016/j.enpol.2019.111119 (cit. on p. 130).

Appendix A

Electricity infrastructure in the North

Among the 80 communities in the North, 53 rely exclusively on diesel generators as their primary source of their electricity (see Table 2.1 and Fig. A.1 - A.2). For other places such as Yukon and NWT, it is a mixture of diesel and hydropower; many of which were constructed in the 1950-60s. The Northern Canada Power Corporation (NCPC) used to own and operate these facilities before it was transferred to the Northern communities in the 1980s [9].

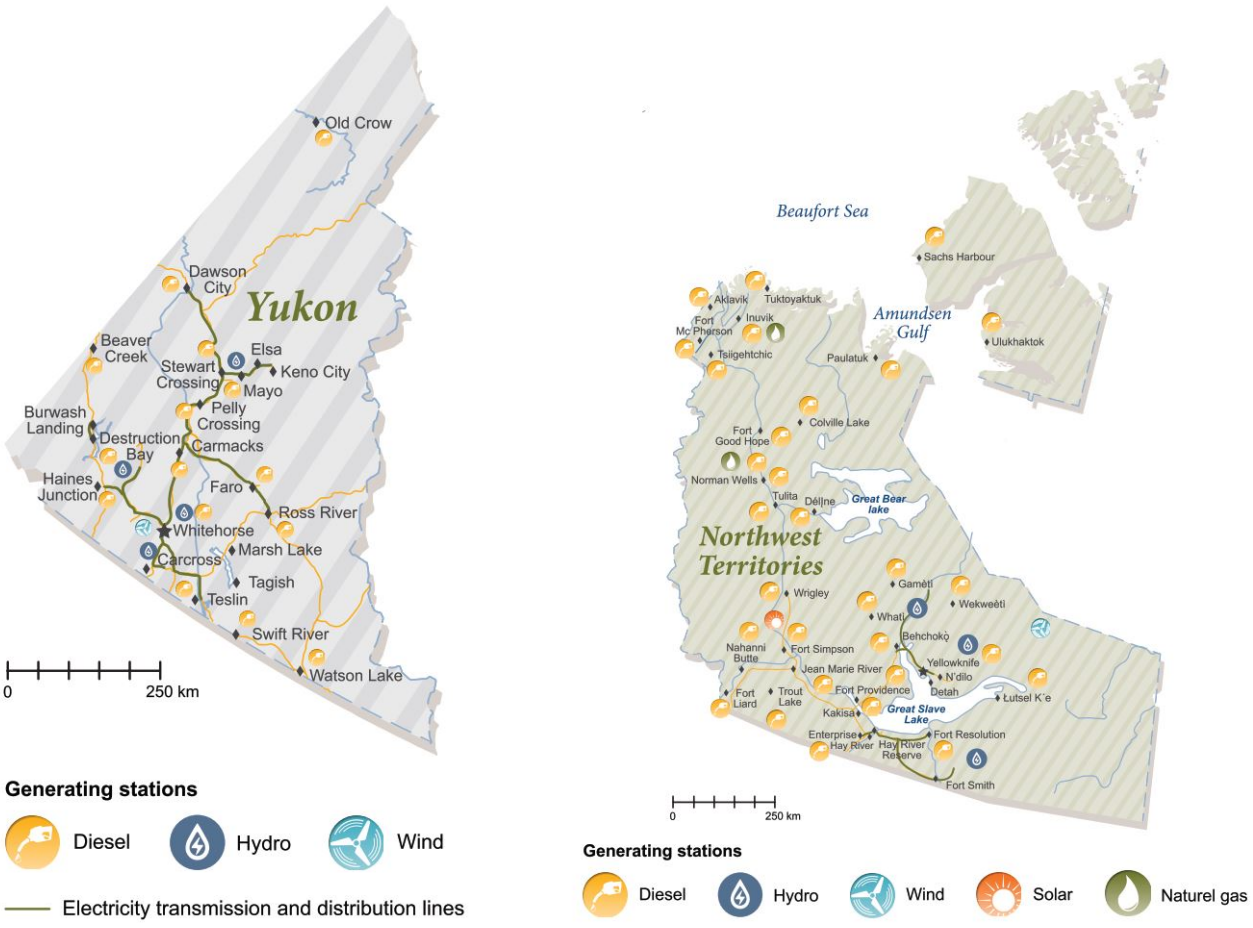

(a) Yukon (b) Northwest Territories

Figure A.1: Power generation facilities in Yukon and the Northwest Territories [9]

Power generation in Nunavut is being provided by Qulliq Energy Corporation

(QEC), a corporation owned by the Government of Nunavut. QEC has a total installed diesel capacity of 54 MW. Power is being transmitted through 26 stand-alone diesel plants and approximately 275 km of distribution lines [26].

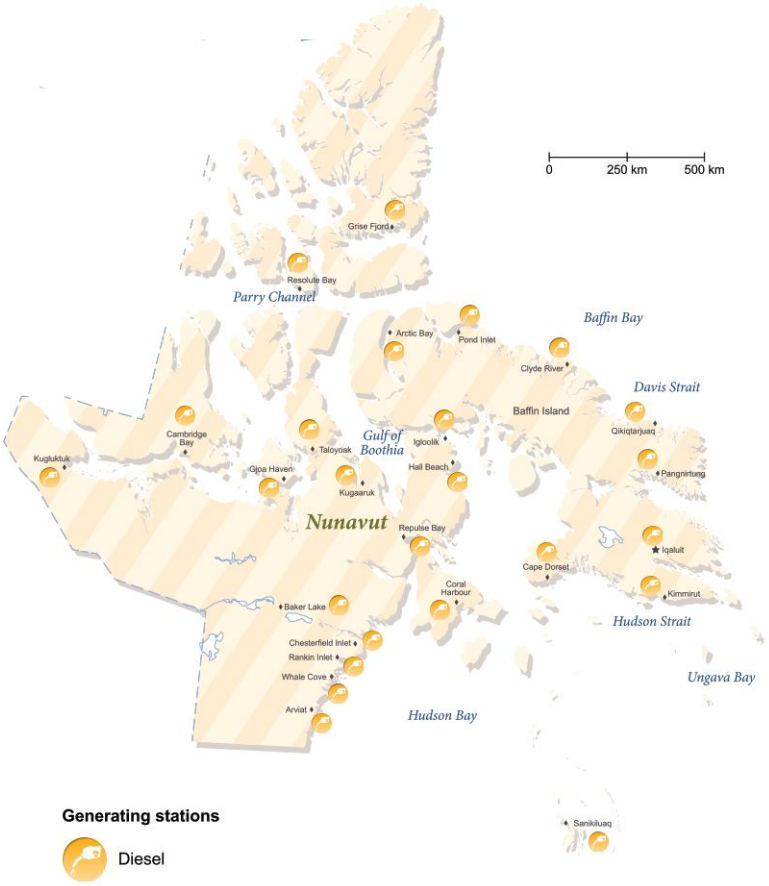

Figure A.2: Communities in Nanavut rely 100% on diesel [9]

Appendix B

CRediT author statement

This appendix is in reference to the contributions made by each author in Chapters 2, 3 and 4 of this dissertation.

As adapted from Elsevier, CRediT (Contributor Roles Taxonomy) was introduced with the intention of recognizing individual author contributions, reducing authorship disputes and facilitating collaboration.

- **Conceptualization:** Ideas; formulation or evolution of overarching research goals and aims
- **Methodology:** Development or design of methodology; creation of models
- **Software:** Programming, software development; designing computer programs; implementation of the computer code and supporting algorithms; testing of existing code components
- **Validation:** Verification, whether as a part of the activity or separate, of the overall replication/ reproducibility of results/experiments and other research outputs
- **Formal analysis:** Application of statistical, mathematical, computational, or other formal techniques to analyze or synthesize study data
- **Investigation:** Conducting a research and investigation process, specifically performing the experiments, or data/evidence collection
- **Resources:** Provision of study materials, reagents, materials, patients, laboratory samples, animals, instrumentation, computing resources, or other analysis tools
- **Data Curation:** Management activities to annotate (produce metadata), scrub data and maintain research data (including software code, where it is necessary for interpreting the data itself) for initial use and later reuse
- **Writing - Original Draft:** Preparation, creation and/or presentation of the published work, specifically writing the initial draft (including substantive translation)

- **Writing - Review & Editing:** Preparation, creation and/or presentation of the published work by those from the original research group, specifically critical review, commentary or revision – including pre-or postpublication stages
- **Visualization:** Preparation, creation and/or presentation of the published work, specifically visualization/ data presentation
- **Supervision:** Oversight and leadership responsibility for the research activity planning and execution, including mentorship external to the core team
- **Project administration:** Management and coordination responsibility for the research activity planning and execution
- **Funding acquisition:** Acquisition of the financial support for the project leading to this publication